Interaction of Chiral Lanthanide complexes with nucleic acids

Bobba, Gabriella

INTERACTION OF CHIRAL LANTHANIDE COMPLEXES WITH NUCLEIC ACIDS

Gabriella Bobba

A thesis submitted for the degree of Doctor of Philosophy

Department of Chemistry
University of Durham

2002

We are chemists, that is hunters: ours are 'the two experiences of adult life' Pavese spoke about, success and failure, killing the white whale or wrecking the ship; we must not surrender to the incomprehensible substance, we must not give up. We are here for this, to make mistakes and correct them, to receive knocks and return them. We must never feel disarmed: nature is immense and complex, but it is not impermeable to intelligence; you have to go round it, prick it, probe it, look for a way through or make it yourself.

Siamo chimici, cioé cacciatori: nostre sono 'le due esperienze della vita adulta' di cui parlava Pavese, il successo e l'insuccesso,
uccidere la balena bianca o sfasciare la nave; non ci si deve arrendere alla materia incomprensibile, non ci si deve sedere. Siamo qui per
questo, per sbagliare e correggerci, per incassare colpi e renderli. Non ci si deve mai sentire disarmati: la natura é immensa e complessa,
ma non é impermeabile all'intelligenza; devi girarle intorno, pungere, sondare, cercare il varco o fartelo.

Primo Levi - "Il sistema periodico"

Acknowledgements

Sincere thanks to:

Professor David Parker for having faith in me, always being available to discuss my problems and for teaching me not to surrender to the challenges of chemistry;

Dr Andrew Beeby for enlightening discussions about photochemistry and help with the lifetime, phosphorescence and fluorescence anisotropy experiments;

Dr Alan Kenwright, Ian McKeag and Catherine Heffernan for running the VT and 2D NMR spectra;

Dr Mike Jones and Lara Turner for their assistance with the mass spectrometry measurements;

Dr Ritu Kataky and Lisa Wiley for their help with the cyclic voltammetry experiments;

the current and past members of the DP group: the postdocs (Juan Carlos Frias, Rachel Dickins, Kanthi Senanayake, Yann Bretonniere, Horst Puschmann, James Bruce, Mark Lowe, Justin Perry, Ofer Reany, Suzy Kean, Linda Govenlock) and the PhD students (Alessandra Badari, Aileen Congreve, Nicola Thompson, Simon Welsh, Mark O'Halloran, Dimitri Messeri, Stephanie Blair, Celine Mathieu) for helping me with the chemistry, sharing with me my successes and failures and making the lab an enjoyable and friendly place to work in;

all the other friends I met in Durham, for making these three years a wonderful life experience, and my Italian friends, for staying close to me, despite the distance;

my sister Barbara, my Mum and Dad, for encouraging my choice and loving me immensely.

Declaration

The research described in this thesis was undertaken at the Department of Chemistry of the University of Durham between January 2000 and November 2002. All of the work is my own; no part of it has previously been submitted for a degree at this or any other university.

Statement of copyright

Abstract

Enantiopure Δ and Λ lanthanide complexes, bearing a phenanthridinium or a dipyridoquinoxaline chromophore as a sensitiser, have been designed with the aim of developing structural and reactive probes for nucleic acids. Their interaction with DNA was studied using various spectroscopic techniques.

A certain degree of stereoselectivity in DNA binding was discerned. The Λ enantiomers of the Eu tetramide and of the $EuPh_3dpq$ complexes interacted with nucleic acids in a predominantly intercalative binding mode, by inserting their planar aromatic chromophore between the base-pairs. The former showed a preference for C-G sites, while the latter bound preferentially to A-T base-pairs. A rather different binding mode, probably involving the minor groove, was revealed in the interaction of the Δ enantiomer of the $EuPh_3dpq$ complex with nucleic acids, with a higher affinity for C and G bases.

In the presence of nucleic acid, a charge transfer process occurred in each case, which quenched the singlet excited state of the phenanthridinium moiety or the lanthanide excited state (in Ph_3dpq complexes). In the unique case of the $EuNp_3dpq$ complexes, the interaction resulted in an increase in the metal emission intensity and lifetime, as a consequence of the protection of the molecule, probably accommodated in the DNA minor groove, from a quenching process. This 'light switch' effect can be exploited in the development of spectroscopic probes.

The $TbNp_3dpq$, on the other hand, was found to generate singlet oxygen efficiently and could therefore act as a reactive probe.

Moreover, the $EuPh_3dpq$ and $TbPh_3dpq$ complexes showed extraordinarily high emission quantum yields in aqueous media, due to the favourable photophysical properties of the dpq antenna as well as the nonadentate nature of the Ph_3dpq ligand. This makes them valuable luminescent probes.

Contents

CHAPTER 5

Abbreviations

A	adenine
T	thymine
G	guanine
C	cytosine
poly(dAdT)	polydeoxyadenylic-deoxythymidylic acid
poly(dGdC)	polydeoxyguanylic-deoxycytidylic acid
CT-DNA	calf-thymus deoxyribonucleic acid
phi	9,10-phenanthrenequinone diimine
dppz	dipyrido [3,2-a:2',3'-c] phenazine
phen	phenanthroline
bpy	bipyridyl
hat	1,4,5,8,9,12-hexaazatriphenylene
tap	1,4,5,8-tetraazaphenanthrene
dpq	dipyrido [3,2-f:2',3'-h] quinoxaline
cyclen, $12N_4$	1,4,7,10-tetraazacyclododecane
DOTA	1,4,7,10-tetraazacyclododecane-1,4,7,10-tetraacetic acid
DO3A	1,4,7,10-tetraazacyclododecane-1,4,7-triacetic acid
Boc	*tert*-butoxycarbonyl
Ln	lanthanide
Np	1-naphthyl
HEPES	N-(2-hydroxyethyl)piperazine-N'-(2-ethanesulfonic acid)
NOESY	nuclear Overhauser enhancement spectroscopy
COSY	correlation spectroscopy
CD	circular dichroism
ICD	induced circular dichroism
CPL	circularly polarised luminescence
ISC	intersystem crossing
MLCT	metal-to-ligand charge transfer
LMCT	ligand-to-metal charge transfer

CHAPTER 1

Introduction

1.1. Nucleic Acid Structure and Interactions

1.1.1. Nucleic Acid Conformations

As DNA contains all the information necessary for the life of a living organism, it is important to understand how this information is stored and decoded. The answer lies in the internal structure of DNA.[1]

To a first approximation, DNA can be viewed as a **double helix** with a backbone of alternating phosphate groups and deoxyribose sugars and pairs of nitrogenous bases hydrogen bonded together (Fig.1.1). The double helix is antiparallel, normally right-handed, and, owing to the flexibility of the sugar-phosphate chains, can assume a wide range of different conformations.

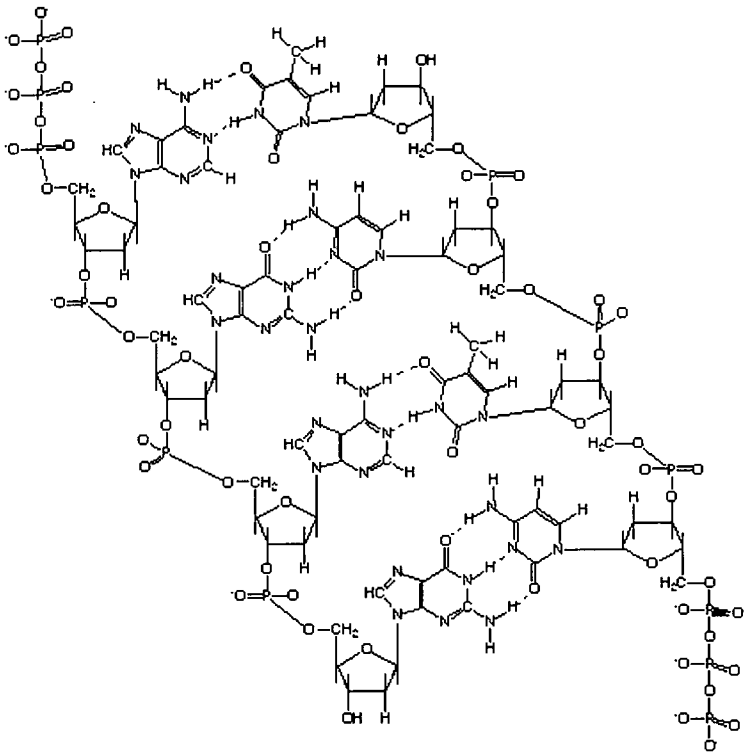

Fig.1.1 Structure of a double-stranded DNA fragment.

The interactions between adenine (A) and thymine (T) and between guanine (G) and cytosine (C) can give rise to Watson-Crick or Hoogsteen **base-pairs** (Fig.1.2).

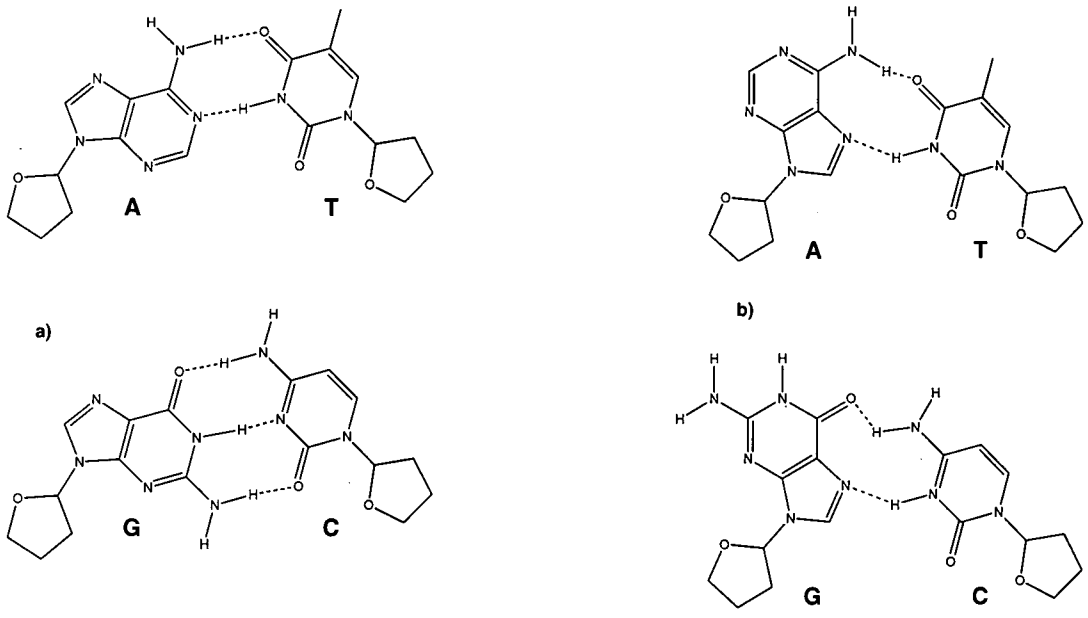

Fig.1.2 Watson-Crick base-pairs (a) and Hoogsteen base-pairs (b), showing hydrogen bonding.

While both A-T base-pairs have roughly equal stability, the Hoogsteen G-C pair is less stable than the Watson-Crick analogue, having two instead of three hydrogen bonds. Moreover, the Hoogsteen G-C pair is only stable at low pH (≤ 5), since one of the nitrogens on C must be protonated. This is the main reason why practically all DNA double helices contain Watson-Crick rather than Hoogsteen pairs. Hoogsteen pairs, however, show up in complexes of DNA with anticancer drugs and in triple helices.

The two sugars to which a base-pair are attached lie closer to one side of the base-pair than the other. This is called the minor groove side because early structural models of DNA showed two spiral **grooves** lying between the two sugar-phosphate chains: a minor (smaller) and a major (larger) groove. This is true for the B-form, but in other helices the so-called minor groove is actually as large as or larger than the so-called major groove.

It is the hydrophobicity of the bases that provides the driving force for helix formation: they escape from contact with water by interacting with one another at the core of the helix. The bases thus form base-pairs that stack on one another. To increase the overlap of consecutive pairs, the bases forming a pair rotate about their long axes in opposite directions (Fig.1.3). This motion is called 'propeller twist' and tends to be higher in regions containing mostly A-T base-pairs.

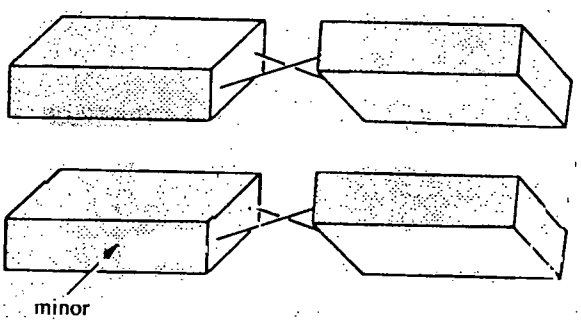

Fig.1.3 Propeller-twisted base-pairs. Note how the hydrogen bonds between bases are distorted by this motion, yet remain intact. The minor groove edges of the bases are indicated.[1]

In addition to this, which is a property of a single base-pair, there are three significant relative motions of two base-pairs that lie over each other at any base-pair step: two rotations (twist and roll) and a translation (slide) (Fig.1.4).

- 'Twist' (T) corresponds to a rotation about the local twist axis that runs vertically through the centres of any two neighbouring base-pairs;
- 'Roll' (R) describes the rolling-open of base-pairs along their long axes;
- 'Slide' (S) describes the relative sliding of neighbouring base-pairs along their long axes.

Two base-pairs can adopt conformations with different values of T, R and S, in order to maximise hydrogen bonding or stacking interactions and to avoid steric clashes.

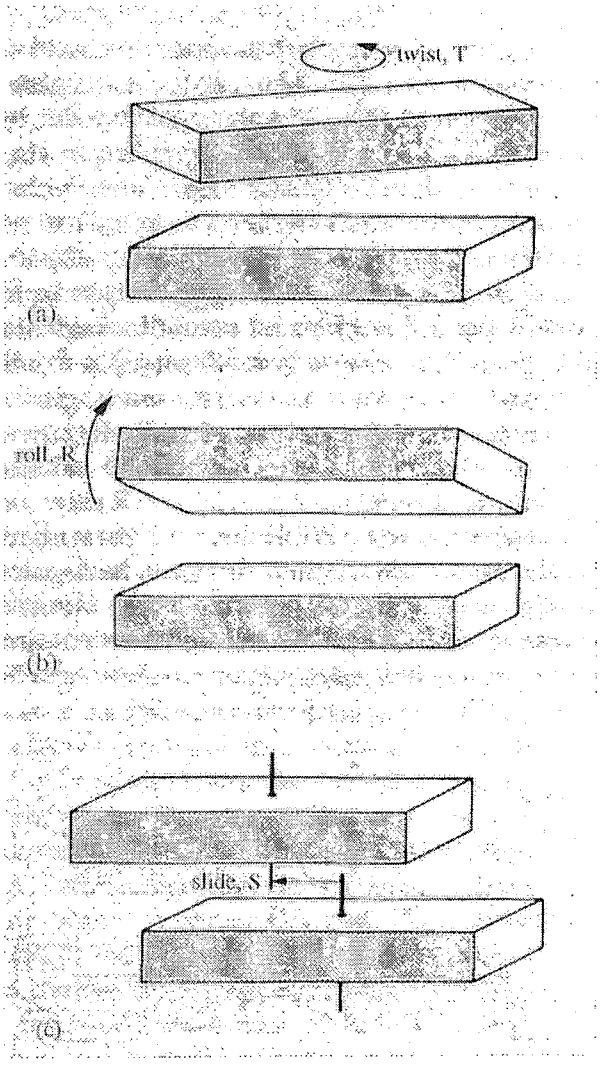

Fig.1.4 Twist, roll and slide motions at a base-pair step. The arrows define the positive sense of each motion.[1]

The stacking of bases on one another is influenced not only by the hydrophobic effect, but also by partial electric charges within the bases themselves (Fig. 1.5). The preferred positions will maximise attractive interactions between a partially positively charged atom from one base and a negatively charged atom from the base directly above or below and minimise the repulsive juxtapositions.

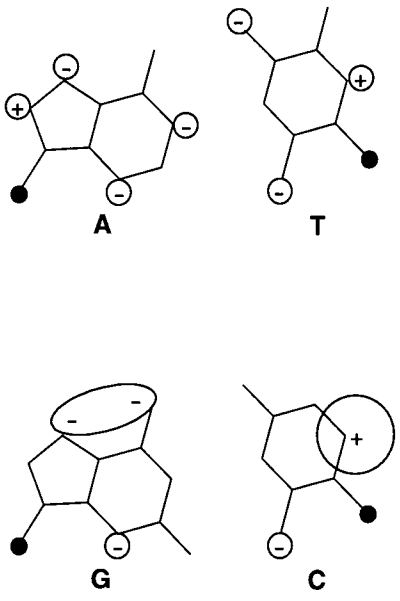

Fig.1.5 Regions of 'partial charge' for A-T and C-G base-pairs. The base-pairs have the same relative orientations as in Fig.1.2 (a).[1]

A dense accumulation of negative charge along the major groove edge of G can be noticed, as well as a concentration of positive charge on the major groove edge of C. Two successive G-C base-pairs, therefore, will not stack directly on top of one another, due to a strong like-to-like charge repulsion.

Another force that controls the interactions between base-pairs is the repulsion between the negatively charged upper and lower surfaces of any base, due to their aromatic nature. Thus the base-pairs tend to lie offset from one another, which is the opposite of the hydrophobic effect. It is the amount of water surrounding the bases that determines which of the two is stronger: when the DNA fibre is wet, the hydrophobic forces are dominant and the result is the B-form (S = 0 Å), but when it is dry, the repulsive effect becomes stronger and the A-form (S = -1.5 Å) appears. A left-handed Z-form, in which the base-pairs lie offset from one another, can also be seen in relatively dry fibres (Fig.1.6).

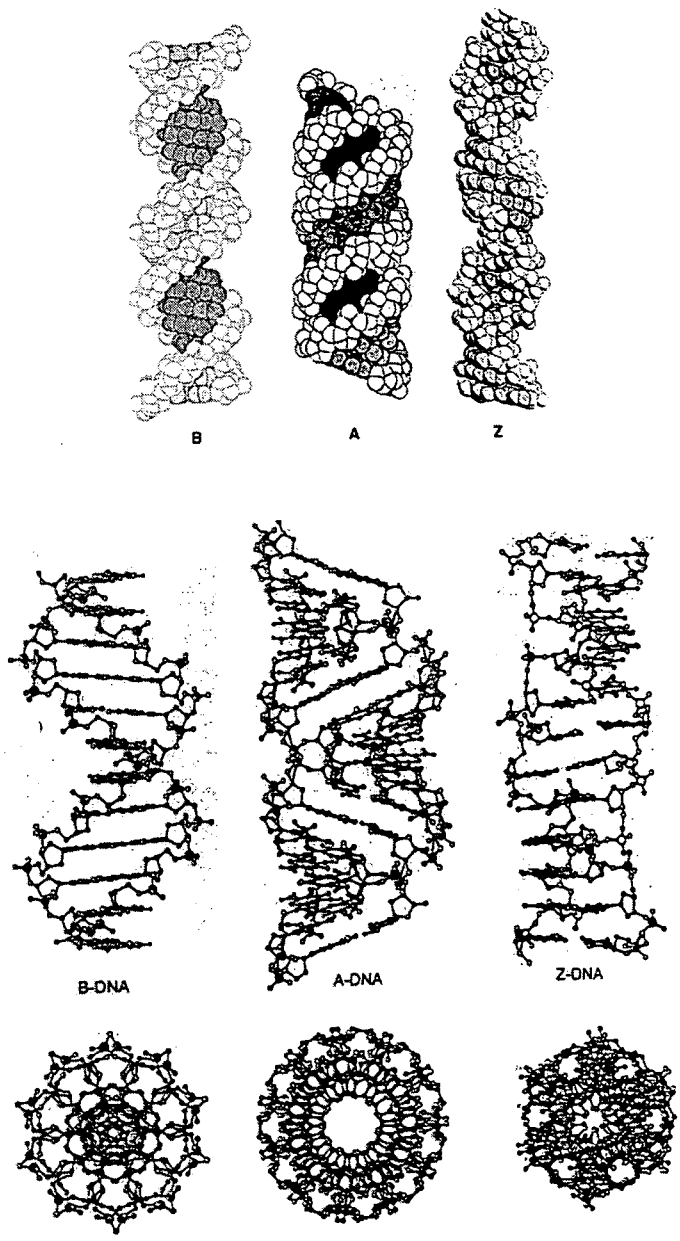

Fig.1.6 B-, A- and Z-DNA viewed perpendicular to the helix axis and down the helix axis.[53]

These polymorphs are generated by different values of slide, roll and twist, favoured at a local level by the base composition of the step. These three parameters are broadly related to each other and give rise to the external form of the helix, affecting, first of all, the dimension of the grooves (Table 1.1).

Table 1.1 Typical geometric parameters for standard A-, B- and Z-forms of DNA.[53]

Parameter	A-DNA	B-DNA	Z-DNA
Roll	12°	0°	1°
Twist	32°	36°	11/50°
Slide	0.15 nm	0 nm	0.2 nm
Helix diameter	2.55 nm	2.37 nm	1.84 nm
Bases/turn of helix	11	10	12
Base rise/base-pair	0.23 nm	0.33 nm	0.38 nm
Major groove	narrow, deep	wide, deep	flat
Minor groove	broad, shallow	narrow, deep	narrow, deep

Although it is often assumed that **RNA** adopts a single stranded geometry,[2] it contains extensive duplex regions in which adenine forms base-pair with uracil instead of thymine. Double helical RNA[2] adopts the A-form geometry. Mismatched regions are a common secondary structural motif and act as potential protein recognition sites.

Less known forms of DNA are **triple helices** and **quadruplexes**,[2] generated by particular sequences. A third nucleic acid strand comprising pyrimidines can associate with a duplex, consisting of purines on one strand and pyrimidines on the other, to form Hoogsteen hydrogen bonded base triplets T··A-T and C^+··G-C. The third strand occupies the major groove of the initial duplex.

Four stranded structures can be formed by the telomeric sequences at the ends of chromosomes. C-rich sequences form two parallel-stranded duplexes with C-C base-pairs intercalated into each other (Fig.1.7).

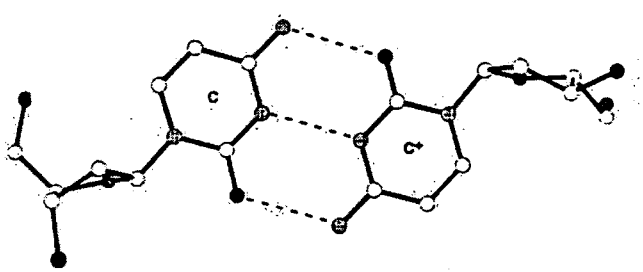

Fig.1.7 C-C^+ base-pair, of the type found within the C-rich quadruplex structures.[2]

On the other hand, the G-rich single strand of telomeres can form different quadruplexes by intramolecular folding of several consecutive repeats, by intermolecular association of four strands or by a combination of both (Fig.1.8).

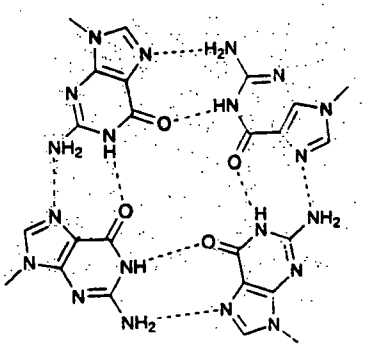

Fig.1.8 The hydrogen bonding arrangement in the guanine quadruplex.[2]

In summary, hydrophobic forces and electrostatic interactions between partial charges and between negatively charged surfaces influence the conformation of nucleic acids by altering the preferred values of roll, slide and twist on a local scale, thus affecting the outward features of DNA. These, in turn, are connected to the functions of DNA through the recognition of particular sequences by a protein or the easy unwinding of the promoter sequences that start transcription or replication.

1.1.2. Interactions with Water

The hydration of DNA[3] is essential for the maintenance of its structural integrity. There are some differences between A- and B- helical types, in terms of available surface area in the grooves, as well as between A-T and G-C base-pairs. The B-DNA major groove is dominated by the large, hydrophobic thymine methyl group, therefore water networks have not been observed. On the contrary, a 'spine of hydration' is present in the narrow minor groove in A-T regions. A-DNA shows higher hydration of G-C base-pairs compared to A-T. In A-DNA, successive phosphate groups are close enough for water molecules to be able to form bridges between them. They are more separated in the B-form, where water molecules hydrogen bond to the anionic phosphate oxygen atoms rather than to the ester oxygen

atoms. The sugar oxygen atom frequently participates in water networks, especially in A-form structures.

Studying the interaction with water is important because the extent of DNA hydration provides an indication of accessibility to ligands other than water itself.

1.1.3. Reversible Binding Modes

Nucleic acids interact reversibly not only with water and metal ions, but also with small organic molecules and proteins. Studies of non-covalent interactions with small molecules[2,3,4] have provided important information about nucleic acid binding specificity, ligand-induced conformational transitions, mode of action of antibiotics and anti-cancer drugs.

There are three primary types of reversible interaction:

- electrostatic binding: non specific, along the exterior of the helix;
- groove-binding: with the edges of base-pairs;
- intercalation: between adjacent base-pairs (Fig.1.9).

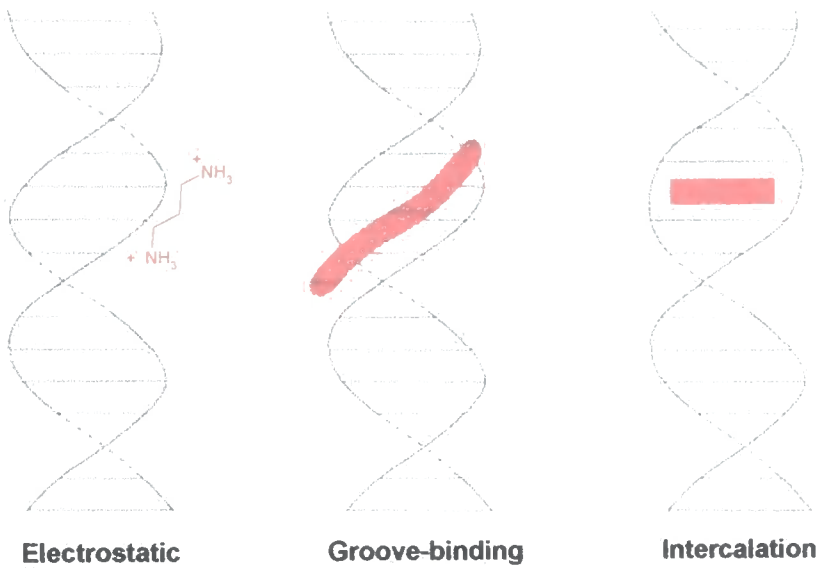

Fig.1.9 The three primary reversible binding modes.[4]

Electrostatic binding[4]

Metal ions such as Na^+ and K^+ associate with the negatively charged phosphate groups and, by reducing the effective charge on nucleic acids, strongly affect their binding interactions. Any cation can interact with nucleic acids through electrostatic binding. The observed equilibrium constant for this process strongly depends on salt concentration: it decreases with increasing Na^+ concentration. The kinetics of association and dissociation are quite rapid. Indeed, kinetic studies indicate that cations which at equilibrium bind to DNA through groove-binding or intercalation, initially associate with the duplex through electrostatic binding. They can then diffuse rapidly along the duplex backbone to their specific binding site.

Groove-binding[2,3,4]

As described above, the major and minor grooves differ significantly in electrostatic potential, hydrogen bonding characteristics, steric effects and hydration. Many proteins exhibit major groove interactions, while small molecules in general prefer the minor groove of DNA. Such molecules typically contain several small aromatic ring systems, linked with torsional freedom, to allow a twist complementary to that of the minor groove (Fig.1.10).

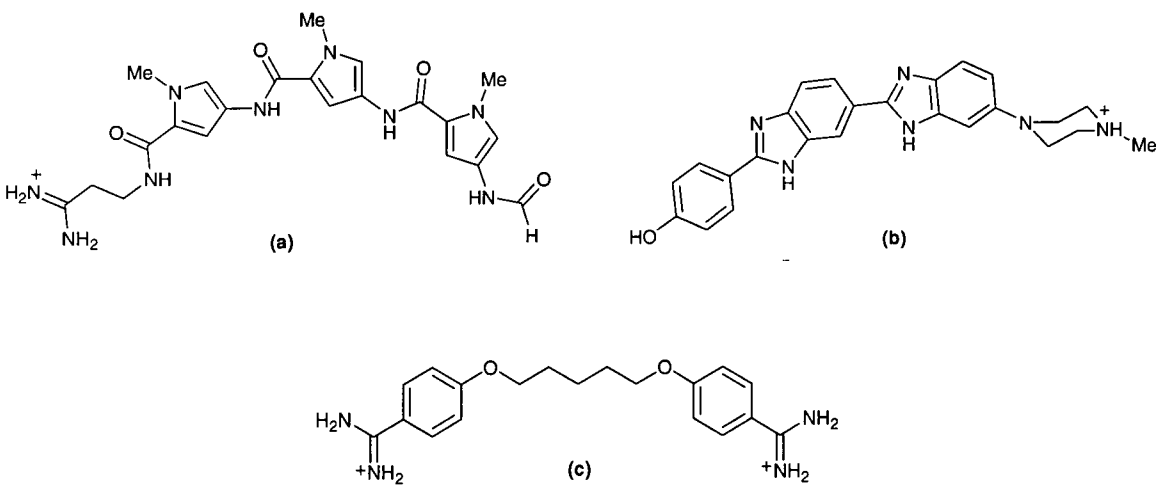

Fig.1.10 Structures of groove-binding molecules: distamycin (a), Hoechst 33258 (b) and pentamidine (c).

This binding mode is based on van der Waals and hydrogen bonding interactions. Hydrogen bonds can be accepted by A-T base-pairs, from the bound molecule to the C-2 carbonyl oxygen of T or the N-3 nitrogen of A. Although similar groups are present on G-C base-pairs, the amino group of G presents a steric block to hydrogen bond formation at N-3 of G and at the C-2 carbonyl of C. The hydrogen bond between the amino group of G and the carbonyl oxygen of C in G-C base-pairs lies in the minor groove and sterically inhibits penetration of molecules into this groove in G-C rich regions. Moreover, the negative electrostatic potential is greater in the A-T minor groove than in G-C rich regions, which provides an additional important source for A-T specific minor groove binding of cations.

Intercalation[2,3,4]

Planar aromatic molecules can insert between base-pairs, causing a lengthening of the double helix and a decrease in the helical twist at the intercalation site (unwinding). Most simple intercalators display either no binding specificity or a slight G-C preference. In fact, the intercalating moiety is typically an extended electron-deficient planar aromatic ring system and tends to interact with the more electron-rich G-C base-pair. On the other hand, groove binders display significantly greater binding selectivity, because they can contact more base-pairs as they lie along the groove and this gives them a greater recognition potential.
Simple intercalators, such as proflavine and ethidium bromide, consist solely of an intercalating group, often carrying a positive charge (Fig.1.11).

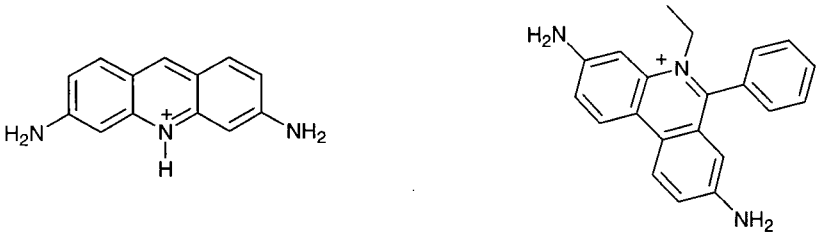

Fig.1.11 Structures of simple intercalators: proflavine (left) and ethidium (right).

They are stacked with their long axis parallel to the long axis of the adjacent base-pairs. The amino groups point toward diester oxygens of the DNA phosphate groups and provide additional electrostatic and hydrogen bonding stabilization of the complex. In the case of ethidium, the out-of-plane phenyl group limits full intercalation of the phenanthridinium ring; the phenyl and ethyl substituents lie in the minor groove of the complex.

More complex intercalators, such as the anti-cancer drugs shown in Fig.1.12, contain side-chains, sugar rings or peptide units, which reside in a DNA groove. Van der Waals interactions and hydrogen bonds with the grooves provide higher sequence specificity.

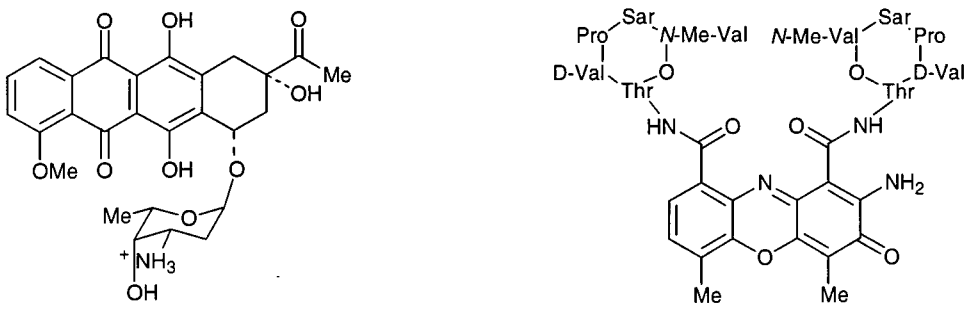

Fig.1.12 Structures of complex intercalators: daunomycin (left) and actinomycin (right).

Although simple intercalators could bind at every potential intercalation site between base-pairs, solution studies indicate that they reach saturation at a maximum of one intercalator per two base-pairs. This empirical observation has led to the **'neighbour exclusion principle'** which states that intercalators can at most bind at alternate possible base-pair sites on DNA.[5] This has been explained on the basis of the conformational changes induced by the intercalator binding at adjacent sites or as a consequence of a decrease in the equilibrium constant: When intercalators bind to DNA they neutralize some of its charge. The favourable release of condensed ions is reduced as intercalators bind to the helix and the observed equilibrium constant is also reduced.

It is important to establish **experimental criteria** that demonstrate intercalation in the absence of crystallographic data. Considering the changes occurring upon intercalation, the following experiments have been proposed:[6,7]

- Experiments that show perturbations in the DNA structure: changes in the viscosity and electrophoretic mobility of DNA caused by the lengthening and unwinding of the helix; downfield shifts in the ^{31}P NMR spectrum of the phosphodiester backbone; disruption of sequential internucleotide nuclear Overhauser enhancement (NOE) connectivities, since the intercalating ligand separates the nucleotide residues beyond the 0.5 nm proximity limits observable with NOESY experiments.
- Experiments that indicate an electronic interaction between the intercalator and DNA bases: hypochromism and a shift to longer wavelength of the transition of the intercalated chromophore are observed. Emission enhancements or quenching in those molecules that luminesce reflect changes also in the excited state electronic structure. Also applicable are ^{1}H NMR upfield shifts in the aromatic protons of the intercalated molecule, which result from ring currents from the stacked aromatic bases.
- Experiments that demonstrate molecular orientation and rigidity of the intercalator: dichroic techniques evaluate the bound orientation of the intercalator relative to the oriented helical axis. Luminescence polarization experiments establish the time over which the molecule is rigidly bound within the helix.

1.2. Luminescence Properties of Lanthanide Complexes

1.2.1. Lanthanide Luminescence[8]

The trivalent lanthanide ions and their complexes are known to luminesce, giving rise to narrow bands corresponding to transitions within f orbitals. Since the 4f orbitals are shielded from the environment by an outer shell of 5s and 5p orbitals, they are only minimally involved in bonding. Due to this small interaction between ligand and f orbitals, ligand-field splittings are very small, thus emission bands do not broaden and shift upon complexation.

Samarium, europium, terbium, dysprosium and ytterbium exhibit strong luminescence, owing to the large energy gap between the lowest excited state and the

highest ground state levels, which makes the competing radiationless decay less likely to occur. Eu^{3+} and Tb^{3+} emit in the visible region of the spectrum upon excitation at 580 and 485 nm respectively (Fig.1.13).

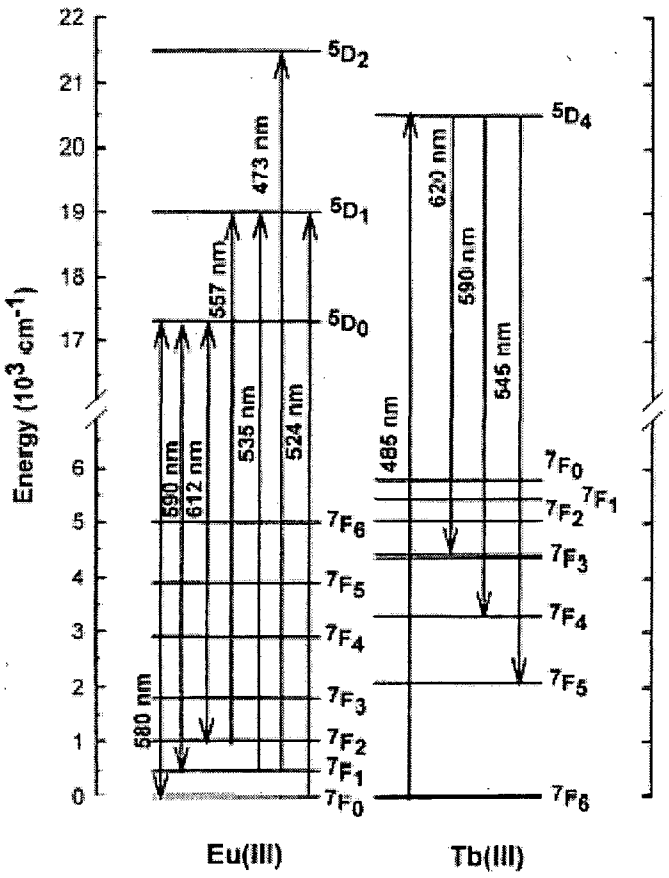

Fig.1.13 Energy levels for Eu(III) and Tb(III) showing their excitation wavelengths and their most intense emissive transitions.[8]

For **Eu(III)** complexes, the strongest emissions generally arise from $^5D_0 \rightarrow {}^7F_{1,2}$ transitions at 590 and 612 nm respectively. The $^5D_0 \rightarrow {}^7F_1$ ($\Delta J = 1$) transition is magnetic dipole in character and largely independent on the coordination sphere, whereas the electric dipole $^5D_0 \rightarrow {}^7F_2$ ($\Delta J = 2$) transition is extremely sensitive to the nature and symmetry of the coordination sphere, its intensity being enhanced by distortion of the symmetry around the ion. The number of bands in the $\Delta J = 2$ manifold is determined by the site symmetry: two bands are observed for C_4-

symmetric complexes, whereas less symmetric complexes display at least three bands. The $^5D_0 \rightarrow {}^7F_4$ transition is also relatively intense and sensitive to the ligand field, being predominantly electric dipole in character. The remaining $^5D_0 \rightarrow {}^7F_j$ transitions are generally weak. The $^5D_0 \rightarrow {}^7F_0$ transition, at 580 nm, is weak but sensitive to the ligand environment and is used as a probe of Eu^{3+} coordination homogeneity. In fact, since the $^5D_0$ and $^7F_0$ states are non-degenerate, the number of absorption or emission bands observed is related to the number of chemically distinct environments of the ion.

In the case of **Tb(III)**, all emissions arise from the $^5D_4$ level. The $^5D_4 \rightarrow {}^7F_5$ ($\Delta J = 1$) emission band, at 545 nm, is the most intense and is hypersensitive, but not as sensitive to the ion environment as the $^5D_0 \rightarrow {}^7F_2$ transition of Eu^{3+}. The analysis of the fine structure of the spectrum does not provide much information about the local symmetry of the metal ion, because emission bands normally consist of a large number of transitions, which can rarely be fully resolved. In fact, the J values of the levels involved in the transitions are high, resulting in splitting of the J levels into many sublevels.

1.2.2. Sensitised Emission

As mentioned before, the interaction of the ligand with f orbitals is very weak, therefore its contribution to the 4f wavefunction is so small that transitions among f orbitals remain forbidden by the parity (Laporte) selection rule also upon complexation. This explains the low molar absorption coefficients observed for Ln(III) ions ($\varepsilon < 1\ M^{-1}cm^{-1}$). The lanthanide absorbance bands are thus very weak and the excited states are not readily populated by conventional light sources. Sensitised emission[9] provides a solution to this problem: the lanthanide is indirectly excited by energy transfer from a neighbouring chromophore, which can be incorporated into the ligand. The so-called 'antenna' must absorb strongly at a suitable wavelength and transfer its excitation energy to the metal, which becomes excited to the emissive state (Fig.1.14).

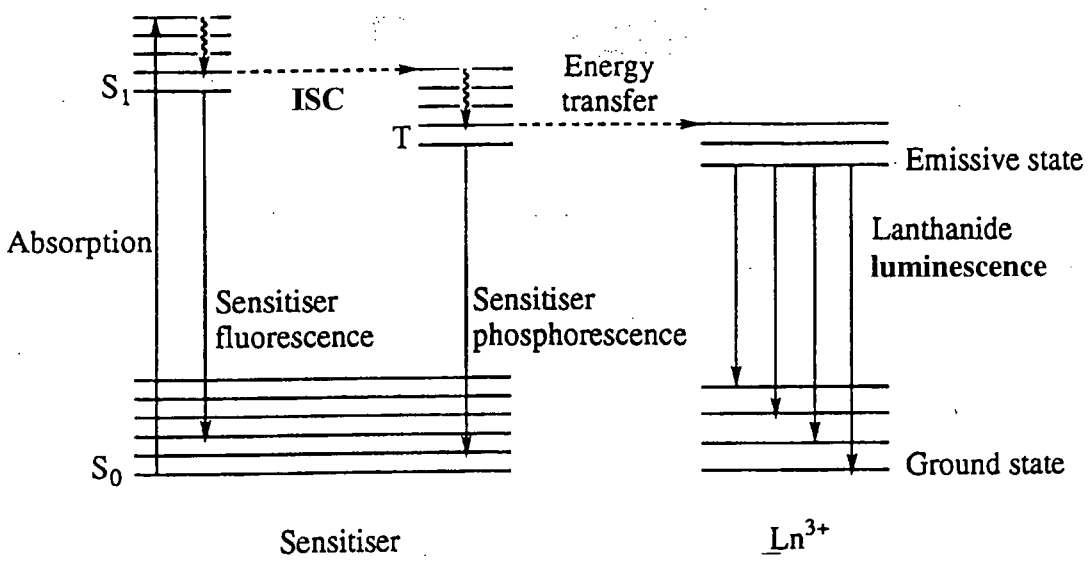

Fig.1.14 Jablonski diagram for sensitised emission.

If the antenna has a high absorption coefficient (typically > 10^4 $M^{-1}cm^{-1}$) and the energy transfer process is efficient, then intense luminescence may result upon excitation by conventional light sources.[10]

The efficiency of the energy transfer process depends on the extent of overlap of the emission spectrum of the antenna with the absorption spectrum of the lanthanide ion. In other words, the energies of the triplet state of the sensitiser and the emissive state of the lanthanide ($^5D_0$ Eu = 17,240 cm^{-1}, $^5D_4$ Tb = 20,400 cm^{-1}) must be close, with the former being slightly higher (at least 1700 cm^{-1}), to ensure that the process is exothermic. If the energy gap is too small (< 1500 cm^{-1}), however, thermally activated back energy transfer can occur, resulting in a reduction of the emission intensity and lifetime. Back energy transfer is more likely to be a problem for terbium, whose emissive state is quite high in energy. In the case of europium, a photoinduced electron transfer from the chromophore to the metal can occur, owing to the ease of reduction of Eu^{3+} to Eu^{2+}. This process often deactivates the singlet excited state of the antenna in a non-radiative way, thus reducing its efficiency as a sensitiser.

1.2.3. Deactivation of the Lanthanide Excited State

The intensity and lifetime of the emission can also be reduced by deactivation of the metal emissive state, without the intermediacy of the antenna.[9] Energy transfer can occur from the metal excited state to the O-H stretching vibrations of coordinated or closely diffusing water molecules and to N-H amide bonds in the ligand. Both O-H and N-H bonds, in fact, have high vibrational stretching frequencies (> 3000 cm^{-1}), close to the energy levels of the lanthanide emissive states. This process becomes less probable as the energy gap between the emissive and the next lower level increases, therefore Eu^{3+} (ΔE = 12,300 cm^{-1}) is more affected than Tb^{3+} (ΔE = 14,700 cm^{-1}).

The luminescence of Eu^{3+} and Tb^{3+} complexes is more intense in D_2O than in H_2O because energy transfer to O-D oscillators is slower than to O-H, due to the lower vibrational frequency of the O-D vibration. The difference in measured rate constants for depopulation of the lanthanide excited state in H_2O and D_2O is proportional to the quenching effect of exchangeable XH oscillators (OH and NH). As the energy transfer process is distance dependent, OH oscillators of coordinated water molecules give the biggest quenching effect. It is possible, therefore, to calculate the number of water molecules bound to the complex (q) with the following equations:

$$q_{Eu} = 1.2\ (k_{H2O} - k_{D2O} - 0.25)$$

$$q_{Tb} = 5\ (k_{H2O} - k_{D2O} - 0.06)$$

These revised equations[11] include a term accounting for closely diffusing water molecules. For Eu complexes, an additional subtraction of 0.075 ms^{-1} should be made, per coordinated amide NH group.

1.3. Designing Probes for Nucleic Acids

A better knowledge of nucleic acid structure, site-specific recognition and interactions is the first step in the development of new nucleic acid interactive drugs. In fact, once specific interactions between a molecule and a DNA sequence can be

predicted on the basis of their three-dimensional geometries and binding abilities, the design of drugs acting as gene regulators will follow.

The search for chemical rather than enzymatic probes for the study of nucleic acid structures is dictated by their higher stability in a wider range of conditions of pH, ionic strength and temperature.

1.3.1. Spectroscopic and Reactive Probes

Transition metal complexes can be particularly useful probes,[12,6] owing to the spectroscopic sensitivity of intense metal-to-ligand charge transfer (MLCT) bands to the local DNA environment. Together with electrostatic association with nucleic acids, they offer well-defined geometries that can be useful in designing reagents to match specific local DNA conformations.

Octahedral metallointercalators[13] have attracted particular interest as spectroscopic and reactive probes for DNA. The insertion of aromatic heterocyclic ligands, such as 9,10-phenanthrenequinone diimine (phi) or dipyrido [3,2-a:2',3'-c] phenazine (dppz) (Fig.1.15), between the base-pairs results in high binding affinities and well-defined orientation of all the functionalities on the metal complex with respect to the DNA duplex. Phenanthroline (phen) and bipyridyl (bpy) are among the most widely used ancillary ligands (Fig.1.15).

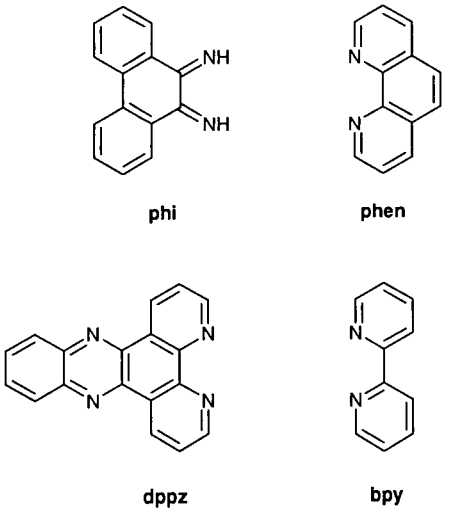

Fig.1.15 Intercalating (left) and ancillary (right) ligands used in transition metal probes.

Complexes containing the phi ligand are well-known major groove intercalators.[13] Although an intercalative binding mode was also proved for dppz complexes, it is still not clear from which groove it occurs.[14,15,16]

Ruthenium, rhenium and osmium complexes containing the dppz ligand represent valuable photophysical probes of nucleic acids, because they can act as **'molecular light switches'** (Fig.1.16).[17,18]

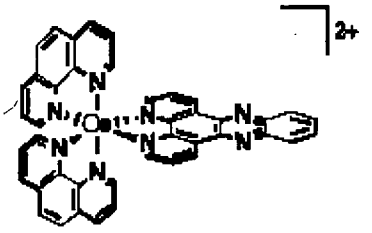

Fig.1.16 $[Os(phen)_2(dppz)]^{2+}$: a molecular light switch.[13]

Luminescence is observed only upon addition of DNA to an aqueous solution of these complexes, reflecting the shielding of the intercalating ligand from the solvent, provided by the interaction with the nucleic acid. The excited state of the complex cannot be deactivated anymore by hydrogen bonding of water molecules to the nitrogens of the pyrazine ring.

Among the reactive probes, particularly interesting are the **photocleavers**, whose reactivity is activated by light.[19] They offer several advantages: chemical reagents need not be added to the system and in vivo application can be envisaged, because the timing of the reaction can be controlled. Selective excitation of the photocleavage agent can be achieved if it contains a chromophore absorbing at wavelengths longer than 330 nm, where nucleic acids and most proteins are transparent. This limits the number of side reactions in the system and facilitates the analysis of the reaction mechanism.

Photocleavage of nucleic acids typically involves an initial oxidative reaction with either a sugar residue or a nucleobase. The photocleaver, in its excited state, may generate a reactive intermediate, i.e. a radical, which initiates nucleic acid cleavage. Observation of spontaneous cleavage is strong evidence that a hydrogen atom

abstraction from the sugar residues has occurred. On the contrary, attack at the nucleobase does not cause an immediate strand break, which occurs only after incubation with hot piperidine or aniline.

Non-specific DNA cleaving agents, targeting the backbone sugars, are useful to visualize the site-specific binding of proteins to DNA through footprinting.[12] The presence of a protein bound to DNA blocks the normal cleavage by the reagent and the binding site appears as a blank spot (or 'footprint') when the end-labelled products of the reaction are denaturated and electrophoresed. Rhodium complexes containing the phi ligand are examples of footprinting reagents that undergo photoactivation. The radical produced upon irradiation on the intercalated phi ligand via an intra-ligand charge transfer[20] is not diffusible, so the footprints are precise to single nucleotide resolution.

Although deoxyribose oxidation in itself is non-selective, phi complexes have been synthesised which exhibit different sequence selectivities, depending on the ancillary ligands. Bulky ligands such as phenanthroline impart selectivity, because full intercalation is possible only at sites with high propeller twisting toward the major groove (Fig.1.17).[21]

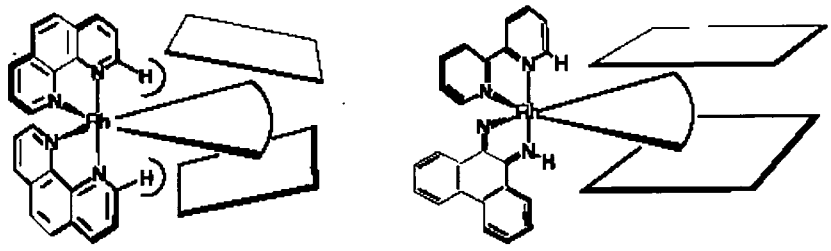

Fig.1.17 Steric interactions of $[Rh(phen)_2(phi)]^{3+}$ with a propeller-twisted intercalation site (left) and of $[Rh(phi)_2(bpy)]^{3+}$ with an ordinary intercalation site (right).[13]

Alternatively, the non-intercalated ligands can form hydrogen bonding[22] and/or van der Waals interactions[23] with the DNA bases in the major groove, thus achieving some binding and cleavage selectivity (Fig.1.18).

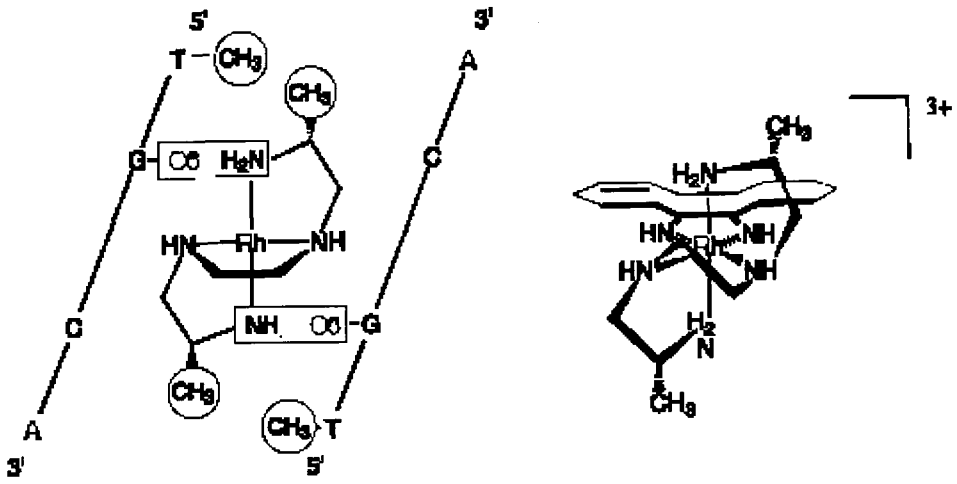

Fig.1.18 Interaction of Δ-α-[Rh[(R,R)Me_2trien](phi)]$^{3+}$ with the 5'-TGCA-3' intercalation site: van der Waals interactions between thymine and ligand methyl groups and hydrogen bonding between axial amines of the ligands and O6 of guanines are highlighted.[13]

Reaction with the nucleobases of DNA can occur in three different ways: direct electron transfer from the base to the excited-state photocleaver; triplet energy transfer from the excited state photocleaver to O_2, producing singlet oxygen, which then reacts with the base; formation of an adduct with the base. In the first two mechanisms, cleavage occurs almost exclusively at guanine, being the most easily oxidised base[24] as well as the most reactive toward singlet oxygen. Oxidation of guanine by electron transfer has been reported for Ru(II) complexes with strongly oxidizing ligands such as hat or tap (Fig.1.19).[25] On the other hand, Ru(II) dppz complexes in their excited state are sensitisers of singlet oxygen.[26]

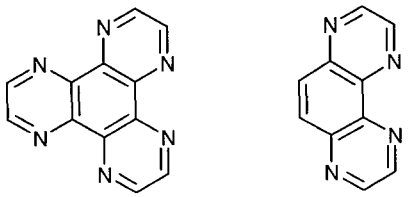

Fig.1.19 Hat and tap ligands.

A photocleaver that ruptures nucleic acids by a hydrolytic mechanism would be advantageous for structure determination. Indeed, if it can recognise certain

conformations, such as cruciforms, single stranded regions or left-handed helices, their exact location would be determined more easily than with oxidative agents, which often produce diffusible radical species. Moreover, the cleavage products could be re-linked and used for the synthesis of recombinant DNA.

Due to the repulsion between the negatively charged backbone and potential nucleophiles, the phosphodiester bonds in DNA are not easily hydrolysed. The half-life for **hydrolysis** at neutral pH and 25°C has been estimated to be 130,000 years.[27]

Copper, zinc and lanthanide ions have been used in synthetic nucleases[28] because, being strong Lewis acids, they can activate the phosphodiester bonds towards nucleophilic attack via charge neutralisation and they can significantly lower the pK_a of a coordinated water, thereby providing a metal-bound hydroxide nucleophile at near neutral pH.

Although hydrated Ln(III) ions have been shown to be effective DNA cleavers, the free ions tend to precipitate as the hydroxides around pH 9 and are toxic to biological systems because of their similarity to Ca(II). Hence, they have to be included into complexes possessing high kinetic and thermodynamic stability as well as open coordination sites for solvent and substrate. Both linear and macrocyclic ligands have been used[29] for mono and dinuclear Ln(III) complexes, the latter being generally more effective in promoting RNA and DNA hydrolysis.

The Ce(IV) ion is the most active for DNA hydrolysis[30,31] because it can accept electrons from the phosphate residues. For the other lanthanides, the tetravalent state is not easily accessible and reduction of Ln(III) ions is difficult, due to the instability of the Ln(II) species. Recently, a dicerium complex has been reported, capable of double-strand DNA hydrolysis at 37°C (Fig.1.20).[32] By targeting the 3'-O-P bond of the phosphodiester linkage regioselectively, it mimics restriction enzymes.

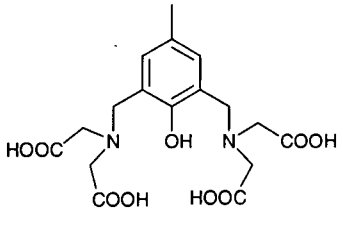

Fig.1.20 HXTA ligand used in Ce_2(HXTA), a synthetic nuclease.

To develop a synthetic nuclease with the desired sequence specificity, a recognition element, such as an oligonucleotide or a short peptide, can be covalently attached to the ligand. This methodology, called 'antisense approach', has been widely used to exploit the recognition potential of a single-strand DNA target sequence by a complementary oligonucleotide[33,34] or of a duplex DNA by a protein.[35,36]

1.3.2. Lanthanide Probes

The chiral lanthanide complexes discussed in chapter 2 and 3 (Fig.1.21) have been proposed as luminescent probes for DNA structural recognition.

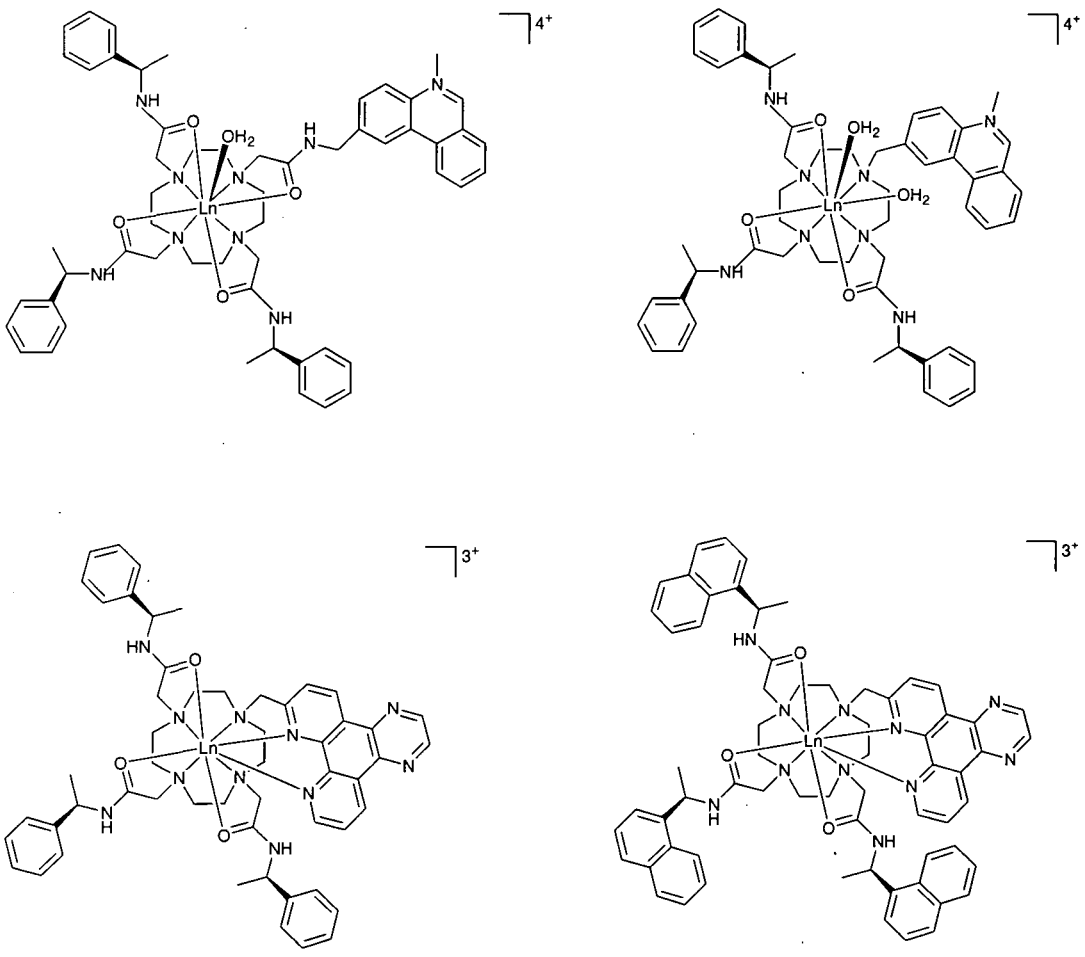

Fig.1.21 Structures of the lanthanide complexes under investigation.

In the design of these complexes the following features have been evaluated, regarding:

a. The metal

Lanthanide ions have been chosen because they possess long luminescence lifetimes (ms). This allows a time-resolved detection procedure to be employed, in order to minimise the interference of background luminescence in biological media.[9] A delay is set between the excitation pulse and the measurement of the lanthanide luminescence, during which time the short-lived (ns to μs) background fluorescence and scattered light decay to negligible levels.

b. The ligand

Ligands based on the 1,4,7,10-tetraazacyclododecane (cyclen) have been used to obtain complexes with high kinetic and thermodynamic stability with respect to metal ion dissociation. They also provide a good shielding of the lanthanide ion from the solvent water molecules which quench its excited state, especially when all the coordination sites are saturated by the ligand.

The **chirality** of these complexes is designed to achieve chiral discrimination through the formation of diastereomeric adducts with the nucleic acid. In order to be useful as a chiral probe, a single enantiomer of the complex is desirable that is conformationally rigid on the time scale of metal-based emission lifetime.

In lanthanide complexes of DOTA (1,4,7,10-tetraazacyclododecane-N,N',N'',N'''-tetraacetic acid), two elements of chirality need to be defined: the conformation of the macrocyclic ring (λ or δ), associated with the N-C-C-N torsion angle (Fig.1.22a), and the orientation of the acetate arms (Λ or Δ), associated with the N-C-C-O torsion angle (Fig.1.22b).[37]

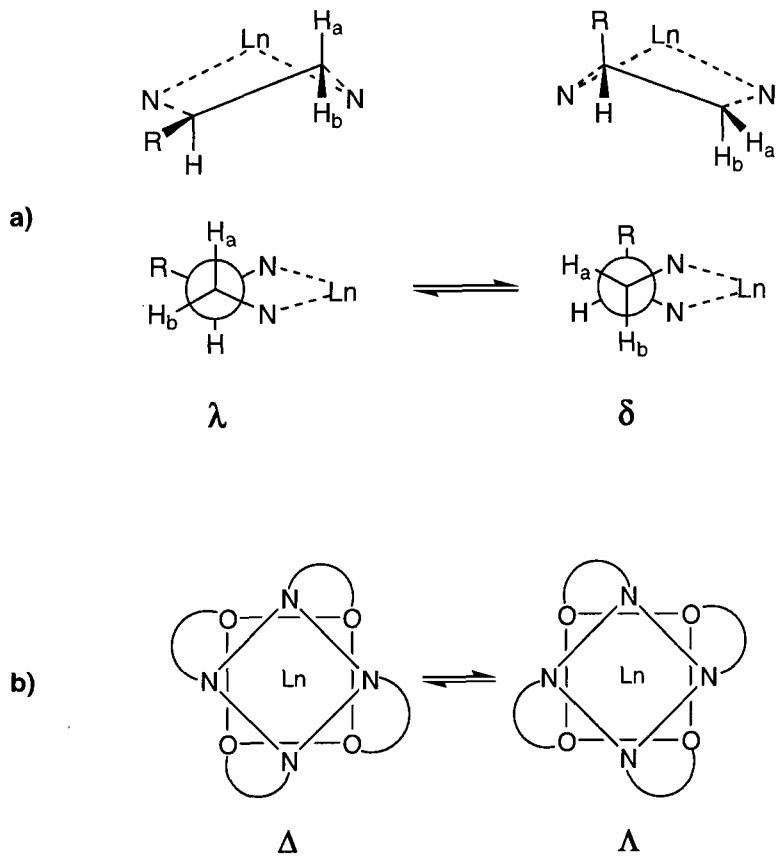

Fig.1.22 Possible conformations of the ring (a) and orientations of the arms (b).

Four stereoisomers result, related as two pairs of enantiomers, which may interconvert in solution via ring inversion (λλλλ ↔ δδδδ) or independent arm rotation (Λ ↔ Δ) (Fig.1.23). An angle of ca 40° between the planes of the nitrogen (N_4 plane) and oxygen (O_4 plane) donors is associated with a square antiprismatic geometry (Λ(δδδδ) and Δ(λλλλ)), while a value of ca -30° defines a twisted square antiprismatic structure (Δ(δδδδ) and Λ(λλλλ)). Ring inversion or arm rotation alone result in exchange between these two geometries, while the combination of both processes results in exchange between the enantiomeric pairs.

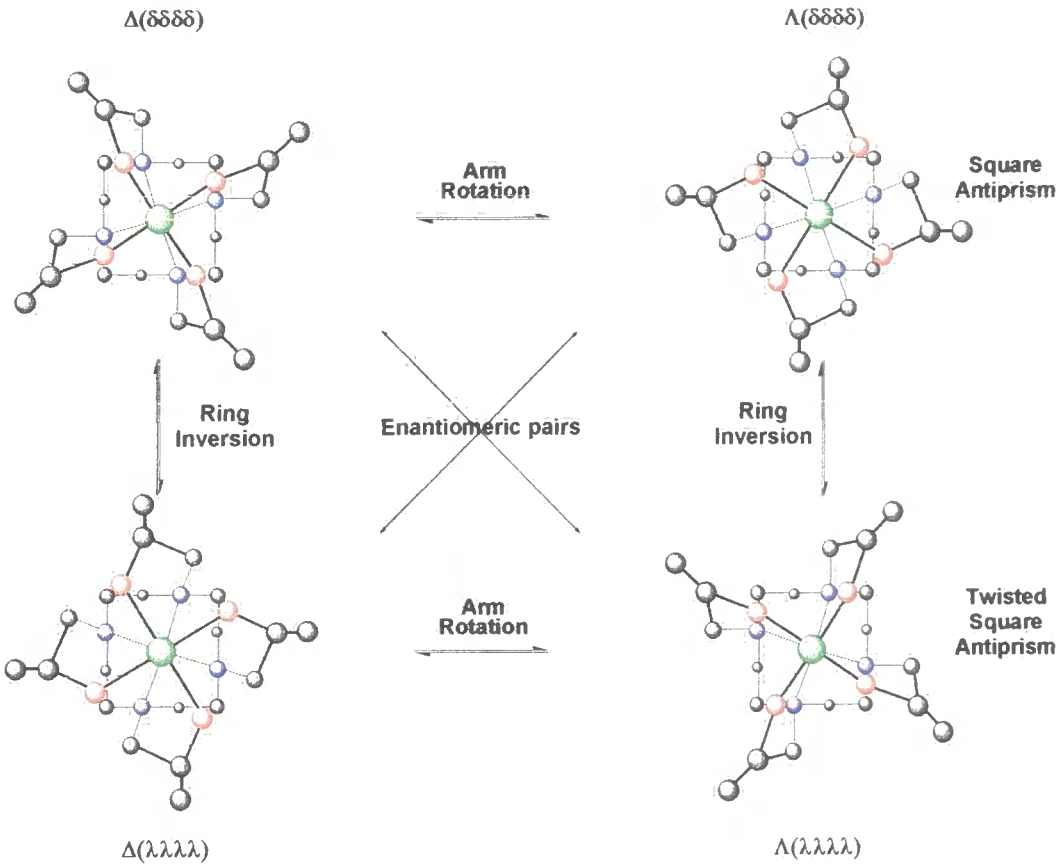

Fig.1.23 Stereoisomers of Ln(DOTA)$^-$ complexes.

The introduction of a chiral centre δ to the ring N in tetraamide Ln(III) complexes imparts conformational rigidity.[38] Arm rotation is inhibited, and ring inversion is slow (50 s^{-1} at 298 K), thus one isomer may be preferred in solution. The configuration of the stereocentre determines the helicity of the complex and the configuration of the macrocyclic ring, with the R and S isomers producing the Λ(δδδδ) and Δ(λλλλ) configurations respectively, in a regular square antiprismatic geometry.

Crystal structures of the chiral tetraamide complex $LnPh_4$[38] (Fig.1.24) show that the twelve-membered ring adopts a square antiprismatic geometry, with a 37° twist between the N_4 and O_4 planes.

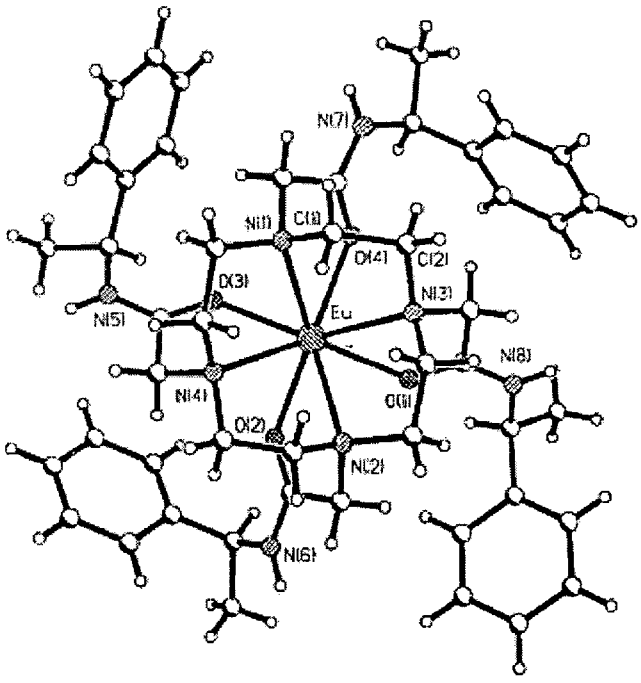

Fig.1.24 View up the z-axis (containing the Ln-OH_2 bond) of the 'parent' $EuPh_4$ complex with an S configuration at the chiral centres.

c. The chromophore

The chromophore has been chosen not only on the basis of its photophysical properties, but also for its structural analogy with well-known nucleic acid interactive molecules.

Besides being a good **sensitiser** for the lanthanide luminescence, it should absorb above 340 nm to avoid co-absorption by other molecules present in biological samples, DNA above all. Both the phenanthridinium and the dipyrido[3,2-f:2',3'-h]quinoxaline (dpq) chromophores can be excited at $\lambda > 330$ nm and are effective antennae for europium.[39]

The former does not efficiently transfer its excitation energy to terbium, because its triplet state is only 800 cm^{-1} higher in energy than the metal emissive state, so that back energy transfer competes.[40] On the contrary, 2:1 complexes of dpq with both Eu^{3+} and Tb^{3+} show very high luminescence quantum yields, due to efficient intersystem crossing, an essentially irreversible energy transfer step, and a high ratio

between radiative and non-radiative decay rates of the lanthanide ion.[41] The dpq group in our complexes is meant to directly coordinate the lanthanide to ensure fast energy transfer through a short distance between sensitiser and metal ion.

Both chromophores are reminiscent of well-known intercalators: ethidium in the case of phenanthridinium and dppz[17] in the case of dpq. The dpq ligand itself, contained in different ruthenium complexes,[42,43,44,45,26] is believed to intercalate DNA from the minor groove. Although a large surface area of the intercalative moiety provides greater stabilization, dpq has been preferred to dppz because the latter is not able to sensitise Eu^{3+} and Tb^{3+} luminescence.[41]

Intercalation has been chosen as the binding mode because it defines the positions in space of all portions of the rigid metal complex relative to the helix axis. Through this well-defined system, specific contacts between the non-intercalated parts of the complex and the base-pairs may be designed. By including a naphthyl instead of a phenyl group in the chiral arms (Fig.1.25), the possibility of an increased hydrophobic interaction with the grooves was investigated.

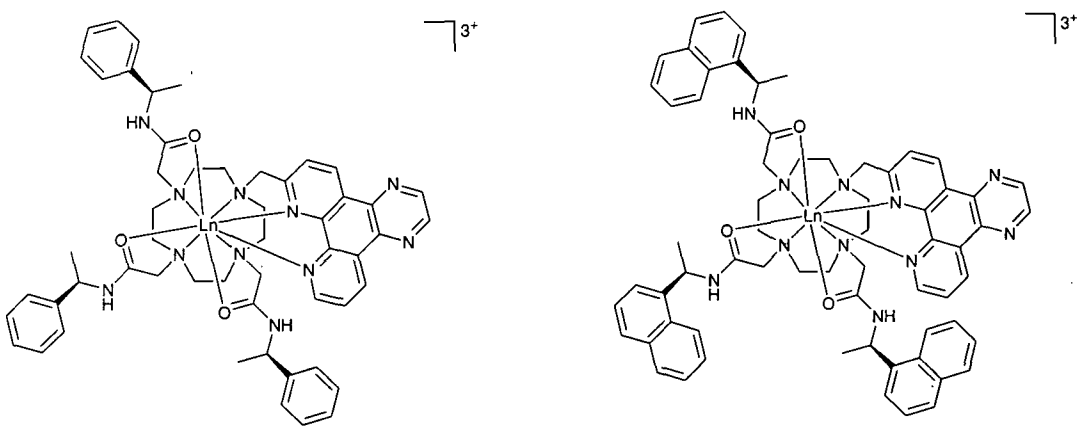

Fig.1.25 Phenyl and naphthyl complexes containing the dpq chromophore.

Each of the complexes has a large positive charge, due to functionalisation of the cyclen with amide groups, which favours a strong Coulombic interaction with the DNA polyanion.

d. Reactive Probes

With the aim of developing reactive probes for nucleic acids, the **terbium** complexes of these ligands were synthesised. As demonstrated for the complexes containing a phenanthridinium chromophore,[40] the triplet state of the antenna could undergo oxygen quenching, giving rise to formation of singlet oxygen. This process is particularly efficient in Tb^{3+} complexes, where the sensitising aryl triplet state can be repopulated by back energy transfer.

Electron transfer from guanine has been demonstrated for ruthenium intercalators containing dppz and dpq ligands.[26] Oxidative damage is due to the Ru(III) species, generated in situ through a flash/quench method[46] by quenching of the photoexcited intercalated Ru(II) complex by a non-intercalated electron acceptor.

Although this technique provides powerful ground state oxidants, even more useful would be the production of excited state oxidants upon photoactivation. Direct guanine oxidation from the Ru(II) excited state would be possible for the dppz complexes on the basis of their excited state reduction potentials,[26] but it has not been observed. Damage at guanines occurs, instead, via production of singlet oxygen.

Among the dppz complexes, $[Cr(phen)_2(dppz)]^{3+}$ proved a particularly strong photooxidant, capable of both guanine and adenine oxidation.[47] Its emission quenching in the presence of DNA has been associated with the direct oxidation of the nucleobases. The same behaviour has been reported for $Ru(hat)_3^{2+}$ and $Ru(tap)_3^{2+}$, which are particularly oxidizing in their MLCT excited state,[25,48] although each is a relatively poor DNA binder.

Derivatisation of the dppz ligand can be employed to tune the reduction potential of these complexes, in order to increase their oxidizing power.[49] Two recent examples are $[Ru(phen)_2(dicnq)]^{2+}$ and $[Ru(phen)_2(qdppz)]^{2+}$ (Fig.1.26), which show DNA photocleavage in their MLCT excited state, although the mechanism of this activity has not been clarified.[50]

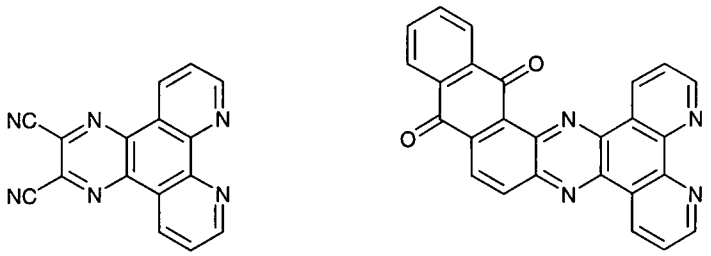

dicnq qdppz

Fig.1.26 Dicnq and qdppz ligands.

DNA damage could be achieved also by exploiting the redox properties of **cerium**. The Ce(III) complexes discussed in chapter 4 (Fig. 1.27) have been designed to investigate the possibility of oxidative damage.

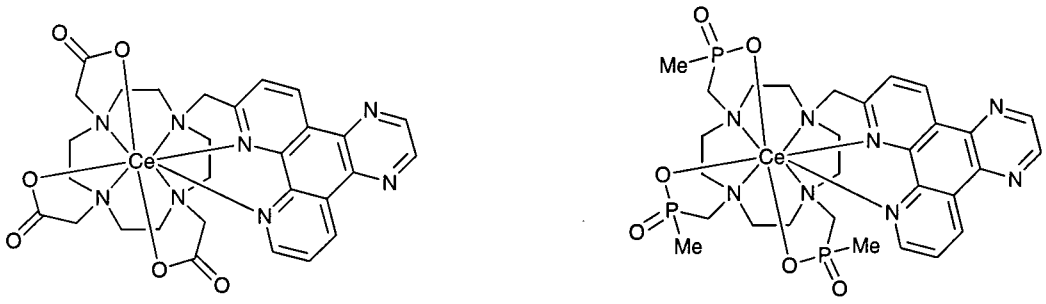

Fig.1.27 Structures of the cerium complexes under investigation.

Cerium is the only lanthanide with a stable tetrapositive state, therefore we considered whether in its complexes with ligands containing the electron deficient dpq moiety, an MLCT transition may be present. Only recently, the first example of a Ce(III) complex with an MLCT excited state has been reported.[51] If an MLCT state is formed, it might act as a photooxidant upon irradiation.

Ce(III) complexes could also generate ground state oxidants through formation of Ce(IV) species by chemical or electrochemical oxidation. Previous work[52] on the

$Ce(III)Ph_4$ complex showed the unsuitability of this ligand: the amide group was preferentially oxidised instead of the Ce(III) ion. Acetate and phosphinate arms were therefore considered instead, giving rise to neutral Ce(III) complexes. The dpq group is here meant to increase the binding affinity to DNA via intercalation, in order to achieve an efficient oxidative process.

1.4. Techniques

Several techniques have been used to measure the changes in the physical properties of nucleic acid interactive molecules upon binding. We have focused on photophysical parameters and employed different spectroscopic methods: absorption and emission spectroscopies, circular dichroism, circularly polarised luminescence and fluorescence anisotropy.

1.4.1. Circular Dichroism

Circular dichroism spectroscopy is one of the most commonly used techniques to study the conformations of nucleic acids in solution.[53,54] It measures the difference in absorption of left and right circularly polarised light as a result of chirality. Being achiral, the nucleic bases themselves are intrinsically optically inactive, but the linkage to the chiral sugar in a nucleotide results in a CD induced into their $\pi \rightarrow \pi^*$ transitions. The CD spectrum of a polynucleotide, however, is dominated by the CD induced into the transitions of the bases from their coupling with each other, rather than by the CD induced from the coupling with the backbone transitions.

CD spectra can probe DNA conformational changes due to different conditions of humidity, ionic strength, temperature as well as interactions with small molecules.[54,55] In the latter case, the interaction may be monitored by observing either the CD of the nucleic acid or a CD induced into the molecule upon binding to DNA (ICD). It is possible to distinguish between intercalative and groove binding on the basis of the magnitude of the ICD, the former being about 1/20 that of the latter ($< 10\ \Delta\varepsilon/M^{-1}cm^{-1}$). However, the correlation between the intensity and sign of ICD

and the orientation of the molecule in its binding site has been only partially explained.[56,57]

If the CD intensity changes as a function of ligand:DNA ratio, but the shape of the spectrum remains the same, it can be deduced that the ligand binding mode is unchanged. If the ligand binds in a single binding mode, binding constants and site sizes can be determined. If, however, there is a change in the shape of the spectrum, this can be due to a change in the occupancy of more than one binding site as the ligand:DNA ratio increases, to changes in the DNA conformation or to ligand-ligand interactions.

Unfortunately, CD spectra are often difficult to interpret, therefore quantitative data analysis and detailed structural information about macromolecules cannot be easily obtained.

1.4.2. Circularly Polarised Luminescence

Circularly polarised luminescence is the emission analogue of circular dichroism.[58] It measures the difference in emission of left and right circularly polarised light by a chiral molecule. While CD probes the geometry of molecules in the ground state, CPL probes that of the excited state. CPL is particularly valuable to investigate transitions that cannot easily be studied in absorption, such as the f-f electronic transitions of the lanthanide complexes.

CPL studies on chiral lanthanide complexes showed that the local helicity at the metal centre determines the rotatory strength associated with a transition.[59] A change in the shape and intensity of the CPL spectra may therefore occur if the interaction with DNA changes the degree of helicity about the lanthanide.

1.4.3. Fluorescence Anisotropy

Steady-state measurements of fluorescence anisotropy[60] provide useful indications on the rigidity of the orientation of a molecule with respect to the DNA helix. The molecule bound to DNA is excited with polarised light and, if on the time scale of

the emission it is rigidly held on the helix, polarisation is retained in the emitted light.

Polarised emission depends on the existence of transition moments for absorption and emission which lie along specific directions within the fluorophore structure. In homogeneous solution, the ground state fluorophores are all randomly oriented. When exposed to polarised light, however, those having their absorption transition moments oriented along the electric vector of the incident light are preferentially excited. Depolarisation of the emission is primarily caused by rotational diffusion of fluorophores. The anisotropy measurements reveal the average angular displacement of the fluorophore that occurs between absorption and subsequent emission of a photon. This displacement is dependent on the rate and extent of rotational diffusion during the lifetime of the excited state. For small fluorophores in solutions of low viscosity, the rate of rotational diffusion is typically faster than the rate of emission, therefore the emission is depolarised and the anisotropy is close to zero. On the contrary, if the fluorophore is associated with a macromolecule, its rotational motion decreases and its emission retains the polarisation.

This technique has often been used to demonstrate intercalation;[61,62,63] no retention of polarisation is observed for surface-bound molecules. It has also been proposed as a measure of chiral selectivity.[64] Non-enantiomeric factors such as intrinsic anisotropy or fluorescence lifetime are identical for two enantiomers, therefore a difference in their anisotropies, upon interaction with a chiral selector, is related to a difference in the strength of the interaction.

The anisotropy is calculated as:

$$r = \frac{I_{//} - I_{\perp}}{I_{//} + 2I_{\perp}}$$

where $I_{//}$ is the intensity observed when the emission polariser is oriented parallel to the direction of the polarised excitation and $I_{\perp}$ is the intensity observed when the polariser is perpendicular to the excitation. As shown in Fig.1.28, the sample is excited with vertically polarised light, whose electric vector is oriented parallel to the z-axis.

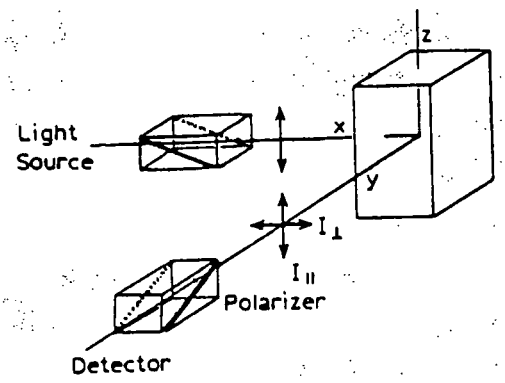

Fig.1.28 Schematic diagram for measurement of fluorescence anisotropies.[60]

In practice, however, the emission is observed through a monochromator, which usually has a different transmission efficiency for vertically and horizontally polarised light. Consequently, rotation of the emission polariser changes the measured intensities even if the sample emits unpolarised light. To measure the actual intensities $I_{//}$ and $I_\perp$, a G factor, which is the ratio of the sensitivities of the detection system for vertically and horizontally polarised light, must be determined. This G factor is measured using horizontally polarised excitation, so that both polariser orientations are perpendicular to the polarisation of the excitation. Both the horizontally and vertically polarised components are thus equal and proportional to $I_\perp$. Any measured difference in I_{HV} (corresponding to horizontally polarised excitation and vertically polarised emission) and I_{HH} (both excitation and emission are horizontally polarised) must be due to the properties of the detection system (Fig.1.29).

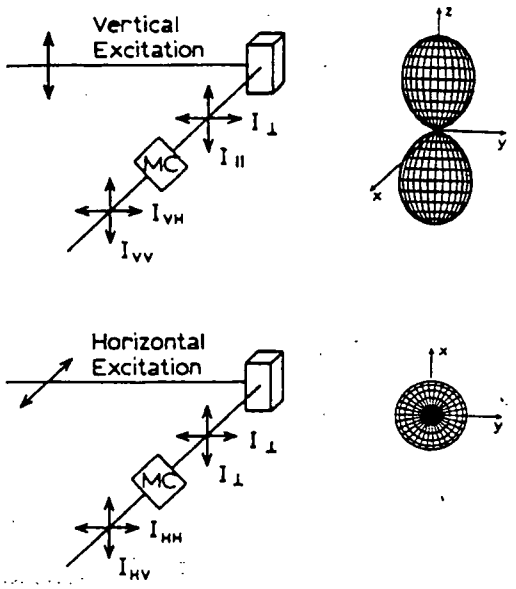

Fig.1.29 Schematic diagram for L-format measurements (MC: monochromator). The shapes at the right are the excited-state distributions.[60]

Since $G = \frac{I_{HV}}{I_{HH}}$, the anisotropy can be expressed as:

$$R = \frac{I_{VV} - GI_{VH}}{I_{VV} + 2GI_{VH}}$$

In practice, only four measurements are required: I_{VV}, I_{VH}, I_{HV} and I_{HH}.

1.4.4. Equilibrium Dialysis

In order to evaluate the binding affinity of a ligand to a nucleic acid and the stereoselectivity of the binding, equilibrium dialysis experiments[65] may be performed.

The two compartments of the dialysis cell must be separated by a membrane that permits the diffusion of the ligand only, but not of the nucleic acid. The buffered solution containing the ligand is introduced in one chamber, the DNA solution in the other chamber. At equilibrium (after 24-48 hours) both compartments will contain

the same free ligand concentration. The difference in absorption between samples from the two compartments thus provides the bound ligand concentration and the binding constant can be calculated.

If a DNA solution is dialysed against a racemic mixture of chiral ligands, the preferential binding of one enantiomer to the nucleic acid can be demonstrated.[66,67] In fact, after equilibration, the CD spectrum of the dialysate will show an optical enrichment of the unbound enantiomer.

References

1 C. R. Calladine and H. R. Drew, 'Understanding DNA', Academic Press, San Diego, 1997.

2 S. Neidle and C. M. Nunn, *Natural Product Reports*, 1998, **15**, 1.

3 S. Neidle, 'DNA Structure and Recognition', Oxford University Press, 1994.

4 'Nucleic Acids in Chemistry and Biology', edited by G. M. Blackburn and M. J. Gait, Oxford University Press, 1996.

5 J. D. Mc Ghee and P. H. von Hippel, *Journal of Molecular Biology*, 1974, **86**, 469.

6 C. M. Dupureur and J. K. Barton in 'Comprehensive Supramolecular Chemistry', edited by J. L. Atwood, J. E. D. Davies, F. Vogtle, and D. D. Mac Nicol, Pergamon Press, 1996.

7 E. C. Long and J. K. Barton, *Accounts of Chemical Research*, 1990, **23**, 271.

8 J. I. Bruce, M. P. Lowe and D. Parker in 'The Chemistry of Contrast Agents in Medical Magnetic Resonance Imaging', edited by A. Merbach and E. Toth, Wiley, New York, 2001.

9 D. Parker and J. A. G. Williams, *Journal of the Chemical Society-Dalton Transactions*, 1996, 3613.

10 S. J. Weissman, *Journal of Chemical Physics*, 1942, **10**, 214.

11 A. Beeby, I. M. Clarkson, R. S. Dickins, S. Faulkner, D. Parker, L. Royle, A. S. de Sousa, J. A. G. Williams, and M. Woods, *Journal of the Chemical Society-Perkin Transactions 2*, 1999, 493.

12 A. M. Pyle and J. K. Barton, *Progress in Inorganic Chemistry*, 1990, **38**, 413.

13 K. E. Erkkila, D. T. Odom, and J. K. Barton, *Chemical Reviews*, 1999, **99**, 2777.

14 E. Tuite, P. Lincoln, and B. Norden, *Journal of the American Chemical Society*, 1997, **119**, 239.

15 R. E. Holmlin, E. D. A. Stemp, and J. K. Barton, *Inorganic Chemistry*, 1998, **37**, 29.

16 A. Greguric, I. D. Greguric, T. W. Hambley, J. R. Aldrich-Wright, and J. G. Collins, *Journal of the Chemical Society-Dalton Transactions*, 2002, 849.

17 A. E. Friedman, J. C. Chambron, J. P. Sauvage, N. J. Turro, and J. K. Barton, *Journal of the American Chemical Society*, 1990, **112**, 4960.

18 E. J. C. Olson, D. Hu, A. Hormann, A. M. Jonkman, M. R. Arkin, E. D. A. Stemp, J. K. Barton, and P. F. Barbara, *Journal of the American Chemical Society*, 1997, **119**, 11458.

19 B. Armitage, *Chemical Reviews*, 1998, **98**, 1171.

20 C. Turro, A. Evenzahav, S. H. Bossmann, J. K. Barton, and N. J. Turro, *Inorganica Chimica Acta*, 1996, **243**, 101.

21 D. Campisi, T. Morii, and J. K. Barton, *Biochemistry*, 1994, **33**, 4130.

22 T. P. Shields and J. K. Barton, *Biochemistry*, 1995, **34**, 15037.

23 A. H. Krotz, B. P. Hudson, and J. K. Barton, *Journal of the American Chemical Society*, 1993, **115**, 12577.

24 S. Steenken and S. V. Jovanovic, *Journal of the American Chemical Society*, 1997, **119**, 617.

[25] J. P. Lecomte, A. KirschDeMesmaeker, M. M. Feeney, and J. M. Kelly, *Inorganic Chemistry*, 1995, **34**, 6481.

[26] S. Delaney, M. Pascaly, P. K. Bhattacharya, K. Han, and J. K. Barton, *Inorganic Chemistry*, 2002, **41**, 1966.

[27] A. Radzicka and R. Wolfenden, *Science*, 1995, **267**, 90.

[28] E. L. Hegg and J. N. Burstyn, *Coordination Chemistry Reviews*, 1998, **173**, 133.

[29] S. J. Franklin, *Current Opinion in Chemical Biology*, 2001, **5**, 201.

[30] M. Komiyama, N. Takeda, Y. Takahashi, H. Uchida, T. Shiiba, T. Kodama, and M. Yashiro, *Journal of the Chemical Society-Perkin Transactions 2*, 1995, 269.

[31] M. Komiyama, N. Takeda, and H. Shigekawa, *Chemical Communications*, 1999, 1443.

[32] M. E. Branum, A. K. Tipton, S. R. Zhu, and L. Que, *Journal of the American Chemical Society*, 2001, **123**, 1898.

[33] M. Komiyama, *Journal of Biochemistry*, 1995, **118**, 665.

[34] L. Y. Huang, L. L. Chappell, O. Iranzo, B. F. Baker, and J. R. Morrow, *Journal of Biological Inorganic Chemistry*, 2000, **5**, 85.

[35] J. T. Welch, M. Sirish, K. M. Lindstrom, and S. J. Franklin, *Inorganic Chemistry*, 2001, **40**, 1982.

[36] K. D. Copeland, M. P. Fitzsimons, R. P. Houser, and J. K. Barton, *Biochemistry*, 2002, **41**, 343.

[37] D. Parker, R. S. Dickins, H. Puschmann, C. Crossland, and J. A. K. Howard, *Chemical Reviews*, 2002, **102**, 1977.

[38] R. S. Dickins, J. A. K. Howard, C. W. Lehmann, J. Moloney, D. Parker, and R. D. Peacock, *Angewandte Chemie-International Edition in English*, 1997, **36**, 521.

[39] I. M. Clarkson, A. Beeby, J. I. Bruce, L. J. Govenlock, M. P. Lowe, C. E. Mathieu, D. Parker, and K. Senanayake, *New Journal of Chemistry*, 2000, **24**, 377.

[40] D. Parker, P. K. Senanayake, and J. A. G. Williams, *Journal of the Chemical Society-Perkin Transactions 2*, 1998, 2129.

[41] E. B. van der Tol, H. J. van Ramesdonk, J. W. Verhoeven, F. J. Steemers, E. G. Kerver, W. Verboom, and D. N. Reinhoudt, *Chemistry-a European Journal*, 1998, **4**, 2315.

[42] I. Greguric, J. R. AldrichWright, and J. G. Collins, *Journal of the American Chemical Society*, 1997, **119**, 3621.

[43] J. G. Collins, A. D. Sleeman, J. R. Aldrich-Wright, I. Greguric, and T. W. Hambley, *Inorganic Chemistry*, 1998, **37**, 3133.

[44] J. G. Collins, J. R. Aldrich-Wright, I. D. Greguric, and P. A. Pellegrini, *Inorganic Chemistry*, 1999, **38**, 5502.

[45] E. M. Proudfoot, J. P. Mackay, and P. Karuso, *Biochemistry*, 2001, **40**, 4867.

[46] E. D. A. Stemp, M. R. Arkin, and J. K. Barton, *Journal of the American Chemical Society*, 1997, **119**, 2921.

[47] K. D. Barker, B. R. Benoit, J. A. Bordelon, R. J. Davis, A. S. Delmas, O. V. Mytykh, J. T. Petty, J. F. Wheeler, and N. A. P. Kane-Maguire, *Inorganica Chimica Acta*, 2001, **322**, 74.

[48] C. G. Coates, P. Callaghan, J. J. McGarvey, J. M. Kelly, L. Jacquet, and A. Kirsch-De Mesmaeker, *Journal of Molecular Structure*, 2001, **598**, 15.

[49] R. E. Holmlin, J. A. Yao, and J. K. Barton, *Inorganic Chemistry*, 1999, **38**, 174.

[50] A. Ambroise and B. G. Maiya, *Inorganic Chemistry*, 2000, **39**, 4256 and 4264.

[51] H. Kunkely and A. Vogler, *Journal of Photochemistry and Photobiology A-Chemistry*, 2002, **151**, 45.

[52] S. D. Kean, University of Durham, 2001.

[53] A. Rodger and B. Norden, 'Circular Dichroism and Linear Dichroism', Oxford University Press, 1997.

[54] W. C. Johnson, M. Ardhammar, B. Norden and T. Kurucsev in 'Circular Dichroism: Principles and Applications', edited by N. Berova, K. Nakanishi, and R. W. Woody, John Wiley & Sons, 2000.

[55] C. Zimmer and G. Luck in 'Advances in DNA Sequence Specific Agents', edited by L. H. Hurley, JAI Press, 1992.

[56] R. Lyng, A. Rodger, and B. Norden, *Biopolymers*, 1991, **31**, 1709.

[57] R. Lyng, A. Rodger, and B. Norden, *Biopolymers*, 1992, **32**, 1201.

[58] H. P. J. M. Dekkers in 'Circular Dichroism: Principles and Applications', edited by N. Berova, K. Nakanishi, and R. W. Woody, John Wiley & Sons, 2000.

[59] J. I. Bruce, D. Parker, S. Lopinski, and R. D. Peacock, *Chirality*, 2002, **14**, 562.

[60] J. R. Lakowicz, 'Principles of Fluorescence Spectroscopy', Kluwer Academic/Plenum Publishers, 1999.

[61] J. K. Barton, J. M. Goldberg, C. V. Kumar, and N. J. Turro, *Journal of the American Chemical Society*, 1986, **108**, 2081.

[62] A. E. Friedman, C. V. Kumar, N. J. Turro, and J. K. Barton, *Nucleic Acids Research*, 1991, **19**, 2595.

[63] P. Lincoln and B. Norden, *Journal of Physical Chemistry B*, 1998, **102**, 9583.

[64] M. E. McCarroll, F. H. Billiot, and I. M. Warner, *Journal of the American Chemical Society*, 2001, **123**, 3173.

[65] K. A. Connors, 'Binding Constants', Wiley-Interscience, 1987.

[66] J. K. Barton, J. J. Dannenberg, and A. L. Raphael, *Journal of the American Chemical Society*, 1982, **104**, 4967.

[67] R. J. Morgan, S. Chatterjee, A. D. Baker, and T. C. Strekas, *Inorganic Chemistry*, 1991, **30**, 2687.

CHAPTER 2

Lanthanide Complexes with a Phenanthridinium Chromophore

The interaction of nucleic acids with two cationic chiral lanthanide complexes bearing a phenanthridinium chromophore (Fig.2.1) is described in this chapter.

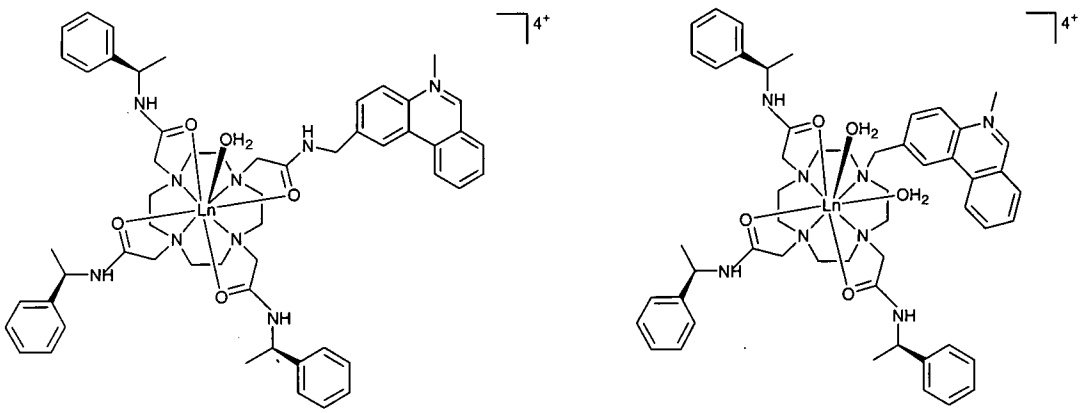

Fig.2.1 Tetraamide (left) and triamide (right) lanthanide complexes bearing a phenanthridinium chromophore.

Previous studies showed that the Eu tetraamide complex can intercalate between the base-pairs of $[(CG)_6]_2$ and $[(AT)_6]_2$ oligonucleotides. A higher binding affinity for the former dodecamer was observed.[1] We investigated its interaction with polymeric nucleic acids, focusing our attention on those containing C and G bases.

The behaviour of the triamide complex was also examined, which possesses two coordinated water molecules and an intercalative phenanthridinium moiety closer to the lanthanide centre.

In each case, both (RRR)- and (SSS)- complexes were compared. These have been shown to give rise to one major diastereoisomer in solution, with a regular square antiprismatic array. An R configuration at the chiral centre favours the formation of the $\Lambda(\delta\delta\delta\delta)$ isomer, while an S configuration gives rise to a preferred $\Delta(\lambda\lambda\lambda\lambda)$ isomer.[2] The interaction with nucleic acids was investigated for each enantiomer, between which chiral discrimination was expected. As B-DNA is a chiral molecule, with a right-handed helicity, it may form diastereomeric adducts of differing free energy, leading to a preferred interaction with one enantiomer of the complex.

2.1. Synthesis

2.1.1. Phenanthridine Derivatives

Functionalisation of phenanthridine at C-2 was carried out as shown in Scheme 1:

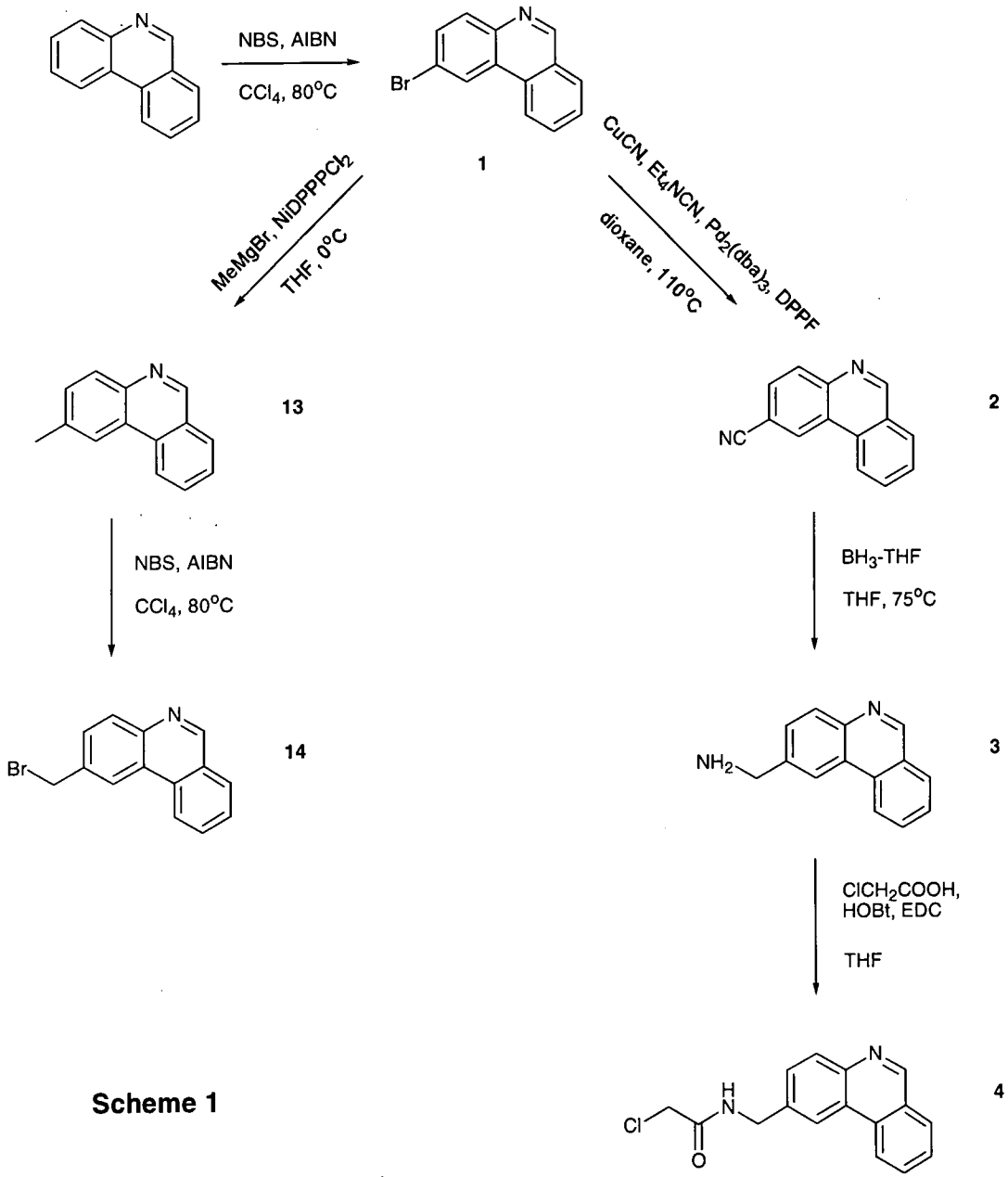

Scheme 1

For the preparation of 2-bromomethylphenanthridine, **14**, regioselective bromination of phenanthridine in the 2-position was followed by alkylation, using a nickel catalysed Grignard coupling reaction.[3] Benzylic bromination of 2-methylphenanthridine, **13**, was achieved using N-bromosuccinimide.

The synthesis of the α-haloamide, **4**, also required bromination of phenanthridine. Cyanation of 2-bromophenanthridine, **1**, was followed by nitrile reduction and coupling of the resultant amine, **3**, with chloroacetic acid.

The first synthesis[4] of the cyanophenanthridine, **2**, undertaken in the absence of the catalyst, yielded a mixture of products which proved rather difficult to separate. Therefore, a new procedure[5] was followed. Although the cyano group source was the same, i.e. cuprous cyanide, the use of a palladium (0) catalyst (tris(dibenzylideneacetone)dipalladium) allowed milder reaction conditions to be used. Heating in DMF required high temperature (170°C) and long reaction time (48 hours), whereas, in the catalysed cyanation, 1,4-dioxane was used as solvent at the reflux temperature (101°C) and the reaction was complete after 4 hours.

The ^{1}H NMR spectrum of 2-bromophenanthridine was assigned on the basis of a COSY and compared to the results from a NOESY spectrum of 2-methylphenanthridine. Cross-peaks between the methyl group and the neighbouring protons, on the same ring, confirmed the assignment of the signals due to H1 and H3. The substituent in the 2 position affects mainly the protons on the same ring, while the chemical shifts of the protons on the other rings (H6 to H10) maintained their correlated positions.

2.1.2. Ligands and Complexes

The synthesis of the (RRR) octadentate ligand, **8**, and the (RRR) heptadentate analogue, **16**, was carried out as shown in Scheme 2:

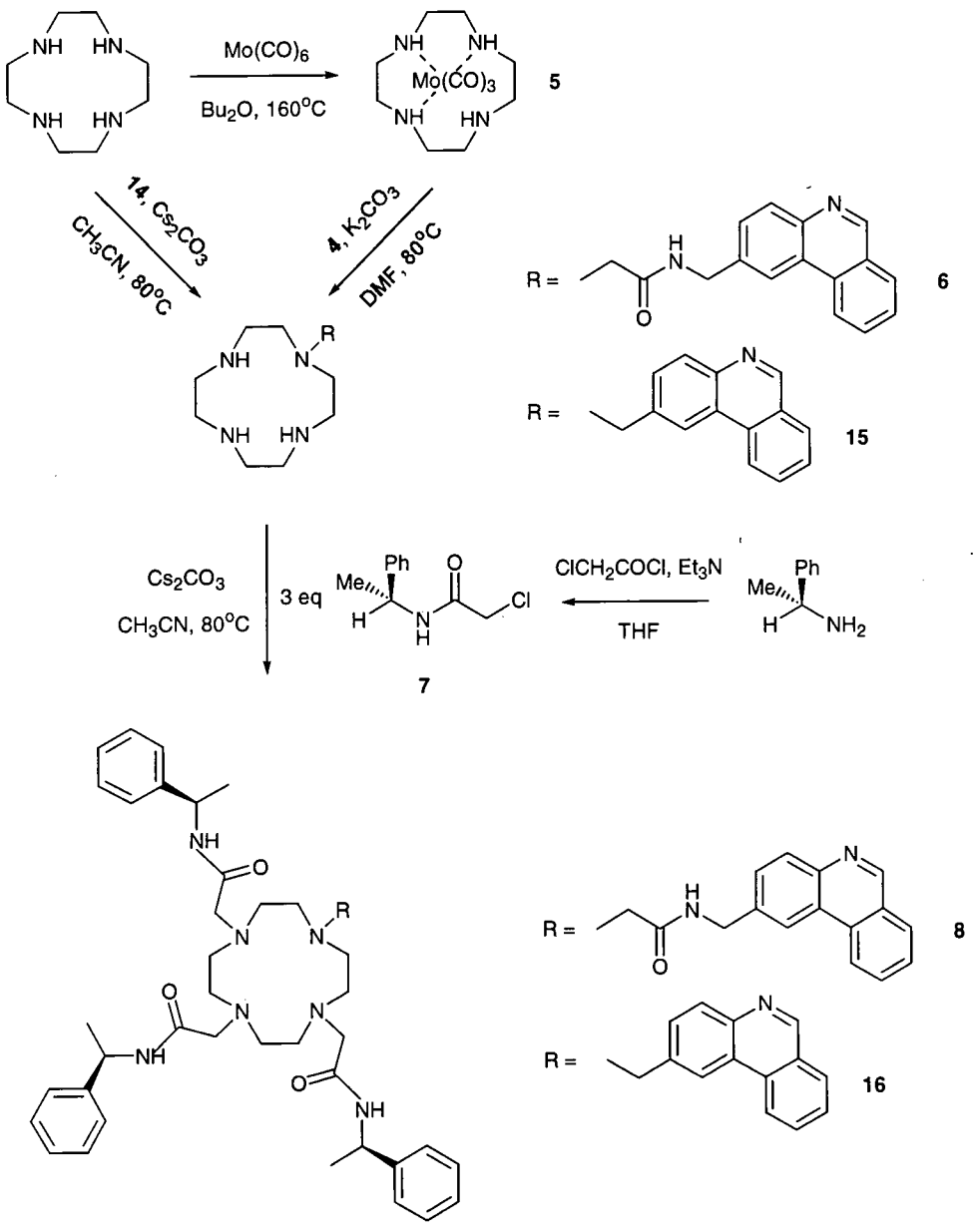

Scheme 2

Monoalkylation of cyclen with the α-chloroamide, **4**, was achieved via the intermediacy of a molybdenum tricarbonyl cyclen complex, **5**.[6] In the case of the bromomethylphenanthridine, **14**, it had previously been established that allylic and benzylic halides tend to react with **5** to give a 1,7-disubstituted product. Monoalkylation of the macrocycle was therefore undertaken via a different route, using an excess of cyclen to favour monosubstitution.

The (R)-α-chloroamide arms, **7**, were synthesised from the enantiopure amine[4] and introduced on to the macrocycle in the presence of caesium carbonate.

The lanthanide complexes **9**, **11**, **17** were prepared in anhydrous acetonitrile, following reaction of the given macrocyclic ligand with the appropriate trifluoromethanesulphonate salt, and purified by precipitation onto diethyl ether.

Selective N-methylation of the phenanthridine group in the complex occurred under mild conditions (excess CH_3I, CH_3CN, 40°C) to yield the final products **10**, **12**, **18** (Scheme 3). The final products were estimated to be 95% pure. ^1H NMR spectra of ligand **8** and complex **9** are included in appendix.

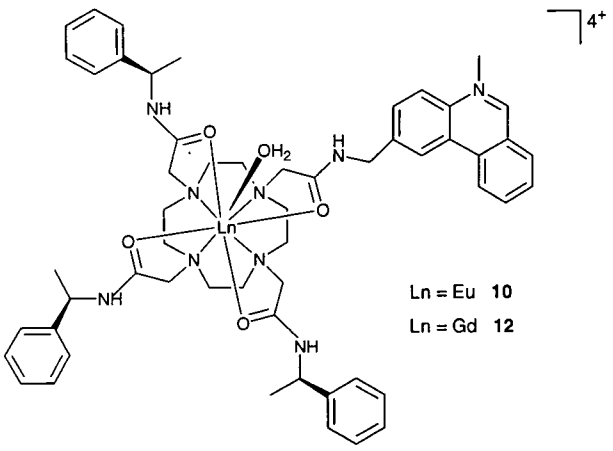

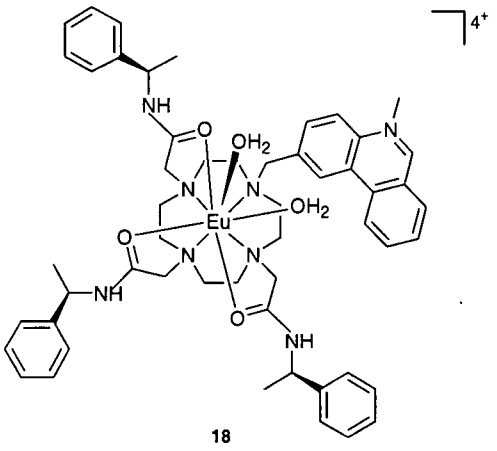

Scheme 3

2.2. Interaction of Δ- and Λ- Eu Tetraamide Complexes with Nucleic Acids

2.2.1. Absorption and Emission Spectra

Changes in the absorption and emission spectra of the complexes were monitored as a function of added DNA. The aqueous solutions of the complexes and nucleic acids were prepared with a pH 7.4 buffer (HEPES 10 mM, NaCl 10 mM) and the concentrations determined on the basis of their absorbance at 320 nm and 260 nm respectively, considering ε = 8000 $M^{-1}cm^{-1}$ for the phenanthridinium chromophore (320 nm), ε = 6600 $M^{-1}cm^{-1}$ for calf-thymus DNA (42% CG rich) and poly(dAdT) and ε = 8400 $M^{-1}cm^{-1}$ for poly(dCdG) (260 nm). The values obtained for the nucleic acids were divided by two, in order to express the concentrations in terms of base-pairs.

After each addition, an absorption spectrum of the phenanthridinium chromophore (280-480 nm) and emission spectra of the phenanthridinium fluorophore and the lanthanide (385-750 nm) were recorded. In the titrations with oligonucleotides[1] the absorbance at 302 and 378 nm did not change significantly as a function of added DNA (isosbestic points). Accordingly, the latter was chosen as the excitation wavelength, to ensure that observed changes in emission may be ascribed to the complex interaction and not to any change in absorption.

Addition of CT-DNA and poly(dGdC) to Δ- and Λ-Eu tetraamide caused a decrease in the intensity of the absorption bands at 320 and 370 nm (hypochromism) and a small shift to the red. Formation of two well-defined isosbestic points at 298 and 383 nm was observed (Fig.2.2). Hardly any change in the absorption spectra of either enantiomer was obtained in the presence of poly(dAdT).

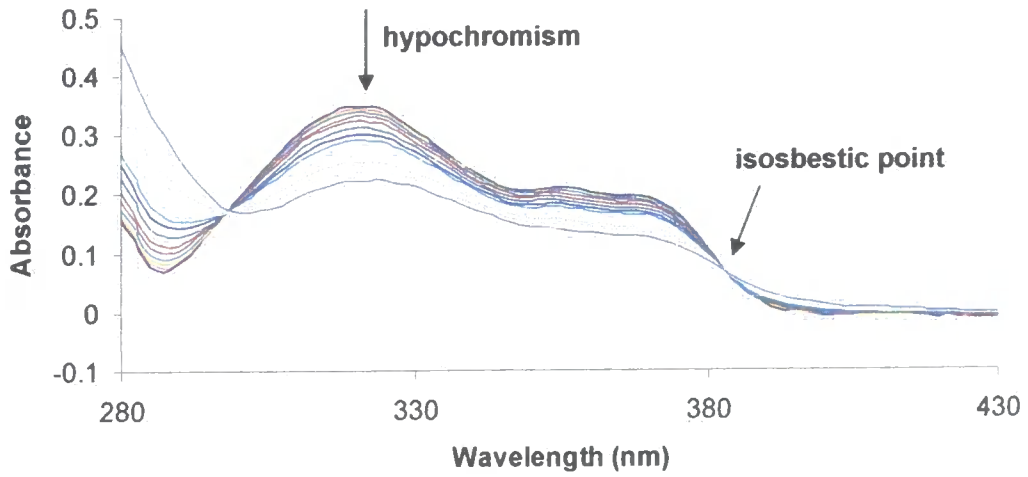

Fig.2.2 Absorption spectra of Λ-Eu tetraamide (44 μM) upon addition of poly(dGdC) (0.5 mM), from 0 to 3 base-pairs per complex, showing hypochromism and isosbestic points (pH 7.4, 10 mM HEPES, 10 mM NaCl, 295 K).

The variation of observed hypochromism at 320 nm, expressed as the percentage difference between the absorbance calculated at each addition to account for dilution and the A_{320} observed, was plotted as a function of DNA concentration, reported as the number of base-pairs per complex (Fig.2.3). Very similar curves were obtained for the Δ and Λ isomers in the presence of each nucleic acid.

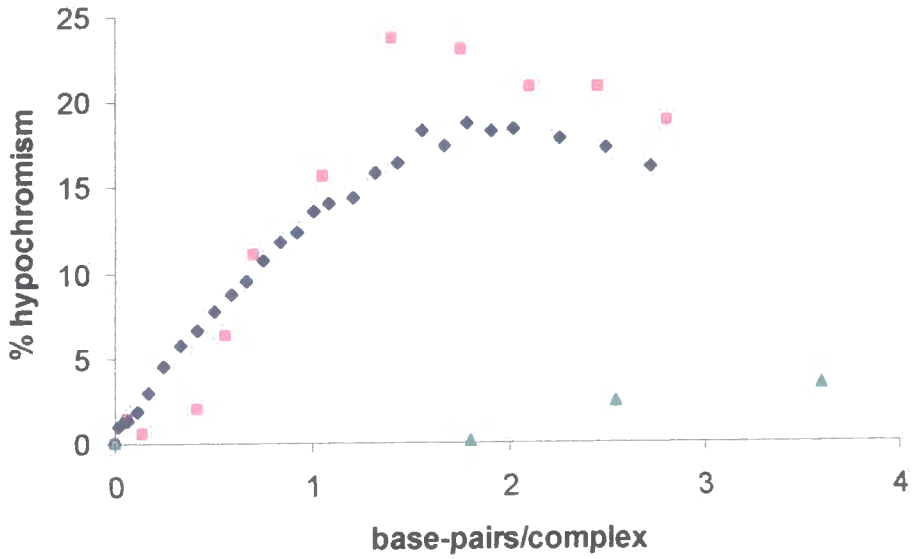

Fig.2.3 Percentage hypochromism at 320 nm for Λ-Eu tetraamide as a function of added CT-DNA (■), poly(dGdC) (♦) and poly(dAdT) (▲).

Hypochromism and red shift are suggestive of an intercalative binding mode, as a result of a charge transfer interaction between the more electron-rich C and G bases and the electron-poor phenanthridinium moiety. This is reflected in the higher extent of hypochromism found, for each enantiomer, in the presence of both CT-DNA and poly(dGdC). In each case examined, the Λ isomer gave the sharper isosbestic point at 383 nm and the more intense long-wavelength tail, suggesting that this enantiomer binds in a more 'well-defined' manner.

The hypochromic effect reaches a plateau at about 2·base-pairs/complex, which is in agreement with the neighbour exclusion principle,[7] that states that an intercalator can bind at most to alternate base-pair sites on DNA. This result, however, cannot be taken as a measure of the binding site size, because the nucleic acids used for the titrations contained strands of different lengths. A quantitative analysis of the experimental data using the method of McGhee and von Hippel[7] was attempted. The problems encountered in the fitting of the curves were related to the lack of a well-defined molecule size.

Quenching of the phenanthridinium fluorescence at 406 nm, upon addition of nucleic acid, was observed in each case. The europium emission intensity decreased to approximately the same extent, ruling out any direct quenching of the metal emissive state. Moreover, the form of the spectrum did not change, indicating that the binding did not distort the coordination environment around the lanthanide (Fig.2.4).

Furthermore, the corresponding Tb tetraamide complex showed a similar behaviour: the decrease in the terbium emission at 545 nm mirrored the quenching of the antenna at 406 nm.

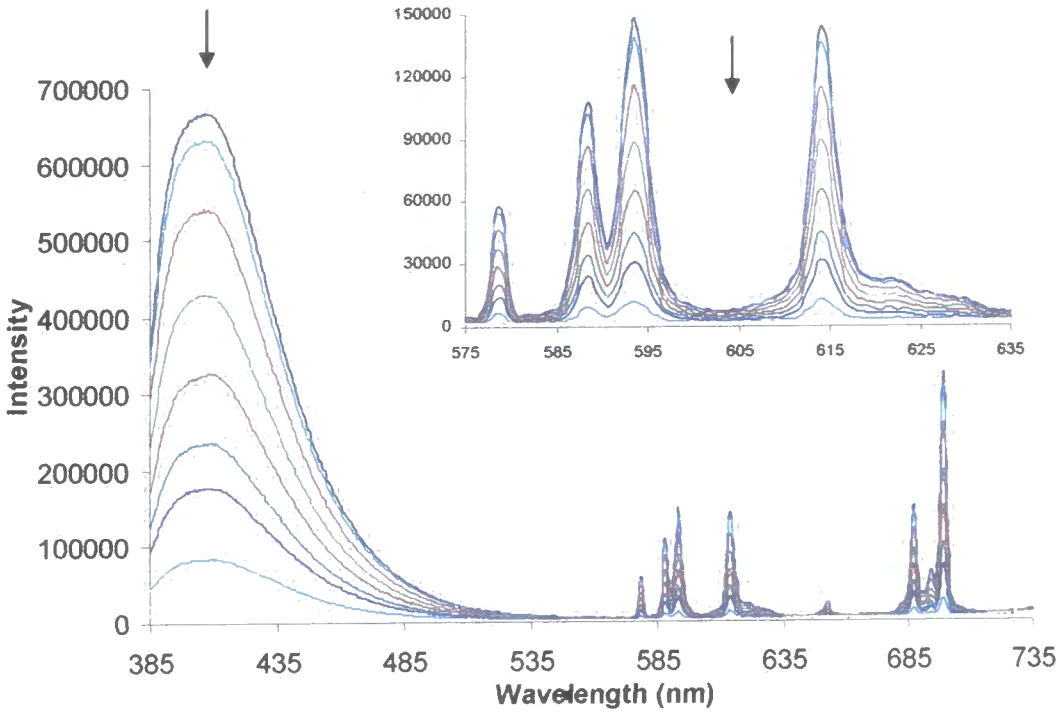

Fig.2.4 Emission spectra of Λ-Eu tetraamide (44 μM) upon addition of poly(dGdC) (0.5 mM), from 0 to 3 base-pairs per complex, showing quenching in the fluorescence of the phenanthridinium moiety (406 nm) and the lanthanide ion (λ_{ex} 378 nm, pH 7.4, 10 mM HEPES, 10 mM NaCl, 295 K).

The change in fluorescence quenching was examined as a function of added nucleic acid (Fig.2.5). Calf-thymus DNA and poly(dGdC) showed a greater effect compared to poly(dAdT), for each enantiomer.

The hypochromism and quenching curves obtained for Δ- and Λ-Eu tetraamide in the presence of poly(dGdC) were very similar. Therefore, they might be considered to reflect an interaction involving a predominantly intercalative binding mode, where a charge transfer from the nucleobases occurs, which deactivates the singlet excited state of the chromophore.

Poly(dAdT) seemed to show a preference for the Δ isomer and bound in a manner in which any charge transfer process in the ground or excited state was much less.

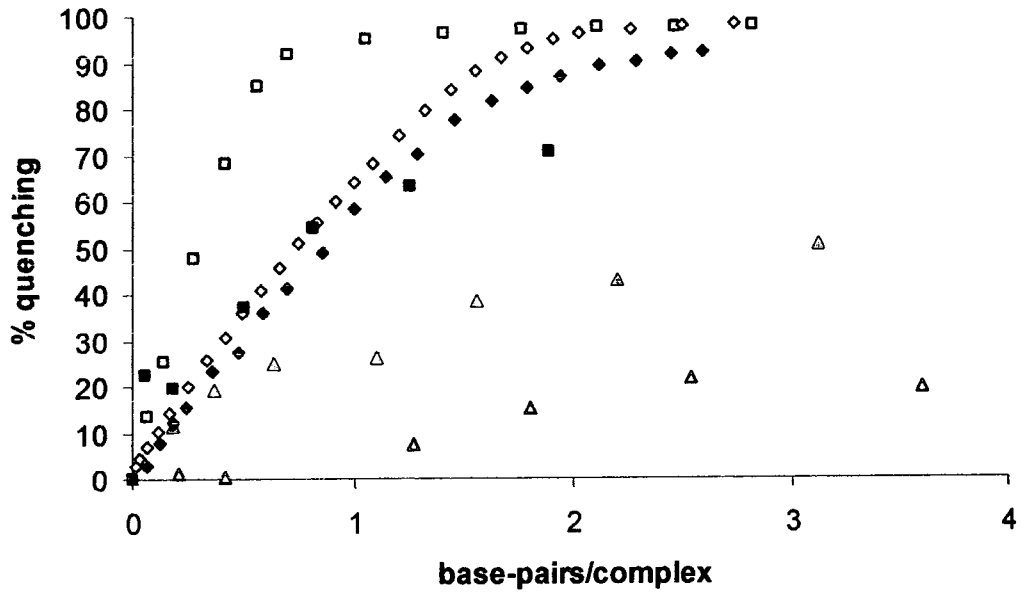

Fig.2.5 Percentage quenching at 406 nm for Λ- (empty symbol) and Δ-Eu tetraamide (filled symbol) as a function of added CT-DNA (□), poly(dGdC) (◊) and poly(dAdT) (Δ).

In the titrations with CT-DNA, a higher binding affinity was observed for the Λ rather than the Δ isomer. The quenching curve representing the interaction with Λ-Eu tetraamide reaches a maximum at lower base-pair/complex ratio compared to the hypochromism curve. This behaviour, which would be in contradiction to the neighbour exclusion principle if only intercalation was taken into account, might be due to additional binding modes, which are favoured in the presence of A and T bases. In order to show the contribution of C-G base-pairs to the DNA quenching curve, the base-pair/complex values for CT-DNA, which is 42% CG rich, have been divided by 0.42 (Fig.2.6). The curve obtained for this 'normalised' DNA is similar to that of poly(dGdC), with the same base-pair/complex saturating value. This indicates that the extent of quenching is primarily associated with an interaction with C-G base-pairs.

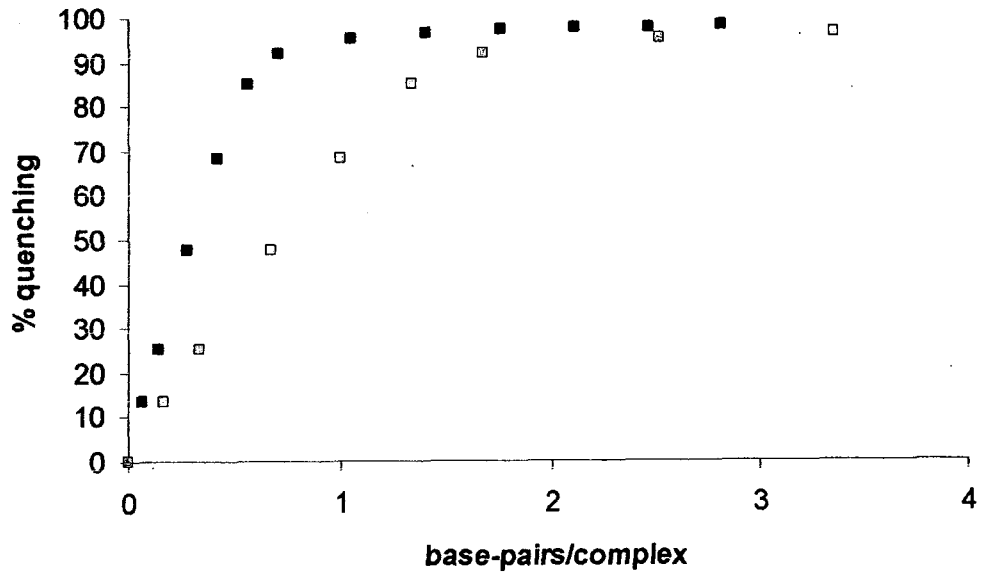

Fig.2.6 Percentage quenching at 406 nm for Λ-Eu tetraamide as a function of added CT-DNA. The blue symbols represent the titration curve, the pink symbols the normalized curve.

2.2.2. CD Spectra

CD spectra have been used to confirm the binding mechanism of intercalating cationic molecules such as ethidium bromide.[8] Since the DNA CD is due to the orientation of the bases, a decrease in the helical twist at the intercalation site, due to the interaction, causes a change in the CD spectrum.

The circular dichroism spectrum of poly(dGdC) was monitored as a function of added tetraamide complex between 220 and 380 nm. This spectral region contained also the signal of the chiral complex. Therefore, a CD difference spectrum was obtained by subtracting the contribution of the complex at each point of the titration.

The CD spectrum of free poly(dGdC) reveals the features characteristic of B-DNA: a positive band centred at 282 nm and a negative band at 252 nm (Fig.2.7). Upon addition of each complex, the CD intensity changed at both wavelengths, but the overall form of the spectrum did not change substantially. It can be deduced that the polynucleotide maintains a B-conformation.

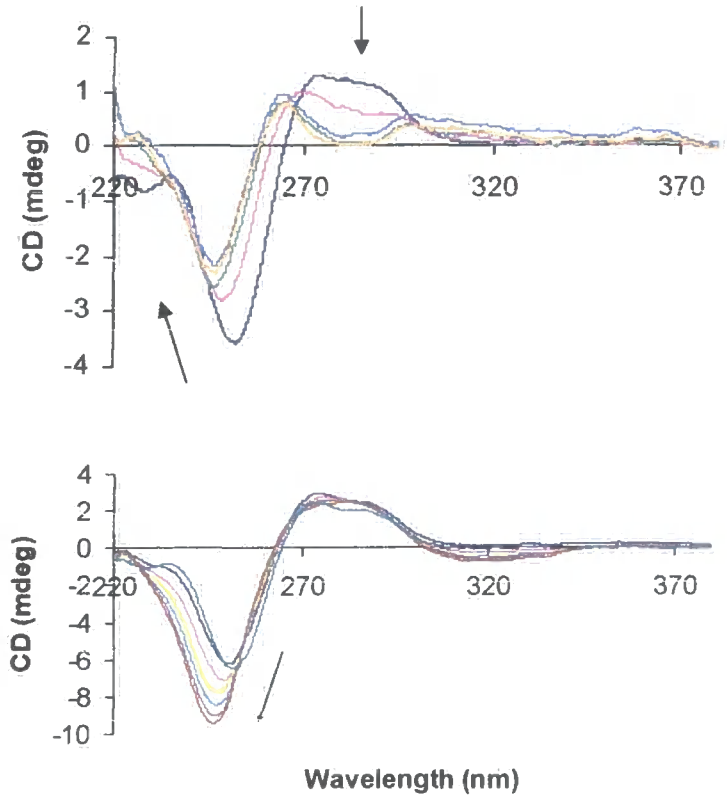

Fig.2.7 CD difference spectra of poly(dGdC) upon addition of Λ- (upper) and Δ- (lower) Eu tetraamide from 0 to 0.7 complex molecules per base-pair (pH 7.4, 10 mM HEPES, 10 mM NaCl, 295 K).

Upon binding of the Λ isomer, the 252 nm band decreased in intensity by 40% and shifted to the blue by 5 nm, while the positive band decreased slightly in intensity and shifted from 282 to 265 nm. Addition of the Δ isomer, on the contrary, led to a 60% increase in the intensity of the negative band, which also shifted by 6 nm to lower wavelength. A similar behaviour was observed in binding to the oligonucleotide $[(CG)_6]_2$.[2]

This suggests that a change in the base orientation has occurred, which may be due to the untwisting of DNA caused by the intercalation of the complex. Although it is not possible to explain why the CD at 252 nm changes in opposite directions in the presence of the Λ and Δ isomers, it is clear that the helical structure of the nucleic acid is distinctly different in the diastereomeric complexes.

2.2.3. Equilibrium Dialysis

An equilibrium dialysis experiment was carried out in an attempt to estimate the binding affinity of the Λ-Eu tetraamide complex to poly(dGdC).

A cellulose acetate membrane with a molecular weight cut-off of 5000 was used to separate the two chambers of a dialysis cell, so that only the complex (MW = 1646) could diffuse through it. A solution of the complex (60 μM) was put in compartment 1 and dialysed against a solution of poly(dGdC) (12 μM) contained in compartment 2.

After 24 hours, the absorbance at 320 nm of samples taken from the two compartments was measured. The sample from compartment 1 gave the concentration of the free complex (21 μM), which is the same in both chambers at equilibrium (Fig.2.8). The difference in absorption between the two samples represents the effect of the bound complex and is proportional to its concentration.

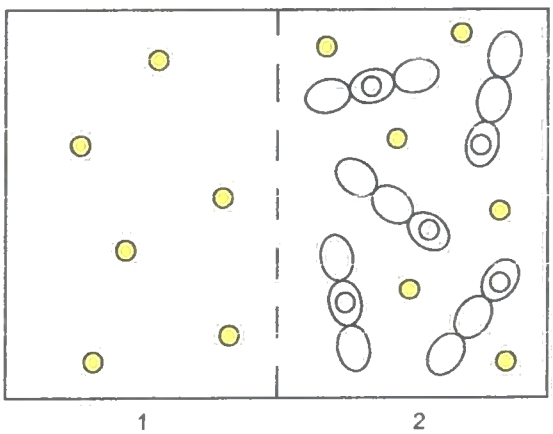

Fig.2.8 Representation of the situation at equilibrium: free complex in compartment 1 and free and bound complex in 2. The intensity of the colour is proportional to the absorbance of the chromophore in the free and bound complex.

Considering the concentration of the bound complex in compartment 2 (18 μM) and the percentage hypochromism observed in the interaction between Λ-Eu tetraamide and poly(dGdC) (18%), the contribution of the bound form to the total absorbance

was calculated. The absorbance at 320 nm measured for the sample taken from compartment 2 was in good agreement with the expected value.

The small difference between the two A_{320} values (8%) was ascribed to a possible adsorption of the complex to the membrane or to an error in the estimated concentrations in compartment 2, due to the slightly larger volume in 2 compared to 1. The membrane, in fact, is impermeable to the macromolecule and the osmotic pressure gradient that arises causes a solvent flow toward the compartment containing the macromolecule. The actual concentrations of free and bound complex in this chamber are thus lower than expected, resulting in a smaller value of absorbance at 320 nm.

An indicative binding constant was obtained for the equilibrium:

$$\text{Free complex} + \text{poly(dGdC)} \leftrightarrow \text{Bound complex}$$

using the values calculated for the free (21 μM) and bound (18 μM) complex and the concentration of poly(dGdC) in base-pairs (6 μM). A value of $K = 1.4 \cdot 10^5\ M^{-1}$ resulted, indicating a fairly strong interaction.

If the actual concentration of nucleic acid was known, the average number of complex molecules bound per macromolecule could be obtained.[9]

2.2.4. Fluorescence Anisotropy

The anisotropy of the Λ-Eu tetraamide complex was measured to evaluate if this technique was suitable for studying its interaction with nucleic acids.

An aqueous solution of the complex was excited at 378 nm and its emission intensities I_{VV}, I_{VH}, I_{HV} and I_{HH} measured in the range 380-750 nm. The same measurement was repeated with increasing amounts of glycerol; the corresponding anisotropies are shown in Table 2.1. It must be pointed out that the anisotropy is a dimensionless quantity, independent of the total intensity and of the concentration of the sample.

Table 2.1 Anisotropy of Λ-Eu tetraamide in aqueous solutions containing different percentages of glycerol (v/v) (298 K).

% glycerol	Anisotropy
0	0.016
25	0.028
62.5	0.047
90.6	0.094
99.5	0.130

The fundamental anisotropy of the fluorophore (r_0), that is the anisotropy observed at time 0, in the absence of depolarising processes, was determined for N-methyl phenanthridinium iodide. In order to avoid diffusive motion during the excited state lifetime, a 75:25 glycerol/water (v/v) solution was prepared and cooled to -60°C. The anisotropy measured in these conditions (r_0 = 34.35), is the maximum anisotropy of the fluorophore. Therefore, a value between 0 and 34.35 was expected for the complex upon interaction with a nucleic acid.

The anisotropies of the solutions corresponding to the last point in the titrations of Λ-Eu tetraamide with poly(dGdC) and with CT-DNA were close to zero. This result has two possible interpretations: either the complex and the nucleic acids do not interact at all, which is not consistent with the results discussed so far, or the fluorescence of the bound complex is completely quenched by the nucleic acid and only the small fraction of free complex that is in equilibrium with the bound form emits. The emission of the free complex, however, is quickly depolarised by rotational diffusion, giving rise to near zero anisotropy.

2.2.5. Lifetime Measurements

It is only by comparing the singlet state lifetimes of the phenanthridinium fluorophore in the absence and presence of nucleic acid that the emission of the bound complex can be distinguished from that of the free form.

The excited state lifetimes of the phenanthridinium fluorophore were measured for the interaction between Λ-Eu tetraamide and poly(dGdC), varying the base-pairs per complex ratio from 0 to 4. The decay curve fitted well to a single mono-exponential in each case and gave a value of 2.9 ns for the lifetime of the antenna in the free complex, which reduced only very slightly, to 2.5 ns, at a base-pairs per complex ratio of 4.

It must be concluded that only the free complex fluoresces. If the bound complex emitted, a multiexponential decay would arise, being a combination of the lifetimes of the free and bound forms. The inability of the bound complex to luminesce obviously inhibits the further development of such systems as structural or reactive probes for DNA.

2.3. Interaction of Δ- and Λ- Eu Triamide Complexes with Nucleic Acids

2.3.1. Absorption and Emission Spectra

The spectroscopic behaviour of the Δ and Λ-Eu triamide complexes (Fig.2.9) was studied in the presence of poly(dGdC) and CT-DNA.

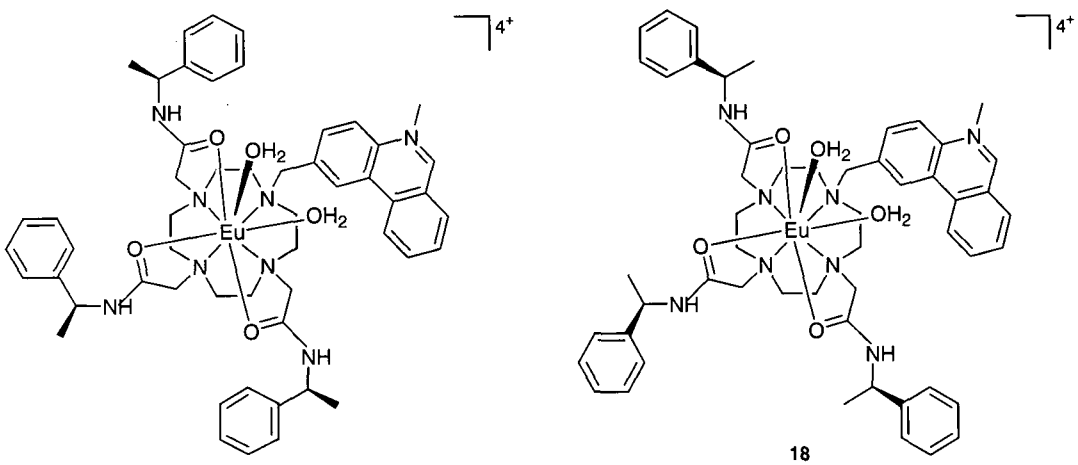

Fig.2.9 Enantiomeric Δ (left) and Λ (right) Eu triamide complexes.

Neither significant hypochromism nor red shift was observed in their absorption spectra, following addition of each nucleic acid.

The emission spectra showed a quenching of the phenanthridinium fluorescence, which was almost complete for Λ-Eu triamide in the presence of each nucleic acid (Fig.2.10). An apparent saturation limit of 1.5 base-pairs per complex was obtained for both the Λ and the Δ enantiomer upon addition of CT-DNA, while a limit of less than one base-pair per complex was reached with poly(dGdC).

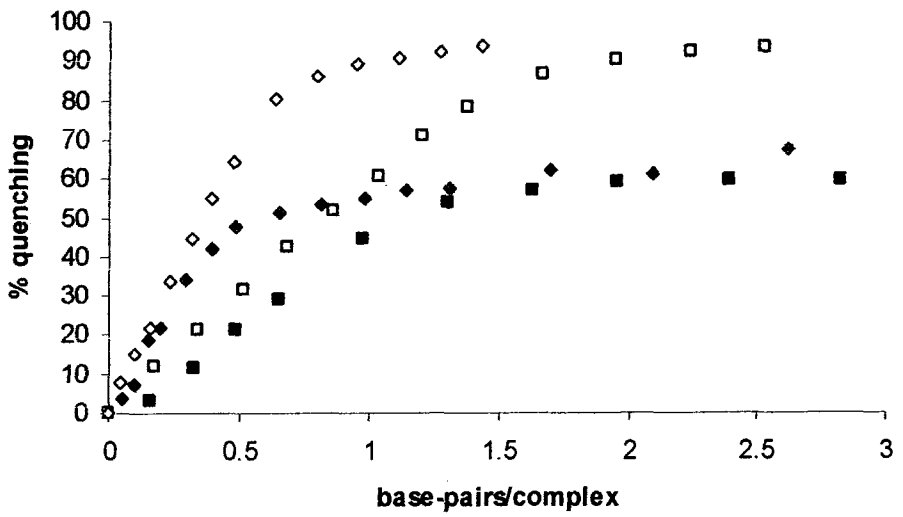

Fig.2.10 Percentage quenching at 406 nm for Λ- (empty symbol) and Δ-Eu triamide (filled symbol) as a function of added CT-DNA (□) and poly(dGdC) (◊).

Upon interaction with DNA, not only the intensity of the Eu emission decreased, but also the form of the spectrum changed, for each enantiomer. The biggest change was observed in the manifold of the $\Delta J = 4$ band, which is sensitive to the ligand field and is normally perturbed by variations in the Eu coordination environment (Fig.2.11).

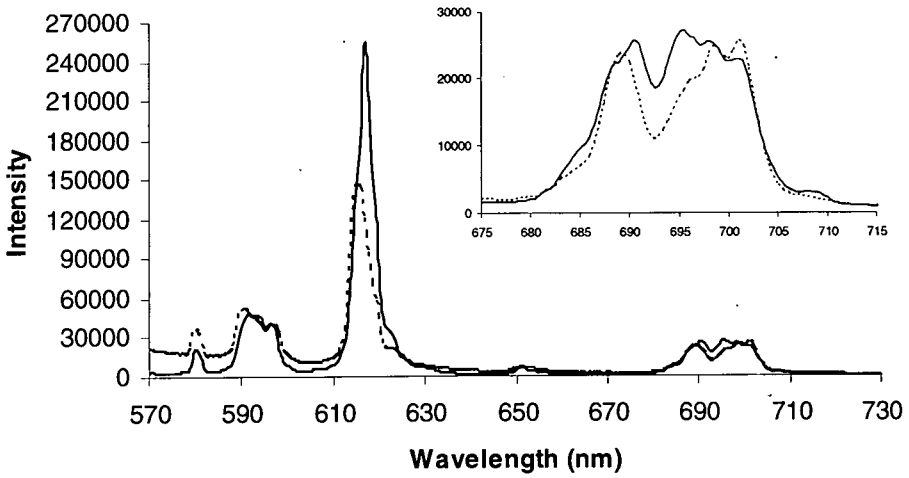

Fig.2.11 Europium emission spectra of Λ-Eu triamide in the absence (solid line) and in the presence (dotted line) of excess CT-DNA (λ_{ex} 378 nm, pH 7.4, 10 mM HEPES, 10 mM NaCl, 295 K). Changes in the ΔJ = 4 band are shown in the inset.

The similarity of the emission spectrum of the complex in the presence of CT-DNA to that in the presence of NaH_2PO_4[10] suggests that the interaction occurs through coordination of the phosphate groups in the DNA backbone to the lanthanide centre. Analogous changes in the Eu emission spectrum have been reported upon addition of oligonucleotides and the displacement of one coordinated water molecule by the DNA phosphate has been confirmed by an increase in the lifetime of the lanthanide excited state,[11] as it normally occurs when coordinating anions bind to heptacoordinate complexes.[10]

2.3.2. CPL Spectra

Circularly polarised emission spectra for the enantiomeric complexes were observed in the absence and presence of excess added nucleic acid.

The CPL spectrum of Λ-Eu triamide in the presence of poly(dGdC) closely resembled that obtained following addition of NaH_2PO_4 (particularly the ΔJ = 1 and

ΔJ = 2 patterns) (Fig.2.12). This supports the hypothesis of a direct electrostatic binding mode of the metal to the phosphate backbone of DNA.

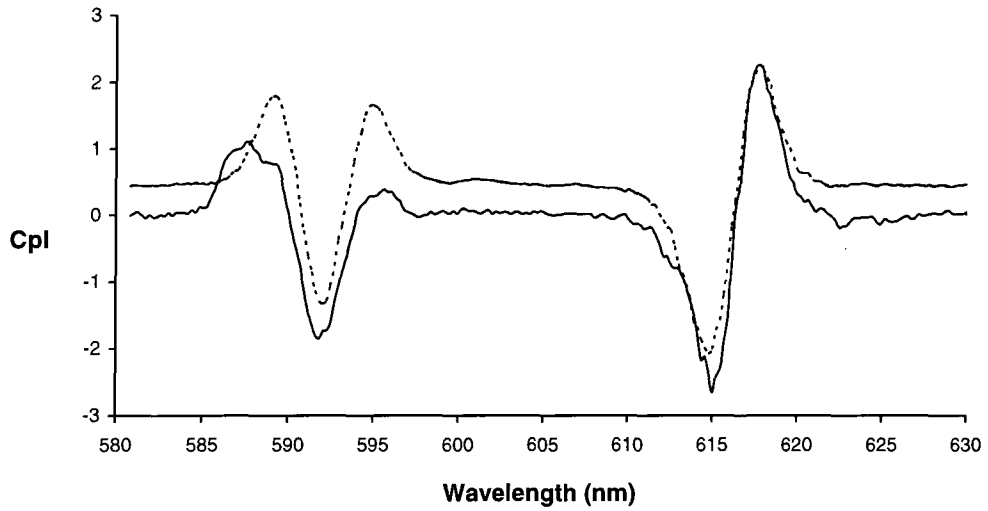

Fig.2.12 CPL spectra of Λ-Eu triamide in the presence of 2 base-pairs of poly(dGdC) per complex (solid line) and of 10 equivalents of NaH_2PO_4 (dotted line) (λ_{ex} 378 nm, pH 7.4, 10 mM HEPES, 10 mM NaCl, 295 K).

2.4. Summary and Conclusions

The Δ and Λ tetraamide complexes bind to nucleic acids preferentially at C-G sites. The interaction is primarily intercalative, with a more well-defined interaction established for the Λ enantiomer, as revealed by absorption spectral changes and fluorescence quenching experiments.

In the bound form, the luminescence of the phenanthridinium chromophore is completely quenched by charge transfer from the electron-rich nucleobases, thus no sensitisation of the lanthanide centre can occur. This limits further developments of the europium complexes as luminescent probes and of the terbium analogues as reactive probes for nucleic acids.

The production of singlet oxygen, which occurs with an overall quantum yield of 20% for the free Tb complex,[12] cannot occur in the bound form, because the triplet state of the chromophore is not populated.

The binding of the triamide complex seems to be mainly electrostatic, involving a coordinative interaction with the phosphate groups of the DNA backbone. The phosphate acts as a monodentate ligand, leaving one water molecule coordinated to the metal which could, in principle, hydrolyse the phosphodiester link. The hydrolytic mechanism (Fig.2.13) would be similar to that described for $Eu(THED)^{3+}$, a macrocyclic complex that cleaves RNA by nucleophilic attack of the phosphate linkage via a metal-activated hydroxyl group.[13]

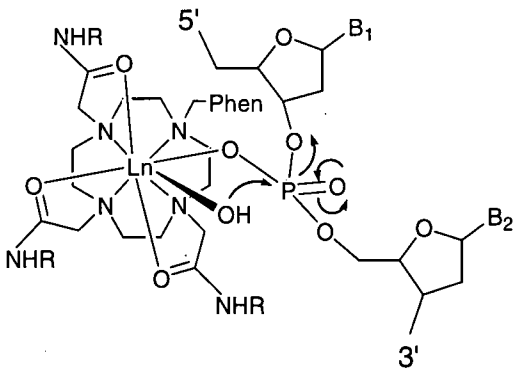

Fig.2.13 Hypotetical nucleophilic attack of the phosphate linkage of DNA by the Eu triamide complex.

The hydrolytic activity of a cleaving agent increases in the presence of intercalating groups in the ligand, which bring the lanthanide ion closer to the phosphodiester links.[14] Unfortunately, it is not possible to exploit this strategy with the Eu triamide complex, because the phenanthridinium moiety does not intercalate.

Moreover, problems arise from the quenching of the antenna, which is probably brought into proximity of the C and G bases despite the non-intercalative interaction.

In order to obtain efficient probes, new chromophores need to be identified in which highly efficient intersystem crossing occurs at a rate which is faster than or competitive with the DNA quenching of the singlet state.

References

1 L. J. Govenlock, C. E. Mathieu, C. L. Maupin, D. Parker, J. P. Riehl, G. Siligardi, and J. A. G. Williams, *Chemical Communications*, 1999, 1699.

2 G. Bobba, R. S. Dickins, S. D. Kean, C. E. Mathieu, D. Parker, R. D. Peacock, G. Siligardi, M. J. Smith, J. A. G. Williams, and C. Geraldes, *Journal of the Chemical Society-Perkin Transactions 2*, 2001, 1729.

3 K. Tamao, S. Kodama, I. Nakajima, and M. Kumada, *Tetrahedron*, 1982, **38**, 3347.

4 D. Parker, P. K. Senanayake, and J. A. G. Williams, *Journal of the Chemical Society-Perkin Transactions 2*, 1998, 2129.

5 T. Sakamoto and K. Ohsawa, *Journal of the Chemical Society-Perkin Transactions 1*, 1999, 2323.

6 D. Parker, 'Macrocycle Synthesis', Oxford University Press, 1996.

7 J. D. Mc Ghee and P. H. von Hippel, *Journal of Molecular Biology*, 1974, **86**, 469.

8 C. Zimmer and G. Luck in 'Advances in DNA Sequence Specific Agents', edited by L. H. Hurley, JAI Press, 1992.

9 K. A. Connors, 'Binding Constants', Wiley-Interscience, 1987.

10 J. I. Bruce, R. S. Dickins, L. J. Govenlock, T. Gunnlaugsson, S. Lopinski, M. P. Lowe, D. Parker, R. D. Peacock, J. J. B. Perry, S. Aime, and M. Botta, *Journal of the American Chemical Society*, 2000, **122**, 9674.

11 C. E. Mathieu, PhD Thesis, Durham, 2000.

12 G. Bobba, S. D. Kean, D. Parker, A. Beeby, and G. Baker, *Journal of the Chemical Society-Perkin Transactions 2*, 2001, 1738.

13 B. F. Baker, H. Khalili, N. Wei, and J. R. Morrow, *Journal of the American Chemical Society*, 1997, **119**, 8749.

14 J. Rammo, R. Hettich, A. Roigk, and H. J. Schneider, *Chemical Communications*, 1996, 105.

CHAPTER 3

Lanthanide Complexes with a Dipyridoquinoxaline Chromophore

Two new ligands have been designed (Fig.3.1), bearing a dipyridoquinoxaline (dpq) chromophore, which is an established and efficient sensitiser for lanthanide luminescence.[1] Here, the antenna has been integrated into the complex structure and acts as a bidentate ligand, preventing the coordination of water molecules that quench the lanthanide excited state.

Inspection of CPK space-filling models showed that chelation of the metal by the pyridine nitrogens of dpq could occur, if the antenna was linked to cyclen through a short methylene bridge from C-7.

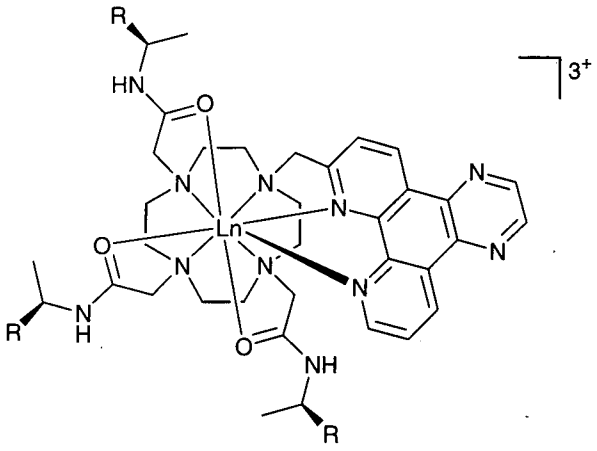

	Ln = Eu	Tb	Gd
R = Phenyl	**40**	**41**	**42**
R = 1-Naphthyl	**45**	**46**	**47**

Fig.3.1 Structure of the lanthanide complexes with the Ph_3dpq (**39**) and Np_3dpq (**44**) ligands, showing the chelation of the metal.

The desired 7-functionalised dpq systems were considered to be most readily prepared via the 7-chloromethyl derivative, which in turn could be synthesised from a 7-methyl precursor.

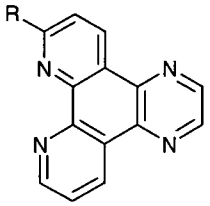

R = Me 7-methyldpq

R = CH_2Cl 7-chloromethyldpq

3.1. Synthesis

3.1.1. Dipyrido[3,2-f:2',3'-h]quinoxaline Derivatives

In order to link the dipyridoquinoxaline chromophore to cyclen, functionalisation at C-7 was undertaken. Three different routes were evaluated for the synthesis of 7-halomethyldpq via 7-methyldpq. Common to each is the formation of the condensed ring system, as shown in Scheme 1:

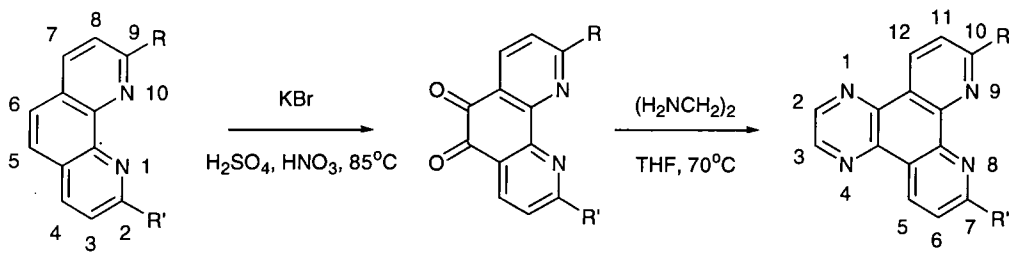

R=H, R'=Cl	**21**	**22**	**23**
R=R'=CH_3	neocuproine	**24**	**25**
R=H, R'=CH_3	**28**	**29**	**30**

Scheme 1

Each of the dpq derivatives was synthesised starting from 1,10-phenanthroline-5,6-quinones, obtained by oxidation of phenanthroline derivatives with bromine (generated in situ from H_2SO_4 and KBr) and HNO_3, according to a literature procedure.[2] Condensation of the 1,10-phenanthroline-5,6-diones with ethylenediamine gave the corresponding Schiff bases, which, upon oxidation by oxygen from the air, afforded the dpq derivatives, as described previously.[1]

Route 1

This route was designed on the basis of the synthetic strategy adopted for 2-bromomethylphenanthridine (**14**): halogenation of the heterocycle, followed by alkylation and benzylic bromination.

Regioselective chlorination at the position α- to the nitrogen was considered easier on 1,10-phenanthroline than on dpq, and was achieved using a literature procedure[3] (Scheme 2).

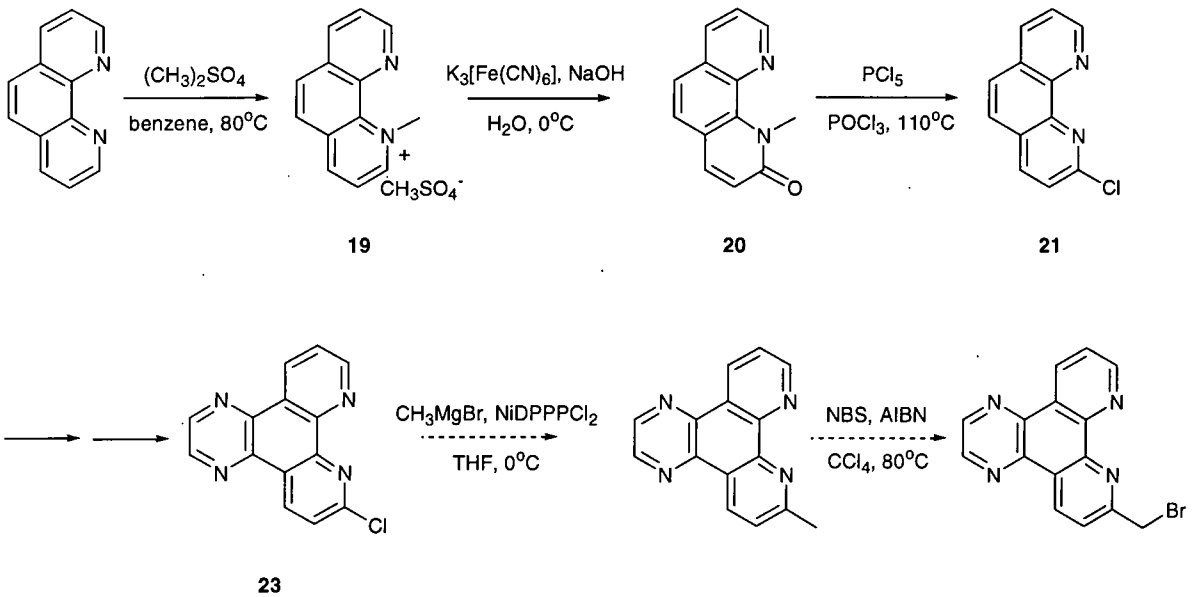

Scheme 2

Formation of the 1-methylphenanthrolinium salt, **19**, was followed by oxidation in the α- position by simultaneous addition of solutions of ferricyanide and alkali. Chlorination and demethylation of the product, **20**, afforded the monochloro derivative **21**.

Following the formation of the pyrazine ring, nucleophilic substitution of the halide was attempted for **23** using a nickel catalysed Grignard coupling reaction,[4] but the expected 7-methyldpq was not obtained.

A different approach was thus used, in which the methyl group was already present in the phenanthroline derivative, prior to the formation of the fourth ring.

Route 2

The route shown in Scheme 3 was inspired by the monofunctionalisation of neocuproine described in the literature.[5]

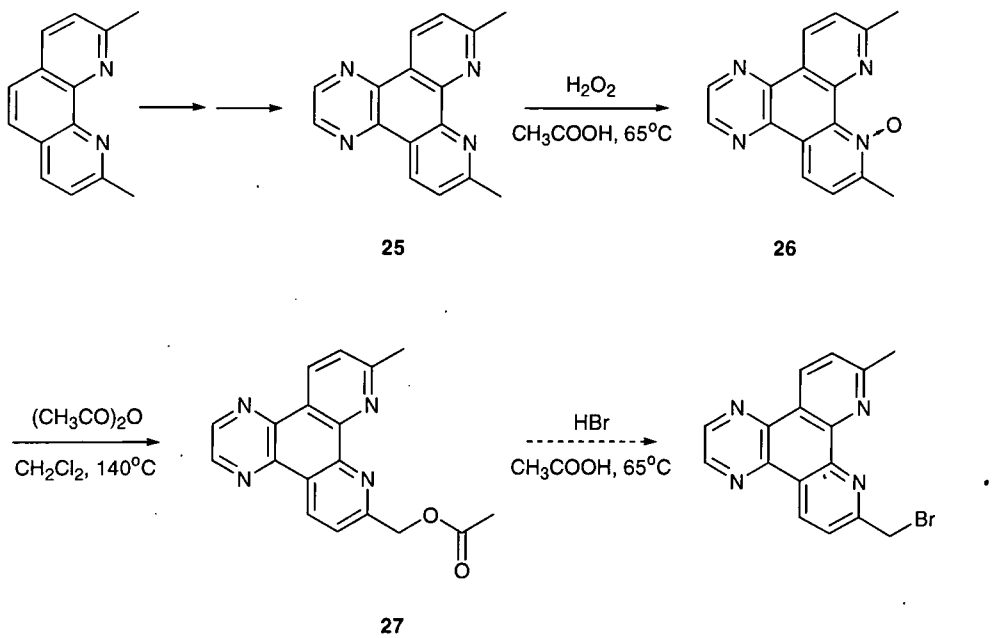

Scheme 3

For the condensed ring system, **25**, oxidation at nitrogen took place selectively at one of the pyridine rings rather than on the pyrazine ring. The resulting mono-N-oxide underwent a Boekelheide rearrangement: reaction of **26** with acetic anhydride gave the monofunctionalised product **27** in good yield. Nucleophilic substitution of the acetoxy group was attempted using hydrobromic acid in glacial acetic acid, but a mixture of tri and tetrabrominated products was obtained, as revealed by mass spectrometry.

Basic hydrolysis of the ester and chlorination of the resultant alcohol, as described in the same literature procedure, was considered to be an alternative. However, this strategy was abandoned for several reasons. The presence of a methyl group in the 10-position might cause steric hindrance and prevent the coordination of the lanthanide centre in the final complex. Moreover, the same synthetic route is not

applicable to the 7-methyldpq derivative, because oxidation would occur more easily at the nitrogen in the 9- position.

Route 3

The third route starts with the synthesis of monomethyldpq, which is then functionalised in two different ways (Scheme 4).

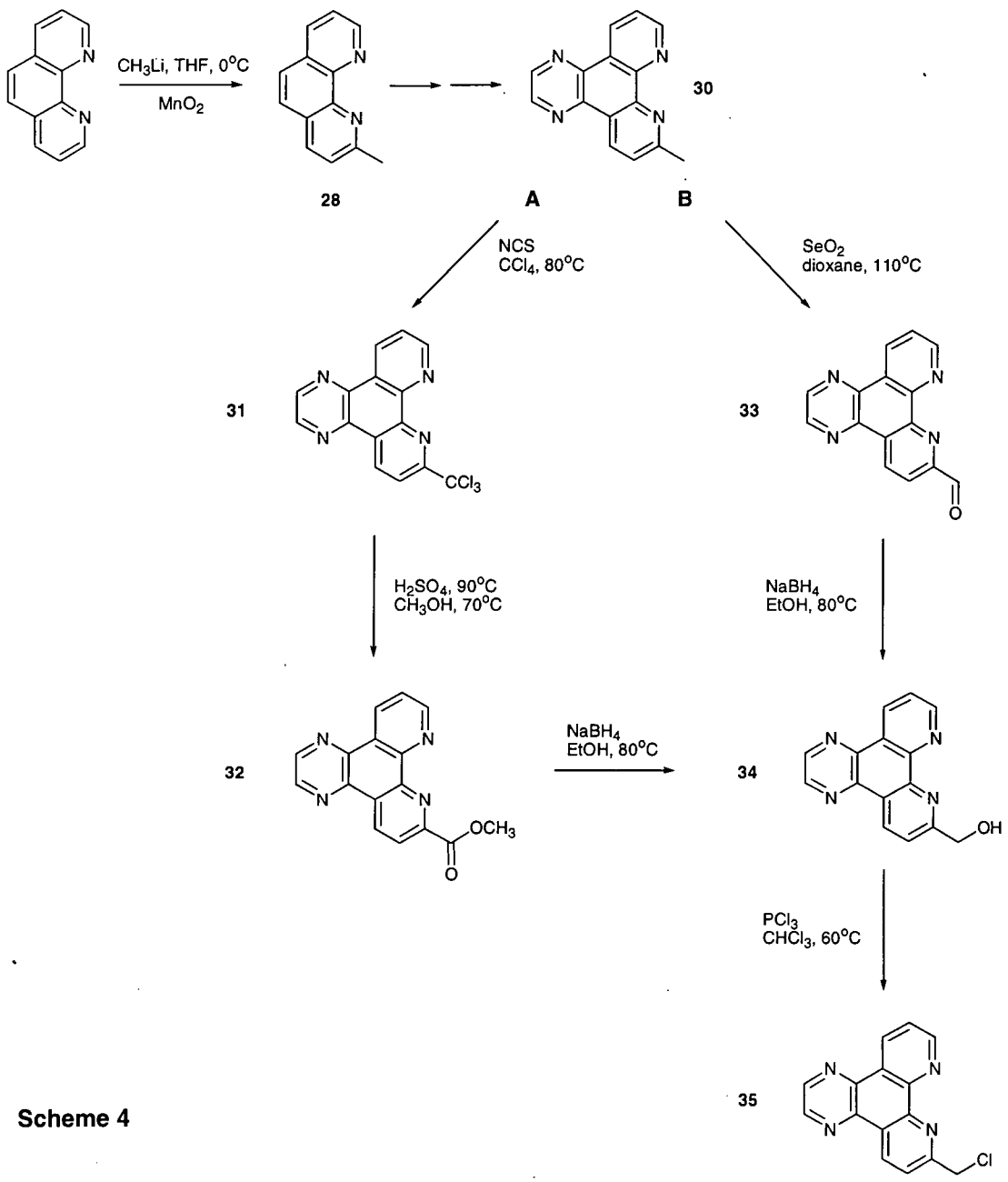

Scheme 4

Regioselective methylation of 1,10-phenanthroline in the 2-position was achieved using methyl lithium. The intermediate dihydrophenanthroline was re-aromatised by oxidation with manganese dioxide. Upon condensation with ethylenediamine, route **A** was followed first.

As for 2,9-dimethyl-1,10-phenanthroline,[6] functionalisation of the α-methyl group by radical halogenation with one equivalent of N-chlorosuccinimide was unsuccessful. An excess of this reagent, instead, gave the trichloromethyl derivative **31** in good yield.[7] Hydrolysis in concentrated sulphuric acid and esterification with methanol afforded compound **32**, which was then reduced to the alcohol **34**.[7] As reduction with sodium borohydride proved to be not reproducible, reaction with $LiAlH_4$ at low temperature was attempted,[8] but afforded the alcohol in low yield, as part of a complex mixture of products.

Another strategy (**B**) was then adopted to obtain the alcohol: mild oxidation of methyldpq with selenium dioxide,[9] followed by reduction of the aldehyde, **33**, with $NaBH_4$.[6] Chlorination of the alcohol with phosphorus trichloride[5] yielded the desired chloromethyl derivative **35**. This route was therefore used to prepare the target compound, **35**.

3.1.2. Ligands and Complexes

The synthesis of the two ligands, **39** and **44**, is shown in Scheme 5.

In order to achieve monofunctionalisation, triprotection of the macrocycle with 2.4 equivalents of Boc was undertaken.[10] Alkylation with the chloromethyl derivative, **35**, was followed by removal of the protecting groups, using trifluoroacetic acid.

This approach proved more convenient than the use of an excess of cyclen, as described in the previous chapter for the triamide ligand. Chromatographic separation of the monoalkylated product **38** from residual cyclen was not possible in that case, leading to formation of a small quantity of ligand bearing four chiral arms in the following step. The presence of this by-product, whose R_F is close to that of the dpq ligand **39**, made the purification of the desired product difficult to achieve.

The phenyl and naphthyl α-chloroamides, synthesised from the respective chiral amines as reported,[11,12] were then added to the macrocycle, by an alkylation reaction in acetonitrile.

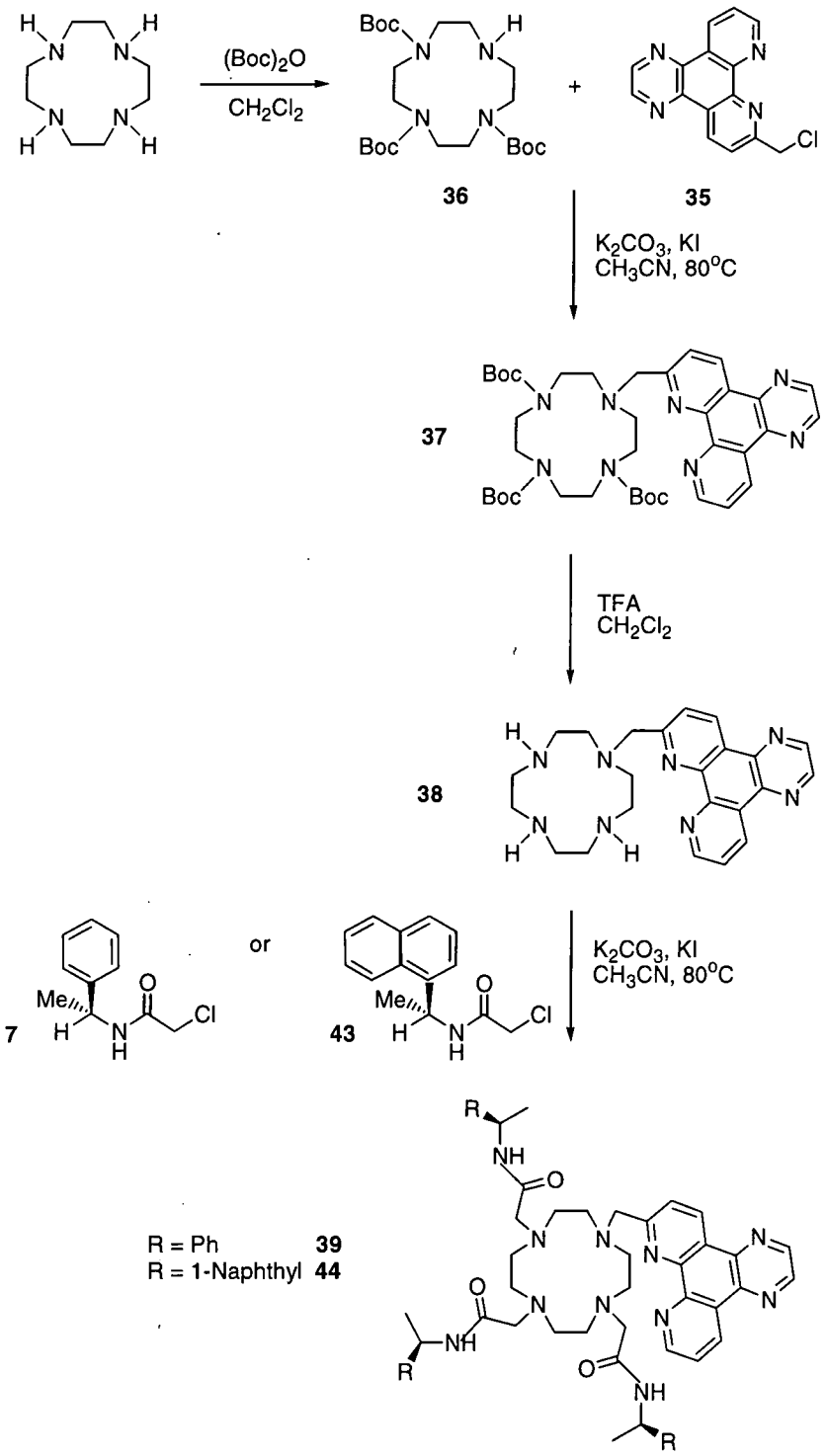

Scheme 5

The europium (**40**, **45**), terbium (**41**, **46**) and gadolinium (**42**, **47**) complexes were prepared in anhydrous acetonitrile by reaction of the ligands with the appropriate trifluoromethanesulphonate salt and purified by repeated precipitation onto dry diethyl ether. The final products were estimated to be 95% pure.

3.2. Characterisation of Δ- and Λ- $LnPh_3dpq$ Complexes

3.2.1. Solution ^1H NMR Studies

Proton NMR studies provided information about the structure of the complexes in solution. The spectra recorded in D_2O (see appendix) and CD_3OD at ambient temperature for Δ- and Λ-$EuPh_3dpq$ revealed a similar pattern, which resembled that observed for related triamide Eu complexes.[13,14] The most paramagnetically shifted 'pseudo-axial' ring protons of the macrocycle resonated as one set of four broadened singlets in the range 32-20 ppm. Such chemical shifts are consistent with the presence of a major species, adopting a square antiprismatic geometry. Previous work has established that this is the Λ(δδδδ) isomer for the complexes with an R configuration at each stereogenic centre at carbon and Δ(λλλλ) for those with an S configuration.

Increasing the temperature over the range 278-313 K in D_2O and 243-293 K in CD_3OD led to the shift to lower frequency and the broadening of the resonances expected as a consequence of the temperature dependence of the paramagnetic susceptibility. At low temperatures, additional small signals were observed, with chemical shifts close to the ones of the major species (within 2 ppm), which might indicate the presence of a minor isomer adopting the same geometry. If this is the case, the broadening of the signals upon temperature increase is most likely to be due to the interconversion of the two isomers as a consequence of an increased rate of ring inversion.

A ^1H-^1H COSY spectrum (CD_3OD, 500 MHz) was recorded at 243 K in order to confirm the partial assignment of the spectrum. In the region above 20 ppm, where four 'axial' protons of the $12N_4$ ring resonate, an additional signal was observed (31

ppm), which was identified with the proton in 10 on the dpq group. Chelation of the lanthanide ion by the nitrogens on the pyridine rings brings the *H10* on dpq close to the z-axis of the molecule, where it experiences a large positive paramagnetic shift.

3.2.2. CPL and Emission Spectra

The absolute configuration of the complexes was confirmed by circularly polarised luminescence spectroscopy. Mirror image CPL spectra were obtained for the Eu and Tb enantiomeric complexes (Fig.3.2).

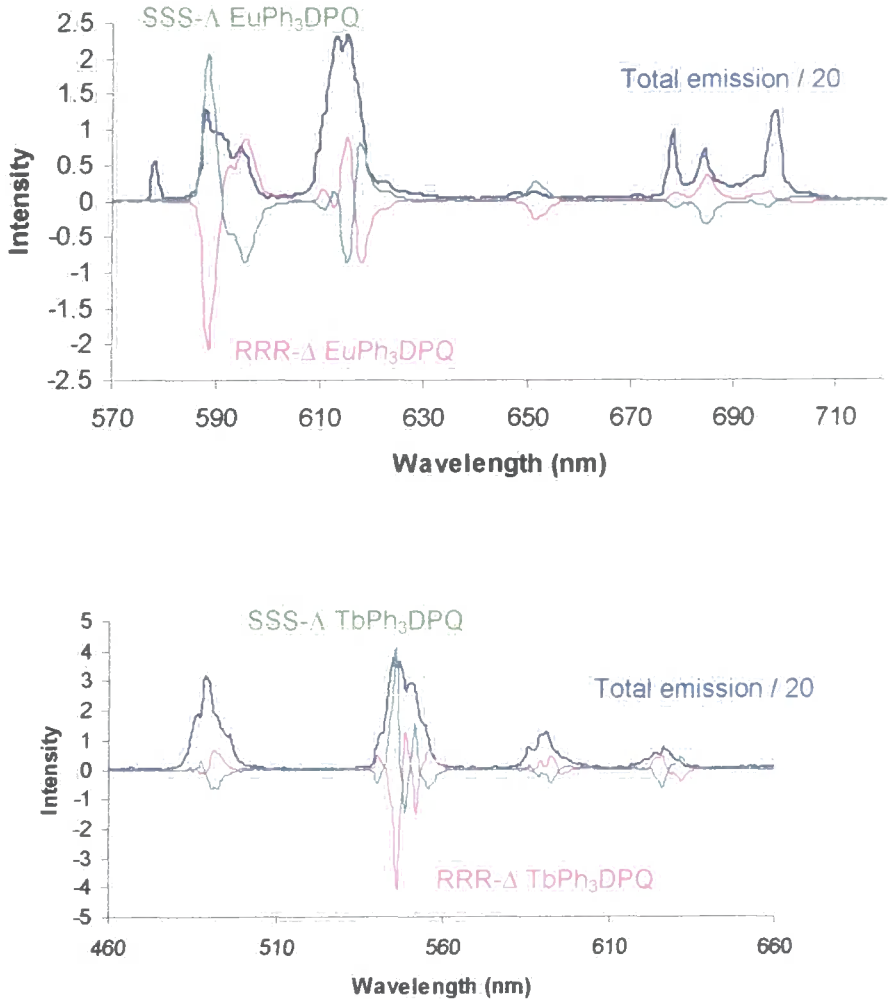

Fig.3.2 Mirror image CPL spectra of Δ- and Λ-$EuPh_3$dpq (upper) and Δ- and Λ-$TbPh_3$dpq (lower). The blue trace represents the corresponding total emission spectrum (λ_{exc} 340 nm, pH 7.4, 10 mM HEPES, 10 mM NaCl, 295 K).

Comparison of the sign and magnitude of the CPL of two complexes can provide structural information, because these parameters are determined by the helicity about the lanthanide centre.[15] The sequence of the sign of the transitions was the same as for the parent tetraamide $EuPh_4$ and $TbPh_4$ complexes,[11,16] except for the $\Delta J = 2$ band in the Eu spectra. This, on the one hand, confirms that the configuration of the (SSS) complexes was Δ and that of the (RRR) complexes Λ. On the other hand, it points out the sensitivity of the $\Delta J = 2$ band to the polarisability of the axial donor.[16] $EuPh_3dpq$ is peculiar in this respect, having a pyridine nitrogen donor in the axial position instead of a water molecule. The emission dissymmetry factors measured for the Ph_3dpq complexes in H_2O were compared to those reported for the Ph_4 analogues (Table 3.1).

Table 3.1 Emission dissymmetry factors measured, at different wavelength, for $LnPh_3dpq$ and $LnPh_4$ complexes (H_2O, 295 K).

	Δ-$EuPh_3dpq$	Δ-$EuPh_4$
g^{588}	+0.18	+0.09
g^{596}	-0.16	-0.09
g^{614}	-0.04	+0.08
	Δ-$TbPh_3dpq$	Δ-$TbPh_4$
g^{547}	+0.12	+0.27

The g factors found for the $\Delta J = 1$ band are of the same sign and almost double for Δ-$EuPh_3dpq$ compared to Δ-$EuPh_4$. A large difference is noticeable at 614 nm, where a negative factor was measured for the complex containing the dpq group. Negative values of g^{614} were found, for Δ-$EuPh_4$, only in HMPA, where the axial position is occupied by a molecule of this solvent, in which the P(V) oxygen is much more polarisable than the water oxygen.[16] The dissymmetry factor measured for Δ-

$TbPh_3dpq$ at 547 nm was about 50% lower than that of the Δ-$TbPh_4$ complex.[11] This also highlights the sensitivity of this transition to the nature of the axial donor atom.

The total emission spectrum of $EuPh_3dpq$ (blue in Fig.3.2) shows the features characteristic of complexes lacking axial symmetry: a $\Delta J = 1$ band including more than two transitions and an intense $\Delta J = 2$ band. The intensity of the latter also reflects the high degree of polarisability of the axial donor.[17]

No fluorescence was observed from the dpq chromophore, consistent with the expected high efficiency of the intersystem crossing process, as revealed in earlier studies with this chromophore.[1]

3.2.3. Hydration State

The number of water molecules coordinated to the lanthanide ion (q) was assessed by measuring the rate constants for depopulation of the Eu $^5D_0$ and Tb $^5D_4$ excited states in H_2O and D_2O and applying the following equations:[18]

$$q_{Eu} = 1.2\ (k_{H2O} - k_{D2O} - 0.25 - 3 \cdot 0.075)$$

$$q_{Tb} = 5\ (k_{H2O} - k_{D2O} - 0.06)$$

In each case, the complex was shown to possess no bound water molecules (Table 3.2). This result is in agreement with the relaxivity value measured, at 293 K and 65 MHz, for $GdPh_3dpq$ (3.5 $mM^{-1}s^{-1}$), which is only slightly higher than those reported for non-hydrated complexes of Gd with polyaminopolycarboxylic ligands (2-3 mM^{-1} s^{-1}).[19] This small difference, as well as the non-integral q value calculated for the Tb complex, may be interpreted in terms of a significant contribution to the measured relaxivity from the second-sphere of hydration, in which the amide carbonyl groups may act as hydrogen bond acceptors for closely diffusing water molecules.

Table 3.2 Radiative rate constants for decay of the lanthanide excited state, calculated q values and overall emission quantum yields in H_2O and D_2O (λ_{exc} 340 nm, pH 7.4, 10 mM HEPES, 10 mM NaCl, 295 K).

	k_{H_2O}	k_{D_2O}	q	φ_{H_2O}	φ_{D_2O}
$EuPh_3dpq$	0.95 ms^{-1}	0.61 ms^{-1}	0	21 %	27 %
$TbPh_3dpq$	0.54 ms^{-1}	0.42 ms^{-1}	0.3	36 %	46 %

3.2.4. Emission Quantum Yield

The quantum yield of emission (φ_{em}), defined as the ratio of the number of photons emitted to the number of photons absorbed, measures the efficiency of the emissive process. For sensitised emission, the overall quantum yield is related to the quantum yield for the formation of the antenna triplet state (φ_T), the efficiency of the energy transfer process (η_{ET}), the natural radiative rate constant (k^o) and the observed luminescence lifetime of the lanthanide (τ_{obs}) by the following equation:[20]

$$\varphi_{em} = \varphi_T \eta_{ET} k^o \tau_{obs}$$

The overall emission quantum yields of $EuPh_3dpq$ and $TbPh_3dpq$ were measured, in H_2O and D_2O, relative to known complexes (Fig.3.3).[14,21] The excitation wavelength used corresponds to the lowest-energy maximum in the excitation spectrum (i.e. the 0-0 transition of the antenna).

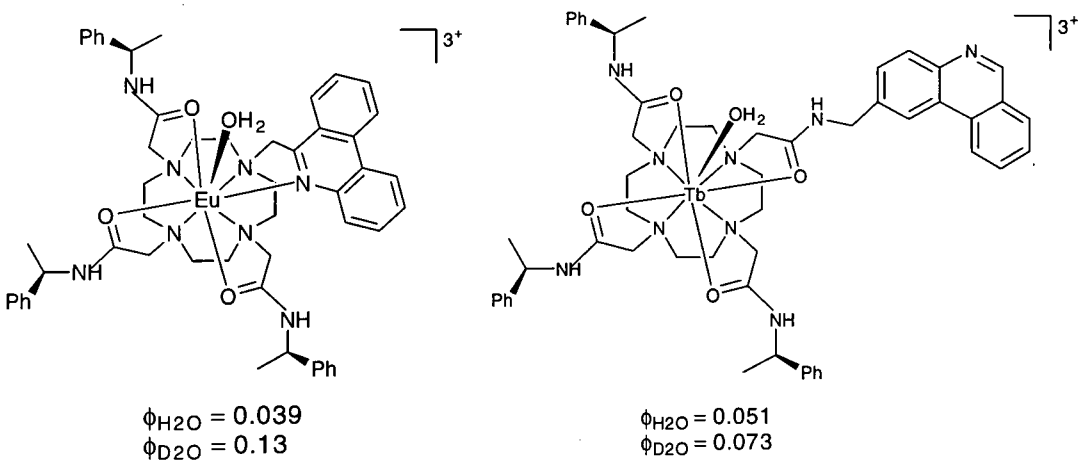

ϕ_{H2O} = 0.039
ϕ_{D2O} = 0.13

ϕ_{H2O} = 0.051
ϕ_{D2O} = 0.073

Fig.3.3 Complexes used as standards for quantum yield determination.

Very high quantum yields were obtained in each case (Table3.2). These represent the highest values reported for lanthanide complexes in aqueous media using excitation above 320 nm.

The values measured in D_2O do not differ much from those in H_2O, reflecting the absence of vibrational quenching by OH oscillators of coordinated water molecules and confirming the hydration state (q = 0).

Two other factors contribute to the high overall quantum yields observed: a high triplet quantum yield (φ_T), consistent with the absence of fluorescence from dpq, and an efficient energy transfer process (η_{ET}), due to the short distance between the dpq and the lanthanide centre, ensured by direct coordination.

The efficiency of energy transfer depends on the energy difference between the triplet state of the antenna and the emissive state of the lanthanide. The triplet energy of the dpq chromophore was measured for the Gd complex at 77 K in a MeOH/EtOH glass. Complexes of this lanthanide are normally used for the determination of the antenna triplet energy, as Gd cannot be sensitised, its first excited state (32,150 cm^{-1}) being well above the aryl triplet states.[17] From the shortest-wavelength transition (425 nm) in the phosphorescence spectrum (Fig.3.4) a value of 23,500 cm^{-1} was

derived, which is significantly higher than the Eu (17,200 cm^{-1}) and Tb (20,400 cm^{-1}) emissive states. Such a high energy difference precludes a thermally activated back energy transfer process at ambient temperature and ensures that the energy transfer step is very efficient.

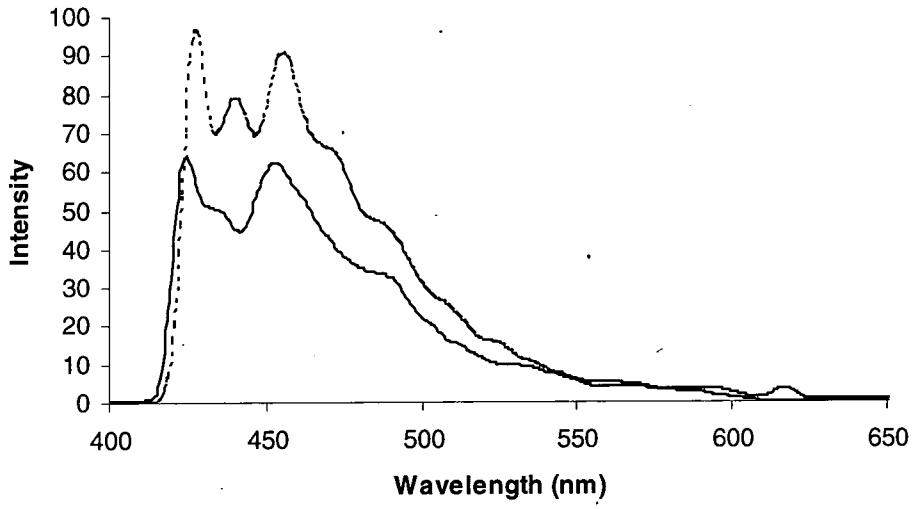

Fig.3.4 Phosphorescence spectrum of $GdPh_3dpq$ (solid line) compared to that of the antenna (dotted line) (λ_{exc} 340 nm, MeOH/EtOH 4:1, 77 K).

The high efficiency of energy transfer was consistent with the insensitivity of the radiative decay constants k to sample deoxygenation. Degassed solutions of Eu and $TbPh_3dpq$ gave the same values of k_{H2O} as those reported in Table 3.1 for oxygenated solutions. This means that quenching by molecular oxygen cannot compete with energy transfer for the depopulation of the triplet state, because the latter process occurs at a much higher rate.

3.2.5. Absorption and CD spectra

The absorption and CD spectra of the complexes were recorded at room temperature in aqueous solution. The absorption spectrum was compared to that of dpq itself: the shift to longer wavelength of the main two bands is further indirect evidence that the chromophore is coordinated to the metal (Fig.3.5).

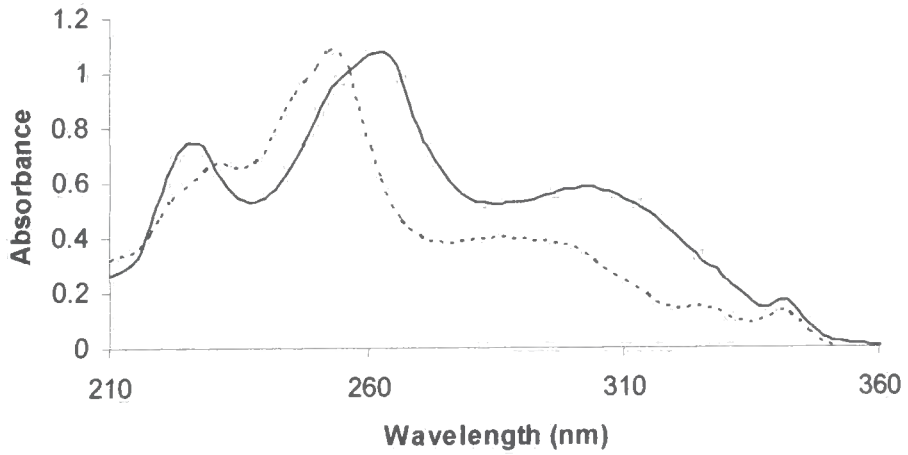

Fig.3.5 Absorption spectra of $EuPh_3dpq$ (H_2O, solid line) and dpq (MeOH, dotted line) (298 K).

The long-wavelength band at 340 nm allows selective excitation in biological media and averts the need for quartz optics. Moreover, the relatively high extinction coefficient at this wavelength (3000 $M^{-1}cm^{-1}$) makes the first step of the sensitisation process efficient and therefore contributes to the high overall quantum yield.

Weak, mirror-image signals, corresponding to the 340 nm band, were observed in the CD spectra of Δ- and Λ-$EuPh_3dpq$ (Fig.3.6).

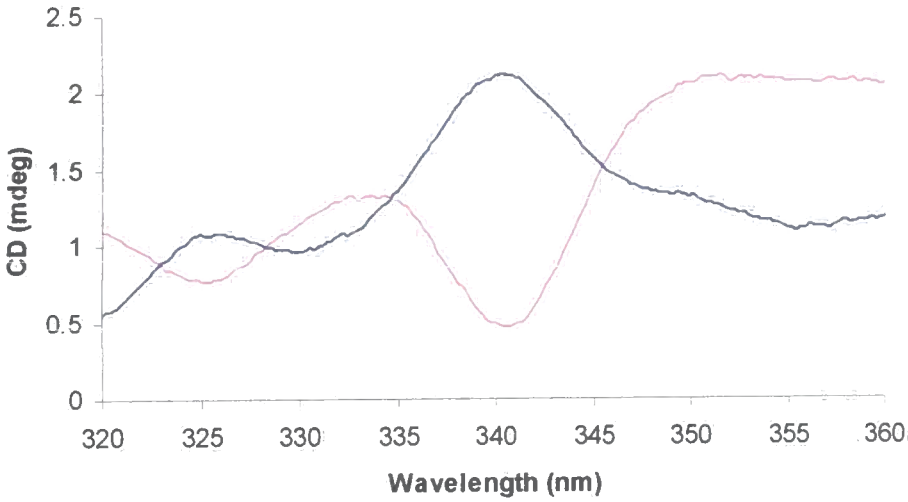

Fig.3.6 Mirror image CD spectra of dpq in Δ- (pink line) and Λ-$EuPh_3dpq$ (blue line) (H_2O, 298 K).

The intensity of the CD is low because it is a secondary effect of the chiral arms inducing a CD in the chromophoric but achiral dpq.

3.3. Interaction of Δ- and Λ- $LnPh_3dpq$ Complexes with Nucleic Acids

Spectroscopic studies of the interaction of Δ- and Λ- Eu and $TbPh_3dpq$ with poly(dAdT), poly(dGdC) and CT-DNA were carried out as described in chapter 2.

3.3.1. Absorption Spectra

Changes in the absorption spectra of the Eu and $TbPh_3dpq$ complexes were monitored as a function of added nucleic acid.

Incremental addition of poly(dAdT) to Δ- and Λ-Eu and to Λ-$TbPh_3dpq$ resulted in a decreased intensity of the band at 340 nm and a red shift, with formation of a well-defined isosbestic point at 345.5 nm (Fig.3.7). The same effect was observed upon addition of CT-DNA to Δ-$EuPh_3dpq$, whereas poly(dGdC) caused very small changes in the absorption spectra of each of the complexes under study.

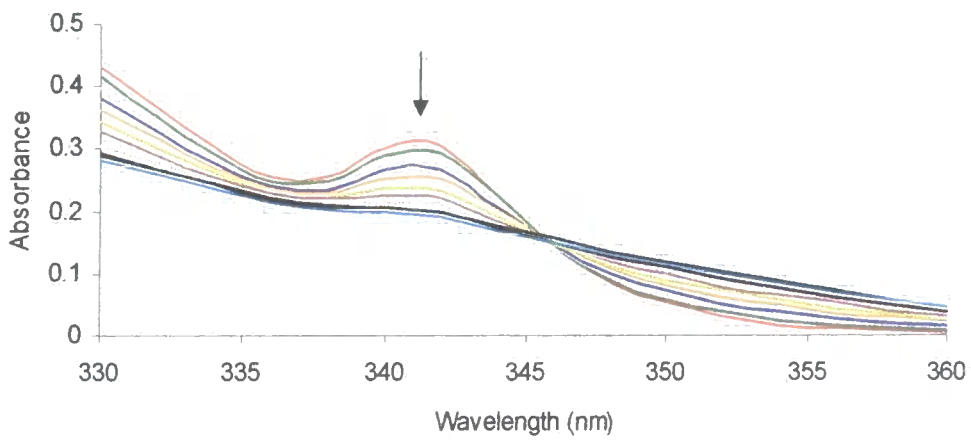

Fig.3.7 Changes in the absorption spectra of Λ-$EuPh_3dpq$ (60 μM) following addition of poly(dAdT) (4.5 mM) from 0 to 4 base-pairs per complex (pH 7.4, 10 mM HEPES, 10 mM NaCl, 295 K).

A rather high percentage of hypochromism (20%) was obtained for Λ-$EuPh_3dpq$ in the presence of poly(dAdT), while 10-15% hypochromism was observed in the other three cases.

The changes described are consistent with a charge transfer interaction between the metal-bound chromophore and the DNA bases, suggesting, but not proving, an intercalative binding mode, especially where the hypochromic effect observed was large.

3.3.2. CD Spectra

The binding interaction was also examined by circular dichroism difference spectroscopy. Addition of Λ-$EuPh_3dpq$ to a solution of poly(dAdT) resulted in a change in the intensity of the nucleic acid CD spectrum at 246 and 264 nm. No change occurred in the gross features of the spectrum, ruling out any transition from B-DNA to either an A- or a Z-form (Fig.3.8).

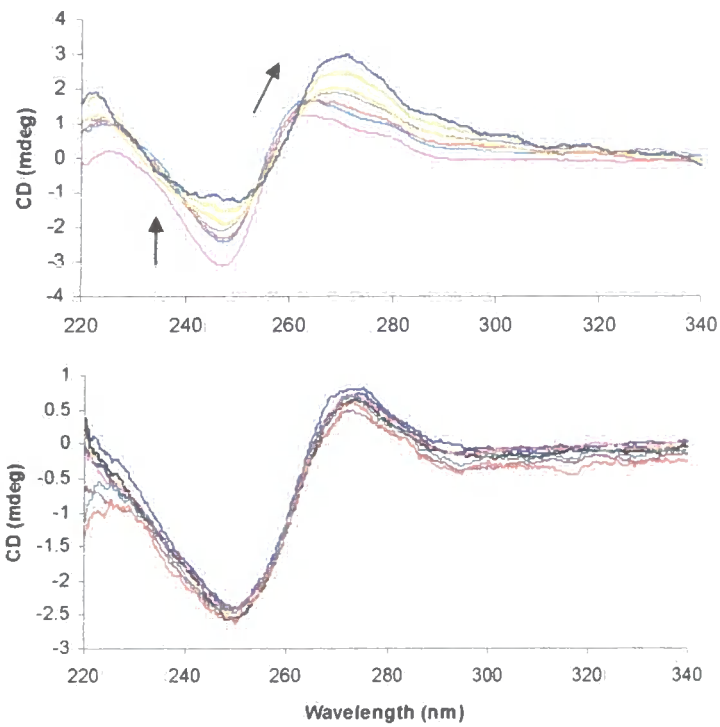

Fig.3.8 CD difference spectra of poly(dAdT) in the presence of increasing ratios (0-1.3 complex molecules per base-pair) of Λ- (upper) and Δ-$EuPh_3dpq$ (lower) (pH 7.4, 10 mM HEPES, 10 mM NaCl, 295 K).

The negative band at 246 nm showed a 65% reduction in intensity and the positive band a 200% increase, together with a 7 nm shift to the red. No significant changes were observed upon interaction of the Δ complex with poly(dAdT) (Fig.3.8), nor for either enantiomer with poly(dGdC).

Changes in the CD spectra of the dpq chromophore were also monitored. Following addition of poly(dAdT), Λ-$EuPh_3$dpq showed a decrease in the intensity at 340 nm and a red shift of 5 nm (Fig.3.9).

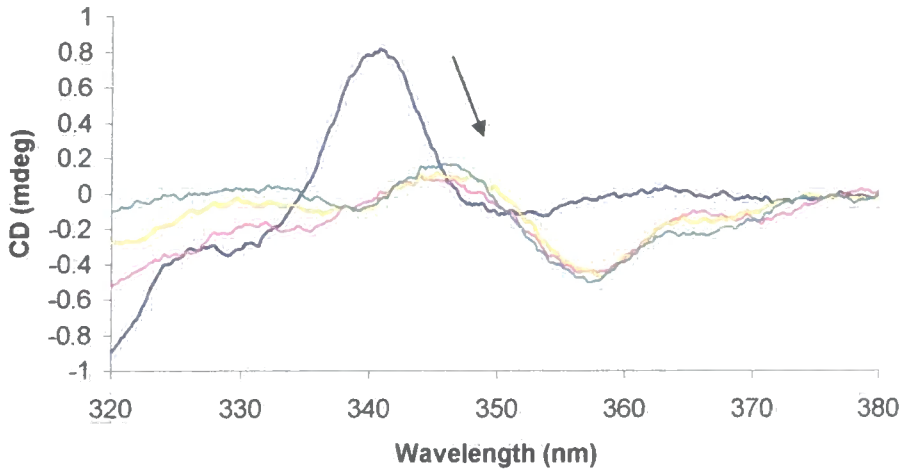

Fig.3.9 CD difference spectra for Λ-$EuPh_3$dpq (0.1 mM) following addition of poly(dAdT) (1.8 mM) from 0 to 2 base-pairs per complex (pH 7.4, 10 mM HEPES, 10 mM NaCl, 295 K).

No change in this region was apparent in the CD spectrum of Λ-$EuPh_3$dpq when poly(dGdC) was added, nor in the spectra of Δ-$EuPh_3$dpq in the presence of either polynucleotide.

Thus, for the system Λ-$EuPh_3$dpq/poly(dAdT), the correlated changes in the CD spectra of the nucleic acid and of dpq confirm the hypothesis of an intercalative binding interaction based on the hypochromic effect described above.

Intercalation brings the chromophore close to the DNA bases, resulting in an induced CD in its transition at 340 nm. On the other hand, the interaction also causes a change in the local helicity and pitch of the nucleic acid, which is reflected in its CD spectrum.

3.3.3. Emission Spectra

Changes in the emission spectra of the europium and terbium complexes were recorded as a function of added polynucleotide following excitation at 345.5 nm. In general, quenching of the lanthanide emission was observed, which was more efficient for the Δ isomers (Fig.3.10-3.11). For Eu, the decrease in intensity at 590 nm is believed to represent only the quenching effect, because the $\Delta J = 1$ transition is magnetic dipole allowed and its intensity is relatively independent of changes in the electronic coordination environment.

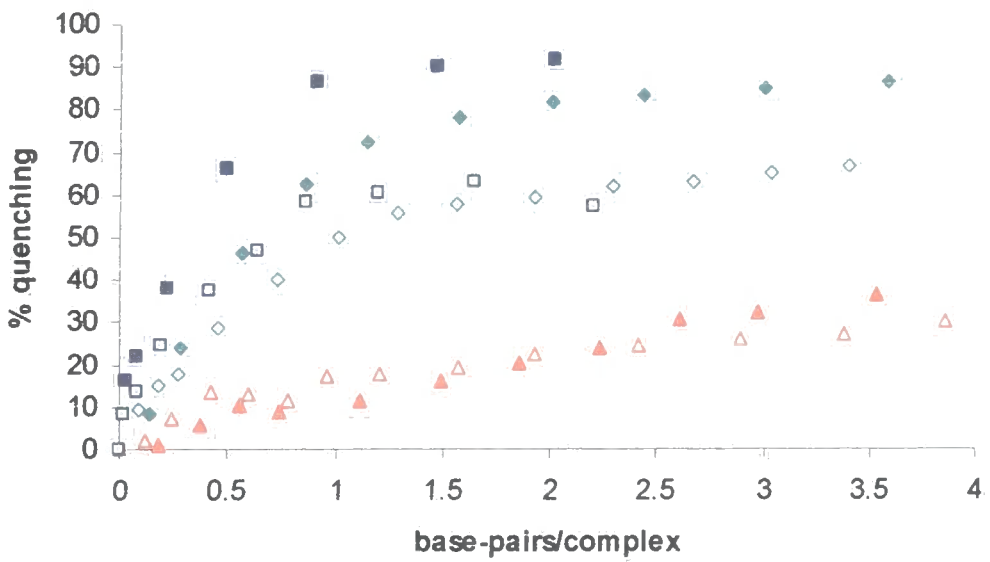

Fig.3.10 Percentage quenching at 590 nm for Λ- (empty symbol) and Δ-$EuPh_3dpq$ (filled symbol) as a function of added CT-DNA (□), poly(dGdC) (◊) and poly(dAdT) (Δ).

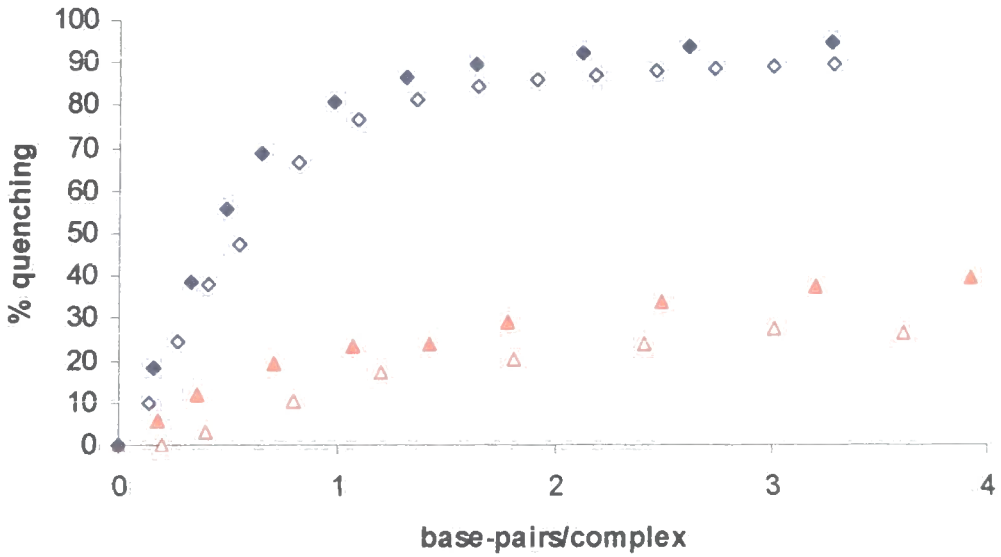

Fig.3.11 Percentage quenching at 543 nm for Λ- (empty symbol) and Δ-$TbPh_3dpq$ (filled symbol) as a function of added poly(dGdC) (◊) and poly(dAdT) (Δ).

The nucleic acids containing the more electron-rich C and G bases gave rise to a greater quenching effect (60-90% compared to 20-30% in the presence of poly(dAdT)), which apparently reached a maximum at lower base-pairs per complex ratio (1-1.5 compared to 3-4 base-pairs/complex). A saturating limit of 1.5 base-pairs per complex also corresponds to neutralisation of the tripositive charge of the complex by the negative phosphate groups of the nucleotides.

The quenching process was associated with a decrease in the lifetime of the lanthanide emission (Table 3.3), consistent with direct quenching of the metal-based excited state. The changes in emission lifetime mirrored the differences in intensity highlighted above (Δ > Λ and CG >> AT). Moreover, the effect was greater for Tb than Eu and was insensitive to the degree of sample deoxygenation.

Table 3.3 Lifetimes (τ/ms ±10%) for europium and terbium complexes in the absence and presence of poly(dAdT) and poly(dGdC) at saturation state (λ_{exc} 340 nm, pH 7.4, 10 mM HEPES, 10 mM NaCl, 295 K).

	Free complex	+ poly(dGdC)	+ poly(dAdT)
Δ-$EuPh_3dpq$	1.05	0.79	1.04
Λ-$EuPh_3dpq$	1.05	0.88	1.18
Δ-$TbPh_3dpq$	1.85	0.85	1.59
Λ-$TbPh_3dpq$	1.85	1.11	1.75

Only the emission spectrum of Λ-$EuPh_3dpq$ changed in form following addition of nucleic acid. The changes were more evident in the presence of poly(dAdT) than poly(dGdC), with CT-DNA showing an intermediate situation. Addition of polynucleotide resulted in enhanced resolution of the $\Delta J = 1$ band and a greater decrease in the intensity at 681 nm compared to 687 nm, within the $\Delta J = 4$ manifold (Fig.3.12).

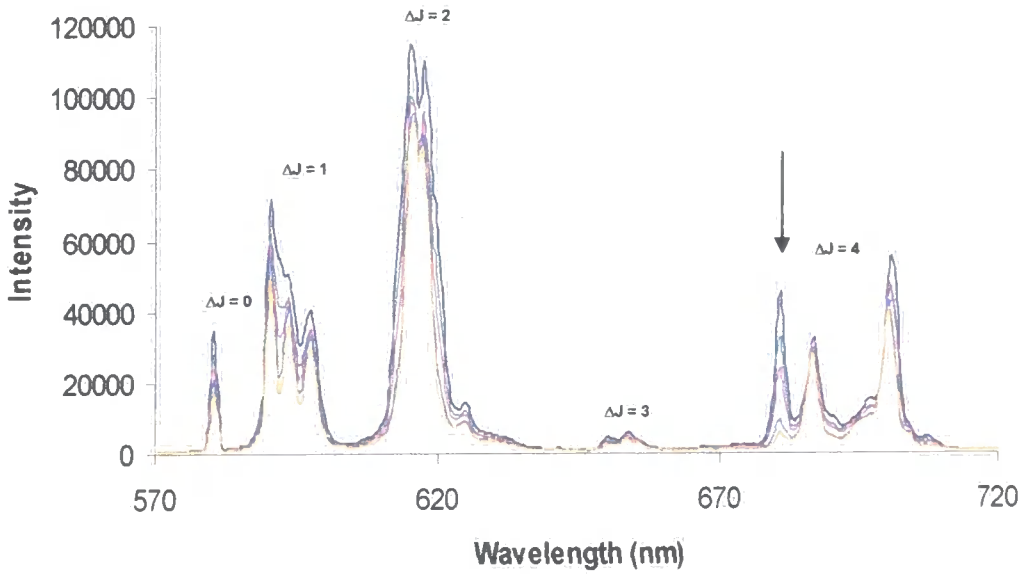

Fig.3.12 Emission spectra of Λ-$EuPh_3dpq$ (60 μM) upon addition of poly(dAdT) (4.5 mM) from 0 to 4 base-pairs per complex (λ_{exc} 340 nm, pH 7.4, 10 mM HEPES, 10 mM NaCl, 295 K).

These changes were tentatively ascribed either to the presence of two stereoisomers with different binding affinity or to a perturbation of the polarisability of the axial donor. The form of the ΔJ=1 band suggests the presence of a minor isomer because it seems to contain a fourth component at 592 nm, in addition to the three transitions expected for an asymmetric complex. This species may be favoured by the interaction and quenched at higher rate, thus allowing the three peaks of the major isomer to show more clearly.

The second interpretation is based on the sensitivity of the ΔJ = 4 band to the nature and polarisability of the axial donor atom.[22] The interaction with the nucleobases may perturb the electronic distribution in the dpq moiety and the polarisability of the axially-positioned pyridine N-donor.

The changes in the form of the emission spectrum of Λ-$EuPh_3$dpq can be correlated to the hypochromism manifested in the absorption spectra in the presence of poly(dAdT). By plotting the % hypochromism and the ratio of the emission intensity at 681 and 687 nm versus the number of base-pairs per complex, the same trend was observed (Fig.3.13).

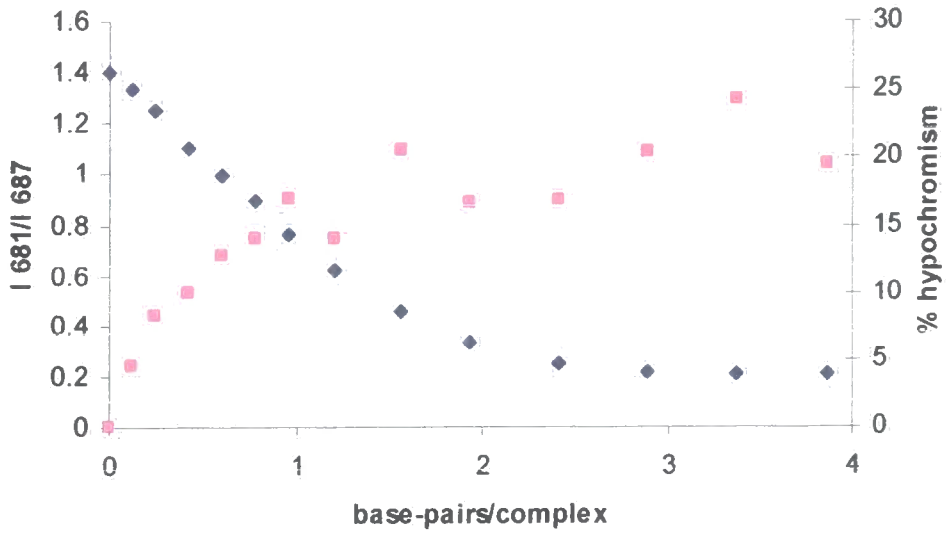

Fig.3.13 Degree of hypochromism (■) and changes in the ratio of the intensity at 681 and 687 nm (◆) as a function of poly(dAdT) base-pairs per Λ-$EuPh_3$dpq complex.

A limiting value of 2 base-pairs per complex is obtained in each case, which is consistent with the 'neighbour exclusion' principle[23] that characterises the intercalative binding mode.

These results, together with the CD spectral changes, suggest that intercalation occurs only in the absence of C and G bases and is enantioselective (Λ isomer only). On the contrary, in the presence of C and G, a different interaction prevails, which causes the quenching of the lanthanide luminescence and shows higher affinity for the Δ enantiomer.

A charge transfer interaction of the complex with the bases may explain the deactivation of the lanthanide excited state. Considering the reduction potentials measured for Tb and Eu in similar complexes ($E_{1/2}$ = -3.5 V for Tb^{3+}, -1.1 V for Eu^{3+}),[24] Eu is expected to be more sensitive to quenching, if an electron transfer process occurs from the nucleobases. However, the extent of quenching obtained for $TbPh_3dpq$, particularly in the presence of C-G base-pairs, was higher than for $EuPh_3dpq$. To explain this, an MLCT state may be proposed to participate in the electron transfer process. Such an excited state would be produced more easily in Tb complexes, as a consequence of a charge transfer from the metal to the dpq group. Although there is no direct evidence for an MLCT state, either in absorption or emission spectra, it may represent a transient species, which can be detected only in time-resolved studies.

3.3.4. Competitive Quenching Experiments

Iodide ions are efficient quenchers of aryl singlet excited states.[25] The quenching is collisional in nature and can be described by the Stern-Volmer equation:

$$F_o/F = 1 + k_q \tau_o [Q] = 1 + K_{SV} [Q]$$

where F_o and F are the fluorescence intensities in the absence and presence of quencher, k_q is the bimolecular quenching constant, τ_o is the emission lifetime in the

absence of quencher and [Q] is the concentration of quencher. The Stern-Volmer quenching constant, K_{SV}, is given by $k_q \tau_o$.

The plot of F_o/F versus [Q] is normally linear and its slope is equal to K_{SV}, from which k_q can be derived. The bimolecular quenching constant provides information about the efficiency of the process.

Experiments with the tetraamide complexes described in the previous chapter showed that iodide efficiently quenches the phenanthridinium singlet excited state.[21] In similar experiments with Λ- and Δ-$EuPh_3$dpq, quenching of the lanthanide emissive state was observed instead. Incremental addition of iodide ions caused a decrease in the emission intensity, accompanied by a decrease in the lifetime of the metal excited state, which obviously would not occur if only the excited dpq chromophore was quenched.

A Stern-Volmer plot was obtained for each enantiomer (Fig.3.14), which gave K_{SV} values of the order of $10^2\ M^{-1}$. Considering τ_o = 1.05 ms (Table 3.3), a k_q value of $10^5\ M^{-1}s^{-1}$ was calculated. This value is low compared to those normally found for iodide quenching of aryl excited states ($10^{10}\ M^{-1}s^{-1}$),[25] due to the longer emission lifetimes of lanthanide ions. A small value of k_q is consistent with the inefficiency of the quenching process, due to the inaccessibility of the nine-coordinate metal, which is shielded within the complex, to the quencher.

Competitive quenching experiments with I^- were performed in the presence of polynucleotides. Competition between charge transfer quenching by nucleobase interaction and quenching involving electron transfer from I^- gives useful comparative information.

Addition of poly(dAdT) reduced the initial K_{SV} values by about 50%, independent of complex helicity. In the presence of poly(dGdC), an 80% decrease was observed for Δ-$EuPh_3$dpq, while the K_{SV} of Λ-$EuPh_3$dpq remained unchanged (Fig.3.14).

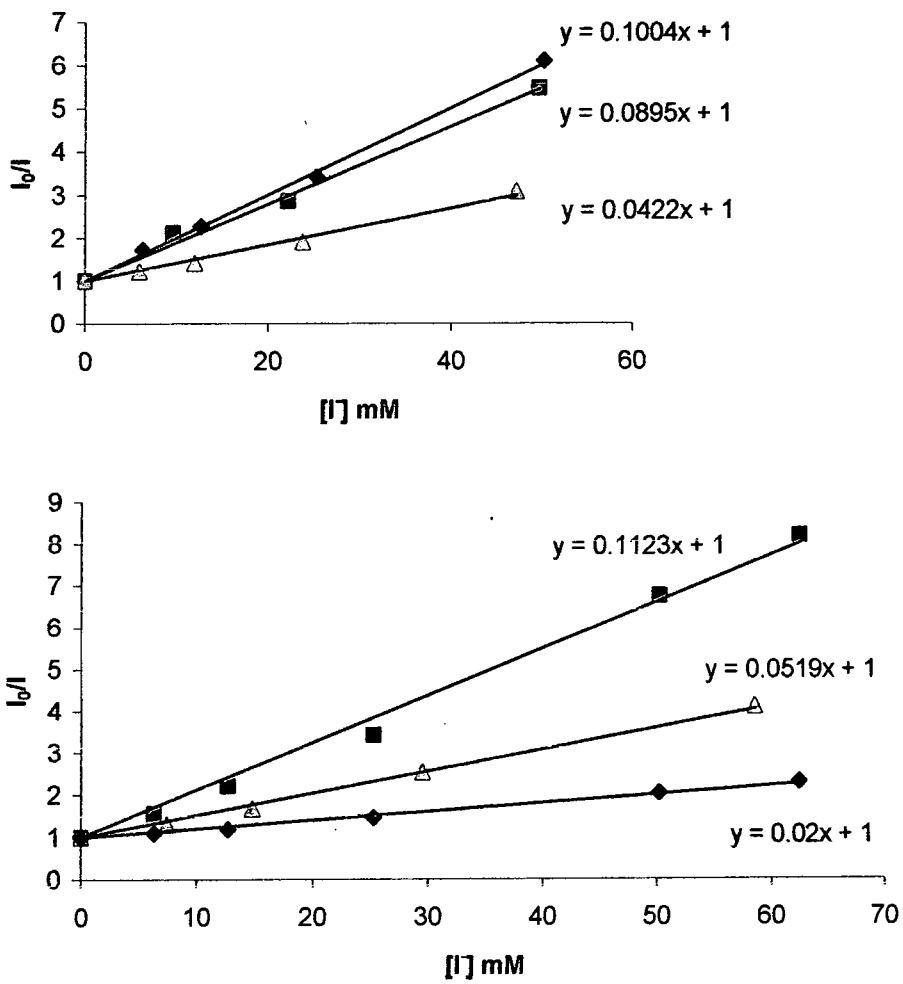

Fig.3.14 Stern-Volmer plots for iodide quenching of Λ- (upper) and Δ-$EuPh_3dpq$ (lower) in the absence (■) and in the presence of poly(dGdC) (♦) and poly(dAdT) (▲)(λ_{exc} 340 nm, pH 7.4, 10 mM HEPES, 10 mM NaCl, 295 K).

The extent of quenching is decreased as a consequence of the interaction with the nucleic acid, which shields the lumophore from the iodide ions and electrostatically prevents their approach. The order of quenching inhibition can be correlated to the apparent affinities estimated on the basis of the emission spectral changes. Δ-$EuPh_3dpq$ shows indeed the biggest change in K_{SV} following addition of poly(dGdC), while the changes in the presence of poly(dAdT) are smaller and equal for the two enantiomers. Only the behaviour of Λ-$EuPh_3dpq$ in the presence of

poly(dGdC) does not follow the same trend, which indicates that, in this case, the metal is equally exposed to I^- quenching in the free and bound states, suggesting that the complex is unlikely to penetrate well into the DNA grooves.

Quenching experiments have often been used to prove intercalation of transition metal complexes between the DNA base-pairs.[26,27] However, emission from dpq is not observed in our complexes, therefore quenching experiments cannot provide any information about the binding mode of the molecule. Quenching of europium luminescence cannot give this information because it is the dpq, and not the lanthanide, that is inserted between the nucleobases and is shielded to a greater extent in an intercalative binding mode.

3.3.5. Control Experiments

a. In order to understand the contribution of the electrostatic interaction between the positively charged complexes and the negatively charged DNA to the overall binding, changes in the absorption and emission spectra of Λ-$EuPh_3$dpq were monitored upon addition of a solution of Na_2HPO_4. The range between 0 and 8 phosphate molecules per complex was considered, which is comparable to 0-4 base-pairs per complex. It was found that both the absorption and emission spectra maintained their form, therefore it can be concluded that the spectral changes observed in the titrations with nucleic acids were not simply due to the interaction of the tripositively charged complexes with the phosphate groups on the DNA backbone. After accounting for dilution, a small decrease (10%) in the absorbance at 340 nm was calculated, mirrored by a similar decrease in the emission intensity. This confirms that the small percentage of hypochromism observed for Δ-$EuPh_3$dpq and Λ-$TbPh_3$dpq in the presence of poly(dAdT) was probably not due to intercalation, consistent with the absence of changes in the CD spectra, but may be associated with the contribution of the electrostatic interaction to the overall binding.

b. The effect of the ionic strength on the spectral features of Λ-$EuPh_3$dpq was also studied, by increasing the concentration of NaCl between 0 and 100 mM. Again, no change in the form of the absorption and emission spectra was apparent. Only a small decrease in the emission intensity occurred, which may be due to quenching by chloride ions. In parallel experiments with Λ-$EuPh_3$dpqC, containing a cyclohexyl derivative of dpq,[28] the ionic strength proved to affect the binding affinity between the complex and poly(dAdT). Titrations carried out in the presence of different concentrations of NaCl gave rise to the same maximal value of hypochromism. However, saturation was reached at higher base-pairs per complex ratios in solutions of high ionic strength, reflecting a decreased affinity, due to the presence of an intercalative binding not associated to an electrostatic interaction. A similar combination of intercalative and electrostatic contributions to the overall binding is believed to occur in the interaction between Λ-$EuPh_3$dpq and poly(dAdT).

c. The kinetics of the interaction was followed by recording the changes in the absorption and emission spectra of Λ-$EuPh_3$dpq in a solution containing 2 base-pairs of poly(dAdT) per complex. An overall 20% decrease in the emission intensity occurred in the first 4 hours, after which time no further decrease was observed. All the titration experiments were typically run in a shorter time (2-3 hours), so an experimental error of the order of 10% should be considered for the quenching values obtained.

d. Changes in the absorption and emission spectra of Λ-$EuPh_3$dpq in the pH range 1-7 were monitored following addition of trifluoroacetic acid. The absence of change showed that protonation of the pyrazine nitrogen atoms does not perturb the polarisability of the dpq chromophore and cannot be at the origin of the emission spectral changes observed for this complex in the presence of each nucleic acid. The high stability of the complex with respect to acid catalysed dissociation was also confirmed.

e. An emission spectrum of Λ-EuPh$_3$dpq was recorded in acetonitrile to investigate the role of solvent polarity. The form of this spectrum was slightly different from that obtained in water (Fig.3.15).

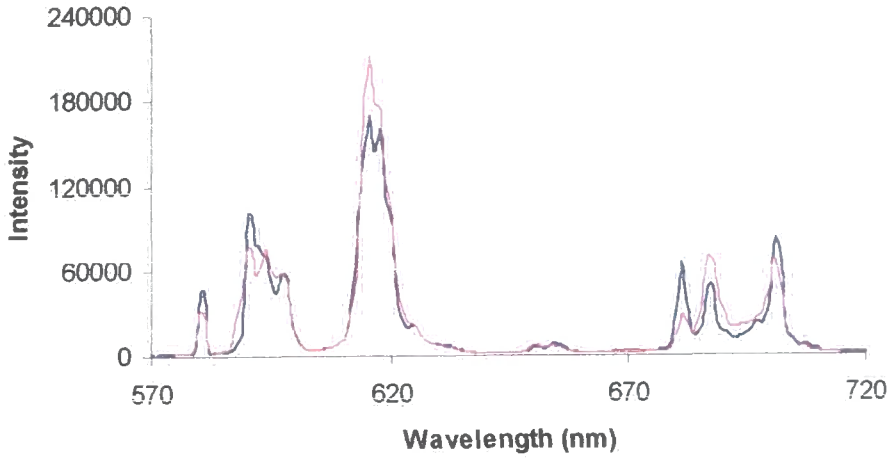

Fig.3.15 Emission spectra of EuPh$_3$dpq in H_2O (blue line) and CH_3CN (pink line) (λ_{exc} 340 nm, 295 K).

The $\Delta J = 1$ band showed three well-defined transitions, whereas in the $\Delta J = 2$ manifold, one main transition was apparent at 615 nm. Within the $\Delta J = 4$ manifold, the band at 681 nm was lower than that at 686 nm. Their relative intensities were reversed in the spectrum of the aqueous solution. The features of the emission in acetonitrile were found to be similar to those observed for the same complex in the presence of nucleic acids. A different solvation of the overall complex is therefore likely to be the cause of these changes. Two sources of hydrogen bonding may be identified in the molecule: the nitrogens on the pyrazine ring of dpq (H-bond acceptors) and the amide groups (with the nitrogens as H-bond donors and the oxygens as H-bond acceptors). That water can form hydrogen bonds to the amide groups was revealed by X-ray analysis of hydrated tetraamide Eu complexes[29] and is consistent with the relaxivity values measured for GdPh$_3$dpq. In acetonitrile, which cannot act as a hydrogen bond donor and is only a very weak acceptor, the electronic distribution in the amide

groups is different. As the amide carbonyls are linked to the lanthanide, the latter will experience a slightly different ligand field, which is reflected by changes in the form of the emission spectrum. The ^{1}H NMR spectrum of the complex in CD_3CN was also expected to show the effect of a different solvation. However, no significant change in the value of the chemical shifts was observed, upon comparison with the ^{1}H NMR spectra recorded in CD_3OD and D_2O. It must be concluded that the effect of this perturbation is more evident in the excited state (reflected by emission spectra) than in ground state (reflected by NMR spectra).

3.3.6. Phosphorescence Spectra

In order to investigate whether the interaction with nucleic acids results in a perturbation of the triplet energy level of the chromophore, a phosphorescence spectrum of $GdPh_3dpq$ in the presence of poly(dGdC) was recorded.

Glycerol was added to a buffered aqueous solution of $GdPh_3dpq$ and poly(dGdC) in a ratio of 2.5 base-pairs per complex, higher than the saturation value found in emission experiments with this polynucleotide.

A 1:1 mixture of glycerol/water was used, instead of MeOH/EtOH, to avoid any change in the conformation of the nucleic acid. CD studies have previously shown that these two alcohols have a big effect on the DNA secondary structure and can reduce the number of bases per turn of helix.[30]

The spectrum obtained was similar to that recorded in the absence of DNA (Fig.3.16), with a shortest wavelength transition at 431 nm, corresponding to a triplet energy of 23,200 cm^{-1}.

This experiment shows that the quenching observed in the emission spectra of the complexes, as a consequence of the interaction with nucleic acids, does not involve a significant perturbation of the dpq triplet energy level.

The oligonucleotide $[(AT)_6]_2$ was used in this case, because it possesses a known and well-defined molecular weight, so that an amount corresponding to 2 base-pairs per complex could be weighed and added to the NMR sample of Λ-$EuPh_3dpq$. A spectral titration experiment, analogous to those performed with polynucleotides, had revealed the same changes in the form of the emission spectrum, reaching saturation close to 1 base-pair per complex.

No differences in the position of the proton resonances nor in the intensity of the minor isomer signals were observed. The complex, therefore, does not seem to undergo any structural change as a consequence of the interaction, supporting the conclusion, drawn on the basis of the CPL spectra, that the local symmetry about the lanthanide ion and the overall coordination geometry of the complex are conserved. The hypothesis of a minor isomer which interacts preferentially with DNA may thus be discarded.

A two-dimensional NMR experiment was also performed, with the aim of clarifying the regioselectivity in the interaction of the Ph_3dpq complexes with nucleic acids containing a mixed sequence of bases. The palindromic oligonucleotide $[CGCGAATTCGCG]_2$ was used, because its ^1H NMR spectrum has been fully assigned.[31] The paramagnetic effect of Gd was exploited: it gives rise to relaxation of the nucleobases nearest to the complex binding site and suppresses their resonances without causing a shift.

The disappearance of cross-peaks in the COSY spectrum of the oligonucleotide was monitored, following addition of low concentrations of Λ-$GdPh_3dpq$. Addition of 0.01 equivalents led to loss of the cross-peaks corresponding to G-4 and A-5. When 0.02 equivalents were added, some signals of C-3 began to be lost and disappeared completely at 0.05 equivalents, together with peaks belonging to T-8 and G-12. The signals for C-1, C-9 and C-11 were clearly evident even after addition of 0.05 equivalents of $GdPh_3dpq$.

Although the resonances for the other four bases of the oligomer could not be unequivocally identified in the initial ^1H NMR spectrum, making their suppression impossible to follow, some information can still be obtained from this experiment. The complex seemed to bind with higher affinity toward the centre of the

oligonucleotide, in the AATT region, supporting the higher affinity of the Λ isomer for these bases, observed in the absorption and CD titrations with poly(dAdT).

3.4. Summary and Conclusions

Europium and terbium complexes with the Ph_3dpq ligand proved to be strongly luminescent, as a result of the favourable photophysical properties of the dpq chromophore, as well as the nonadentate nature of the ligand. They represent improved luminescent probes with respect to the complexes described in the previous chapter. Despite the higher extinction coefficient at the excitation wavelength, the phenanthridinium antenna did not lead to highly efficient sensitisation, due to radiative deactivation of the singlet excited state and depopulation of the triplet state by molecular oxygen quenching. The dpq based complexes, on the contrary, showed high quantum yields of sensitisation, as a consequence of efficient intersystem crossing and energy transfer processes.

The interaction with nucleic acids is signalled by the two systems in rather different ways. In the complexes with a phenanthridinium chromophore, the singlet excited state of the antenna was perturbed, while in the Ph_3dpq complexes the emissive state of the lanthanide ion was quenched. Both quenching processes are believed to involve a charge transfer interaction with the electron-rich nucleobases. The efficiency was found to increase in the presence of guanine, which is the most readily oxidised of the DNA bases.

A certain degree of stereoselectivity can be discerned in the interaction of the Ph_3dpq complexes with nucleic acids. The greater quenching effect shown by Δ-EuPh_3dpq in the presence of cytosine and guanine may indicate a higher affinity for these bases, compared to the Λ isomer. The binding mode, however, is still uncertain. Purely electrostatic binding has been ruled out on the basis of the results obtained in control experiments. The absence of change in the CD spectra and of hypochromism in the absorption spectra indicates that intercalation does not occur. A groove-binding interaction may be present, which, however, should give rise to induced CD spectral changes.

The Λ isomer of $EuPh_3dpq$, on the other hand, shows a well-defined interaction with poly(dAdT), consistent with a predominantly intercalative binding mode, as strongly indicated by the large absorption and CD spectral changes. Insertion of dpq between the nucleobases causes a perturbation in the polarisability of the axial donor atom, which is reflected in a change in the form of the Eu emission spectrum, but not in the geometry around the lanthanide.

The fact that the interaction is stereoselective suggests that the groove is involved. A possible model is for intercalation of the Λ isomer from the minor groove, in a manner that is not accessible for the Δ isomer.

3.5. Characterisation of Δ- and Λ- $LnNp_3dpq$ Complexes

The naphthyl analogues of the Ph_3dpq complexes were synthesised (Fig.3.17), in order to investigate the effect of larger aromatic groups in the pendant arms on binding affinity and base selectivity.

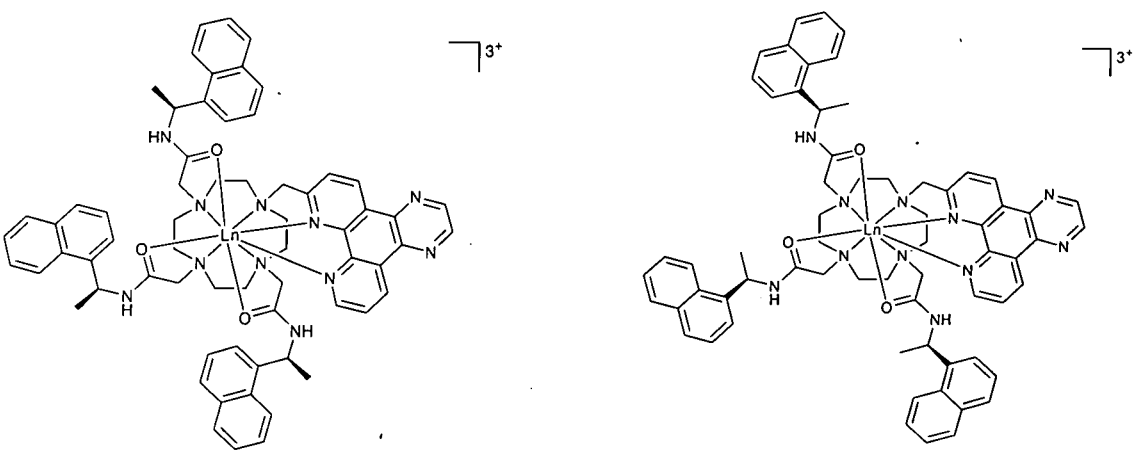

Fig.3.17 Enantiomeric Δ (left) and Λ (right) $EuNp_3dpq$ complexes.

As for the complexes bearing phenyl groups, ^1H NMR spectra revealed the presence of one major stereoisomer in solution, adopting a square antiprismatic geometry. No minor isomer was apparent in this case, probably due to the higher rigidity of the molecule. The bulky naphthyl groups may further decrease the rate of arm rotation

and ring inversion is slow on the NMR timescale at ambient temperature (< 40 s^{-1} at 298 K for typical ninecoordinate Ln complexes).[15]

3.5.1. CD Spectra

The correlation between the absolute configuration at the chiral centres and the clockwise or anticlockwise arrangement of the pendant arms in the complex was made possible by circular dichroism studies.

Mirror image CD spectra were recorded for (RRR)- and (SSS)-$EuNp_3dpq$. The weak signal at 340 nm, corresponding to the dpq chromophore, was positive for the former and negative for the latter, as observed for the Ph_3dpq complexes (Fig.3.6). By analogy, Λ(δδδδ) and Δ(λλλλ) configurations were assigned to the R and S enantiomers respectively.

The most striking feature of the CD spectra was the presence of two bands of opposite sign in the naphthyl absorption region, which was associated with exciton coupling (Fig.3.18).

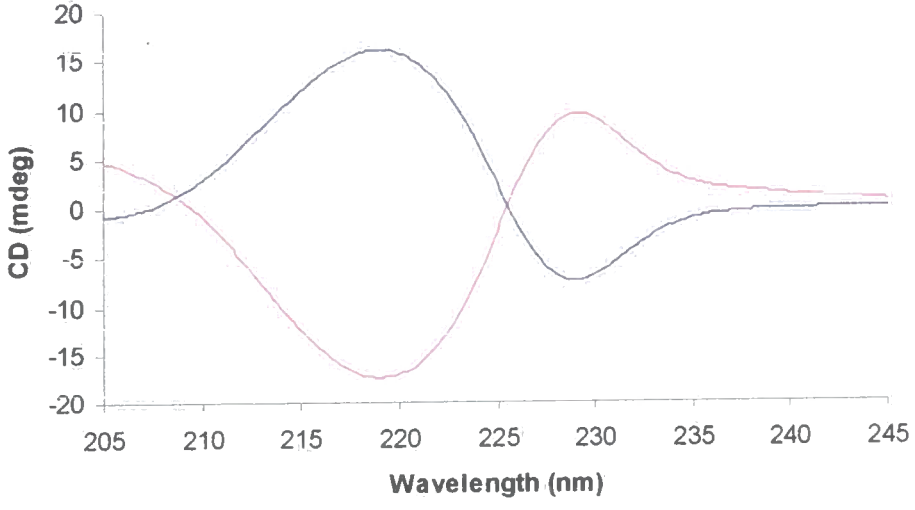

Fig.3.18 Mirror image CD spectra of Δ- (blue line) and Λ-$EuNp_3dpq$ (pink line), showing exciton coupling between adjacent naphthyl chromophores (H_2O, 298 K).

This coupling is ascribed to a dipole-dipole interaction between the electric transition moments of two naphthyl chromophores which gives rise to the bisignate profile.

The sign of the band at the longer wavelength defines the chirality of the molecule.[32] The parent tetranaphthyl $EuNp_4$ complexes showed similar exciton coupling, with the same Davydov splitting between the two bands (10 nm), of positive chirality for the R enantiomer and negative for the S. The R and S enantiomers proved to possess a Λ and Δ disposition of the chiral arms respectively,[33] which is consistent with the assignment made previously by comparing $EuNp_3dpq$ and $EuPh_3dpq$.

The amplitude of exciton coupling depends on the mutual orientation of the two chromophores and is maximised when the angle between the two transition moments is close to 70°.[34] Crystallographic studies on $GdNp_4$ revealed dihedral angles between adjacent pairs of naphthyl groups close to 80° (Fig.3.19).[35] Given that the degree of exciton coupling is similar ($g^{219} = -1.8 \cdot 10^{-3}$ for Λ-$EuNp_3dpq$ and $-2.2 \cdot 10^{-3}$ for Λ-$NaNp_4$), a similar disposition may occur in the Np_3dpq complexes.

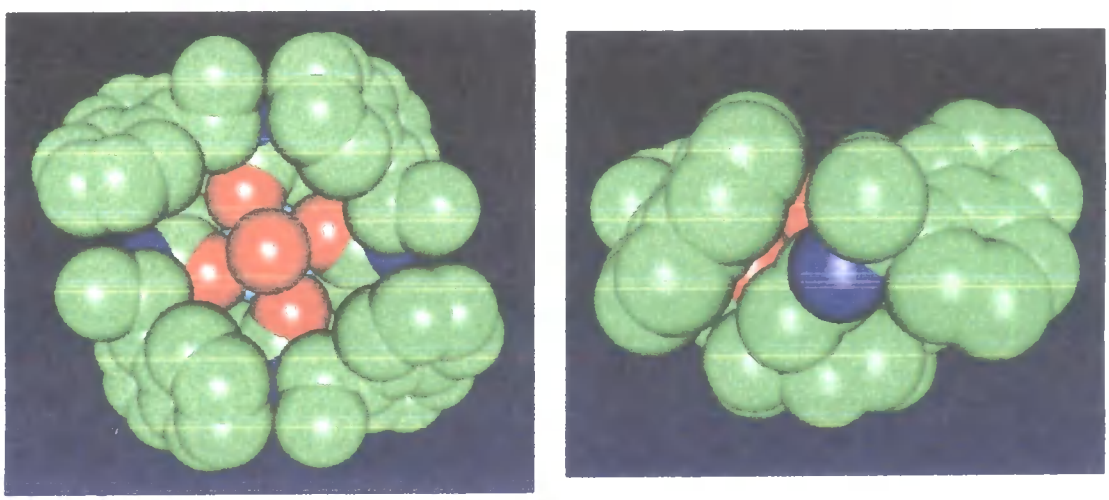

Fig.3.19 Models of the $GdNp_4$ complex, showing the molecule from the top and the side.

3.5.2. Europium Emission Spectra and Lifetimes

The emission spectrum of $EuNp_3dpq$ was recorded, in water, following excitation at 340 nm, and compared to that obtained for an equi-absorbant solution of $EuPh_3dpq$ (Fig.3.20). The only difference observed in the form of the two spectra was the absence of a proper band at 681 nm for the Np_3dpq complex. On the other hand, a

large difference was detected in the luminescence intensity, with $EuNp_3dpq$ emitting more than 100 times less strongly than the phenyl analogue.

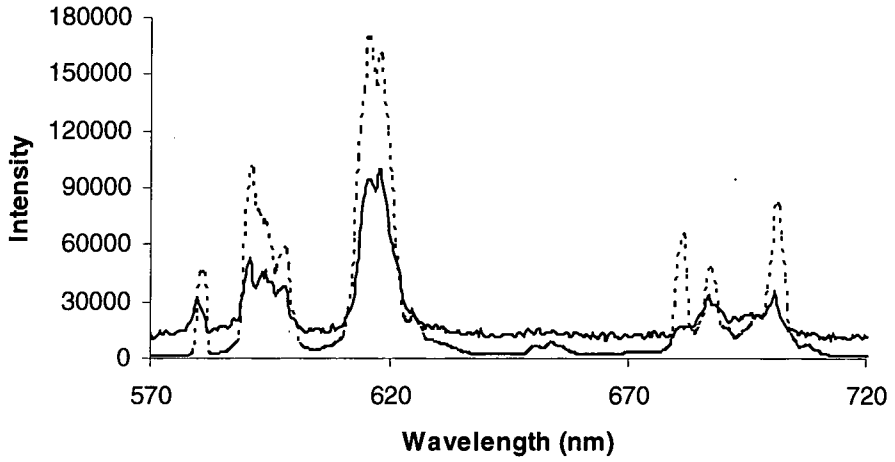

Fig.3.20 Emission spectra of $EuNp_3dpq$ (solid line, scaled to allow comparison) and $EuPh_3dpq$ (dotted line) (λ_{exc} 340 nm, H_2O, 298 K).

The lifetime of the europium emissive state was measured, in H_2O and D_2O, following excitation at 355 nm by a pulsed laser (Table 3.4). The value obtained for $EuNp_3dpq$ in water was about 40% smaller than that found for $EuPh_3dpq$, while in D_2O the difference was not so evident (20%). Sample deoxygenation did not result in increased τ_{H2O}, ruling out a possible involvement of oxygen quenching of the antenna triplet state in the depopulation of the lanthanide excited state. The two processes are not normally connected in europium complexes, because the energy difference between the aryl triplet and the metal emissive state is too large to allow a thermally activated back energy transfer process at ambient temperature.

Table 3.4 Lifetimes of the Eu excited state in H_2O and D_2O (λ_{exc} 355 nm, 298 K), calculated q values and relaxivities of the Gd complexes with Ph_3dpq and Np_3dpq ligands (65 MHz, 293 K, H_2O).

	τ_{H2O} (ms)	τ_{D2O} (ms)	q	r_{1p} ($mM^{-1}s^{-1}$)
Np_3dpq	0.60	1.27	0.5	2.9
Ph_3dpq	1.05	1.65	0	3.6

From the rate constants for depopulation of the Eu excited state, in H_2O and D_2O, a non-integral q value (0.5) was calculated. This may suggest the presence of an equilibrium between two species, having one and no coordinated water molecules respectively.

However, the relaxivity measured for $GdNp_3dpq$ (Table 3.4) falls in the range of values typical of complexes lacking a first coordination sphere of hydration. Moreover, it is smaller than the relaxivity found for the phenyl analogue, as expected on the basis of the higher hydrophobicity, which makes the approach of closely diffusing water molecules more difficult.

A different coordination environment around the lanthanide centre for the hydrated species, on the other hand, would result in additional bands in the Eu emission spectrum as well as a different pattern of resonances in the shifted ^1H NMR spectrum.

It can be concluded that the Np_3dpq complexes possess no bound water molecules and that the shorter lifetime of the lanthanide excited state is not due to vibrational quenching by water OH oscillators.

3.5.3. Absorption and Phosphorescence Spectra

In order to characterise the triplet state involvement in the sensitisation of the lanthanide, a phosphorescence spectrum of $GdNp_3dpq$ was recorded at 77 K in a MeOH/EtOH glass. The complex was excited at 340 nm, a wavelength at which only the dpq chromophore absorbs, but not the naphthyl groups, as shown by their absorption spectra (Fig.3.21).

The phosphorescence spectrum of $GdNp_3dpq$ was very different from that obtained for $GdPh_3dpq$, with a relatively weak band corresponding to the dpq triplet state (Fig.3.22). The more intense bands, in the region 470-580 nm, represent the emission from the naphthyl triplet state, as deduced by comparison with the phosphorescence spectrum recorded for the naphthyl arm, upon excitation at 280 nm.

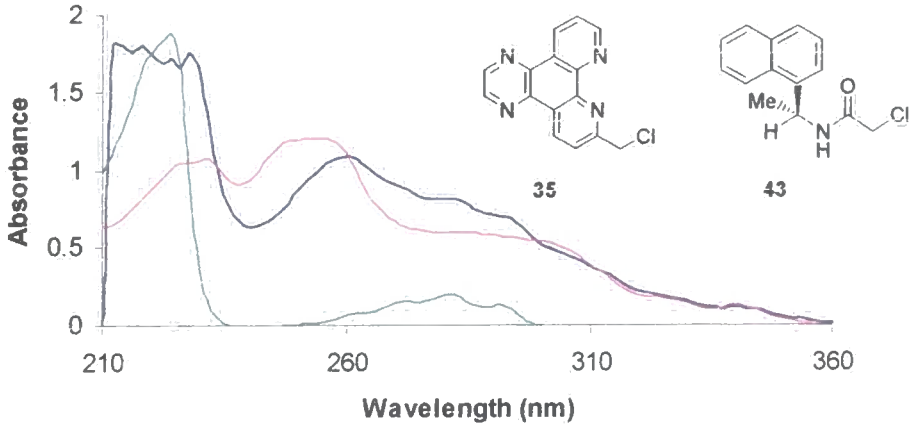

Fig.3.21 Absorption spectra of $GdNp_3dpq$ (blue line), dpq arm **35** (pink line) and naphthyl arm **43** (green line) (EtOH/MeOH 3:1, 298 K).

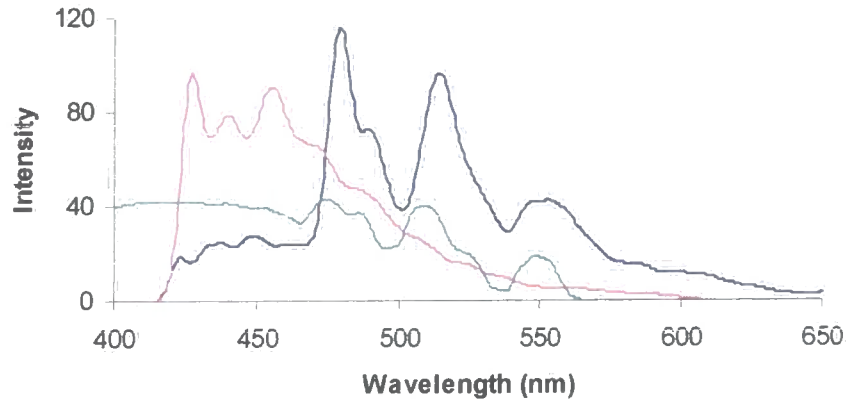

Fig.3.22 Phosphorescence spectra of $GdNp_3dpq$ (blue line), dpq arm **35** (pink line) and naphthyl arm **43** (green line) (EtOH/MeOH 3:1, 77 K).

A triplet-triplet energy transfer process is believed to occur in these complexes, which populates the naphthyl triplet excited state indirectly, without involving its singlet state. The dpq chromophore, following excitation, undergoes intersystem crossing, then transfers part of its energy to the naphthyl groups. This hypothesis is based on the observation that the triplet state of the naphthyl (20,900 cm^{-1}) lies 2600 cm^{-1} lower than that of dpq (Fig.3.23). On the contrary, its singlet state is higher in energy than the dpq singlet state, which makes a singlet-singlet energy transfer process impossible. Moreover, intramolecular triplet-triplet energy transfer between aryl chromophores is a fast process, which can occur at long distance, with a limiting r_o value of 20 Å.[36,37]

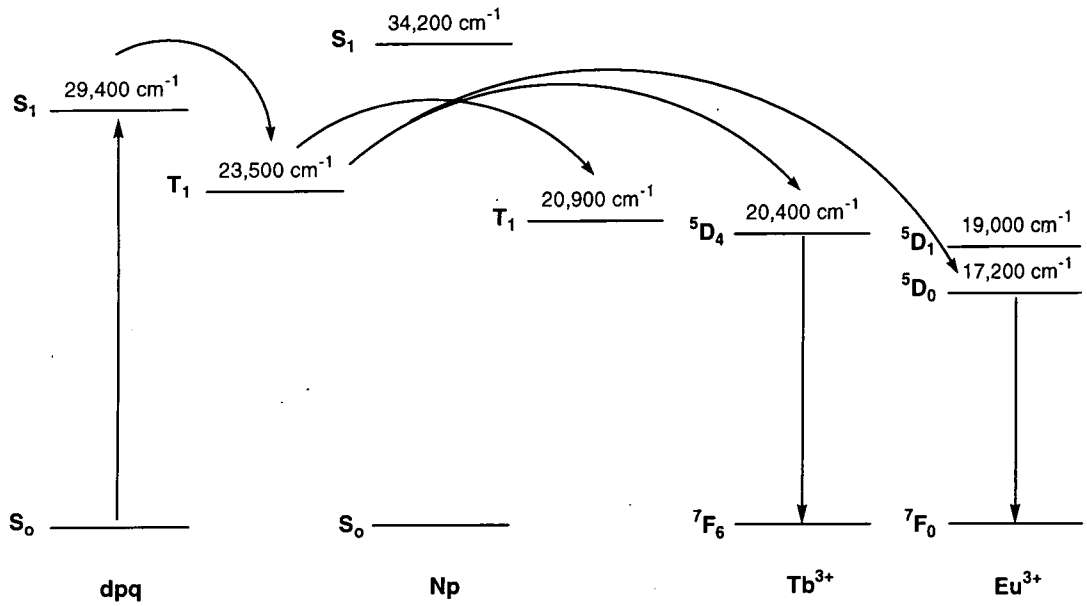

Fig.3.23 Jablonski diagram showing the processes occurring upon excitation of Eu and $TbNp_3dpq$ complexes at 340 nm.

As energy transfer from the dpq triplet to the lanthanide emissive state is in competition with triplet-triplet energy transfer, dpq is a much less efficient sensitiser in the presence of naphthyl groups. This explains, in part, the lower emission intensity observed for $EuNp_3dpq$.

The naphthyl groups themselves may give rise to lanthanide ion sensitisation. In fact, energy transfer from the naphthyl triplet state to the Eu and Tb emissive states has been observed in the parent tetranaphthyl complexes.[38] However, the contribution of these chromophores to the overall sensitisation process is likely to be reduced in Np_3dpq complexes, because the naphthyl groups are more distant from the metal ion than the coordinating dpq moiety.

3.5.4. Terbium Emission Spectra and Lifetimes

The emission spectrum of $TbNp_3dpq$ was recorded, in water, following excitation at 340 nm (Fig.3.24). The intensity observed was extremely weak, less than 3% of that recorded for an equi-absorbant solution of $TbPh_3dpq$.

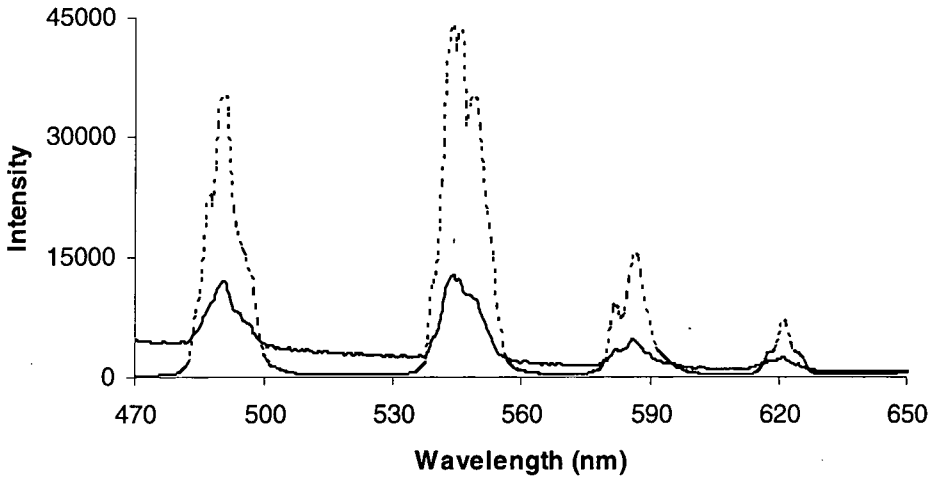

Fig.3.24 Emission spectra of $TbNp_3dpq$ (solid line, scaled to allow comparison) and $TbPh_3dpq$ (dotted line) (λ_{exc} 340 nm, H_2O, 298 K).

The lifetime of the Tb excited state was measured, in H_2O and D_2O, following excitation by a pulsed laser at 355 nm. A value of 4 μs was obtained in each case, which increased to 114 μs when the solution in H_2O was degassed.

Molecular oxygen is a known quencher of the naphthyl triplet state and has been demonstrated to play a role in the depopulation of the Tb emissive state in complexes bearing naphthyl groups on the pendant arms.[39] By analogy, a back energy transfer process was invoked to explain this behaviour, which is consistent with the small energy difference (500 cm^{-1}) between the Tb $^5D_4$ excited state and the naphthyl triplet state (Fig.3.23). On the contrary, a thermally activated back energy transfer process from the Eu $^5D_0$ emissive state of $EuNp_3dpq$ is unlikely to occur at ambient temperature, as this level lies 3700 cm^{-1} lower than the aryl triplet. This is consistent with the insensitivity of the Eu emission lifetime to deoxygenation. The energy of the Eu $^5D_1$ state, however, is closer to the naphthyl triplet (ΔE = 1900 cm^{-1}), so that back energy transfer might take place from this excited state.

In $TbNp_3dpq$, the naphthyl triplet state is populated via two processes: a triplet-triplet energy transfer from the dpq triplet state and a back energy transfer from the Tb excited state. Quenching by molecular oxygen was thus expected to generate singlet oxygen in high yields. This quantum yield was measured, in methanol, by observing the emission from singlet oxygen, at 1270 nm, following excitation at 355 nm by a pulsed laser. Perinaphthenone, which possesses a quantum yield of 97% in MeOH,

was used as a standard. The overall quantum yield for singlet oxygen formation was measured to be 51% (±10%) for $TbNp_3dpq$. Production of singlet oxygen was also detected for $EuNp_3dpq$ and may tentatively be related to a back energy transfer process involving the Eu $^5D_1$ state.

As pointed out above, the triplet state of the naphthyl group is higher in energy than the Tb $^5D_4$ excited state, therefore the back energy transfer process requires thermal activation. By lowering the temperature, the extent of back energy transfer is expected to be reduced and the Tb lifetime increased.

The metal emission lifetimes of $TbNp_3dpq$ and $EuNp_3dpq$ were measured, in ethanol, upon gradual temperature decrease from 293 to 120 K (Fig.3.25).

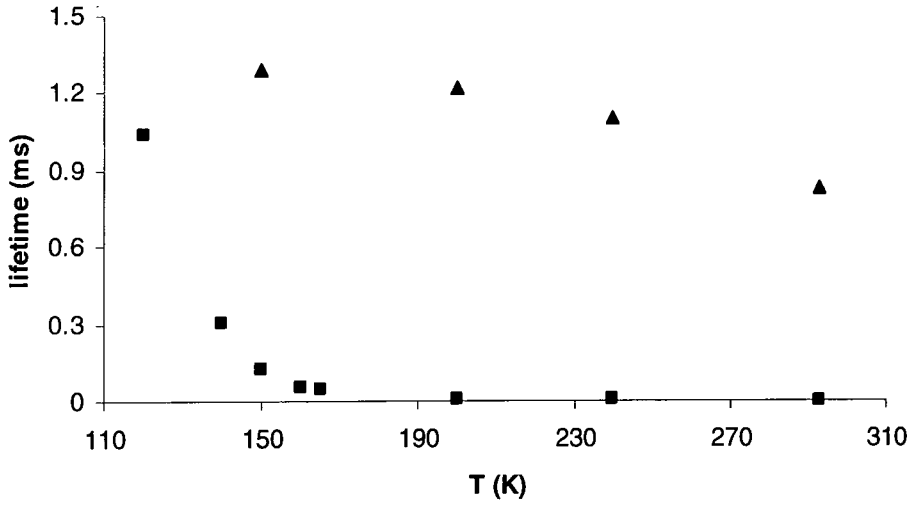

Fig.3.25 Temperature dependence of the lanthanide emissive state lifetime of $TbNp_3dpq$ (■) and $EuNp_3dpq$ (▲)(λ_{exc} 355 nm, EtOH, aerated solutions).

Only a small increase (35%) in the metal excited state lifetime was observed for $EuNp_3dpq$, consistent with the freezing out of vibrational quenching due to solvent OH oscillators.

On the other hand, the Tb emission lifetime underwent a large change, which was particularly evident in the temperature range 160-120 K. This confirms that the back energy transfer process is indeed thermally activated and that, at low temperatures, is much less efficient in depopulating the metal emissive state.

The thermodynamic parameters for back energy transfer can be obtained using the Eyring equation, which describes the temperature dependence of reaction rates:

$$\ln\frac{k}{T} = -\frac{\Delta H^{\#}}{R}\frac{1}{T} + \ln\frac{k_B}{h} + \frac{\Delta S^{\#}}{R}$$

where k is the reaction rate, R the gas constant, k_B Boltzmann's constant, h Planck's constant, $\Delta H^{\#}$ and $\Delta S^{\#}$ the activation enthalpy and entropy respectively.

As the rate for back energy transfer is the main temperature dependent component of the rate constant for decay of the Tb excited state, the latter was used in plotting ln(k/T) versus 1/T (Fig.3.26). The line obtained showed a small curvature, which was associated with the temperature dependence of oxygen solubility. An activation enthalpy of 9.6 kJ/mol was calculated from the slope, and an activation entropy of -100 J/mol K from the intercept on the y axis.

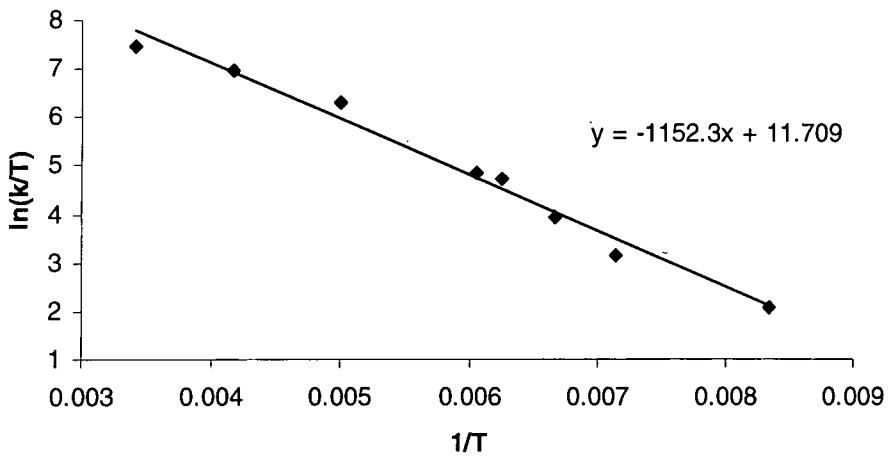

Fig.3.26 Plot representing Eyring equation, used to determine the activation enthalpy and entropy for the back energy transfer process occurring in $TbNp_3dpq$.

3.6. Interaction of Δ- and Λ- $LnNp_3dpq$ Complexes with Nucleic Acids

3.6.1. Absorption and CD Spectra

Changes in the absorption spectra of Δ- and Λ- Eu and $TbNp_3dpq$ were monitored as a function of added poly(dAdT), poly(dGdC) and CT-DNA.

In general, little or no change was observed. Only Λ-EuNp$_3$dpq, in the presence of poly(dAdT), showed a small hypochromism (10%) and red shift of the band at 340 nm. Although the hypochromic effect was small, the possibility of an intercalative interaction was considered and the same system was studied by circular dichroism spectroscopy.

The CD difference spectra of poly(dAdT) were recorded in the presence of increasing ratios of Λ-EuNp$_3$dpq. Both the form and the intensity of the CD bands remained unchanged, indicating that the small hypochromism observed is probably not associated with intercalation. CD difference spectra of poly(dGdC) were also recorded, following addition of Λ-EuNp$_3$dpq: again, no variation was apparent.

The presence of exciton coupling in the spectra of the Np$_3$dpq complexes was considered a useful probe for detecting conformational changes in the complex due to its interaction with the nucleic acids.

Changes in the exciton coupling signals of Δ- and Λ-EuNp$_3$dpq were observed, upon addition of poly(dAdT) and poly(dGdC). Similar titrations were carried out with the Δ and Λ isomers of the parent tetranaphthyl complexes, LnNp$_4$, for comparison.

A decrease in the intensity of the positive and negative bands was observed in each case (Fig.3.27). However, each complex containing the dpq moiety gave rise to a much larger effect compared to the control (Fig.3.28).

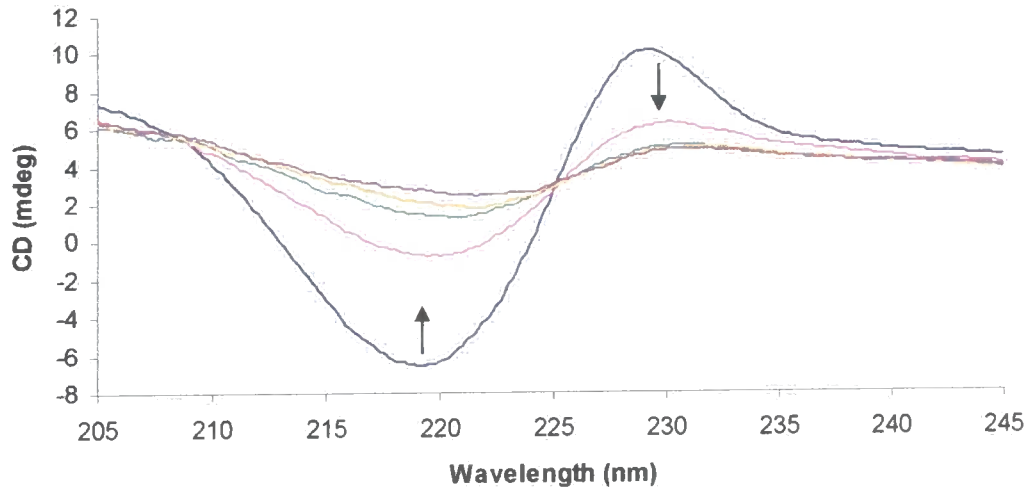

Fig.3.27 CD spectra of Λ-EuNp$_3$dpq (2 μM) following addition of poly(dAdT) (5 μM) from 0 to 0.1 base-pairs per complex (pH 7.4, 10 mM HEPES, 10 mM NaCl, 295 K).

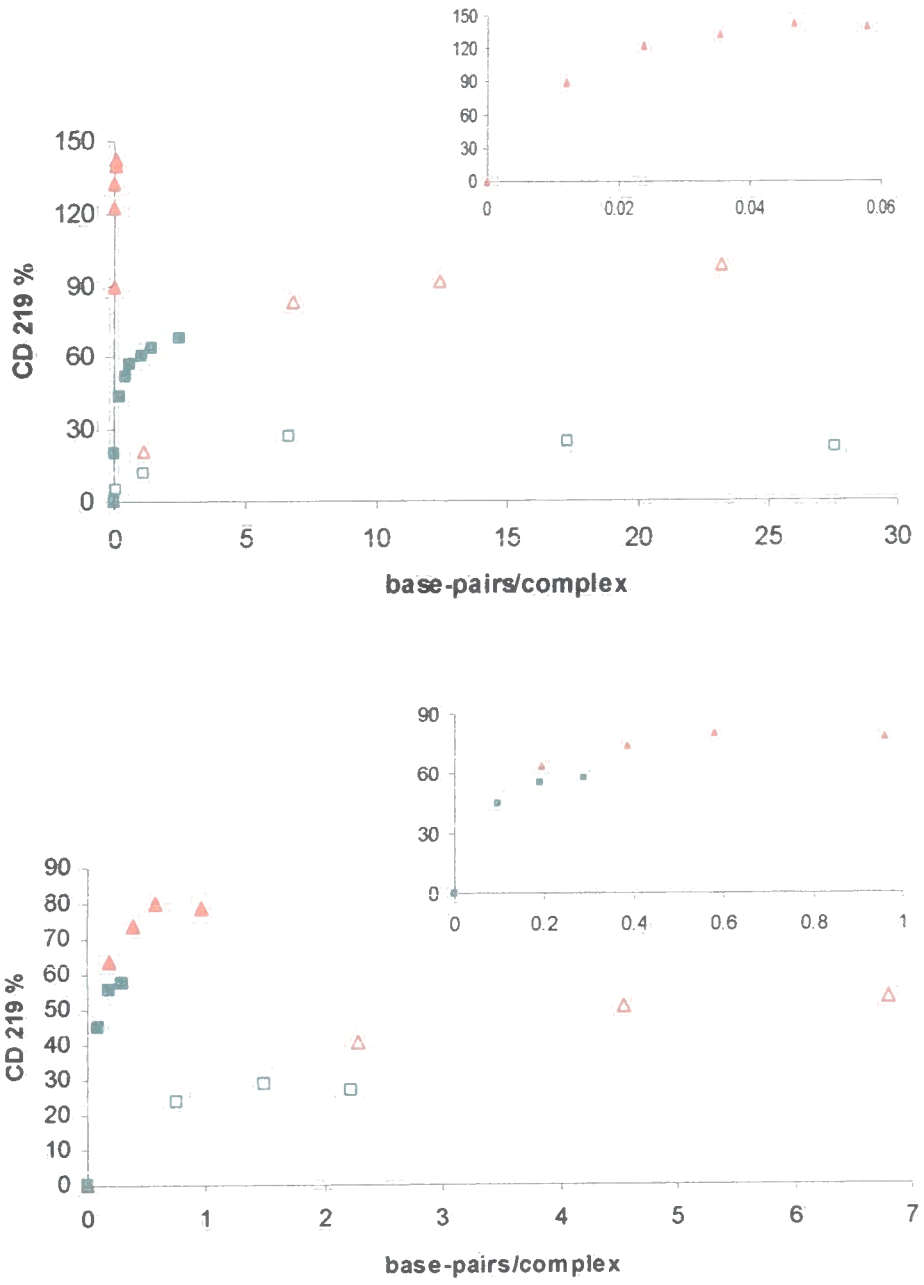

Fig.3.28 Percentage decrease in the exciton coupling band at 219 nm of Δ- (■) and Λ-$EuNp_3dpq$ (▲), compared to Δ-$EuNp_4$ (□) and Λ-$GdNp_4$ (Δ), following addition of poly(dAdT) (upper) and poly(dGdC) (lower). Enlargements of the regions at low base-pairs/complex values (insets) show the behaviour of the Np_3dpq complexes more clearly.

The Λ isomers, both of the Np_3dpq and of the Np_4 complexes, showed a larger decrease than the correspondent Δ isomers. The differences between Λ- and Δ-$EuNp_3dpq$ and between Λ- and Δ-$LnNp_4$ were more marked in the presence of poly(dAdT).

In particular, addition of very small amounts of poly(dAdT) to Λ-EuNp$_3$dpq, corresponding to 0-0.05 base-pairs per complex, caused a 140% reduction in the intensity of the exciton coupling. This may be indicative of a particularly high binding affinity for the Λ isomer. For the Δ isomer, the limiting reduction was 70%, at 2 base-pairs per complex, i.e. at a DNA concentration two orders of magnitude higher.

A decrease in the amplitude of exciton coupling indicates a conformational change, which may be due to an increased distance between the two coupling chromophores, as well as a different reciprocal orientation. As a consequence of the interaction with the nucleic acid, the dihedral angle between two naphthyl groups must vary from an optimal initial value close to 70° to a value that, in the case of the Λ isomer with poly(dAdT), must be closer to 0 or 180°.

The fact that this effect was larger in the presence of the dpq moiety suggests that this group favours the DNA binding interaction.

A certain degree of stereoselectivity has been defined by this experiment: poly(dAdT) clearly showed a preference for the Λ rather than the Δ isomers. A particularly strong interaction occurred between Λ-EuNp$_3$dpq and poly(dAdT).

3.6.2. Europium Emission Spectra and Lifetimes

Emission spectra of Δ- and Λ-EuNp$_3$dpq were recorded in the presence of increasing concentrations of poly(dAdT), poly(dGdC) and CT-DNA. In each case, addition of nucleic acid led to an **increase** in the intensity of the metal-centred emission (Fig.3.29).

Changes in the Eu emission intensity at 590 nm were plotted against the concentration of nucleic acid relative to the complex (Fig.3.30).

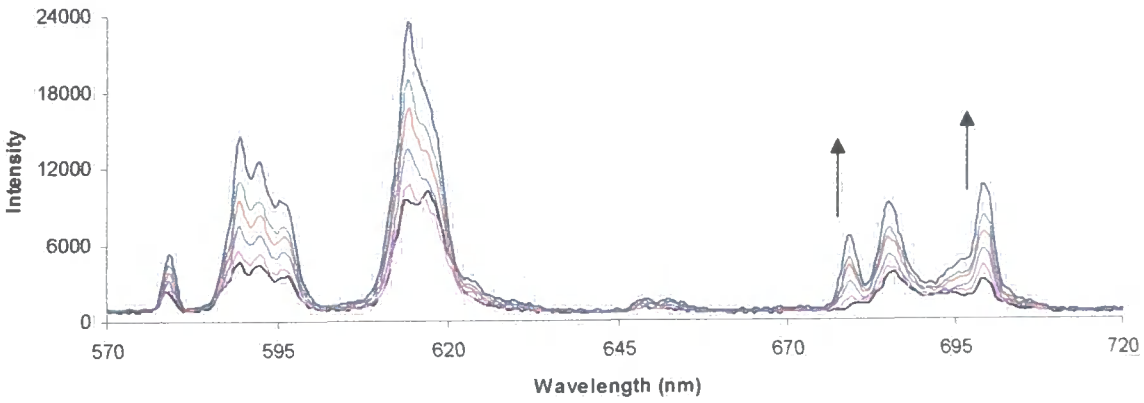

Fig.3.29 Europium emission spectra of Δ-EuNp$_3$dpq (45 μM) upon addition of poly(dGdC) (0.8 mM) from 0 to 1 base-pair per complex (λ_{exc} 340 nm, pH 7.4, 10 mM HEPES, 10 mM NaCl, 295 K).

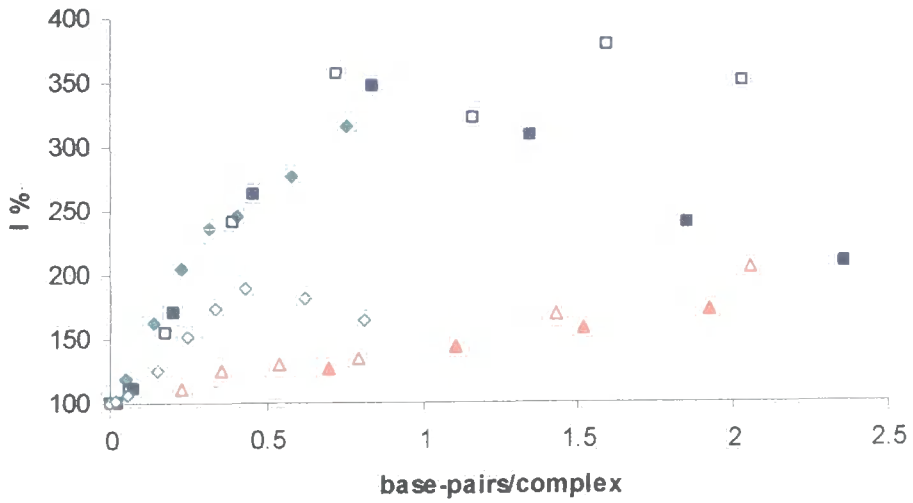

Fig.3.30 Percentage increase in the intensity at 590 nm for Λ- (empty symbol) and Δ-EuNp$_3$dpq (filled symbol) as a function of added CT-DNA (□), poly(dGdC) (◊) and poly(dAdT) (Δ).

A three to four-fold increase in intensity was observed for Δ-EuNp$_3$dpq, following addition of CT-DNA and poly(dGdC), while addition of poly(dAdT) gave rise to a

smaller variation. The behaviour of Λ-EuNp$_3$dpq in the presence of CT-DNA and poly(dAdT) was similar to that of the Δ enantiomer, while the effect of poly(dGdC) for the Λ isomer was 50% less than for the Δ isomer.

In each case, the change in intensity at 615 nm, within the ΔJ = 2 band, was larger. For the Δ isomer only, addition of nucleic acid resulted in a particularly large increase in the intensity at 700 nm. Within the ΔJ = 4 manifold, the relative intensities at 680 and 686 nm changed, for each enantiomer, in the presence of poly(dGdC). For both Δ- and Λ-EuNp$_3$dpq, the ratio of the intensities at 680 and 686 nm doubled in size after addition of small concentrations of poly(dGdC), corresponding to 0.3 base-pairs per complex.

In summary, in each case considered, the presence of C and G bases caused larger variations in the overall Eu emission intensity than did A and T. However, the large stereoselective changes that had been revealed by exciton coupling intensity changes were not so apparent.

The europium emission lifetime was measured at the end of each titration and compared to the lifetime of the complex in the absence of nucleic acid (τ_{H2O} = 0.6 ms) (Table 3.5).

Table 3.5 Percentage increase in the lifetime of the Eu excited state at the end of the titrations of Λ- and Δ-EuNp$_3$dpq with poly(dAdT), poly(dGdC) and CT-DNA.

	+ poly(dAdT)	+ poly(dGdC)	+ CT-DNA
Λ- EuNp$_3$dpq	41%	27%	83%
Δ- EuNp$_3$dpq	9%	2%	58%

Λ-EuNp$_3$dpq showed increased lifetimes with each nucleic acid, while for Δ-EuNp$_3$dpq the change was significant only in the presence of CT-DNA.

The marked variations observed in the lifetime of the Eu excited state mirror the large increase in the emission intensities of both Λ- and Δ-EuNp$_3$dpq obtained upon addition of CT-DNA. The fact that poly(dGdC) did not lead to a similar effect may

suggest that it is the higher order structural features of the overall molecule, and not simply its base-pair composition that plays a role in the interaction with the complex. Correlated changes in the intensity and lifetime of europium emission must be due to deactivation of a quenching process. The interaction with the nucleic acid may provide here a protection of the complex from collisional quenching, which may be more efficient in the presence of a mixed sequence of bases.

CT-DNA, containing all the four nucleobases, possesses higher structural variability than poly(dAdT) and poly(dGdC). Particular sequences, other than $(AT)_n$ and $(CG)_n$, may adopt a conformation that accommodates the complex in one of the grooves, thus shielding it efficiently from a quenching process. Crystal structures of $(AT)_n$ tracts in several oligonucleotides showed narrow minor grooves, with ordered water molecules.[40] On the basis of these features, protection of the complex may not be favoured in the presence of poly(dAdT), as was indeed observed.

Although the nature of the quenching process has not been identified, it must involve the presence of naphthyl groups, as it was not apparent for the Ph_3dpq complexes. The exclusion of oxygen due to the interaction with DNA might explain the increase in intensity. Decreased quenching of the naphthyl triplet state by molecular oxygen might result in a more efficient sensitisation of the Eu $^5D_0$ emissive state, with the intermediacy of the $^5D_1$ state. However, the insensitivity of Eu lifetime to deoxygenation seems to suggest that the protection from oxygen quenching provided by DNA cannot, alone, justify the large increase in the Eu emission lifetime measured in the presence of the nucleic acid.

3.6.3. Terbium Emission Spectra and Lifetimes

Changes in the Tb emission spectra were observed for Λ-TbNp$_3$dpq, following addition of poly(dAdT), poly(dGdC) and CT-DNA, and for Δ-TbNp$_3$dpq, following addition of CT-DNA.

The emission intensity, which was already very weak in the absence of nucleic acid, decreased in each case (Fig.3.31).

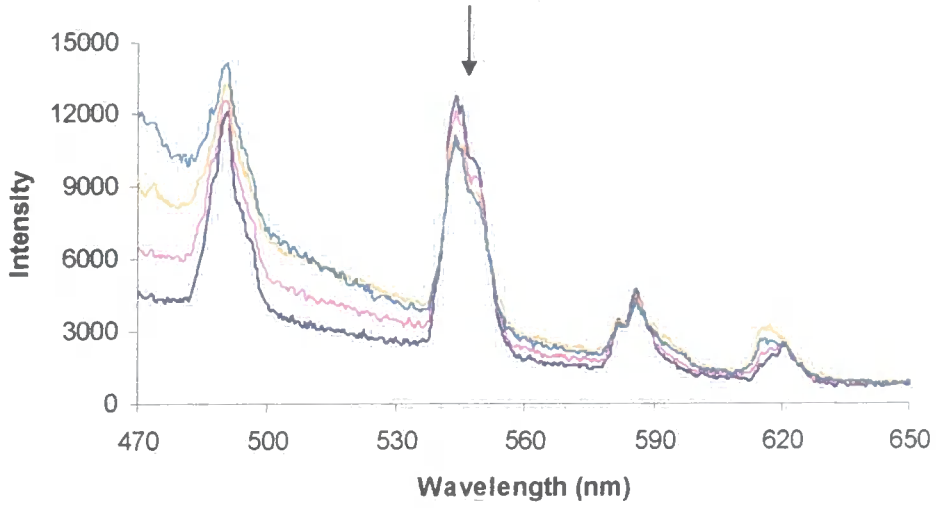

Fig.3.31 Emission spectra of Δ-TbNp$_3$dpq (44 μM) following addition of CT-DNA (1.7 mM) from 0 to 3 base-pairs per complex (λ_{exc} 340 nm, pH 7.4, 10 mM HEPES, 10 mM NaCl, 295 K).

CT-DNA caused a smaller change (20%) in the emission intensity of Λ-TbNp$_3$dpq than did poly(dAdT) (35%) and poly(dGdC) (60%) (Fig.3.32). Δ-TbNp$_3$dpq, in the presence of CT-DNA, showed the same percentage decrease as the Λ enantiomer. Titrations of Δ-TbNp$_3$dpq with the other two polynucleotides were not carried out, because the extent of quenching observed in each case indicated that these complexes do not represent interesting structural or emissive probes.

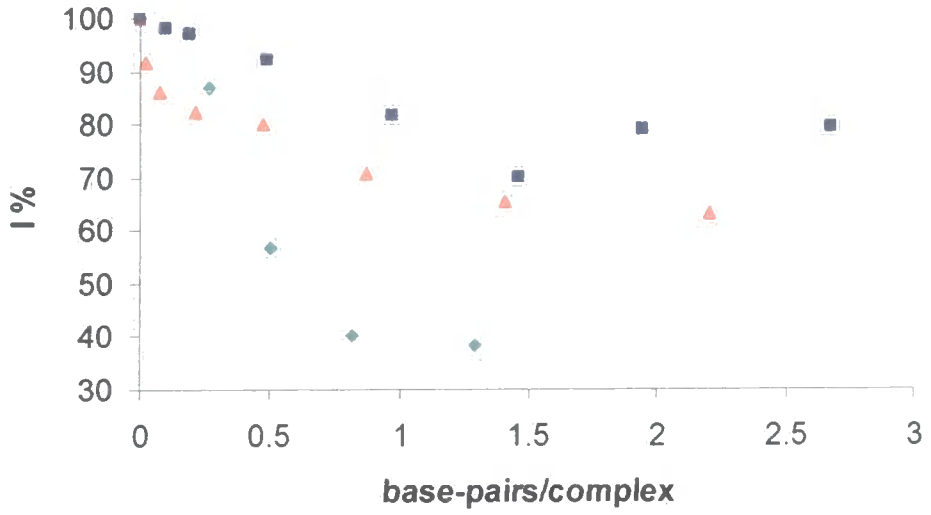

Fig.3.32 Percentage decrease in the intensity at 543 nm for Λ-TbNp$_3$dpq as a function of added CT-DNA (■), poly(dGdC) (♦) and poly(dAdT) (▲).

The lifetimes of Tb emission at the end of the titrations with CT-DNA and poly(dGdC) were measured, following excitation of the sample with a pulsed laser. A slightly longer lifetime (7 μs) than the initial value of 4 μs was obtained for both enantiomers in the presence of CT-DNA, while a smaller value (2 μs) was measured in the presence of poly(dGdC). These changes were not considered to be very important, because the order of magnitude remained similar.

By analogy with the Ph_3dpq complexes, a charge transfer interaction of $TbNp_3$dpq with the nucleobases may explain the deactivation of the Tb excited state. The small quenching observed in each case may represent the result of the competition between a process, analogous to that observed for $EuNp_3$dpq, that would increase the emission intensity, and the charge transfer process, that would decrease it to the same extent observed for $TbPh_3$dpq. In the latter complex, the efficiency of quenching was particularly high in the presence of poly(dGdC), which is consistent with the greater effect obtained for $TbNp_3$dpq in the presence of this polynucleotide.

3.6.4. Control Experiments

Several control experiments were carried out to define more clearly the possible factors giving rise to the observed behaviour.

a. Changes in the absorption and emission spectra of Δ-$EuNp_4$ were monitored as a function of added poly(dGdC). Both spectra maintained their form. A small increase in absorbance at 284 nm was observed, due to concomitant absorption of the nucleic acid at this wavelength. On the other hand, the emission intensity, following excitation at 284 nm, decreased by about 40%. This indicates that an interaction due only to the presence of naphthyl groups in the $EuNp_3$dpq complexes would give rise to decreased emission intensity. The observed increase and the spectral changes obtained, therefore; must result from the presence of the dpq moiety.

b. Changes in the spectra of Δ- and Λ-$EuNp_3$dpq were measured, in the range from zero to eight phosphate molecules per complex, following addition of a solution

of Na_2HPO_4. The overall form of the absorption and emission spectra remained unchanged in each case. After accounting for dilution, a small decrease (15%) in the overall emission intensity was calculated for each enantiomer, which reached a plateau at 1.5 phosphates per complex, as expected for a binding process associated with charge neutralisation. The lifetimes of Eu emission, measured at the end of each titration, showed no change from the value obtained for $EuNp_3dpq$ alone. It must be concluded that the electrostatic component in the interaction between the positively charged $EuNp_3dpq$ complexes and the negatively charged DNA is not associated with the enhancement of Eu emission intensity following DNA binding.

c. Changes in the absorption and emission spectra of Δ-$EuNp_3dpq$, in the pH range 3-7, were monitored following addition of trifluoroacetic acid. The only change observed, at pH 3, was the appearance in the emission spectrum of a band at 415 nm and a broad band centred at 460 nm. These might be due to emission from dpq, as deduced by comparison with a spectrum of the dpq molecule itself (Fig.3.33).

d. The effect of possible intramolecular interactions, between naphthyl groups or between a naphthyl group and dpq, was investigated by observing the differences in the absorption and emission spectra of various $LnNp_3dpq$ complexes as a function of solvent polarity. The absorption spectra of Eu, Tb and $GdNp_3dpq$ were recorded in dry methanol and acetonitrile. As the spectra were similar to those obtained in water, a charge transfer interaction in the ground state between the electron-rich naphthyl and the electron-poor dpq was ruled out. Typically, a charge transfer complex should exhibit an absorption band different to those of the donor and the acceptor, which is sensitive to solvent polarity.[37]

A charge transfer process can also occur in the excited state, between an excited species and a ground state molecule.[37,25] If donor and acceptor are represented by the same molecule, an excimer is formed, whereas, if they are different, an

exciplex results. The charge transfer complex emits, giving rise to broad bands on the red side of the monomer emission.

Intramolecular excimers are indeed formed in complexes bearing naphthyl pendant arms, when two naphthyl groups in close proximity are co-planar.[33] The presence of exciton coupling between two naphthyl groups in $EuNp_3dpq$ indicates that the angle between them is closer to 70° than to the 0° or 180° required for excimer formation. Formation of an intramolecular exciplex between a naphthyl group and dpq was expected to be signalled by differences in the emission spectra of $LnNp_3dpq$ complexes in water, methanol and acetonitrile, as emission from exciplexes is solvent dependent. A broad band was observed for Tb and $GdNp_3dpq$ at 462 nm in CH_3CN, which shifted to 420 nm and broadened in MeOH. EuNp3dpq, however, did not show an analogous signal in these solvents. A similar band was not apparent in the emission spectra of aqueous solution of each complex at neutral pH. However, it appeared at low pH in the spectrum of $EuNp_3dpq$, as described above. By comparison with the emission spectrum of dpq itself (Fig.3.33), these broad bands were identified with emission from dpq.

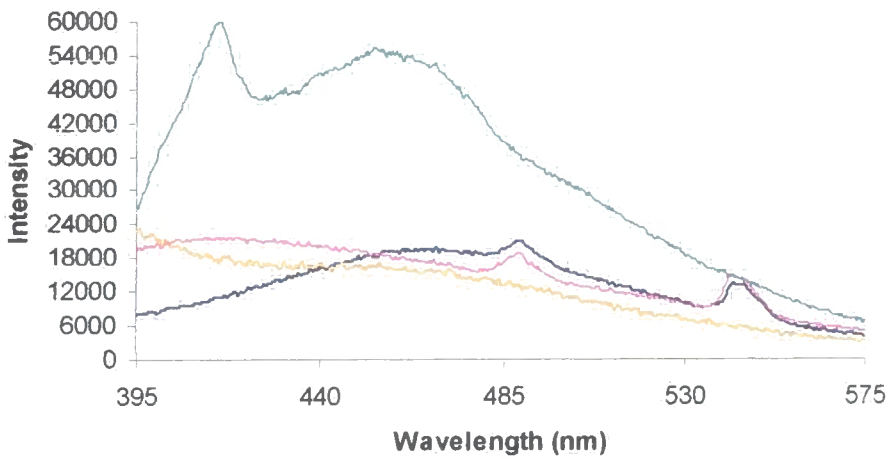

Fig.3.33 Emission spectra of $EuNp_3dpq$ in H_2O at pH 3 (green line), $TbNp_3dpq$ in CH_3OH (pink line) and CH_3CN (blue line), compared to dpq emission in methanol (orange line, scaled to allow comparison) (λ_{exc} 340 nm, 298 K).

The emission spectra recorded for $EuNp_3dpq$ in different solvents were also examined in the region corresponding to metal emission (Fig.3.34).

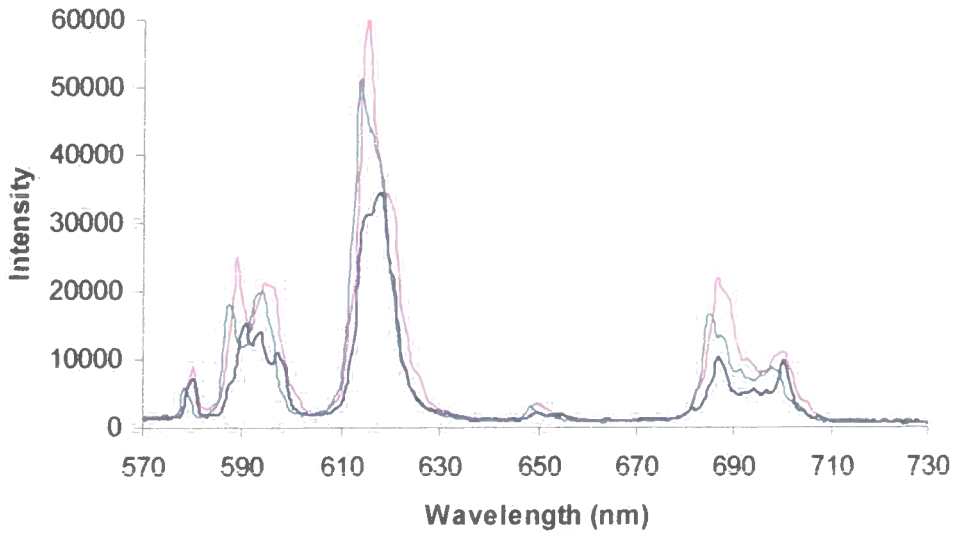

Fig.3.34 Emission spectra of $EuNp_3dpq$ in H_2O (blue line, scaled to allow comparison), CH_3OH (green line) and CH_3CN (pink line) (λ_{exc} 340 nm, 298 K).

The form of the spectra obtained in methanol and acetonitrile was similar, but different to that recorded in water. The $\Delta J = 1$ band appeared as only two, equally intense transitions, instead of the three observed in water. The intensity of the $\Delta J = 2$ band was particularly high at 615 nm. Within the $\Delta J = 4$ manifold, the intensity of the band at 686 nm was larger than that at 700 nm, while the height of the two bands was about the same in water. By analogy with the Ph_3dpq complexes, these differences can tentatively be ascribed to a different degree of solvation of the complex in solvents of different polarity. However, no similarities between the spectra recorded in non-aqueous solvents and those obtained in the presence of DNA were observed.

3.7. Summary and Conclusions

The complexes bearing naphthyl groups on the pendant arms proved to be weakly luminescent because the sensitising efficiency of dpq is lowered by competitive energy transfer to the naphthyl triplet state. In addition, for the TbNp3dpq complexes a back energy transfer process occurs at ambient temperature which deactivates the lanthanide emissive state and repopulates the naphthyl triplet state. Efficient singlet oxygen production results from the quenching of the naphthyl triplet. This could be employed to oxidise DNA in situ, following excitation of the dpq chromophore.

The importance of the dpq moiety in the interaction with nucleic acids was demonstrated by comparing the extent and sense of the changes observed for $EuNp_3dpq$ and $EuNp_4$ in the CD exciton coupling and in the Eu emission intensity.

The nature of the binding interaction appears not to be intercalative, as shown by the absence of changes in the absorption spectra of the complexes and the CD spectra of the polynucleotides. On the other hand, the binding is not simply charge neutralisation by an added anion, as proved by control experiments with phosphate ions. The complexes may bind to the DNA minor groove, as postulated for the phenyl analogues.

For $EuNp_3dpq$, the interaction resulted in an increase in the Eu emission intensity and lifetime, due to protection of the metal from a quenching process which may involve oxygen quenching of the naphthyl triplet state. The higher apparent binding affinity for CT-DNA, compared to poly(dAdT) and poly(dGdC), suggests that a mixed sequence of bases may be required to optimise the interaction. The CD experiments observing exciton coupling changes indicated a striking preference of poly(dAdT) for the Λ enantiomer, which is consistent with the sense of stereoselectivity observed for the Ph_3dpq complexes. The interaction between Λ-$EuNp_3dpq$ and poly(dAdT), however, is not intercalative. This may be due to the steric bulk of the naphthyl groups, which prevent a close approach to DNA and the insertion of the dpq aromatic ring system between the nucleobases.

The main difference in the behaviour of Ph_3dpq and Np_3dpq complexes is the reversal in the variation of the metal emission intensity in the presence of nucleic acid. An increase in the luminescence of the complex, as observed for $EuNp_3dpq$, is

believed to represent an advantage in the use of these molecules as spectroscopic probes for nucleic acids.

The $TbNp_3dpq$ complexes, being able to generate singlet oxygen efficiently, could be employed as reactive probes. However, their use as luminescent probes is limited by the small metal emission intensity observed for the free complex, which is decreased further in the presence of DNA by a quenching process that must involve a charge transfer interaction between the nucleobases, dpq and the Tb ion.

The DNA cleaving ability of the Eu and Tb complexes containing the dpq chromophore is currently being investigated by gel electrophoresis.[41]

References

1 E. B. van der Tol, H. J. van Ramesdonk, J. W. Verhoeven, F. J. Steemers, E. G. Kerver, W. Verboom, and D. N. Reinhoudt, *Chemistry-a European Journal*, 1998, **4**, 2315.

2 M. Yamada, Y. Tanaka, Y. Yoshimoto, S. Kuroda, and I. Shimao, *Bulletin of the Chemical Society of Japan*, 1992, **65**, 1006.

3 J. Lewis and T. D. O' Donoghue, *Journal of the Chemical Society-Dalton Transactions*, 1980, 736.

4 K. Tamao, S. Kodama, I. Nakajima, and M. Kumada, *Tetrahedron*, 1982, **38**, 3347.

5 G. R. Newkome, K. J. Theriot, V. K. Gupta, F. R. Fronczek, and G. R. Baker, *Journal of Organic Chemistry*, 1989, **54**, 1766.

6 C. J. Chandler, L. W. Deady, and J. A. Reiss, *Journal of Heterocyclic Chemistry*, 1981, **18**, 599.

7 G. R. Newkome, G. E. Kiefer, W. E. Puckett, and T. Vreeland, *Journal of Organic Chemistry*, 1983, **48**, 5112.

8 C. A. Panetta, H. J. Kumpaty, N. E. Heimer, M. C. Leavy, and C. L. Hussey, *Journal of Organic Chemistry*, 1999, **64**, 1015.

9 A. M. S. Garas and R. S. Vagg, *Journal of Heterocyclic Chemistry*, 2000, **37**, 151.

10 S. Brandes, C. Gros, F. Denat, P. Pullumbi, and R. Guilard, *Bulletin De La Societe Chimique De France*, 1996, **133**, 65.

11 R. S. Dickins, J. A. K. Howard, C. L. Maupin, J. M. Moloney, D. Parker, J. P. Riehl, G. Siligardi, and J. A. G. Williams, *Chemistry-a European Journal*, 1999, **5**, 1095.

12 S. Aime, M. Botta, R. S. Dickins, C. L. Maupin, D. Parker, J. P. Riehl, and J. A. G. Williams, *Journal of the Chemical Society-Dalton Transactions*, 1998, 881.

13 J. I. Bruce, R. S. Dickins, L. J. Govenlock, T. Gunnlaugsson, S. Lopinski, M. P. Lowe, D. Parker, R. D. Peacock, J. J. B. Perry, S. Aime, and M. Botta, *Journal of the American Chemical Society*, 2000, **122**, 9674.

14 I. M. Clarkson, A. Beeby, J. I. Bruce, L. J. Govenlock, M. P. Lowe, C. E. Mathieu, D. Parker, and K. Senanayake, *New Journal of Chemistry*, 2000, **24**, 377.

15 D. Parker, R. S. Dickins, H. Puschmann, C. Crossland, and J. A. K. Howard, *Chemical Reviews*, 2002, **102**, 1977.

16 J. I. Bruce, D. Parker, S. Lopinski, and R. D. Peacock, *Chirality*, 2002, **14**, 562.

17 J. I. Bruce, M. P. Lowe and D. Parker in 'The Chemistry of Contrast Agents in Medical Magnetic Resonance Imaging', edited by A. Merbach and E. Toth, Wiley, New York, 2001.

18 A. Beeby, I. M. Clarkson, R. S. Dickins, S. Faulkner, D. Parker, L. Royle, A. S. de Sousa, J. A. G. Williams, and M. Woods, *Journal of the Chemical Society-Perkin Transactions 2*, 1999, 493.

19 P. Caravan, J. J. Ellison, T. J. McMurry, and R. B. Lauffer, *Chemical Reviews*, 1999, **99**, 2293.

20 D. Parker and J. A. Williams, *Journal of the Chemical Society-Dalton Transactions*, 1996, 3613.

21 D. Parker, P. K. Senanayake, and J. A. G. Williams, *Journal of the Chemical Society-Perkin Transactions 2*, 1998, 2129.

22 J. I. Bruce, D. Parker, and D. J. Tozer, *Chemical Communications*, 2001, 2250.

23 J. D. Mc Ghee and P. H. von Hippel, *Journal of Molecular Biology*, 1974, **86**, 469.

24 D. Parker, *Coordination Chemistry Reviews*, 2000, **205**, 109.

25 J. R. Lakowicz, 'Principles of Fluorescence Spectroscopy', Kluwer Academic/Plenum Publishers, 1999.

26 J. K. Barton, J. M. Goldberg, C. V. Kumar, and N. J. Turro, *Journal of the American Chemical Society*, 1986, **108**, 2081.

27 A. E. Friedman, C. V. Kumar, N. J. Turro, and J. K. Barton, *Nucleic Acids Research*, 1991, **19**, 2595.

28 G. Bobba, J. C. Frias, and D. Parker, *Chemical Communications*, 2002, 890.

29 S. Aime, A. Barge, J. I. Bruce, M. Botta, J. A. K. Howard, J. M. Moloney, D. Parker, A. S. de Sousa, and M. Woods, *Journal of the American Chemical Society*, 1999, **121**, 5762.

30 W. C. Johnson in 'Circular Dichroism: Principles and Applications', edited by N. Berova, K. Nakanishi, and R. W. Woody, John Wiley & Sons, 2000.

31 D. R. Hare, D. E. Wemmer, S. H. Chou, G. Drobny, and B. R. Reid, *Journal of Molecular Biology*, 1983, **171**, 319.

32 E. L. Eliel, S. H. Wilen, and L. N. Mander, 'Stereochemistry of Organic Compounds', Wiley, 1994.

33 R. S. Dickins, J. A. K. Howard, J. M. Moloney, D. Parker, R. D. Peacock, and G. Siligardi, *Chemical Communications*, 1997, 1747.

34 N. Berova and K. Nakanishi in 'Circular Dichroism: Principles and Applications', edited by N. Berova, K. Nakanishi, and R. W. Woody, John Wiley & Sons, 2000.

35 H. Puschmann, University of Durham, 2002.

36 H. E. Zimmerman and R. D. McKelvey, *Journal of the American Chemical Society*, 1971, **93**,3638.

37 N. J. Turro, 'Modern Molecular Photochemistry', University Science Books, 1991.

38 R. S. Dickins, J. A. K. Howard, C. L. Maupin, J. M. Moloney, D. Parker, R. D. Peacock, J. P. Riehl, and G. Siligardi, *New Journal of Chemistry*, 1998, **22**, 891.

39 A. Beeby, D. Parker, and J. A. G. Williams, *Journal of the Chemical Society-Perkin Transactions 2*, 1996, 1565.

40 S. Neidle, 'DNA Structure and Recognition', Oxford University Press, 1994.

41 J. C. Frias, University of Durham, 2002.

CHAPTER 4

Redox Properties of Cerium (III) Complexes

As described in the previous chapter, an efficient quenching of the luminescence of Tb complexes bearing a dpq chromophore was observed in the presence of C-G base-pairs. It was tentatively attributed to an electron transfer process from guanine to the metal excited state, by analogy with the established effect of this nucleobase on the fluorescence of ruthenium complexes containing hat and tap ligands.[1] Such a photoinduced electron transfer process

$$\text{complex}^* + G \rightarrow \text{complex}^{\cdot -} + G^{\cdot +}$$

produces a guanine radical cation, which can undergo a series of reactions leading to DNA strand breaks. Although there is no simple correlation between the oxidising power of the complex and its ability to cleave DNA, it is important to check the feasibility of the reaction.

Guanine oxidation will occur only if the reduction potential of the complex in the excited state is greater than the oxidation potential of guanine. The reduction potential of the excited state can be estimated from that of the ground state, measured by cyclic voltammetry, and the energy level from where emission occurs.[2] The standard free energy change $\Delta G°_{ET}$ in eV is given by the Rehm-Weller equation:

$$\Delta G°_{ET} = F[E°(G^{\cdot +}/G) - E°(\text{complex/complex}^{\cdot -}) - E_{0,0}(\text{complex})] + \Delta G°(\varepsilon)$$

where F is the Faraday's constant, $E°(G^{\cdot +}/G)$ is the oxidation potential of guanine (1.29 V vs NHE),[3] $E°(\text{complex/complex}^{\cdot -})$ the reduction potential of the complex in the ground state, $E_{0,0}(\text{complex})$ the energy of the emission maximum and $\Delta G°(\varepsilon)$ a solvent term, which can be estimated ≈ -0.1 V for a quenching reaction in H_2O.[4]

Electron transfer is more likely to occur to Tb in its tetravalent, rather than trivalent state, as Tb(II) species are not stable. Tb(IV) may be produced in the excited state as a consequence of a metal-to-ligand charge transfer interaction with dpq:

$$[\text{Tb(III)dpq}]^{3+} \rightarrow [\text{Tb(IV)dpq}^{\cdot -}]^{3+}$$

A similar excited state species, with a radical anion on the tap ligand, is considered to be responsible for guanine oxidation using ruthenium complexes:[5]

$$Ru^{III}(tap^{\bullet-})(tap)(dppz) + G \rightarrow Ru^{II}(tap^{\bullet-})(tap)(dppz) + G^{+}$$

In order to apply the Rehm-Weller equation, the energy of the MLCT state must be measured from its emission maximum. However, no MLCT bands were apparent in the absorption and emission spectra of our Tb complexes. The charge transfer complex may be a transient species that could be detected only in time-resolved luminescence and transient absorption studies, which are underway.

An MLCT transition was considered possible for Ce(III) complexes containing the dpq chromophore, because this is the only lanthanide that can be oxidised more easily than Tb(III). The dpq group was expected to behave as a good electron acceptor, on the basis of the large aromatic area available for charge delocalisation. Only recently an MLCT state has been identified for a Ce(III) complex containing pyrazine-2-carboxylate ligands. This is believed to represent the first example of an f-group metal complex with an MLCT excited state.[6]

In summary, the cerium (III) complexes in Fig.4.1 have been prepared with the aim of obtaining nucleic acid oxidising agents. The complexes CeDO3Adpq and $CeMeP_3dpq$ were expected to show an MLCT transition, which may generate photoactivated Ce(IV) species with DNA cleaving ability, provided that the excited state reduction potentials are adequate for nucleobase oxidation.

Alternatively, Ce(IV) complexes could be obtained, in the ground state, by chemical or electrochemical oxidation of each of the Ce(III) complexes under study. In this case the dpq moiety may not be necessary, but its presence should increase the DNA binding affinity. A direct correlation between the efficiency of guanine oxidation obtained via DNA charge transport and the strength of intercalative binding has been established for Ru complexes containing derivatives of the dppz ligand.[7]

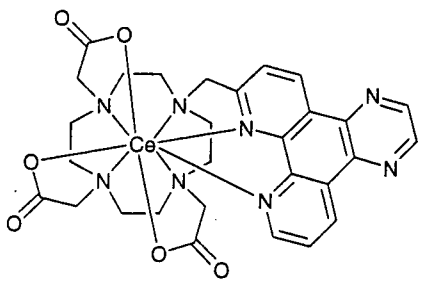

49

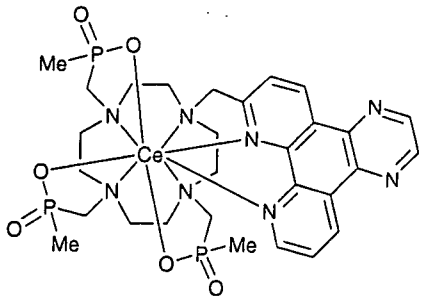

51

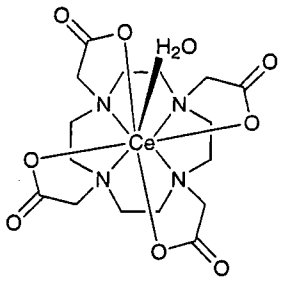

54

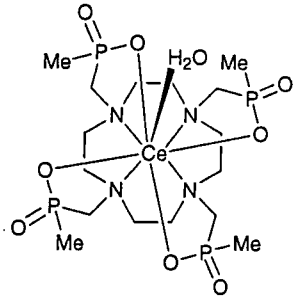

53

Fig.4.1 Structures of CeDO3Adpq (**49**), $CeMeP_3dpq$ (**51**), $[CeDOTA]^-$ (**54**) and $[CeMeP_4]^-$ (**53**).

Previous electrochemical measurements on the Ce(III) complex with the Ph_4 ligand (Fig.1.24) revealed that the redox process was not metal centred and there was evidence for irreversible decomposition of the ligand, possibly via amide oxidation.[8] The amide arms were therefore considered unsuitable and were replaced by acetate and phosphinate arms. Complexes **49**, **51**, **53** and **54** were sought, with the latter two acting as model systems to assess the role of the dpq ligand.

4.1. Synthesis

4.1.1. Complexes Bearing Acetate Arms

The synthesis of the CeDO3Adpq complex is shown in Scheme 1.

Alkylation of the *tert*-butyl ester of DO3A with the dpq chloromethyl derivative, **35**, afforded compound **48** in good yield. Acid hydrolysis of the ester groups, using trifluoroacetic acid, was followed by complexation of the neutral ligand with $Ce(NO_3)_3$. Purification of the complex, **49**, was achieved by chromatography on neutral alumina.

The anionic complex $[CeDOTA]^-$ was prepared in a similar manner to other $[LnDOTA]^-$ complexes, by addition of equimolar quantities of the cerium (III) nitrate salt to the DOTA ligand in aqueous solution.

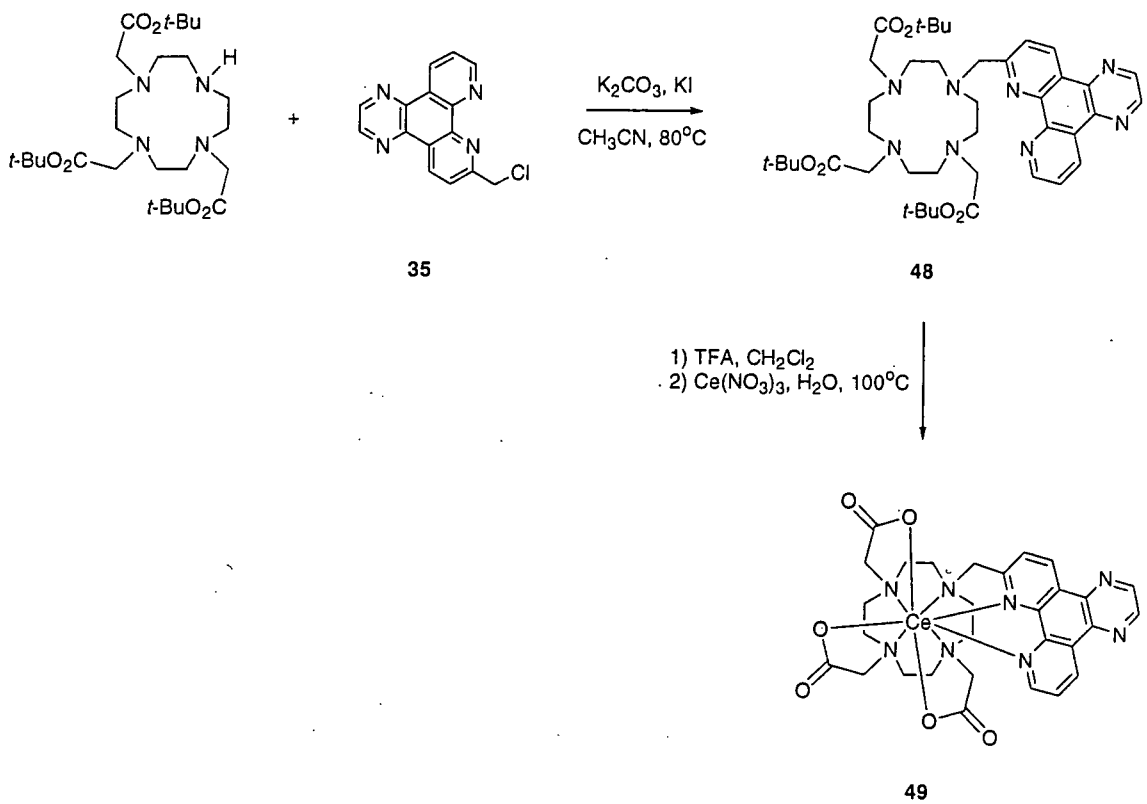

35 **48** **49**

Scheme 1

4.1.2. Complexes Bearing Phosphinate Arms

The synthesis of $CeMeP_3dpq$ and $[CeMeP_4]^-$ (Scheme 2) was carried out using a methodology that has been previously established for the introduction of alkylphosphinate substituents on the cyclen ring.[9]

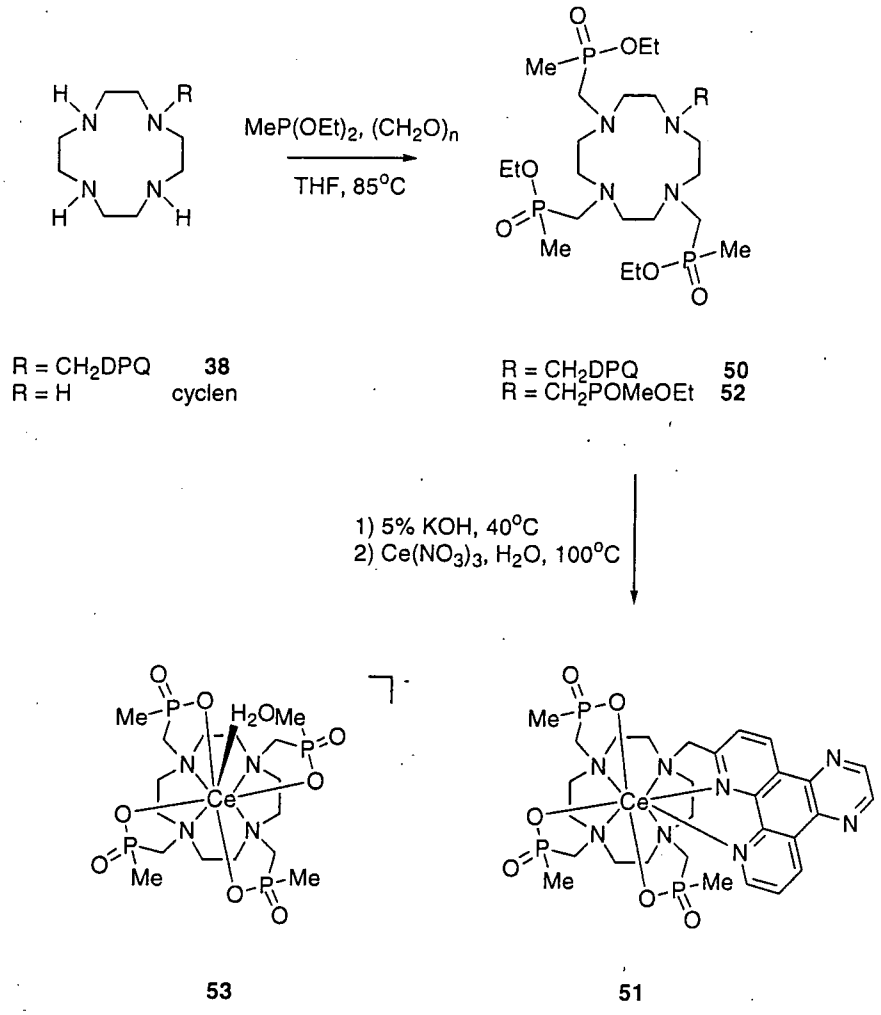

Scheme 2

The phosphinate arms were introduced on the monosubstituted macrocycle **38** and on cyclen by condensation of the secondary amine groups with resublimed paraformaldehyde in the presence of methyldiethoxyphosphine to give, after an Arbuzov rearrangement, the methylene phosphinate esters **50** and **52**. Exclusion of moisture was essential to prevent formation of the hydroxymethylphosphinate ester and 4 Å molecular sieves were used to scavenge any water.

Base hydrolysis with aqueous potassium hydroxide afforded the corresponding phosphinic acids which, after neutralisation, were reacted with cerium nitrate to obtain the Ce(III) complexes **51** and **53**.

4.2. Characterisation

The ^{1}H NMR spectrum of [CeDOTA]$^-$ was assigned following the sequence defined in the literature.[10] In the spectral region between 10 and -10 ppm, only one set of six resonances, each accounting for four protons, was observed. The nature and sequence of the shifts observed corresponds to an isomer adopting a twisted square antiprismatic geometry. The signals of the asymmetric CeDO3Adpq complex covered a wider range of chemical shifts (from 34 to -13 ppm), comparable to that observed for $EuPh_3dpq$ and $EuNp_3dpq$ complexes, which may indicate the presence of a square antiprismatic coordination geometry.

The stereoisomerism of the complexes bearing phosphinate arms is more complicated, because binding of a phosphinate oxygen atom to the metal generates a chiral centre at phosphorus. This results in additional species, compared to the four stereoisomers observed for DOTA complexes (Fig.1.23), corresponding to all the possible combinations of an R or S configuration at each phosphorus centre with the λ or δ conformation of the ring and the Λ or Δ orientation of the arms. Six combinations (RRRR, SSSS, RRRS, SSSR, RRSS, RSRS) are possible in tetraphosphinate complexes, leading to 24 possible stereoisomers (12 pairs of enantiomers) for [CeMeP$_4$]$^-$, and eight (RRR, SSS, RRS, RSS, RSR, SRS, SRR, SSR) in triphosphinate complexes, giving rise to 32 possible stereoisomers (16 pairs of enantiomers) for $CeMeP_3dpq$.[11]

The ^{1}H NMR spectrum of [CeMeP$_4$]$^-$ showed the presence of a single stereoisomer, with resonances strictly related to those of [CeDOTA]$^-$. By analogy, a twisted square antiprismatic geometry is believed to be preferentially adopted in aqueous solution. In the ^{31}P NMR spectrum, one signal, accounting for the four equivalent phosphorus atoms, was apparent, which confirms the presence of only one C_4-symmetric species, presumably with an RRRR or SSSS configuration at the four stereogenic phosphorus centres. The same spectral features were observed for several lanthanide tetrabenzylphosphinate complexes,[12] for which crystal structures were obtained, showing a twisted square antiprismatic geometry. In those complexes, only the larger

lanthanide ions (La to Nd) were able to accommodate a water molecule in the first coordination sphere.[13] $[CeMeP_4]^-$ is thus expected to have one coordinated water.
The ^{31}P NMR spectrum of $CeMeP_3$dpq showed one main set of three, equally intense resonances, which is indicative of one predominant species in solution with three non-equivalent phosphorus nuclei with an RRR or SSS configuration at the stereogenic P centres. The same behaviour has been observed for lanthanide complexes of monoamide triphosphinate derivatives.[11] The chemical shift sequence and range in the ^1H NMR spectrum of $CeMeP_3$dpq was similar to that obtained for the CeDO3Adpq complex, suggesting that a square antiprismatic coordination geometry may be adopted.

4.3. Electrochemical Studies

The redox properties of the cerium complexes were investigated by electrochemical methods in aqueous solution. Cyclic voltammetry experiments were carried out using a glassy carbon working electrode, a platinum counter electrode and a silver/silver chloride reference electrode. The potential was swept between -0.75 and 2 V at different scan rates. A supporting electrolyte of aqueous potassium nitrate was employed at concentrations 100 times higher than that of the analytes, in order to reduce the electrical resistance of the cell and to maintain a constant ionic strength.
For each of the complexes under study, an irreversible process was observed, attributable to the oxidation of Ce(III) to Ce(IV) (Fig.4.2). The voltammograms showed only an anodic wave, with a main peak around 1.6 V, consistent with the potential reported in the literature for Ce(III) → Ce(IV) oxidation (1.59 V vs Ag/AgCl at 25°C). The small peaks at lower potentials (0.6-0.7 V) may be due to oxidation of the ligand.

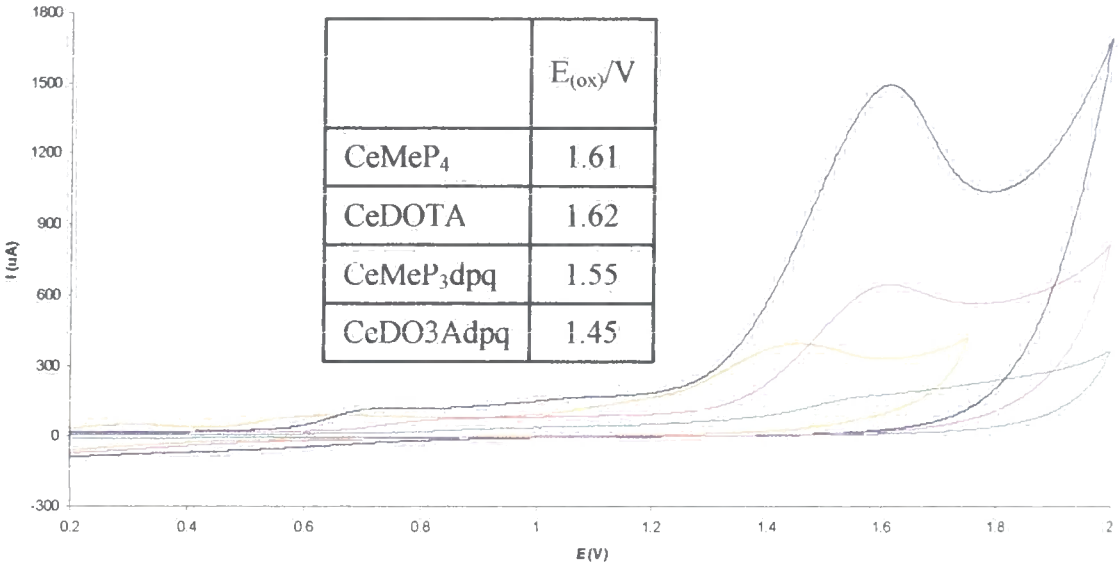

	$E_{(ox)}$/V
$CeMeP_4$	1.61
CeDOTA	1.62
$CeMeP_3dpq$	1.55
CeDO3Adpq	1.45

Fig.4.2 Cyclic voltammograms of $[CeMeP_4]^-$ (blue line), $[CeDOTA]^-$ (pink line), CeDO3Adpq (orange line) and $CeMeP_3dpq$ (green line) (10 mM in aqueous KNO_3 1M, pH 5, 298 K, scan rate 150 mV/s). The table shows the peak potentials vs Ag/AgCl.

The oxidation potential of Ce(III) in the complexes with DOTA and MeP_4 is similar to that of the free ion, while lower values were measured for the complexes containing dpq (Table in Fig.4.2). It can be concluded that the ease of oxidation at the metal centre follows the order CeDO3Adpq > $CeMeP_3dpq$ > $[CeDOTA]^-$ ≈ $[CeMeP_4]^-$.

The current at the peak potential (i_p) provides information about the kinetics of the electrochemical reaction. The intense peak currents observed for $[CeDOTA]^-$ and $[CeMeP_4]^-$ indicated that the oxidation of the ion in these complexes occurred under diffusion control and that the electron transfer process was fast. On the contrary, the complexes containing the bulky dpq moiety gave rise to smaller currents, probably reflecting their lower diffusion coefficients.

4.4. Absorption and Emission Spectra

The absorption spectra of the Ce(III) complexes were recorded in aqueous solution (Fig.4.3).

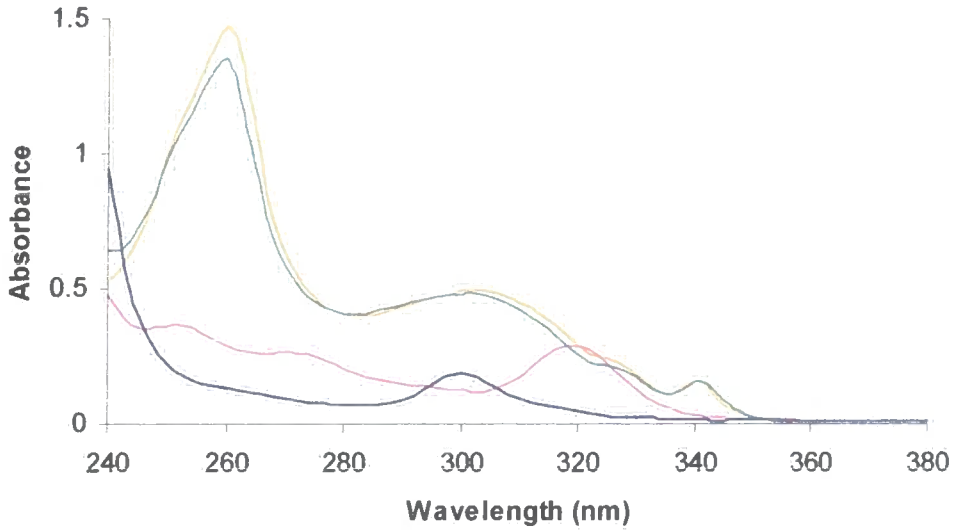

Fig.4.3 Absorption spectra of $[CeMeP_4]^-$ (blue line), $[CeDOTA]^-$ (pink line), CeDO3Adpq (orange line) and $CeMeP_3dpq$ (green line) (H_2O, 298 K).

The bands observed at 318 nm for $[CeDOTA]^-$ and 300 nm for $[CeMeP_4]^-$ were attributed to metal centred transitions. The free Ce^{3+} ion has only one electron in the 4f orbitals. Transitions from the closely spaced $^2F_{5/2}$ and $^2F_{7/2}$ ground state levels to the $5d^1$ excited state configuration give rise to absorption bands between 210 and 260 nm.[14] These bands are shifted to longer wavelengths (typically 300-400 nm) when cerium is included in a complex.[15,16,17]

In the spectra of CeDO3Adpq and $CeMeP_3dpq$, the f-d transitions at the metal are obscured by those of the ligand. The absorption bands correspond mainly to intraligand transitions, as revealed by the close resemblance with the spectra of the $LnPh_3dpq$ complexes, described in the previous chapter. For each of the cerium complexes under study, no metal-to-ligand charge transfer band was apparent.

The luminescence of cerium(III) compounds is usually relatively intense and short lived (ns timescale), since it arises from spin-allowed 5d→4f transitions. The emission spectra of Ce(III) complexes are characterised by bands in the range 340-450 nm.[15,18] Excitation of $[CeDOTA]^-$ and $[CeMeP_4]^-$ in correspondence to the absorption maximum resulted in emission at 460 and 420 nm respectively, consistent with metal-centred transitions (Fig.4.4).

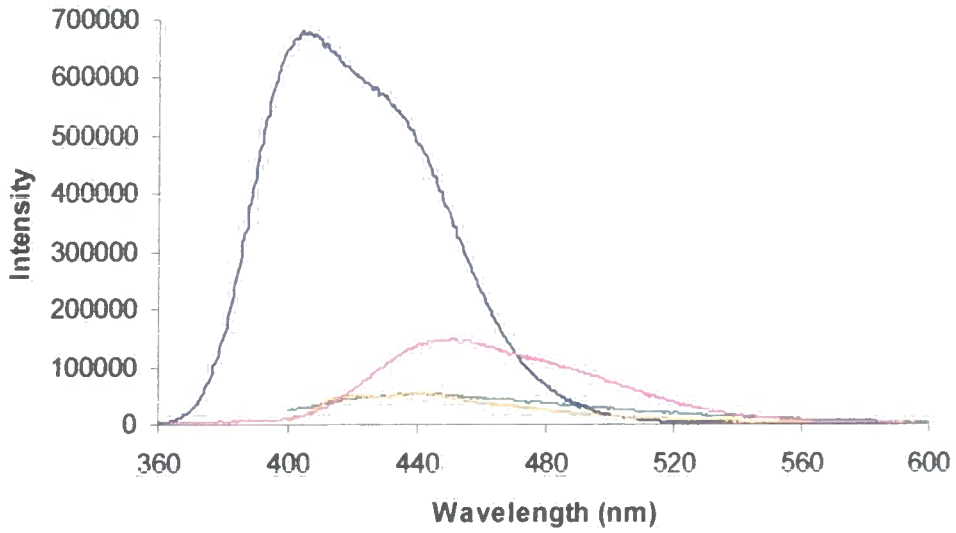

Fig.4.4 Emission spectra of $[CeMeP_4]^-$ (blue line), $[CeDOTA]^-$ (pink line), CeDO3Adpq (orange line) and $CeMeP_3dpq$ (green line), following excitation at 300, 318, 360 and 360 nm respectively (H_2O, 298 K).

No luminescence from CeDO3Adpq and $CeMeP_3dpq$ was observed when the complexes were excited at 340, 320 and 300 nm. Only upon excitation at 360 nm, into the tail of the longest wavelength band, did a weak emission band appear at 450 nm, consistent with a metal-centred d-f excited state. It must be concluded that the emissive state here can be populated only by using the longer excitation wavelength, so that the dpq chromophore does not interfere in the absorption process.

4.5. Chemical Oxidation

The cyclic voltammetry experiments proved that oxidation of the metal centre is possible for each of the four Ce(III) complexes. Chemical oxidation was therefore attempted, in aqueous solution, by addition of an excess of sodium persulfate. This reagent was chosen for its high oxidation potential (2.01 V).[19] The oxidation proved to be very slow and was observed to progress to a considerable extent only in the presence of a saturated solution of persulfate.

Formation of Ce(IV)MeP_4 was monitored by ^{31}P NMR. The peak at 38 ppm, corresponding to the four equivalent phosphorus atoms in the Ce(III) species, progressively disappeared over a period of 10 days. A new resonance appeared at 48.6 ppm, which was attributed to the oxidised Ce(IV)MeP_4 complex.

Similarly, ^1H NMR spectra of $[CeDOTA]^-$ revealed the presence of an increasing amount of the diamagnetic Ce(IV) species, as a set of six resonances between 3 and 4 ppm. In this case, however, the reaction did not go to completion, as the signals of the paramagnetic Ce(III) complex were still apparent, although decreased in intensity by 80%, even after 20 days. A colourless solid appeared upon standing, which was isolated and identified as Ce(IV)DOTA. Its ^1H NMR spectrum in D_2O showed the pattern typical of a diamagnetic lanthanide complex of DOTA. Six resonances were apparent: two doublets, at 3.97 and 3.66 ppm, corresponding to the acetate methylene protons (J_{gem} = 16.8 Hz), two triplets, at 3.80 and 2.97 ppm, attributable to the 'axial' ring protons and two doublets, at 3.14 and 2.88 ppm, arising from the 'equatorial' protons (J_{trans} = 15.0 Hz). Additional broad resonances in the same spectral region may indicate the presence of a minor isomer. The slightly closer resemblance to the spectrum of LuDOTA, rather than LaDOTA,[20] may suggest that the Ce(IV)DOTA complex adopts in solution a square antiprismatic geometry, preferentially. A similar pattern of resonances was also reported for Zr(IV)DOTA,[21] a complex which also showed very low solubility in most polar solvents. The same physical property characterises Ce(IV)DOTA, limiting the range of solution NMR experiments that could be undertaken to clarify the coordination geometry of the complex and the nature of the minor isomer.

Absorption and emission spectra of Ce(IV)MeP_4 and Ce(IV)DOTA were recorded in water. Only a tail of a high energy band, probably due to intraligand transitions, reaching zero absorbance around 350 nm, was apparent in the absorption spectra. Excitation at different wavelength within this tail did not result in any emission from the Ce(IV) species, which is consistent with the absence of a low energy ligand-to-metal charge transfer state.

Addition of an excess of persulfate to $CeMeP_3$dpq and CeDO3Adpq resulted in an exceedingly slow oxidation at the metal centre. For the former complex, the progress of the reaction is being followed by ^{31}P NMR: the Ce(IV) species could not be detected even after 10 days. Monitoring the oxidation by ^{1}H NMR spectroscopy was considered too complicated, therefore only the photophysical behaviour of the two complexes containing the dpq moiety was investigated. No additional bands appeared, in their absorption spectra, on the red side of the intraligand transition at 340 nm. Thus no clear evidence for an LMCT process was provided. A ligand-to-metal charge transfer interaction is unlikely to occur also in the excited state, as suggested by the lack of emission of each complex, following attempted excitation at 340 and 360 nm.

4.6. Conclusions

The Ce(III) complexes containing a dpq chromophore did not show any evidence of a metal-to-ligand charge transfer process. They cannot therefore act as photoactivated reactive probes for nucleic acid cleavage. Although oxidation can be achieved in the ground state, the irreversibility of the reaction, shown by the cyclic voltammetry experiments, makes them unlikely to cause any oxidative damage to DNA. However, the possibility of obtaining stable Ce(IV) complexes with DOTA and MeP_4 ligands has been demonstrated, which represents a good starting point in the design of potential nucleases.

The hydrolytic ability of Ce(IV) can be fully exploited only in complexes with heptadentate ligands, in which two sites are available to coordinate a phosphate

group of the DNA backbone and a water molecule.[22] Moreover, removal of one anionic arm from DOTA and MeP_4 would give rise to cationic Ce(IV) complexes, which could approach the anionic nucleic acid site more easily.

References

1 J. P. Lecomte, A. KirschDeMesmaeker, M. M. Feeney, and J. M. Kelly, *Inorganic Chemistry*, 1995, **34**, 6481.

2 C. Turro, A. Evenzahav, S. H. Bossmann, J. K. Barton, and N. J. Turro, *Inorganica Chimica Acta*, 1996, **243**, 101.

3 S. Steenken and S. V. Jovanovic, *Journal of the American Chemical Society*, 1997, **119**, 617.

4 C. A. M. Seidel, A. Schulz, and M. H. M. Sauer, *Journal of Physical Chemistry*, 1996, **100**, 5541.

5 C. G. Coates, P. Callaghan, J. J. McGarvey, J. M. Kelly, L. Jacquet, and A. Kirsch-De Mesmaeker, *Journal of Molecular Structure*, 2001, **598**, 15.

6 H. Kunkely and A. Vogler, *Journal of Photochemistry and Photobiology A-Chemistry*, 2002, **151**, 45.

7 S. Delaney, M. Pascaly, P. K. Bhattacharya, K. Han, and J. K. Barton, *Inorganic Chemistry*, 2002, **41**, 1966.

8 S. D. Kean, University of Durham, 2001.

9 C. J. Broan, E. Cole, K. J. Jankowski, D. Parker, K. Pulukkody, B. A. Boyce, N. R. A. Beeley, K. Millar, and A. T. Millican, *Synthesis-Stuttgart*, 1992, 63.

10 M. P. M. Marques, C. Geraldes, A. D. Sherry, A. E. Merbach, H. Powell, D. Pubanz, S. Aime, and M. Botta, *Journal of Alloys and Compounds*, 1995, **225**, 303.

11 S. Aime, M. Botta, D. Parker, and J. A. G. Williams, *Journal of the Chemical Society-Dalton Transactions*, 1995, 2259.

12 S. Aime, A. S. Batsanov, M. Botta, J. A. K. Howard, D. Parker, K. Senanayake, and G. Williams, *Inorganic Chemistry*, 1994, **33**, 4696.

13 S. Aime, A. S. Batsanov, M. Botta, R. S. Dickins, S. Faulkner, C. E. Foster, A. Harrison, J. A. K. Howard, J. M. Moloney, T. J. Norman, D. Parker, L. Royle, and J. A. G. Williams, *Journal of the Chemical Society-Dalton Transactions*, 1997, 3623.

14 B. Keller, J. Legendziewicz, J. Przybylski, M. Guzik, and J. Glinski, *Journal of Alloys and Compounds*, 2002, **341**, 197.

15 G. Blasse, G. J. Dirksen, N. Sabbatini, and S. Perathoner, *Inorganica Chimica Acta*, 1987, **133**, 167.

16 E. Toth, E. Brucher, I. Lazar, and I. Toth, *Inorganic Chemistry*, 1994, **33**, 4070.

17 M. Ciampolini, F. Mani, and N. Nardi, *Journal of the Chemical Society-Dalton Transactions*, 1977, 1325.

18 H. Kunkely and A. Vogler, *Journal of Photochemistry and Photobiology A-Chemistry*, 2001, **146**, 63.

19 F. Minisci, A. Citterio, and C. Giordano, *Accounts of Chemical Research*, 1983, **16**, 27.

20 S. Aime, M. Botta, and G. Ermondi, *Inorganic Chemistry*, 1992, **31**, 4291.

21 D. Parker, K. Pulukkody, F. C. Smith, A. Batsanov, and J. A. K. Howard, *Journal of the Chemical Society-Dalton Transactions*, 1994, 689.

22 S. J. Franklin, *Current Opinion in Chemical Biology*, 2001, **5**, 201.

Conclusions and Further Work

On the basis of the results presented in this thesis, it can be concluded that the design of lanthanide probes for nucleic acids is a challenging area of research.

It has been shown that the parameters related to the efficiency of the complexes as luminescent probes can be optimised. In the design of the Ph_3dpq complexes, the favourable photophysical properties of the dpq antenna and the nonadentate nature of the ligand have been exploited, in order to obtain highly emissive europium and terbium complexes. Indeed, their emission quantum yields in aqueous media are remarkably high.

On the other hand, the spectroscopic behaviour of the complexes in the presence of nucleic acids proved to be unpredictable. An interactive unit can be included in the ligand, but its involvement in the sensitisation process, as well as the interaction with DNA, makes it difficult to predict if the lanthanide luminescence will be enhanced or diminished. The reversal in the variation of the metal emission intensity observed for Ph_3dpq and Np_3dpq complexes in the presence of nucleic acid was particularly intriguing.

The differences observed in the interaction of the Δ and Λ isomers of each of the complexes under study with right-handed DNA are consistent with a certain degree of stereoselectivity in binding. Further studies are required to ascertain which groove is involved in the binding process. Molecular modelling based on the X-ray data of related lanthanide complexes could give a useful indication.

The synthesis of new lanthanide complexes containing derivatives of the dpq chromophore can be envisaged. A recognition element can be included, such as an oligonucleotide or a peptide unit, to increase the regioselectivity of the interaction. The recognition moiety can easily be attached to the pyrazine ring of dpq by condensation of the dione with an ethylenediamine derivative.

CHAPTER 5

Experimental

5.1. Synthetic Procedures and Characterisation

Reactions requiring anhydrous conditions were carried out using Schlenk-line techniques under an atmosphere of dry argon. Solvents were dried from an appropriate drying agent when required and water was purified by the 'Purite$_{STILL}$ plus' system.

Thin-layer chromatography was carried out on neutral alumina plates (Merck Art 5550) or silica plates (Merck 5554) and visualised under UV (254 nm) or by staining with iodine. Preparative column chromatography was carried out using neutral alumina (Merck Aluminium Oxide 90, activity II-III, 70-230 mesh), pre-soaked in ethyl acetate, or silica (Merck Silica Gel 60, 230 ± 400 mesh).

Infra-red spectra were recorded on a Perkin-Elmer 1600 FT spectrometer operating with GRAMS Analyst software. ^{1}H, ^{13}C and ^{31}P NMR spectra were recorded on a Varian Mercury 200 (^{1}H at 199.975 MHz, ^{13}C at 50.289 MHz), Varian Unity 300 (^{1}H at 299.908 MHz, ^{13}C at 75.412 MHz), Varian VXR 400 (^{1}H at 399.968 MHz, ^{13}C at 100.572 MHz), or a Bruker AMX 500 spectrometer. Spectra were referenced internally to the residual protio-solvent resonances and are reported relative to TMS. All chemical shifts are given in ppm and coupling constants in Hz. Splitting patterns are described as singlet (s), doublet (d), triplet (t), quartet (q), or multiplet (m). Electrospray mass spectra were recorded on a VG Platform II (Fisons instrument), operating in positive or negative ion mode as stated, with methanol as the carrier solvent. Accurate mass spectra were recorded at the EPSRC Mass Spectrometry Service at the University of Wales, Swansea. Melting points were recorded using a Reichart-Köfler block and are uncorrected.

Compounds **1-18**, **43**, **52** were previously reported by the Parker group and were synthesised with the same procedure (except for **2**, as discussed in chapter 2). **19**, **20**, **21**, **24**, **25**, **36**, **54** are literature compounds and were synthesised with the procedure reported in the literature. The other compounds are entirely new.

1. 2-Bromophenanthridine[1]

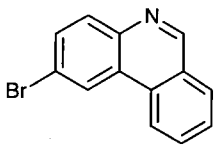

Phenanthridine (5 g, 28 mmol) was dissolved in CCl_4 (150 ml). Excess N-bromosuccinimide (20 g, 112 mmol) and a catalytic amount of AIBN (400 mg) were added and the reaction mixture heated at reflux at 80°C for 6 days. The orange suspension was filtered through a Buchner whilst warm to remove NBS in excess. Removal of the solvent under reduced pressure gave the crude product, which was taken into 400 ml CH_2Cl_2 and washed with 5% $NaHCO_3$ solution (2 × 150 ml). A yellow solid was obtained (7.6 g). Purification by chromatography on silica (gradient elution: CH_2Cl_2 to 1% CH_3OH/CH_2Cl_2, R_f = 0.7, 5% CH_3OH/CH_2Cl_2) and recrystallisation from hot ethanol gave a colourless solid (3.0 g, 12 mmol, 43%). ^1H NMR (300 MHz, $CDCl_3$): δ 7.77 (1H, ddd, J = 0.9, 7.1, H8), 7.84 (1H, dd, J = 2.0, 8.6, H3), 7.92 (1H, ddd, J = 1.5, 6.9, H9), 8.07 (1H, d, J = 8.4, H7), 8.10 (1H, d, J = 8.8, H4), 8.56 (1H, d, J = 8.2, H10), 8.73 (1H, d, J = 2.0, H1), 9.30 (1H, s, H6). M.p. 155-158°C (lit.[9] 160-162.5°C).

2. 2-Cyanophenanthridine[1]

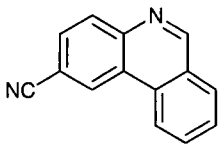

A mixture of compound **1** (2.9 g, 11.4 mmol), copper (I) cyanide (4.9 g, 46 mmol), palladium (0) bis(dibenzylideneacetone) (0.5 g, 0.92 mmol), 1,1'-bis(diphenylphosphino)ferrocene (1.0 g, 1.8 mmol) and tetraethylammonium cyanide (1.8 g, 11.4 mmol) in dry dioxane (50 ml) was boiled under reflux at 110°C under an argon atmosphere. The reaction mixture turned dark red, then grey-green. After 4

hours it was diluted with ethyl acetate, filtered through a celite plug and thoroughly washed with ethyl acetate. The filtrate was washed with saturated aqueous $NaHCO_3$ solution (3 × 100 ml) and dried over $MgSO_4$. The solvent was evaporated under reduced pressure to yield a yellow product which was purified by column chromatography on silica (gradient elution: CH_2Cl_2 to 2% CH_3OH/CH_2Cl_2, R_f = 0.1, CH_2Cl_2) and recrystallisation from hot ethanol, to yield a colourless solid (0.78 g, 3.82 mmol, 33%). ^{1}H NMR (300 MHz, $CDCl_3$): δ 7.84 (1H, ddd, J = 0.9, 7.8, H8), 7.94 (1H, dd, J = 1.5, 8.4, H3), 7.99 (1H, ddd, J = 1.5, 7.5, H9), 8.14 (1H, d, J = 8.1, H7), 8.28 (1H, d, J = 8.4, H4), 8.60 (1H, d, J = 8.1, H10), 8.94 (1H, s, H1), 9.41 (1H, br s, H6). m/z (ES^+) 205 (100%, MH^+), 227 (65%, MNa^+). M.p. 200-205°C (dec.).

3. 2-(Aminomethyl)phenanthridine[1]

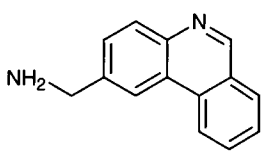

Compound **2** (0.78 g, 3.82 mmol) was taken into a solution of borane-THF (1M, 19 ml, 19 mmol) and boiled under reflux at 75°C for 20 hours under argon. The reaction mixture turned green. ^{1}H NMR (300 MHz, $CDCl_3$, no peaks > 7.7 ppm) revealed that in addition to complete reduction of the cyano group , the N-C6 double bond had also been reduced. Excess borane was quenched by addition of CH_3OH. The solvent was removed by evaporation under reduced pressure and quenching repeated twice more. The residue was taken into HCl (1M, 50 ml) and boiled under reflux at 100°C for 36 hours to re-aromatise the ring. The acidic solution was then washed with diethyl ether (3 × 50 ml) and the pH raised to 13 by addition of KOH pellets. The product was extracted into CH_2Cl_2 (3 × 50 ml), dried over K_2CO_3 and the solvent evaporated to yield a colourless solid (0.51 g, 2.45 mmol, 64%). ^{1}H NMR (300 MHz, $CDCl_3$): δ 1.60 (2H, br s, NH_2), 4.16 (2H, s, CH_2), 7.71 (2H, dd, H3, H8), 7.86 (1H, ddd, J = 1.2, 7.5, H9), 8.04 (1H, d, J = 7.5, H7), 8.16 (1H, d, J = 8.1, H4), 8.52 (1H, s, H1), 8.64 (1H, d, J = 8.1, H10), 9.26 (1H, s, H6).

4. N-(2'-Chloroethanoyl)-2-phenanthridinylmethylamine[1]

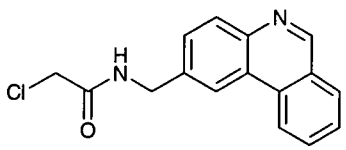

A solution of compound **3** (0.51 g, 2.44 mmol) in anhydrous THF (16 ml) was added to chloroacetic acid (0.23 g, 2.44 mmol). Upon cooling to 0°C, 1-hydroxybenzotriazole (0.33 g, 2.44 mmol) and 1-(3-dimethylaminopropyl)-3-ethylcarbodiimide hydrochloride (0.48 g, 2.53 mmol) were added. The mixture was allowed to warm to room temperature and then stirred for a further hour. The solution was decanted and the solid washed with THF. The solvent was removed by evaporation under reduced pressure and the residue taken into CH_2Cl_2 (75 ml). This solution was washed with saturated aqueous $NaHCO_3$ solution (2 × 50 ml), followed by water (2 × 50 ml) and dried over K_2CO_3. The solvent was removed to yield a white solid, which was used without further purification (0.48 g, 1.69 mmol, 69%). ^{1}H NMR (300 MHz, $CDCl_3$): δ 4.18 (2H, s, CH_2Cl), 4.78 (2H, d, J = 6.0, CH_2NH), 7.10 (1H, br s, NH), 7.68 (1H, dd, J = 1.8, 8.4, H3), 7.75 (1H, dd, J = 7.8, H8), 7.89 (1H, dd, J = 7.8, H9), 8.07 (1H, d, J = 7.5, H7), 8.19 (1H, d, J = 8.4, H4), 8.50 (1H, s, H1), 8.61 (1H, d, J = 8.1, H10), 9.29 (1H, s, H6). M.p. > 250°C.

5. Molybdenum tricarbonyl-1,4,7,10-tetraazacyclododecane complex[2]

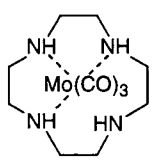

Dry 1,4,7,10-tetraazacyclododecane (0.29 g, 1.69 mmol) was put in an argon filled flask. Dry butyl ether (25 ml) was added and the suspension heated to 100°C under argon. Dry molybdenum hexacarbonyl (0.45 g, 1.69 mmol) was then added and the

reaction mixture refluxed under argon at 160°C for 2 hours, cooled, then filtered under argon. The yellow solid **5** was dried under vacuum and used immediately.

6. 1-(2'-Phenanthridinylmethylcarbamoylmethyl)-1,4,7,10-tetraazacyclododecane[1]

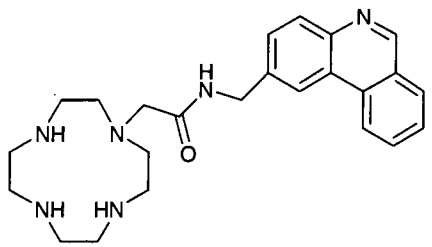

Dry K_2CO_3 (0.23 g, 1.69 mmol) and a solution of compound **4** (0.48 g, 1.69 mmol) in 40 ml of dry, degassed DMF were added to compound **5** (0.60 g, 1.69 mmol). The reaction mixture was stirred under argon at 80°C for 2 hours (it turned from yellow to brown). The DMF was then removed under reduced pressure affording a brown residue which was taken into HCl (1M, 25 ml) and stirred at room temperature overnight. KOH pellets were then added to the solution to attain pH 14. The resulting suspension was centrifuged, the aqueous phase decanted off and then extracted with CH_2Cl_2 (3 × 40 ml), dried over K_2CO_3 and the solvent removed under vacuum to yield a brown oily residue (0.32 g, 0.76 mmol, 45%). ^{1}H NMR (300 MHz, $CDCl_3$): δ 2.45 (8H, m, ring CH), 2.59 (8H, s, ring CH), 3.25 (2H, s, NCH_2), 4.70 (2H, d, J = 5.7, $NHCH_2$), 7.68 (2H, m, H3, H8), 7.83 (1H, dd, J = 1.4, 7.0, H9), 8.01 (1H, d, J = 8.0, H7), 8.10 (1H, d, J = 8.4, H4), 8.51 (1H, s, H1), 8.63 (1H, d, J = 8.2, H10), 9.22 (1H, s, H6). m/z (ES^+) 421 (100%, MH^+).

7. (R)-2-Chloro-N-[1-(phenyl)ethyl]ethanamide[1]

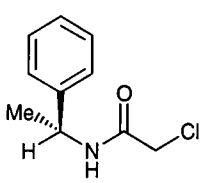

Chloroacetylchloride (8 ml, 101.5 mmol) was added dropwise to a stirred solution of (R)-1-phenylethylamine (11 ml, 83 mmol) and triethylamine (14 ml, 99 mmol) in dry THF (400 ml) at -5°C under argon. The reaction mixture was allowed to warm to room temperature and stirred for 1 hour. The product was extracted into diethyl ether, which was then washed with HCl (0.1M, 50 ml), water (3 × 30 ml) and dried over K_2CO_3. Recrystallisation from diethyl ether yielded white needles (6.1 g, 31 mmol, 31%). ^{1}H NMR (300 MHz, $CDCl_3$): δ 1.55 (3H, d, J = 6.9, CH_3), 4.08 (2H, dd, CH_2), 5.15 (1H, q, J = 7.2, CH), 6.79 (1H, br s, NH), 7.35 (5H, m, Ph). M.p. 92-95°C.

8. 1-(2'-Phenanthridinylmethylcarbamoylmethyl)-4,7,10-tris[(R)-1-(1-phenyl)ethylcarbamoylmethyl]-1,4,7,10-tetraazacyclododecane[1]

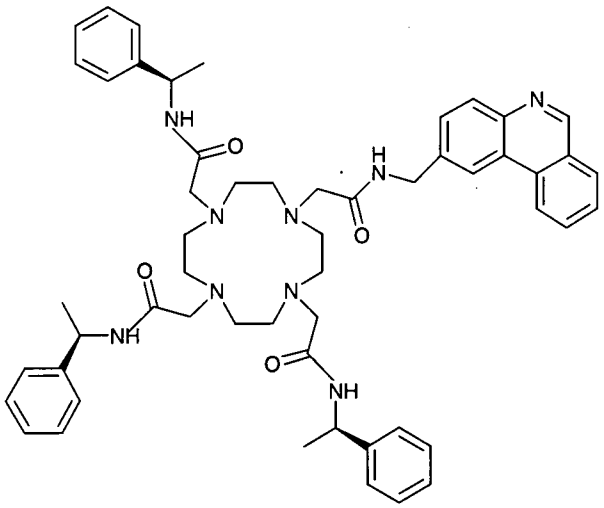

A solution of compound **6** (0.32 g, 0.76 mmol) in a mixture of CH_3CN and CH_2Cl_2 (25 ml) was added to compound **7** (0.45 g, 2.27 mmol) and Cs_2CO_3 (0.74 g, 2.27 mmol). The mixture was stirred under argon at 70°C overnight. The solvent was removed by evaporation and the residue taken into CH_2Cl_2 (20 ml), washed with water (3 × 50 ml), dried over K_2CO_3 and the solvent removed by evaporation to yield a glassy solid, purified by recrystallisation from acetonitrile by addition of ether (0.17 g, 0.19 mmol, 25%). ^{1}H NMR (300 MHz, $CDCl_3$): δ 1.40 (6H, d, J = 6.9, CH_3),

1.43 (3H, d, J = 6.9, CH_3), 2.48 (16H, br m, CH_2 ring), 2.75 (2H, s, NCH_2CO), 2.80 (2H, s, NCH_2CO), 2.82 (2H, s, NCH_2CO), 3.60 (2H, s, NCH_2CO), 4.52 (1H, dd, J = 6, 14.7, phenCH_2NH), 4.68 (1H, dd, J = 6, 14.7, phenCH_2NH), 5.06 (3H, m, J = 7.8, CH), 6.64 (2H, d, J = 8.1, CONH), 6.82 (1H, d, J = 8.1, CONH), 7.24 (15H, m, Ph), 7.60 (1H, dd, J = 8.1, 1.8, H3), 7.74 (1H, dd, J = 7.2, H8), 7.87 (1H, dd, J = 7.2, H9), 8.05 (1H, d, J = 7.5, H7), 8.12 (1H, d, J = 8.4, H4), 8.46 (1H, s, H1), 8.59 (1H, d, J = 8.4, H10), 9.25 (1H, s, H6). m/z (ES^+) 904 (100%, M^+), 926 (90%, MNa^+). M.p. 160-165°C.

9. (RRR)-Eu complex $(CF_3SO_3)_3$ [1]

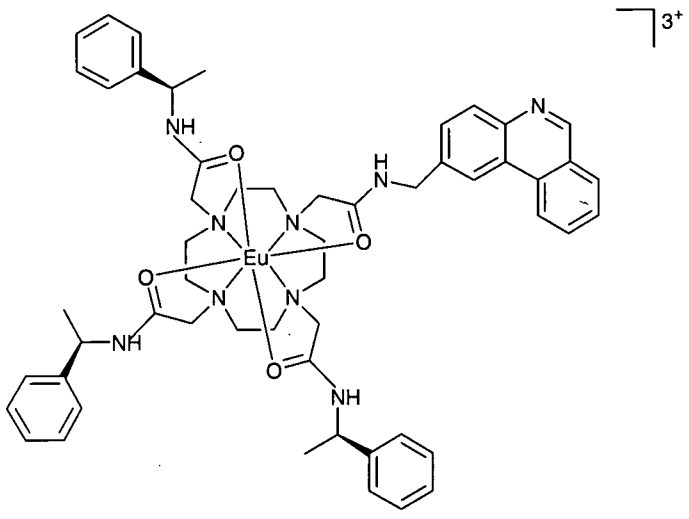

Compound **8** (60 mg, 0.06 mmol) and $Eu(OTf)_3$ (38 mg, 0.06 mmol) were dissolved in anhydrous CH_3CN (2 ml). The pale yellow solution was boiled under reflux at 80°C under argon overnight. The reaction mixture was dropped into ether (200 ml) with stirring: a white precipitate formed, which was separated by centrifugation. The solvent was decanted off, the solid redissolved in CH_3CN and the process repeated. A colourless solid was obtained (44 mg, 0.03 mmol, 50%). ^1H NMR (300 MHz, CD_3OD) partial assignment: δ 29.2 (1H, s, Hax), 28.4 (2H, s, Hax), 27.7 (1H, s, Hax), 9.8, 9.4, 8.7, 8.4, 8.2, 8.1 (8H, phenanthridine signals, coupling not resolved due to lanthanide induced line broadening), 5.8-5.6 (15H, Ph), -1.6 (1H, s, Heq), -2.1 (1H, s, Heq), -2.2 (1H, s, Heq), -2.5 (1H, s, Heq), Hax and Heq at -5.9 (1H, s), -6.3

(1H, s), -7.1 (4H, s), -7.9 (1H, s), -8.0 (1H, s), NCH_2CO at -13.5, -14.1, -14.3, -14.5. m/z (ES^+) 352 (100%, EuL^{3+}), 528 (5%, EuL^{2+}), 602 (45%, $EuLOTf^{2+}$), 1354 (3%, $EuL(OTf)_2^+$). M.p. 200-205°C (dec.).

10. (RRR)-Eutetraamide[1]

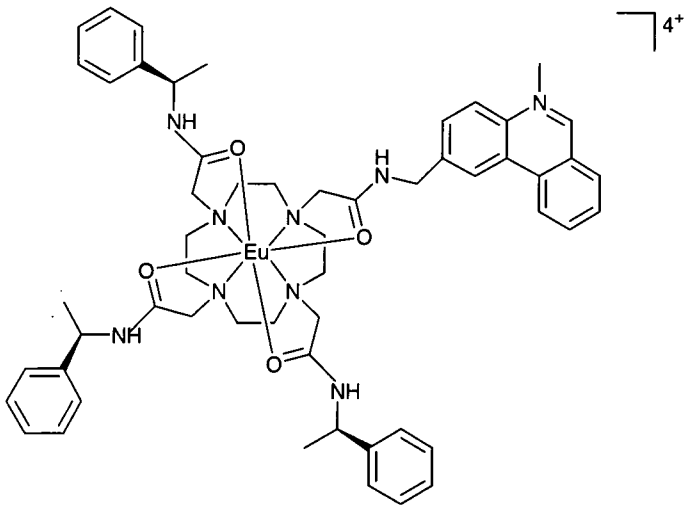

Compound **9** (44 mg, 0.03 mmol) was dissolved in CH_3CN (1 ml) and stirred overnight with an excess of iodomethane (0.5 ml) at 40°C. The excess iodomethane and residual solvent were removed by evaporation under reduced pressure, affording a yellow solid (50 mg, 0.03 mmol, 100%). ^1H NMR (300 MHz, CD_3OD) partial assignment: δ 29.7 (1H, s, Hax), 28.4 (1H, s, Hax), 27.8 (1H, s, Hax), 27.2 (1H, s, Hax), 10.3, 9.9, 9.2, 9.1, 8.9, 8.6 (8H, phenanthridinium signals), 5.9-5.6 (15H, Ph), -0.9 (1H, s, Heq), -2.0 (1H, s, Heq), -2.6 (2H, s, Heq), Hax and Heq at –4.8 (1H, s), -6.4 (1H, s), -6.6 (1H, s), -7.0 (1H, s), -7.4 (2H, s), -8.3 (2H, s), NCH_2CO at –13.5, -13.8, -14.2. m/z (ES^+) 356 (100%, $EuLMe^{3+}$), 535 (15%, $EuLMe^{2+}$), 610 (35%, $EuLMeOTf^{2+}$).

(SSS)-Eutetraamide was synthesised from the (SSS) ligand using the same procedure.

11. (RRR)-Gd complex $(CF_3SO_3)_3$ [1]

Compound **8** (38 mg, MW 903, 0.04 mmol) and $Gd(OTf)_3$ (25 mg, MW 604, 0.04 mmol) were dissolved in dry CH_3CN (2 ml). The procedure followed was identical to that described for compound **9**. m/z (ES^+) 354 (100%, GdL^{3+}), 530 (15%, GdL^{2+}), 605 (30%, $GdLOTf^{2+}$), 1359 (3%, $GdL(OTf)_2^+$).

12. (RRR)-Gdtetraamide[1]

Compound **12** was synthesised in the same way as **10** to yield a colourless solid (42 mg, 0.025 mmol, 63%). m/z (ES^+) 359 (100%, $GdLMe^{3+}$), 537 (15%, $GdLMe^{2+}$), 612 (30%, $GdLMeOTf^{2+}$).

13. 2-Methylphenanthridine[3]

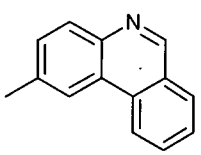

Compound **1** (1.43 g, 5.54 mmol) and a catalytic amount of $NiDPPPCl_2$ (80 mg) were stirred in dry THF (40 ml) at 0°C under a steady flow of argon. A solution of methylmagnesium bromide in diethyl ether (3M, 8 ml, 24 mmol) was added dropwise: the red solution turned brown. The reaction mixture was left stirring at 0°C for a further hour, then allowed to warm to room temperature under argon overnight. The reaction was quenched with aqueous KOH solution (3M, 20 ml) and the THF removed by evaporation. The product was extracted into CH_2Cl_2 (3 × 50 ml), which was then washed with brine (2 × 50 ml) and dried over K_2CO_3. Removal of the solvent under reduced pressure afforded a brown oil which was purified by chromatography over silica (gradient elution: CH_2Cl_2 to 1% CH_3OH/CH_2Cl_2, R_f = 0.3, 5% CH_3OH/CH_2Cl_2) to yield a colourless solid (0.49 g, 2.53 mmol, 46%). ^1H NMR (300 MHz, $CDCl_3$): δ 2.60 (3H, s, CH_3), 7.53 (1H, dd, J = 1.8, 8.4, H3), 7.64

(1H, dd, J = 0.9, 7.2, H8), 7.78 (1H, dd, J = 1.5, 7.2, H9), 7.97 (1H, d, J = 7.8, H7), 8.07 (1H, d, J = 8.4, H4), 8.28 (1H, s, H1), 8.51 (1H, d, J = 8.4, H10), 9.19 (1H, s, H6). m/z (ES^+) 194 (100%, MH^+), 216 (15%, MNa^+). M.p. 89-92°C.

14. 2-(Bromomethyl)phenanthridine[3]

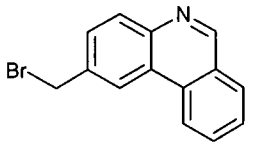

Compound **13** (487 mg, 2.52 mmol) was dissolved in CCl_4 (20 ml), N-bromosuccinimide (449 mg, 2.52 mmol) and a catalytic amount of AIBN were added. The mixture was refluxed at 80°C for 5 hours, then cooled, filtered (to remove the residual succinimide) and the solvent evaporated to give a colourless solid, which was used immediately. Yield (estimated by ^1H NMR): 62% (1.57 mmol). ^1H NMR (300 MHz, $CDCl_3$): δ 4.75 (2H, s, CH_2), 7.75 (2H, m, H3, H8), 7.88 (1H, dd, H9), 8.06 (1H, d, J = 7.8, H7), 8.21 (1H, d, J = 8.7, H4), 8.57 (2H, d, J = 9, H10, H1), 9.29 (1H, s, H6).

15. 1-(2'-Methylphenanthridinyl)-1,4,7,10-tetraazacyclododecane[3]

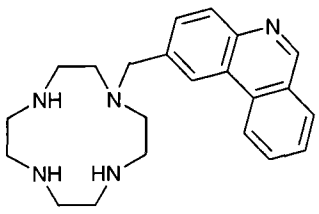

Cyclen (2.7 g, 15.7 mmol) and Cs_2CO_3 (770 mg, 2.36 mmol) were added to a solution of **14** (1.57 mmol) in CH_3CN (15 ml), and the resultant mixture boiled under reflux at 80°C under argon overnight. The suspension was filtered and the solvent removed under reduced pressure leaving a yellow solid. The residue was taken into

CH_2Cl_2 (30 ml) and washed extensively with water (5 × 100 ml) and brine (3 × 50 ml) to remove residual cyclen. The organic layer was dried over Na_2SO_4, filtered and evaporated to dryness to afford a yellow solid (240 mg, 42%, 0.66 mmol). ^{1}H NMR (300 MHz, $CDCl_3$): δ 2.65 (19H, m, ring CH_2, NH), 3.89 (2H, s, CH_2), 7.68 (2H, m, H3, H8), 7.82 (1H, dd, H9), 8:02 (1H, d, J = 7.8, H7), 8.13 (1H, d, J = 8.4, H4), 8.56 (1H, s, H1), 8.65 (1H, d, J = 8.4, H10), 9.23 (1H, s, H6). m/z (ES^+) 182 (100%, $MH^{2+}/2$), 364 (90%, MH^+).

16. 1-(2'-Methylphenanthridinyl)-4,7,10-tris[(R)-1-(1-phenyl)ethyl carbamoylmethyl]-1,4,7,10-tetraazacyclododecane[3]

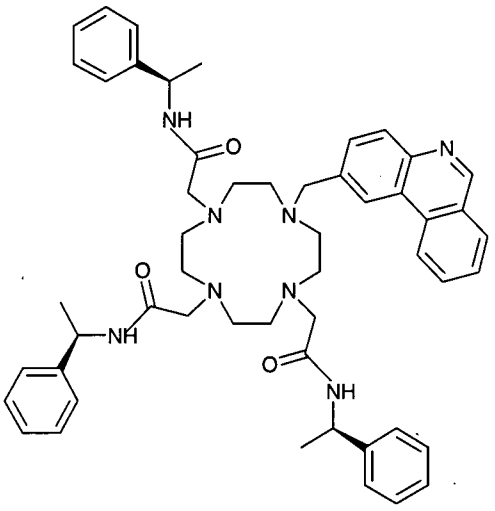

Compound **7** (405 mg, 2.05 mmol) and Cs_2CO_3 (711 mg, 2.18 mmol) were added to a solution of compound **15** (240 mg, 0.66 mmol) in a 1:1 mixture of CH_3CN and CH_2Cl_2 (20 ml). The reaction mixture was refluxed at 80°C under argon overnight. The solution was filtered and the solvent removed under vacuum. The crude residue was purified by chromatography over alumina (gradient elution: CH_2Cl_2 to 1% CH_3OH/CH_2Cl_2, R_f = 0.14, 10% CH_3OH/CH_2Cl_2) to yield a colourless glass (103 mg, 0.12 mmol, 18%). ^{1}H NMR (300 MHz, $CDCl_3$): δ 1.46 (6H, d, J = 6.6, CH_3), 1.55 (3H, d, J = 7.2, CH_3), 2.96 (16H, m, ring CH_2), 3.55 (6H, m, NCH_2CO), 3.90 (2H, s, NCH_2phen), 4.98 (3H, m, CH), 7.23 (15H, m, Ph), 7.35 (3H, m, NH), 7.58 (1H, d, J = 8.4, H3), 7.76 (1H, dd, J = 7.2, H8), 7.93 (1H, dd, J = 7.2, H9), 8.08 (1H,

d, J = 7.8, H7), 8.16 (1H, d, J = 8.4, H4), 8.42 (1H, s, H1), 8.66 (1H, d, J = 8.4, H10), 9.31 (1H, s, H6). m/z (ES^+) 435 (35%, $MHNa^{2+}$), 847 (30%, MH^+), 869 (100%, MNa^+).

17. (RRR)-Eu complex $(CF_3SO_3)_3$ [3]

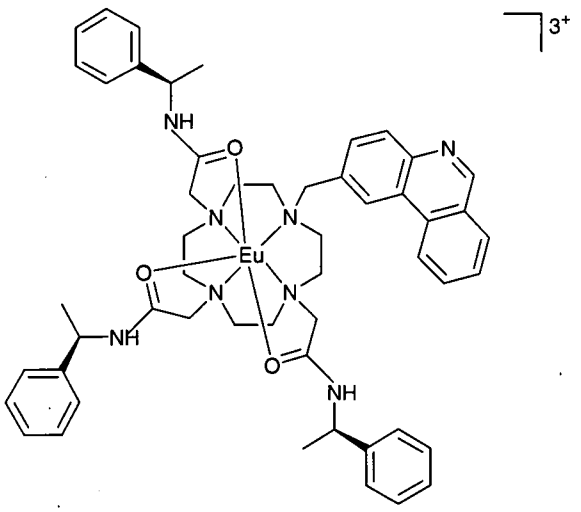

A solution of compound **16** (39 mg, 0.05 mmol) and $Eu(OTf)_3$ (28 mg, 0.05 mmol) in dry CH_3CN (2 ml) was boiled under reflux under argon overnight at 80°C. The solution was then added dropwise to ether (80 ml) with stirring, the precipitate centrifuged and the solvent decanted. The solid was redissolved in CH_3CN and the process repeated. A colourless solid was obtained (50 mg, 0.03 mmol, 60%). ^1H NMR (300 MHz, CD_3OD) partial assignment: δ 24.3 (1H, s, Hax), 22.6 (1H, s, Hax), 21.6 (1H, s, Hax), 19.5 (1H, s, Hax), 11.5, 10.4, 9.7, 9.4, 9.3, 9.1 (8H, phenanthridine signals), 5.3-5.1 (15H, Ph), Hax and Heq at -1.3 (2H, s), -2.5 (1H, s), -3.2 (1H, s), -4.3 (1H, s), -4.7 (1H, s), -5.9 (1H, s), -7.1 (1H, s), -8.4 (1H, s), -9.4 (1H, s), -9.7 (1H, s), -10.4 (1H, s), NCH_2CO at -10.9, -12.8, -13.2, -14.7, NCH_2phen at -18.9, -19.2. m/z (ES^+) after addition of CF_3COOH: 556 (100%, $MCF_3CO_2^{2+}$).

18. (RRR)-Eutriamide[3]

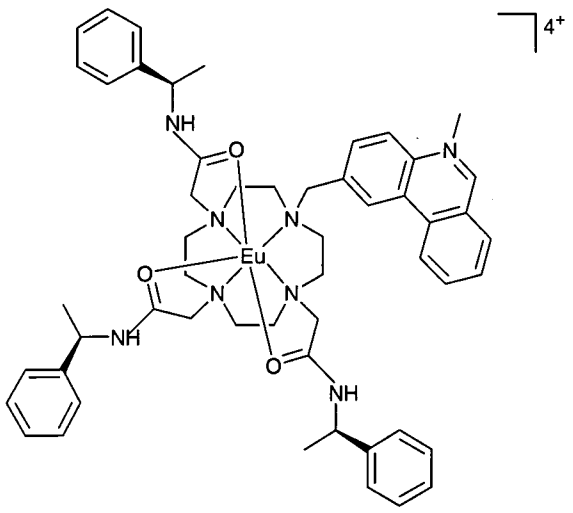

A solution of compound **17** (50 mg, 0.03 mmol) in CH_3CN (1 ml) was stirred with excess iodomethane (1 ml) at 40°C overnight. The solvent and excess iodomethane were removed under vacuum to give a yellow solid (55 mg, 0.03 mmol, 100%). ^1H NMR (300 MHz, CD_3OD) partial assignment: δ 23.2 (1H, s, Hax), 22.4 (1H, s, Hax), 21.0 (1H, s, Hax), 18.7 (1H, s, Hax), 11.9, 10.4, 9.4, 9.1, 8.7 (8H, phenanthridine signals), 4.9-4.4 (15H, Ph), Hax and Heq at -1.9 (2H, s), -3.0 (1H, s), -3.2 (1H, s), –4.3 (1H, s), -5.0 (1H, s), -5.4 (1H, s), -6.5 (1H, s), -7.0 (1H, s), -8.6 (1H, s), -9.9 (1H, s), -10.5 (1H, s), NCH_2CO at -10.9, -11.3, -13.6, -15.4, NCH_2phen at –19.6, -20.3. m/z (ES^+) after addition of CF_3COOH: 375 (65%, $MCF_3CO_2^{3+}$).

(SSS)-Eutriamide was synthesised from the (SSS)-Eu complex using the same procedure.

19. 1-Methyl-1,10-phenanthrolinium methylsulfate[4]

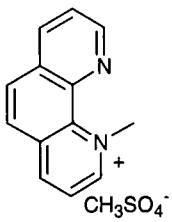

1,10-Phenanthroline (15 g, 0.083 mol) was dissolved in benzene (150 ml) at 60°C. Dimethylsulphate (9.7 ml, 0.102 mol) was added dropwise over 1 hour: a white solid appeared during the addition. The mixture was boiled under reflux for another hour, then allowed to cool to room temperature. Benzene was decanted and the white solid dried under vacuum (23.15 g, 0.079 mol, 95%). ^{1}H NMR (200 MHz, D_2O): δ 5.14 (3H, s, CH_3), 7.78 (1H, dd, J = 8.2, 4.4, H8), 7.98 (2H, dd, J = 8.6, H5, H6), 8.12 (1H, dd, J = 7.6, 6.4, H3), 8.38 (1H, d, J = 8.2, H7), 9.00 (1H, d, J = 8.0, H4), 9.07 (1H, d, J = 4.4, H9), 9.10 (1H, d, J = 6.0, H2). m/z (ES^+) 195 (100%, M^+). M.p. 208-210°C.

20. 1-Methyl-1,10-phenanthrolin-2-one[4]

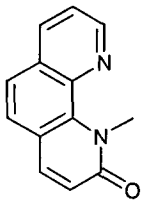

Aqueous solutions of potassium ferricyanide (59 g, 0.179 mol in water (250 ml), sodium hydroxide (64 g, 1.60 mol in 200 ml water) and compound **19** (23.15 g, 0.079 mol in 180 ml water) were prepared and kept in ice for 1 hour. The solutions of NaOH and compound **19** were then added dropwise over 1 hour to the ferricyanide solution at 0°C with rapid stirring. The slurry was stirred for another hour, the solid filtered using a Buchner, washed with water and dissolved in hot $CHCl_3$ (200 ml). Some more product was extracted from the aqueous solution with $CHCl_3$ (100 ml). The yellow organic layer was combined to the solution of the solid, washed with water, dried over $MgSO_4$ and boiled with charcoal before filtering. Removal of the solvent under reduced pressure yielded a light yellow solid (14.85 g, 0.071 mol, 90%). ^{1}H NMR (300 MHz, $CDCl_3$): δ 4.15 (3H, s, CH_3), 6.61 (1H, d, J = 9.3, H3), 7.16 (2H, s, H5, H6), 7.19 (1H, dd, J = 8.1, 4.2, H8), 7.42 (1H, d, J = 9.0, H4), 7.82 (1H, dd, J = 8.4, 1.8, H7), 8.60 (1H, dd, J = 4.2, 1.8, H9). m/z (ES^+) 211 (100%, MH^+), 421 (60%, M_2H^+). IR (KBr) 3053 (ν C-H in aromatic systems), 1657 (ν C=O

in tertiary amides), 1265 (ν C-O), 846 and 738 (out of plane bending C-H) cm^{-1}. M.p. 130-132°C.

21. 2-Chloro-1,10-phenanthroline[4]

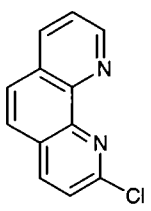

Phosphorus pentachloride (18 g, 0.086 mol) was added to a solution of compound **20** (14.85 g, 0.071 mmol) in phosphorus oxychloride (125 ml, 1.34 mol) and the mixture boiled under reflux at 110°C under argon overnight. Most of the solvent was removed by evaporation and water carefully added at 0°C until no acidic vapours were developed. The pH was raised to 10 by addition of ammonia. The solid was filtered through a sinter, then heated in $CHCl_3$ (150 ml) and filtered again whilst hot. The solution was dried over $MgSO_4$, then charcoal was added to the hot solution. Filtration and removal of the solvent under reduced pressure yielded a brownish solid (14.60 g, 0.068 mol, 96%). ^1H NMR (300 MHz, $CDCl_3$): δ 7.63 (1H, d, J = 8.4, H3), 7.66 (1H, dd, J = 8.1, 4.4, H8), 7.81 (2H, m, H5, H6), 8.20 (1H, d, J = 8.4, H4), 8.27 (1H, dd, J = 8.1, 1.8, H7), 9.23 (1H, dd, J = 4.4, 1.8, H9). ^{13}C NMR (300MHz, $CDCl_3$): δ 123.44 (C8), 124.17 (C3), 125.72 (C6), 126.87 (C5), 128.92 (C4a), 136.23 (C7), 138.77 (C4), 144.61 (C10a), 145.63 (C10b), 150.43 (C9), 151.11 (C2). m/z (ES^+) 215 (100%, M^+), 237 (60%, MNa^+), 429 (30%, M_2^+), 451 (100%, M_2Na^+). M.p. 128-131°C.

22. 2-Chloro-1,10-phenanthrolin-5,6-dione

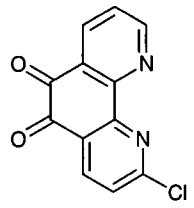

A mixture of compound **21** (1.02 g, 4.75 mmol) and potassium bromide (5.65 g, 47.5 mmol) was placed in an ice bath. Cold concentrated sulfuric acid (20 ml) was carefully allowed to flow along the walls of the flask in small portions: the mixture turned red. Concentrated nitric acid (10 ml) was then added and the solution heated at 85°C for 2 hours. The mixture was cooled, poured into water (400 ml) and neutralised by addition of $NaHCO_3$. The product was extracted with CH_2Cl_2 (3 × 300 ml), which was dried over K_2CO_3 and removed by evaporation. A yellow solid was obtained (0.65 g, 2.66 mmol, 57%). ^1H NMR (300 MHz, $CDCl_3$): δ 7.61 (1H, d, J = 8.4, H3), 7.62 (1H, dd, J = 7.8, 4.8, H8), 8.45 (1H, d, J = 8.1, H4), 8.52 (1H, dd, J = 7.8, 1.8, H7), 9.16 (1H, dd, J = 4.8, 1.8, H9). ^{13}C NMR (300MHz, $CDCl_3$): δ 130.72 (C8), 131.44 (C3), 142.06 (C7), 144.30 (C4), 156.35 (C10a), 158.14 (C10b), 161.26 (C9), 163.72 (C2) 182.31 (C6), 182.80 (C5). m/z (ES^+) 242 (100%, M^+), 267 (20%, MNa^+). IR (KBr) 3069 (ν C-H in aromatic systems), 1683 (ν C=O in quinones), 1561 and 1421 (ν C=N in conjugated cyclic systems), 1380, 1298, 1141, 1116, 834 and 740 (out of plane bending C-H), 622 cm^{-1}. M.p. 112-114°C.

23. 7-Chlorodipyrido[3,2-f:2',3'-h]quinoxaline

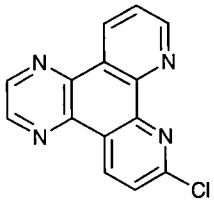

A solution of ethylenediamine (0.18 ml, 2.66 mmol) in THF (10 ml) was added dropwise to a solution of **22** (0.65 g, 2.66 mmol) in THF (500 ml) and the resulting

mixture was boiled under reflux overnight. The solvent was removed by evaporation and the dark red solid taken into CH_2Cl_2 (120 ml) and washed with HCl (1M, 3 × 50 ml). The pH of the brown aqueous layer was raised to 9 by addition of NaOH pellets. After extraction with CH_2Cl_2 (3 × 150 ml), the two organic layers were combined and dried over K_2CO_3. Removal of the solvent under reduced pressure afforded a yellow solid (0.20 g, 0.76 mmol, 29%). ^{1}H NMR (300 MHz, $CDCl_3$): δ 7.71 (1H, d, J = 8.7, H6), 7.75 (1H, dd, J = 8.4, 4.5, H11), 8.91 (2H, m, H2, H3), 9.23 (1H, dd, J = 4.5, 1.8, H12), 9.29 (1H, d, J = 8.7, H5), 9.37 (1H, dd, J = 8.4, 1.8, H10). m/z (ES^+) 267 (60%, MH^+), 289 (50%, MNa^+), 555 (100%, M_2Na^+). M.p. 172-174°C (dec.).

24. 2,9-Dimethyl-1,10-phenanthrolin-5,6-dione[5]

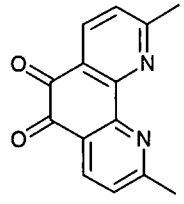

Concentrated sulfuric acid (13 ml) and nitric acid (6.5 ml) were added to a mixture of 2,9-dimethyl-1,10-phenanthroline (0.75 g, 3.60 mmol) and potassium bromide (3.9 g, 32.7 mmol) with the same procedure followed for compound **22**. The reaction mixture was boiled under reflux overnight, then cooled, poured into water (200 ml) and neutralised by addition of $NaHCO_3$. The product was extracted into CH_2Cl_2 (3 × 200 ml), which was then dried over K_2CO_3. Removal of the solvent under reduced pressure yielded a crude solid, which was purified by recrystallisation from hot methanol. Brown-orange needles were obtained (0.17 g, 0.72 mmol, 20%). ^{1}H NMR (300 MHz, $CDCl_3$): δ 2.84 (6H, s, CH_3), 7.41 (2H, d, J = 8.1, H3, H8), 8.36 (2H, d, J = 8.1, H4, H7). m/z (ES^+) 261 (80%, MNa^+), 499 (15%, M_2Na^+).

25. 7,10-Dimethyldipyrido[3,2-f:2',3'-h]quinoxaline[5]

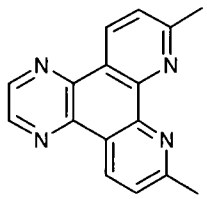

A solution of ethylenediamine (0.05 ml, 0.72 mmol) in THF (3 ml) was added dropwise to a solution of compound **24** (0.17 g, 0.72 mmol) in THF (130 ml). The mixture was heated at 70°C overnight. The orange solid obtained after evaporation of the solvent was dissolved in CH_2Cl_2 (25 ml) and extracted into HCl (1M, 3 × 20 ml). The pH was raised to 9 by addition of NaOH pellets and the solution was held at 4°C for 1 hour. The yellow precipitate was separated by centrifugation (0.10 g, 0.38 mmol, 53%). ^{1}H NMR (300 MHz, $CDCl_3$): δ 3.00 (6H, s, CH_3), 7.67 (2H, d, J = 8.4, H6, H11), 8.95 (2H, s, H2, H3), 9.39 (2H, d, J = 8.4, H5, H12). ^{13}C NMR (300MHz, $CDCl_3$): δ 26.10 (CH_3), 124.49 (C6, C11), 124.97 (C4b, C12a), 133.50 (C5, C12), 140.40 (C4a, C12b), 144.16 (C2, C3), 146.89 (C8a, C8b), 162.02 (C7, C10). m/z (ES^+) 261 (60%, MH^+), 283 (55%, MNa^+), 543 (100%, M_2Na^+).

26. 7,10-Dimethyldipyrido[3,2-f:2',3'-h]quinoxalin-8-oxide

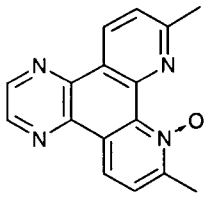

Compound **25** (0.10 g, 0.384 mmol) was dissolved in glacial acetic acid (1.5 ml), hydrogen peroxide (30%, 0.3 ml) was added and the mixture stirred at 65°C for 6 hours. After 2 and 4 hours additional H_2O_2 (0.3 ml) was added, then the solution was cooled to 25°C, diluted with water (1.5 ml) and concentrated under reduced pressure. This procedure was repeated three times, then the solid was neutralised by addition

of saturated aqueous Na_2CO_3. The product was extracted with CH_2Cl_2 (3 × 15 ml), which was then dried over Na_2SO_4. Removal of the solvent by evaporation yielded a yellow solid (0.039 g, 0.141 mmol, 37%). ^1H NMR (300 MHz, $CDCl_3$): δ 2.82 (3H, s, 7-CH_3), 2.97 (3H, s, 10-CH_3), 7.68 (2H, dd, J = 8.4, 2.7, H6, H11), 8.96 (2H, m, H2, H3), 9.02 (1H, d, J = 8.7, H5), 9.43 (1H, d, J = 8.4, H12). m/z (ES^+) 277 (100%, MH^+).

27. 7-Acetoxymethyl-10-methyldipyrido[3,2-f:2',3'-h]quinoxaline

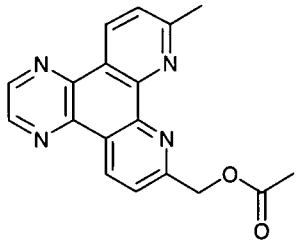

Acetic anhydride (0.13 ml, 1.06 mmol) was added dropwise to a solution of compound **26** (39 mg, 0.141 mmol) in CH_2Cl_2 (5 ml). CH_2Cl_2 was then evaporated under vacuum and the reaction mixture heated at 140°C overnight. After evaporation of the solvent the residue was taken into $CHCl_3$ and washed with saturated aqueous Na_2CO_3 (2 × 10 ml). The organic layer was dried over Na_2SO_4 and the solvent removed under reduced pressure to yield a brown solid (45 mg, 0.134 mmol, 95%). ^1H NMR (300 MHz, $CDCl_3$): δ 2.26 (3H, s, CO_2CH_3), 2.99 (3H, s, CH_3), 5.69 (2H, s, CH_2), 7.68 (1H, d, J = 8.4, H6), 7.86 (1H, d, J = 8.7, H11), 8.96 (2H, m, H2, H3), 9.38 (1H, d, J = 8.4, H5), 9.52 (1H, d, J = 8.4, H12). m/z (ES^+) 259 (100%, $(M-CO_2CH_3)^+$), 341 (50%, MNa^+), 659 (10%, M_2Na^+). M.p. > 250°C.

28. 2-Methyl-1,10-phenanthroline

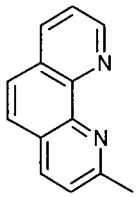

A solution of phenanthroline (10 g, 55 mmol) in dry THF (100 ml) was added dropwise to a solution of methyl lithium (1.6 M in diethyl ether, 40 ml, 64 mmol) in dry THF (300 ml) at 0°C under argon. The mixture was stirred at room temperature overnight under argon. The reaction was quenched by careful addition of water (100 ml) at 0°C, THF was removed under reduced pressure and the product extracted into diethyl ether (3 × 150 ml). Manganese dioxide (53 g, 0.61 mol) was added and the solution stirred for 1.5 hours, then magnesium sulphate was added and the solution further stirred for 2 hours. Filtration through a celite plug and removal of the solvent from the filtrate yielded a white solid. Purification by chromatography on alumina (gradient elution: 10% ethyl acetate/hexane to 50% ethyl acetate/hexane, R_f = 0.19, 70% ethyl acetate/hexane) gave a colourless solid (8.09 g, 42 mmol, 75%). ^{1}H NMR (300 MHz, $CDCl_3$): δ 2.97 (3H, s, CH_3), 7.54 (1H, d, J = 8.1, H3), 7.63 (1H, dd, J = 8.1, 4.2, H8), 7.75 (1H, d, J = 8.7, H6), 7.79 (1H, d, J = 8.7, H5), 8.16 (1H, d, J = 8.4, H4), 8.26 (1H, dd, J = 8.1, 1.5, H7), 9.22 (1H, dd, J = 4.2, 1.2, H9). ^{13}C NMR (75 MHz, $CDCl_3$): δ 25.9 (CH_3), 122.8 (C8), 123.7 (C3), 125.5 (C6), 126.5 (C5), 126.7 (q Ar), 128.8 (q Ar), 136.1 (C7), 136.2 (C4), 145.7 (q Ar), 146.0 (q Ar), 150.3 (C9), 159.5 (C2). m/z (ES^+) 195 (35%, MH^+), 217 (60%, MNa^+), 411 (100%, M_2Na^+). M.p. 72-74°C (lit.[10] 78°C). Elemental analysis: found C 79.55, H 5.44, N 14.57%; $C_{13}H_{10}N_2.0.17H_2O$ requires C 79.19, H 5.23, N 14.21%.

29. 2-Methyl-1,10-phenanthrolin-5,6-dione

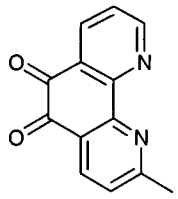

Concentrated sulfuric acid (34 ml) and nitric acid (17 ml) were added to a mixture of compound **28** (1.59 g, 8.18 mmol) and potassium bromide (9.74 g, 82 mmol) with the same procedure followed for compound **22**. The reaction mixture was boiled under reflux overnight, then cooled, poured into water (400 ml) and neutralised by addition of NaOH pellets. The product was extracted into CH_2Cl_2 (3 × 300 ml), which was then dried over K_2CO_3. Removal of the solvent under reduced pressure yielded a green solid (1.49 g, 6.63 mmol, 81%). Further purification was achieved by chromatography on silica (gradient elution: CH_2Cl_2 to 1% CH_3OH/CH_2Cl_2, R_f = 0.34, 5% CH_3OH/CH_2Cl_2) and recrystallisation from methanol. ^1H NMR (300 MHz, $CDCl_3$): δ 2.86 (3H, s, CH_3), 7.44 (1H, d, J = 7.8, H3), 7.58 (1H, dd, J = 7.8, 4.8, H8), 8.40 (1H, d, J = 8.1, H4), 8.50 (1H, dd, J = 7.8, 2.1, H7), 9.14 (1H, dd, J = 4.8, 1.8, H9). ^{13}C NMR (75 MHz, $CDCl_3$): δ 26.2 (CH_3), 125.6 (C8), 125.9 (C3), 126.2 (q Ar), 128.3 (q Ar), 137.5 (C7), 137.7 (C4), 152.7 (q Ar), 153.2 (q Ar), 156.6 (C9), 167.4 (C2), 178.7 (C5), 179.2 (C6). m/z (ES^+) 246 (70%, MNa^+), 279 (70%, MNa^+ + MeOH), 471 (30%, M_2Na^+), 503 (85%, M_2Na^+ + MeOH), 535 (100%, M_2Na^+ + 2 MeOH). IR (KBr) 3074 (ν C-H Ar), 1681 (ν C=O), 1568, 1436 and 1301 (ν C=C Py), 1216, 1123, 1013, 925, 829, 739 cm^{-1}. M.p. 98-100°C (dec.). Elemental analysis: found C 66.28, H 3.46, N 12.19%; $C_{13}H_8N_2O_2.0.67H_2O$ requires C 66.10, H 3.94, N 11.86%.

30. 7-Methyldipyrido[3,2-f:2',3'-h]quinoxaline

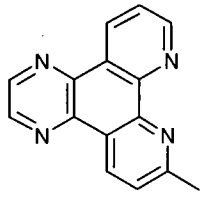

A solution of ethylenediamine (0.23 ml, 3.48 mmol) in THF (15 ml) was added dropwise to a solution of **29** (0.78 g, 3.48 mmol) in THF (400 ml) and the resulting mixture was boiled under reflux overnight. The solvent was removed by evaporation and the dark red solid taken into CH_2Cl_2 (100 ml) and washed with H_2O (3 × 100 ml). The organic layer was dried over K_2CO_3. Removal of the solvent under reduced pressure afforded a yellow solid (0.82 g, 0.33 mmol, 96%). Further purification was achieved by chromatography on silica (gradient elution: CH_2Cl_2 to 1% CH_3OH containing 0.5% NH_3/CH_2Cl_2, R_f = 0.18, 10% CH_3OH containing 0.5% NH_3/CH_2Cl_2). ^1H NMR (300 MHz, $CDCl_3$): δ 2.96 (3H, s, CH_3), 7.64 (1H, d, J = 8.4, H6), 7.74 (1H, dd, J = 8.1, 4.5, H11), 8.91 (2H, m, H2, H3), 9.28 (1H, dd, J = 4.5, 1.8, H10), 9.31 (1H, d, J = 8.4, H5), 9.44 (1H, dd, J = 8.4, 1.8, H12). ^{13}C NMR (75 MHz, $CDCl_3$): δ 26.1 (CH_3), 123.9 (C11), 124.7 (C6), 124.9 (q Ar), 127.1 (q Ar), 133.3 (C12), 133.4 (C5), 140.2 (q Ar), 140.8 (q Ar), 144.2 (C2), 144.6 (C3), 147.1 (q Ar), 147.5 (q Ar), 152.5 (C10), 162.1 (C7). m/z (ES^+) 247 (30%, MH^+), 269 (33%, MNa^+), 515 (100%, M_2Na^+). M.p. 190-193°C. Elemental analysis: found C 71.85, H 3.99, N 22.76%; $C_{15}H_{10}N_4.0.25H_2O$ requires C 71.86, H 4.19, N 22.36%.

31. 7-(Trichloromethyl)dipyrido[3,2-f:2',3'-h]quinoxaline

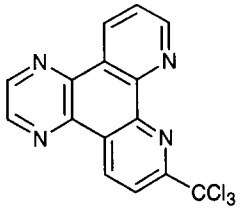

N-chlorosuccinimide (500 mg, 3.7 mmol) and a catalytic amount of benzoyl peroxide were added to a solution of compound **30** (184 mg, 0.75 mmol) in CCl_4 (20 ml). The mixture was heated at reflux overnight. The suspension was filtered and the solvent evaporated. The solid was dissolved in $CHCl_3$ (50 ml) and washed with saturated aqueous Na_2CO_3 solution (3 × 50 ml). The organic layer was dried over K_2CO_3. Evaporation of the solvent afforded a yellow solid (184 mg, 0.53 mmol, 70%). ^1H NMR (300 MHz, $CDCl_3$): δ 7.80 (1H, dd, J = 8.1, 4.5, H11), 8.48 (1H, d, J = 8.7, H5), 8.98 (1H, d, J = 2.1, H2), 9.00 (1H, d, J = 2.1, H3), 9.35 (1H, dd, J = 4.5, 1.8, H10), 9.47 (1H, dd, J = 8.1, 1.5, H12), 9.61 (1H, d, J = 8.7, H6). m/z (ES^+) 371 (30%, MNa^+), 720 (100%, M_2Na^+). M.p. 200-202°C (dec.). Accurate mass spectrum: found MH^+ 348.9810; $C_{15}H_8Cl_3N_4$ requires 348.9814.

32. 7-(Methoxycarbonyl)dipyrido[3,2-f:2',3'-h]quinoxaline

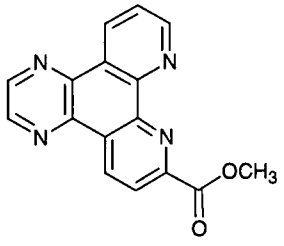

A solution of compound **31** (925 mg, 2.65 mmol) in conc. H_2SO_4 (15 ml) was heated at reflux under argon for 2 hours. Methanol (30 ml) was added slowly to the stirred mixture upon cooling and the solution was heated at reflux overnight. The solution was neutralised by addition of saturated aqueous Na_2CO_3 solution and methanol was evaporated. The product was extracted into CH_2Cl_2, which was dried over $MgSO_4$. Evaporation of the solvent afforded a yellow solid (500 mg, 1.72 mmol, 65%). ^1H NMR (300 MHz, $CDCl_3$): δ 4.14 (3H, s, CH_3), 7.84 (1H, dd, J = 8.1, 3.6, H11), 8.60 (1H, d, J = 8.1, H5), 9.03 (1H, d, J = 2.1, H2), 9.04 (1H, d, J = 2.1, H3), 9.35 (1H, dd, J = 4.5, 1.5, H10), 9.52 (1H, dd, J = 8.1, 1.5, H12), 9.67 (1H, d, J = 8.7, H6). M.p. 220-223°C. Accurate mass spectrum: found MH^+ 291.0879, $C_{16}H_{11}N_4O_2$ requires 291.0882.

33. Dipyrido[3,2-f:2',3'-h]quinoxaline-7-carboxyaldehyde

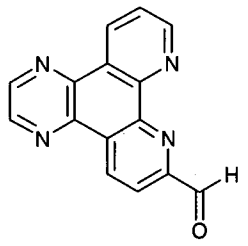

Selenium dioxide (0.77 g, 6.97 mmol) was added to a solution of compound **30** (0.78 g, 3.17 mmol) in dioxane (100 ml). The mixture was heated at reflux for 2 hours, then filtered through celite. Evaporation of the solvent afforded a white solid. Some more product was obtained by stirring the celite in CH_2Cl_2 (0.77 g, 2.96 mmol, 93%). ^{1}H NMR (300 MHz, $CDCl_3$): δ 7.89 (1H, dd, J = 8.1, 4.5, H11), 8.46 (1H, d, J = 8.4, H5), 9.06 (1H, d, J = 1.8, H2), 9.08 (1H, d, J = 1.8, H3), 9.39 (1H, dd, J = 4.2, 1.8, H10), 9.57 (1H, dd, J = 8.1, 1.8, H12), 9.73 (1H, dd, J = 8.4, 0.73, H6), 10.61 (1H, d, J = 0.73, CHO). ^{13}C NMR (75 MHz, $CDCl_3$): δ 121.0 (C5), 124.8 (C11), 127.8 (q Ar), 130.2 (q Ar), 133.7 (C12), 135.1 (C6), 140.0 (q Ar), 141.6 (q Ar), 145.2 (C2), 145.8 (C3), 147.1 (q Ar), 147.7 (q Ar), 152.9 (C10), 154.1 (C7), 194.0 (CHO). m/z (ES^+) 283 (60%, MNa^+), 315 (100%, MNa^+ + MeOH), 543 (60%, M_2Na^+), 575 (10%, M_2Na^+ + MeOH), 607 (40%, M_2Na^+ + 2 MeOH). IR (KBr) 3074, 3029 (ν C-H Ar), 2865 (ν C-H in CHO), 1703 (ν C=O), 1566, 1467 and 1449 (ν C=C Py), 1391 (δ C-H CHO), 1362, 1207, 1077, 767 and 748 cm^{-1}. M.p. > 250 °C. Elemental analysis: found C 67.34, H 3.08, N 20.88%; $C_{15}H_8N_4O.0.33H_2O$ requires C 67.67, H 3.27, N 21.05%.

34. 7-(Hydroxymethyl)dipyrido[3,2-f:2',3'-h]quinoxaline

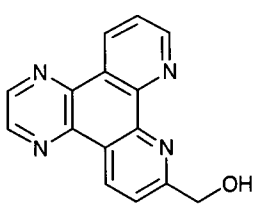

Sodium borohydride (54 mg, 1.43 mmol) was added to a solution of compound **33** (300 mg, 1.15 mmol) in CH_2Cl_2/EtOH 7:1 (120 ml). The mixture was heated at reflux for 2 hours. The solvent was evaporated and the orange solid taken into a saturated solution of Na_2CO_3 (50 ml) and extracted into CH_2Cl_2 (3 × 70 ml). The organic layer was dried over K_2CO_3. Removal of the solvent under reduced pressure afforded a yellow solid (207 mg, 0.79 mmol, 68%), which was used without further purification. ^{1}H NMR (300 MHz, $CDCl_3$): δ 5.20 (2H, s, CH_2), 7.82 (1H, dd, J = 8.1, 4.5, H11), 7.87 (1H, d, J = 8.7, H6), 9.00 (2H, s, H2, H3), 9.27 (1H, dd, J = 4.5, 1.8, H10), 9.51 (1H, d, J = 8.4, H5), 9.54 (1H, dd, J = 8.1, 1.8, H12). ^{13}C NMR (75 MHz, $CDCl_3$): δ 65.4 (CH_2), 121.5 (C11), 124.0 (C6), 126.0 (q Ar), 127.3 (q Ar), 133.5 (C12), 133.9 (C5), 140.2 (q Ar), 140.5 (q Ar), 144.4 (C2), 144.7 (C3), 146.3 (q Ar), 147.0 (q Ar), 152.0 (C10), 163.0 (C7). m/z (ES^+) 262 (100%, M^+), 284 (30%, MNa^+), 546 (20%, M_2Na^+).

35. 7-(Chloromethyl)dipyrido[3,2-f:2',3'-h]quinoxaline

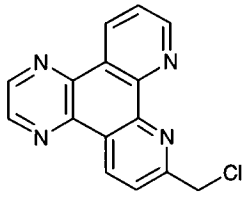

Phosphorus trichloride (0.82 ml, 9.36 mmol) in $CHCl_3$ (5 ml) was added dropwise to a stirred solution of compound **34** (206 mg, 0.78 mmol) in $CHCl_3$ (100 ml). The mixture was heated at reflux for 4 hours. The solution was neutralised by addition of a saturated aqueous Na_2CO_3 solution (100 ml). The organic layer was separated and dried over K_2CO_3. Removal of the solvent under reduced pressure afforded a pink solid. Purification by chromatography on silica (gradient elution: CH_2Cl_2 to 1% CH_3OH/CH_2Cl_2, R_f = 0.47, 10% CH_3OH/CH_2Cl_2) gave a colourless solid (95 mg, 0.34 mmol, 43%). ^{1}H NMR (200 MHz, $CDCl_3$): δ 5.14 (2H, s, CH_2), 7.81 (1H, dd, J = 8.2, 4.4, H11), 8.08 (1H, d, J = 8.4, H6), 8.99 (2H, s, H2, H3), 9.32 (1H, dd, J = 4.4, 1.8, H10), 9.51 (1H, dd, J = 8.2, 1.8, H12), 9.54 (1H, d, J = 8.6, H5). ^{13}C NMR (75 MHz, $CDCl_3$): δ 47.1 (CH_2), 123.1 (C11), 124.9 (C6), 126.1 (q Ar), 127.0 (q Ar),

133.0 (C12), 134.2 (C5), 139.8 (q Ar), 140.1 (q Ar), 144.4 (C2, C3), 146.2 (q Ar), 146.7 (q Ar), 152.2 (C10), 159.2 (C7). m/z (ES^+) 268 (20%, MNa^+ - Cl), 302 (95%, MNa^+), 548 (50%, M_2Na^+ - Cl), 582 (100%, M_2Na^+). M.p. 194-196°C (dec.). Accurate mass spectrum: found MH^+ 281.0593; $C_{15}H_{10}ClN_4$ requires 281.0594.

36. 1,4,7-Tris(tert-butoxycarbonyl)-1,4,7,10-tetraazacyclododecane[6]

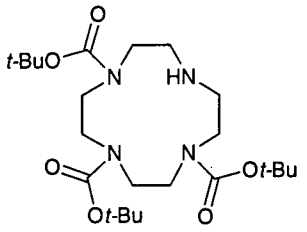

A solution of di-tert-butyl dicarbonate (3.05 g, 13.92 mmol) in CH_2Cl_2 (70 ml) was added dropwise to a stirred solution of 1,4,7,10-tetraazacyclododecane (1 g, 5.80 mmol) in CH_2Cl_2 (290 ml). The mixture was stirred at room temperature for 2 hours. Evaporation of the solvent afforded a transparent oil, which was purified by chromatography on silica (gradient elution: CH_2Cl_2 to 5% CH_3OH/CH_2Cl_2, R_f = 0.29, 10% CH_3OH/CH_2Cl_2) gave a colourless solid (1.85 g, 3.91 mmol, 68%). ^1H NMR (300 MHz, $CDCl_3$): δ 1.39 (18H, s, CH_3), 1.41 (9H, s, CH_3), 2.79 (4H, br s, CH_2), 3.22-3.33 (8H, br s, CH_2), 3.57 (4H, br s, CH_2). ^{13}C NMR (75 MHz, $CDCl_3$): δ 28.4 (CH_3), 28.6 (CH_3), 44.9 (CH_2), 45.9 (CH_2), 48.8 (CH_2), 49.4 (CH_2), 50.9 (CH_2), 79.1 (C), 79.3 (C), 155.6 (C=O). m/z (ES^+) 495 (60%, MNa^+), 967 (100%, M_2Na^+).

37. 1-(7'-Methyldipyrido[3,2-f:2',3'-h]quinoxalinyl)-4,7,10-tris(tert-butoxycarbonyl)-1,4,7,10-tetraazacyclododecane

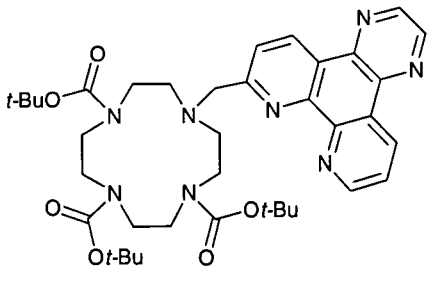

K_2CO_3 (218 mg, 1.58 mmol) and a catalytic amount of KI were added to a solution of compound **36** (148 mg, 0.31 mmol) in CH_3CN (5 ml). The mixture was heated at 60°C and a solution of compound **35** (88 mg, 0.31 mmol) in CH_2Cl_2 (5 ml) was added. The reaction mixture was boiled under reflux under argon overnight. The solution was filtered and the salts washed with CH_2Cl_2. Evaporation of the solvent afforded a crude residue, which was purified by chromatography on silica (gradient elution: CH_2Cl_2 to 3% CH_3OH/CH_2Cl_2, R_f = 0.23, 10% CH_3OH/CH_2Cl_2) to yield a colourless oil (160 mg, 0.22 mmol, 71%). ^1H NMR (300 MHz, $CDCl_3$): δ 1.29 (27H, m, CH_3), 2.78 (4H, br, ring CH_2), 3.50 (12H, m, ring CH_2), 4.27 (2H, s, CH_2), 7.75 (1H, dd, J = 8.1, 4.5, H11), 7.89 (1H, br, H6), 8.94 (2H, m, H2, H3), 9.25 (1H, d, J = 3.0, H10), 9.39 (1H, d, J = 6.6, H5), 9.46 (1H, dd, J = 8.1, 1.5, H12). m/z (ES^+) 716 (3%, M^+), 739 (100%, MNa^+), 1455 (5%, M_2Na^+).

38. 1-(7'-Methyldipyrido[3,2-f:2',3'-h]quinoxalinyl)-1,4,7,10-tetraazacyclododecane

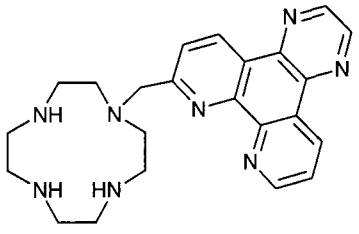

Trifluoroacetic acid (10 ml) was added to a solution of compound **37** (160 mg, 0.22 mmol) in CH_2Cl_2 (3 ml). The mixture was stirred for 2 hours at room temperature. The solvent was evaporated and the residue redissolved in CH_2Cl_2 for 3 times to facilitate elimination of excess acid and tert-butyl alcohol. The resultant orange oil was taken into a KOH solution (5 ml) and the product extracted into CH_2Cl_2 (3 × 5 ml). The organic layer was dried over K_2CO_3. Removal of the solvent under reduced pressure afforded an orange solid (65 mg, 0.16 mmol, 71%). ^1H NMR (300 MHz, $CDCl_3$): δ 2.57 (4H, m, ring CH_2), 2.70 (8H, s, ring CH_2), 2.80 (4H, m, ring CH_2), 4.20 (2H, s, CH_2), 7.71 (1H, dd, J = 8.1, 4.5, H11), 8.07 (1H, d, J = 8.4, H6), 8.87 (1H, d, J = 2.1, H2), 8.88 (1H, d, J = 2.1, H3), 9.25 (1H, dd, J = 4.5, 1.8, H10), 9.41

(1H, dd, J = 8.4, 1.8, H12), 9.43 (1H, d, J = 8.4, H5). ^{13}C NMR (75 MHz, $CDCl_3$): δ 45.1, 46.4, 47.1, 52.0 (ring CH_2), 61.9 (CH_2), 123.1 (C11), 123.5 (C6), 125.8 (q Ar), 126.9 (q Ar), 133.0 (C12), 133.8 (C5), 140.0 (q Ar), 140.5 (q Ar), 144.0 (C2), 144.4 (C3), 146.4 (q Ar), 147.2 (q Ar), 152.2 (C10), 163.5 (C7). m/z (ES^+) 228 (10%, MCa^{2+}), 417 (100%, MH^+), 439 (10%, MNa^+), 833 (3%, M_2H^+). M.p. 175-178°C (dec.). Accurate mass spectrum: found MH^+ 417.2515; $C_{23}H_{29}N_8$ requires 417.2515.

39. 1-(7'-Methyldipyrido[3,2-f:2',3'-h]quinoxalinyl)-4,7,10-tris[(R)-1-(1-phenyl)ethylcarbamoylmethyl]-1,4,7,10-tetraazacyclododecane

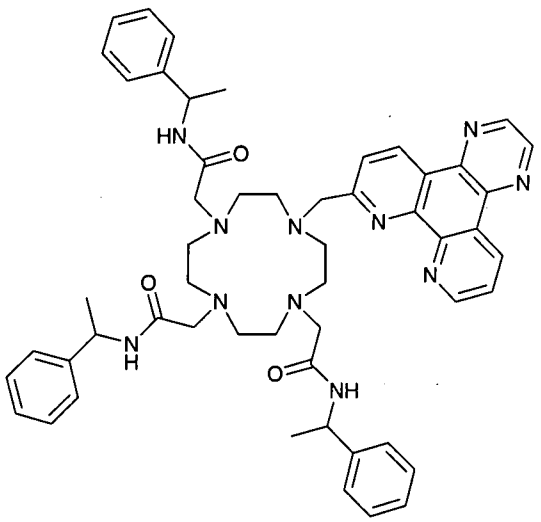

K_2CO_3 (83 mg, 0.6 mmol) and a catalytic amount of KI were added to a solution of compound **38** (50 mg, 0.12 mmol) in CH_3CN (4 ml). The mixture was heated at 60°C and a solution of compound **7** (71 mg, 0.36 mmol) in CH_2Cl_2 (4 ml) was added. The reaction mixture was boiled under reflux under argon overnight. The solution was filtered and the salts washed with CH_2Cl_2. Evaporation of the solvent afforded a crude residue, which was purified by chromatography on alumina (gradient elution: CH_2Cl_2 to 2% CH_3OH/CH_2Cl_2, R_f=0.31, 10% CH_3OH/CH_2Cl_2) to yield a colourless solid (50 mg, 0.06 mmol, 50%). ^1H NMR (300 MHz, $CDCl_3$): δ 1.46 (H, d, J = 2.7, CH_3), 1.48 (H, d, J = 2.7, CH_3), 2.64 (16H, m, ring CH_2), 2.90 (2H, d, J = 6, CH_2), 2.96 (4H, d, J = 6, CH_2), 4.08 (2H, s, CH_2-dpq), 5.14 (3H, m, J = 7.5, CH), 6.88 (2H, br, NH), 7.05 (1H, br, NH), 7.16-7.37 (15H, m, Ph), 7.80 (1H, dd, J = 8.1, 4.2, H11),

7.91(1H, d, J = 8.4, H6), 9.01 (2H, m, H2, H3), 9.28 (1H, dd, J = 4.5, 1.8, H10), 9.41 (1H, d, J = 8.4, H5), 9.54 (1H, dd, J = 8.1, 1.8, H12). ^{13}C NMR (75 MHz, $CDCl_3$): δ 21.4 (CH_3), 21.9 (CH_3), 48.2 (CH), 48.3 (CH), 52.8 (CH_2N), 53.3 (CH_2N), 53.6 (CH_2N), 58.3 (NCH_2CO), 58.9 (NCH_2CO), 62.3 (CH_2-dpq), 123.3 (C11), 123.9 (C6), 126.2 (o-Ar), 127.3 (p-Ar), 128.6 (m-Ar), 133.2 (C12), 133.6 (C5), 143.1 (q-Ar), 144.6 (C2, C3), 140.4 (q-dpq), 152.3 (C10), 161.0 (C7), 169.5 (CO), 170.4 (CO). m/z (ES^+) 469 (40%, MCa^{2+}), 899 (5%, M^+), 922 (100%, MNa^+). M.p. 136-138°C. Accurate mass spectrum: found MH^+ 900.5035; $C_{53}H_{62}N_{11}O_3$ requires 900.5037.

The (SSS) ligand was synthesised with the same procedure. Lanthanide complexes of the two enantiomeric ligands were prepared.

40. $EuPh_3dpq\ (CF_3SO_3)_3$

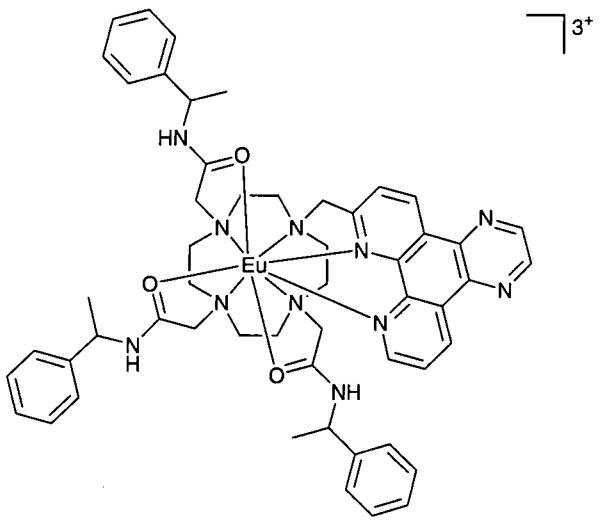

A solution of compound **39** (28 mg, 0.03 mmol) and $Eu(OTf)_3$ (19 mg, 0.03 mmol) in dry CH_3CN (2 ml) was boiled under reflux under argon overnight at 80°C. The solution was then added dropwise to ether (100 ml) with stirring, the precipitate centrifuged and the solvent decanted. The solid was redissolved in CH_3CN and the process repeated. A colourless solid was obtained (35 mg, 0.02 mmol, 75%). ^1H NMR (300 MHz, CD_3OD, -10°C) partial assignment: δ 37.9 (1H, s, Hax), 37.3 (1H,

s, Hax), 31.9 (1H, s, Hax), 27.7 (1H, s, Hax), 26.9 (H10-dpq), 15.7 (dpq), 14.9 (dpq), 11-5 (dpq and Ph signals), -1.8 (6H, s, CH_3), -2.3 (3H, s, CH_3), -3.5 (4H, m, Heq), -7.2 (2H, s, Hax), -7.6 (2H, s, Hax), -9.7 (1H, s, Heq), -10.2 (1H, s, Heq), -15.7 (1H, s, Heq), -15.8 (1H, s, Heq), -16.4 (1H, s, NCH_2CO), -17.0 (1H, s, NCH_2CO), -17.6 (1H, s, NCH_2CO), -17.9 (1H, s, NCH_2CO), -24.0 (2H, s, NCH_2CO). m/z (ES^+) 350 (60%, M^{3+}), 525 (80%, M^{2+}), 534 (50%, $M^{2+}+H_2O$), 600 (30%, $M^{3+}+ CF_3SO_3^-$), 1348 (3%, $M^{3+}+ 2CF_3SO_3^-$). M.p. 176-179°C. Accurate mass spectrum: found $(M + 2CF_3SO_3)^+$ 1350.3208; $C_{55}H_{61}N_{11}O_9EuS_2F_6$ requires 1350.3202.

41. $TbPh_3dpq\ (CF_3SO_3)_3$

Compound **39** (15 mg, 0.02 mmol) and $Tb(Otf)_3$ (10 mg, 0.02 mmol) were dissolved in dry CH_3CN (1 ml). The procedure followed was identical to that described for compound **40**. A colourless solid was obtained (20 mg, 0.01 mmol, 78%). m/z (ES^+) 352 (100%, M^{3+}), 603 (60%, $M^{3+}+ CF_3SO_3^-$), 1356 (5%, $M^{3+}+ 2CF_3SO_3^-$). M.p. 177-179°C. Accurate mass spectrum: found $(M + CF_3SO_3)^{2+}$ 603.6862; $C_{54}H_{61}N_{11}O_6TbSF_3$ requires 603.6866.

42. $GdPh_3dpq\ (CF_3SO_3)_3$

Compound **39** (10 mg, 0.01 mmol) and $Gd(OTf)_3$ (7 mg, 0.01 mmol) were dissolved in dry CH_3CN (1 ml). The procedure followed was identical to that described for compound **40**. A colourless solid was obtained (7 mg, 0.02 mmol, 42%). m/z (ES^+) 352 (100%, M^{3+}), 603 (60%, $M^{3+}+ CF_3SO_3^-$), 1354 (5%, $M^{3+}+ 2CF_3SO_3^-$). M.p. 210-212°C. Accurate mass spectrum: found $(M + 2CF_3SO_3)^+$ 1355.3240; $C_{55}H_{61}N_{11}O_9GdS_2F_6$ requires 1355.3251.

43. (R)-2-Chloro-N-[1-(1-naphthyl)ethyl]ethanamide[7]

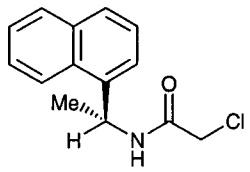

Chloroacetylchloride (0.1 ml, 1.4 mmol) was added dropwise to a stirred solution of (R)-1-naphthylethylamine (0.2 ml, 1.2 mmol) and triethylamine (0.2 ml, 1.4 mmol) in dry THF (5 ml) at 0°C under argon. The reaction mixture was allowed to warm to room temperature and stirred for 1 hour. The product was extracted into diethyl ether, which was then washed with HCl (0.1M, 3 × 15 ml), water (3 × 15 ml) and dried over K_2CO_3. Recrystallisation from diethyl ether yielded white needles (200 mg, 0.80 mmol, 67 %). ^{1}H NMR (200 MHz, $CDCl_3$): δ 1.71 (3H, d, J = 6.8, CH_3), 4.05 (1H, d, J = 15.2, CH_2), 4.09 (1H, d, J = 15.2, CH_2), 5.95 (1H, q, J = 7.0, CH), 6.82 (1H, br s, NH), 7.52 (4H, m, CH Ar), 7.86 (2H, m, CH Ar), 8.08 (1H, m, CH Ar). ^{13}C NMR (50 MHz, $CDCl_3$): δ 21.1 (CH_3), 42.8 (CH_2), 45.5 (CH), 122.8 (CAr), 123.3 (CAr), 125.5 (CAr), 126.2 (CAr), 126.9 (CAr), 128.9 (CAr), 129.1 (CAr), 131.2 (q Ar), 134.2 (q Ar), 137.8 (q Ar), 165.2 (CO). m/z (ES^+) 270 (60%, MNa^+), 517 (100%, M_2Na^+). M.p. 144-145°C.

44. 1-(7'-Methyldipyrido[3,2-f:2',3'-h]quinoxalinyl)-4,7,10-tris[(R)-1-(1-naphthyl)ethylcarbamoylmethyl]-1,4,7,10-tetraazacyclododecane

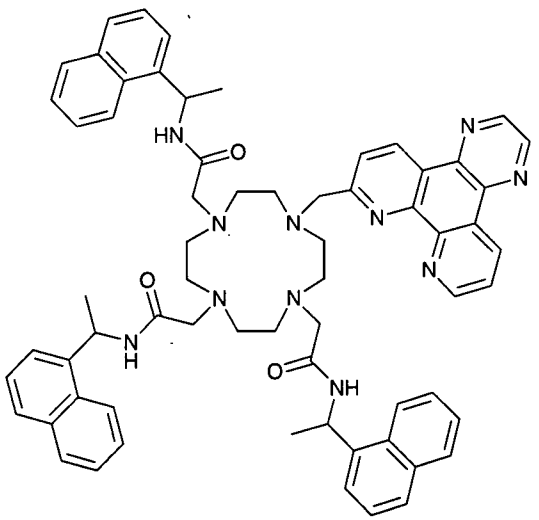

K_2CO_3 (32 mg, 0.23 mmol) and a catalytic amount of KI were added to a solution of compound **38** (19 mg, 0.05 mmol) in CH_3CN (2 ml). The mixture was heated at 60°C and a solution of compound **43** (34 mg, 0.14 mmol) in CH_2Cl_2 (2 ml) was added. The reaction mixture was boiled under reflux under argon overnight. The solution was filtered and the salts washed with CH_2Cl_2. Evaporation of the solvent afforded a crude residue, which was purified by chromatography on alumina (gradient elution: CH_2Cl_2 to 1% CH_3OH/CH_2Cl_2, R_f=0.44, 10% CH_3OH/CH_2Cl_2) to yield a colourless solid (21 mg, 0.02 mmol, 44%). ^1H NMR (200 MHz, $CDCl_3$): δ 1.10-1.65 (9H, m, CH_3), 2.0-4.0 (24H, br, CH_2), 5.4-6.0 (3H, m, CH), 6.9-8.2 (26H, m, NH, Np, H11, H6), 8.8-9.5 (5H, m, dpq). ^{13}C NMR (75 MHz, $CDCl_3$): 20.9 (CH_3), 21.4_(CH_3), 44.3 (CH_2 ring), 44.7 (CH_2 ring), 45.0 (CH_2 ring), 50.6 (CH), 52.2 (CH), 56.0 (NCH_2CO), 57.4 (NCH_2CO), 61.2 (CH_2-dpq), 122.9 (Ar), 123.1 (Ar), 125.4 (Ar), 125.7 (Ar), 125.8 (Ar), 126.0 (Ar), 126.3 (Ar), 127.4 (Ar), 128.6 (Ar), 128.9 (Ar), 130.4 (Ar), 133.4 (Ar), 133.8 (Ar), 140.3 (Ar), 144.6 (Ar), 152.6 (Ar), 159.5 (Ar), 167.6 (CO), 170.0 (CO). m/z (ES^+): 545 (20%, MCa^{2+}), 557 (100%, MNa^+K^+), 1072 (60%, MNa^+). M.p. 154-157°C. Accurate mass spectrum: found MH^+ 1050.5499; $C_{65}H_{68}N_{11}O_3$ requires 1050.5506.

The (SSS) ligand was synthesised with the same procedure. Lanthanide complexes of the two enantiomeric ligands were prepared.

45. $EuNp_3dpq\ (CF_3SO_3)_3$

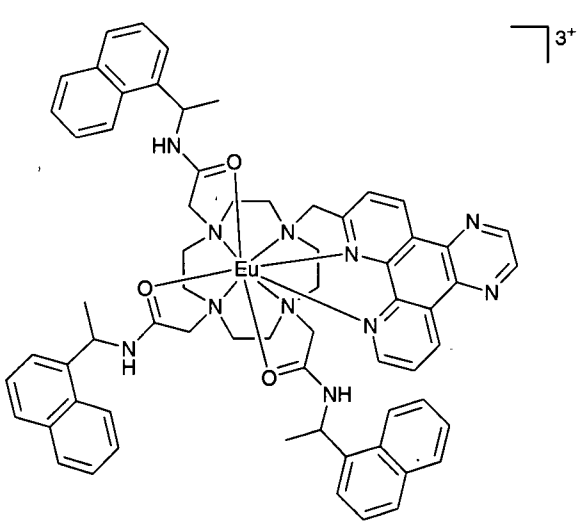

A solution of compound **44** (11 mg, 0.01 mmol) and $Eu(OTf)_3$ (6 mg, 0.01 mmol) in dry CH_3CN (2 ml) was boiled under reflux under argon overnight at 80°C. The solution was then added dropwise to ether (100 ml) with stirring, the precipitate centrifuged and the solvent decanted. The solid was redissolved in CH_3CN and the process repeated. A colourless solid was obtained (11 mg, 0.007 mmol, 67%). ^1H NMR (300 MHz, CD_3OD, -10°C) partial assignment: δ 37.3 (2H, s, Hax), 31.4 (1H, s, Hax), 25.6 (1H, s, Hax), 23.3 (H10-dpq), 15.9 (dpq), 15.0 (dpq), 11-5 (dpq and Np signals), -2.2 (6H, s, CH_3), -2.6 (3H, s, CH_3), Hax and Heq at -3.0 (2H, s), -4.0 (1H, s), -4.8 (2H, s), -6.2 (1H, s), -7.3 (1H, s), -7.8 (1H, s), -8.6 (1H, s), -9.0 (1H, s), -9.8 (1H, s), -11.6 (1H, s), -13.0 (1H, s), -17.0 (2H, s, Heq), -17.5 (1H, s, Heq), -18.0 (2H, s, NCH_2CO), -20.0 (1H, s, NCH_2CO), -21.2 (1H, s, NCH_2CO), -22.9 (1H, s, NCH_2CO), -24.9 (1H, s, NCH_2CO). m/z (ES^+) 400 (100%, M^{3+}), 675 (60%, M^{3+}+ $CF_3SO_3^-$), 1501 (5%, M^{3+}+ $2CF_3SO_3^-$). M.p. > 250°C. Accurate mass spectrum: found $(M + CF_3SO_3)^{2+}$ 675.7148; $C_{66}H_{67}N_{11}O_6EuSF_3$ requires 675.7085.

46. $TbNp_3dpq\ (CF_3SO_3)_3$

Compound **44** (4 mg, 0.003 mmol) and $Tb(OTf)_3$ (2 mg, 0.003 mmol) were dissolved in dry CH_3CN (1 ml). The procedure followed was identical to that described for compound **45**. A colourless solid was obtained (3 mg, 0.002 mmol, 59%). m/z (ES^+) 403 (100%, M^{3+}), 679 (65%, M^{3+}+ $CF_3SO_3^-$), 1507 (3%, M^{3+}+ $2CF_3SO_3^-$). M.p. > 250°C. Accurate mass spectrum: found $(M + CF_3SO_3)^{2+}$ 678.7158; $C_{66}H_{67}N_{11}O_6TbSF_3$ requires 678.7101.

47. $GdNp_3dpq\ (CF_3SO_3)_3$

Compound **44** (4 mg, 0.003 mmol) and $Gd(OTf)_3$ (2 mg, 0.003 mmol) were dissolved in dry CH_3CN (1 ml). The procedure followed was identical to that described for compound **45**. A colourless solid was obtained (3 mg, 0.002 mmol, 41%). m/z (ES^+) 402 (20%, M^{3+}), 679 (85%, M^{3+}+ $CF_3SO_3^-$), 1505 (5%, M^{3+}+ $2CF_3SO_3^-$). M.p. > 250°C.

48. 1-(7'-Methyldipyrido[3,2-f:2',3'-h]quinoxalinyl)-4,7,10-tris(tert-butoxycarbonylmethyl)-1,4,7,10-tetraazacyclododecane

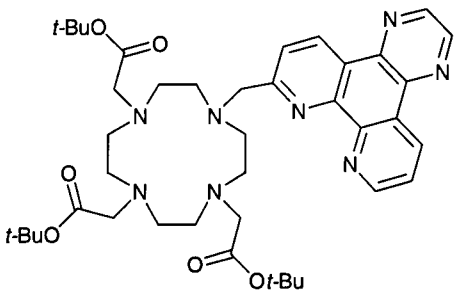

K_2CO_3 (98 mg, 0.71 mmol) and a catalytic amount of KI were added to a solution of compound **?** (73 mg, 0.14 mmol) in CH_3CN (3 ml). The mixture was heated at 60°C and a solution of compound **35** (40 mg, 0.14 mmol) in CH_2Cl_2 (5 ml) was added. The reaction mixture was boiled under reflux under argon overnight. The solution was filtered and the salts washed with CH_2Cl_2. Evaporation of the solvent afforded a solid (88 mg, 0.12 mmol, 83%). ^1H NMR (300 MHz, $CDCl_3$): δ 1.45 (9H, m, CH_3), 1.61 (9H, s, CH_3), 2.00 (9H, s, CH_3), 2.80 (24H, br m, ring and arms CH_2), 7.25 (1H, dd, J = 8.1, 4.5, H11), 7.81(1H, d, J = 8.4, H6), 9.00 (1H, d, J = 2.4, H2), 9.02 (1H, d, J = 2.4, H3), 9.03 (1H, dd, J = 4.5, 1.8, H10), 9.45 (1H, dd, J = 8.1, 1.5, H12), 9.49 (1H, d, J = 8.4, H5). m/z (ES^+) 782 (100%, MNa^+), 798 (100%, MK^+).

49. CeDO3Adpq

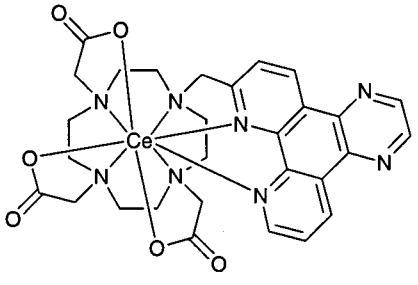

Trifluoroacetic acid (8 ml) was added to a solution of compound **48** (88 mg, 0.12 mmol) in CH_2Cl_2 (3 ml). The mixture was stirred overnight at room temperature. The solvent was evaporated and the residue redissolved in CH_2Cl_2 for 3 times to facilitate elimination of excess acid and tert-butyl alcohol. The product was checked by ^1H

NMR and used for complexation immediately. ^{1}H NMR (300 MHz, CD_3OD): δ 3-4.5 (H, br, ring and arms CH_2), 8.75 (2H, br, H11, H6), 9.55 (2H, br, H2, H3), 9.75 (1H, br, H10), 9.93 (1H, br, H12), 10.4 (1H, br, H5).

The ligand was dissolved in a mixture of methanol and water (1:1, 10 ml) and the pH raised to 6 by addition of a KOH solution. Cerium nitrate (52 mg, 0.12 mmol) was added and the mixture was heated at reflux overnight. Evaporation of the solvent afforded a crude residue, which was purified by preparative TLC on alumina (gradient elution: 10% CH_3OH/CH_2Cl_2 to 20% CH_3OH/CH_2Cl_2, R_f = 0.39, 30% CH_3OH/CH_2Cl_2) to yield a pale yellow solid (25 mg, 0.035 mmol, 29%). ^{1}H NMR (300 MHz, D_2O) partial assignment: δ 34.36 (1H, s, NCH_2CO), 29.30 (1H, s, NCH_2CO), 26.78 (1H, s, NCH_2CO), 19.48 (1H, s, NCH_2CO), 11.56 (1H, s, NCH_2CO), 11-4 (dpq), 2.61 (1H, s, Hax), -0.54 (1H, s, Hax), -2.41 (1H, s, Heq), -3.16 (2H, s, Heq), -4.98 (1H, s, Heq), -5.86 (1H, s, Heq), -8.92 (1H, s, Heq), -9.28 (1H, s, Heq), -9.88 (1H, s, Heq), -10.94 (1H, s, Hax), -11.71 (1H, s, Hax), -12.01 (1H, s, Hax), -13.32 (1H, s, Hax). m/z (ES^-) 363 (100%, M^{2-}), 789 (20%, M+ NO_3^-). M.p. > 250°C (dec.). Accurate mass spectrum: found MH^+ 728.1502; $C_{29}H_{32}N_8O_6Ce$ requires 728.1499.

50. Triethyl 10-(7'-methyldipyrido[3,2-f:2',3'-h]quinoxalinyl)-1,4,7,10-tetraazacyclododecane-1,4,7-triyltrimethylenetri(methylphosphinate)

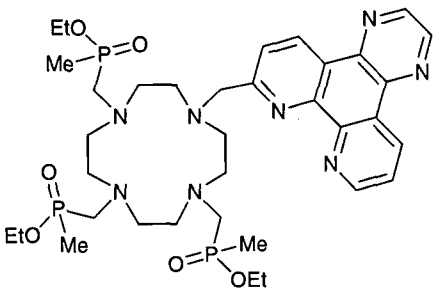

Compound **38** (60 mg, 0.14 mmol) was dissolved in a 6:1 mixture of dry THF and CH_2Cl_2 (7 ml) under argon over 4 Å molecular sieves. Methyldiethoxyphosphine (0.1 ml, 0.65 mmol) and paraformaldehyde (22 mg, 0.72 mmol) were added and the

mixture was heated at reflux under argon overnight. Evaporation of the solvent yielded a brown oil, which was purified by alumina column chromatography (gradient elution: CH_2Cl_2 to 1% CH_3OH/CH_2Cl_2, R_f =0.26, 5% CH_3OH/CH_2Cl_2) to yield a yellow oil (90 mg, 0.12 mmol, 80%). ^1H NMR (300 MHz, $CDCl_3$): δ 1.25 (3H, t, J = 6.9, OCH_2CH_3), 1.33 (3H, t, J = 6.9, OCH_2CH_3), 1.34 (3H, t, J = 6.9, OCH_2CH_3), 1.54 (9H, m, PCH_3), 2.6-3.2 (19H, br, ring CH_2 and PCH_2), 3.86 (2H, CH_2dpq), 4.10 (6H, m, OCH_2CH_3), 7.80 (1H, dd, J = 8.1, 4.2, H11), 8.25 (1H, d, J = 8.4, H6), 9.00 (2H, s, H2, H3), 9.32 (1H, d, J = 3.3, H10), 9.47 (1H, d, J = 8.1, H5), 9.53 (1H, dd, J = 8.4, 1.2, H12). ^{31}P NMR (81 MHz, $CDCl_3$): δ 53.2 (3P, br). m/z (ES^+): 408 (100%, MCa^{2+}).

51. $CeMeP_3dpq$

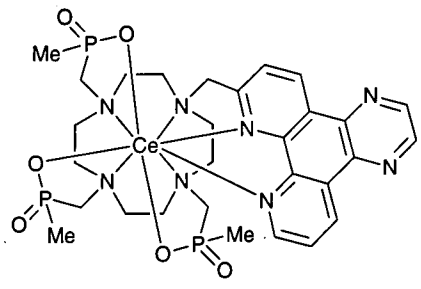

Compound **50** (90 mg, 0.12 mmol) was stirred in a solution of KOH (2 ml, 5% solution in a 3:1 mixture of water and methanol) at 40°C overnight. The solution was neutralised with HCl. The product was checked by ^1H NMR and used for complexation immediately. ^1H NMR (300 MHz, D_2O): δ 1.19 (9H, m, PCH_3), 2.2-4.0 (24H, br m, ring and arms CH_2), 7.24 (1H, br, Ar), 7.40 (1H, d, J = 7.2, Ar), 7.76 (1H, br, Ar), 7.90 (1H, br, Ar), 7.99 (1H, br, Ar), 8.07 (1H, br, Ar), 8.47 (1H, br, Ar). ^{31}P NMR (81 MHz, D_2O): δ 37.7 (3P, br).

Cerium nitrate (50 mg, 0.116 mmol) was added to a solution of the ligand in water (8 ml). The mixture was heated at reflux overnight. Evaporation of the solvent afforded a crude residue, which was purified by preparative TLC on alumina (10% CH_3OH/CH_2Cl_2, R_f=0.40, 20% CH_3OH/CH_2Cl_2) to yield a pale yellow solid (11 mg,

0.014 mmol, 12%). ^{1}H NMR (200 MHz, D_2O) partial assignment: δ 40.11 (1H, s, NCH_2P), 37.33 (1H, s, NCH_2P), 29.59 (1H, s, NCH_2P), 23.61 (1H, s, NCH_2P), 13.79 (1H, s, NCH_2P), 12.39 (3H, s, NCH_2P and NCH_2dpq), 11-4 (dpq), 0.05 (3H, s, PCH_3), -0.80 (1H, s, Hax), -2.64 (3H, s, PCH_3), -3.40 (3H, s, PCH_3), -4.66 (2H, s, Hax), -5.75 (1H, s, Hax), -6.36 (1H, s, Heq), -8.93 (1H, s, Heq), -10.10 (1H, s, Heq), -11.08 (1H, s, Heq), -13.49 (1H, s, Hax), -13.85 (1H, s, Hax), -14.48 (1H, s, Hax), -15.35 (1H, s, Hax). ^{31}P NMR (81 MHz, D_2O): δ 33.8 (1P, br), 38.6 (1P, br), 41.6 (1P, br). m/z (ES^+) 852 (100%, MNa^+). M.p. > 250°C. Accurate mass spectrum: found MH^+ 830.1418; $C_{29}H_{41}N_8O_6P_3Ce$ requires 830.1416.

52. Tetraethyl-1,4,7,10-tetraazacyclododecane-1,4,7,10-tetrayltetramethylenetetra(methylphosphinate)[8]

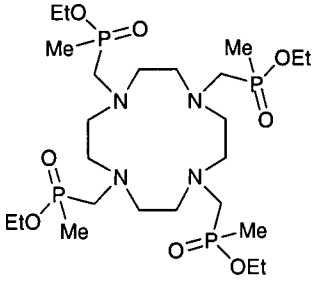

1,4,7,10-Tetraazacyclododecane (70 mg, 0.41 mmol) was dissolved in dry THF (4 ml) under argon over 4 Å molecular sieves. Methyldiethoxyphosphine (0.4 ml, 2.44 mmol) and paraformaldehyde (73 mg, 2.44 mmol) were added and the mixture was heated at reflux under argon overnight. Evaporation of the solvent yielded a pale yellow oil, which was purified by alumina column chromatography (gradient elution: CH_2Cl_2 to 1% CH_3OH/CH_2Cl_2, R_f =0.6, 10% CH_3OH/CH_2Cl_2) to yield a yellow oil (101 mg, 0.15 mmol, 38%). ^{1}H NMR (200 MHz, $CDCl_3$): δ 1.27 (12H, t, J = 7.0, OCH_2CH_3), 1.50 (12H, d, J = 14.2, PCH_3), 2.5-3.3 (24H, br, ring CH_2 and PCH_2), 4.04 (8H, q, J = 7.0, OCH_2CH_3). ^{31}P NMR (81 MHz, $CDCl_3$): δ 53.0 (4P, br). m/z (ES^+): 346 (100%, MCa^{2+}), 675 (80%, MNa^+).

53. [CeMeP$_4$]$^-$

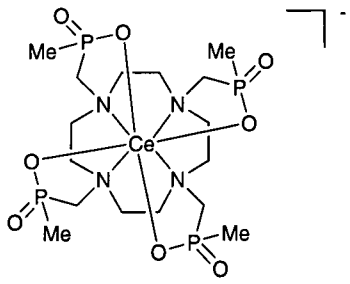

Compound **52** (53 mg, 0.08 mmol) was stirred in a solution of KOH (2 ml, 5% solution in water) at 40°C for 4 hours. The reaction was followed by ^{31}P NMR (81 MHz, D_2O): δ 40.7 (4P) and by m/z (ES^+): 269 (25%, MH_2^{2-}), 288 (90%, MCa^{2-}), 577 (50%, $MHCa^-$), 599 (25%, $MNaCa^-$), 615 (40%, $MKCa^-$). The solution was neutralised by addition of HCl solution and cerium nitrate (35 mg, 0.08 mmol) was added. The mixture was heated at reflux overnight. Evaporation of the solvent afforded a pale yellow solid. ^{1}H NMR (200 MHz, D_2O): δ 14.18 (4H, br s, CH_2 arm), 8.18 (4H, br s, Hax), 6.26 (4H, br s, CH_2 arm), 3.86 (12H, br s, PCH_3), 0.00 (4H, br s, Heq), -1.24 (4H, br s, Heq), -14.26 (4H, br s, Hax). ^{31}P NMR (81 MHz, D_2O): δ 38.0 (4P). m/z (ES^-): 676 (50%, M^-).

54. [CeDOTA]$^-$

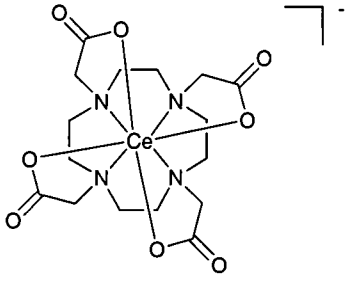

DOTA (50 mg, 0.12 mmol) was dissolved in water (8 ml) and the pH raised to 6 by addition of a KOH solution. Cerium nitrate (54 mg, 0.12 mmol) was added and the mixture was heated at reflux overnight. Evaporation of the solvent afforded a pale yellow solid. ^{1}H NMR (200 MHz, D_2O): δ 9.88 (4H, br s, CH_2 acetate), 7.40 (4H, br s, Hax), 6.98 (4H, br s, CH_2 acetate), 1.41 (4H, br s, Heq), 0.53 (4H, br s, Heq), -10.25 (4H, br s, Hax). m/z (ES^-): 540 (100%, M^-).

5.2. Photophysical Measurements

Ultraviolet absorbance spectra were recorded on a Unicam UV2-100 spectrometer operating with Unicam Vision software. Samples were contained in quartz cuvettes with a path length of 1 cm. All spectra were run against a reference of pure solvent contained in a matched cell. Absorption coefficients were calculated, using the Beer-Lambert law, from the absorbance at a number of different solution concentrations.

Circular dichroism spectra were recorded using a JASCO J-810 spectropolarimeter. Quartz cuvettes with a path length of 1 cm were employed.

Luminescence spectra were recorded using a Perkin-Elmer LS 50B, operating with FL Winlab software, or an Instruments S.A. Fluorolog 3-11, operating with DataMax software. The low temperature spectra were recorded using an Oxford Instruments DN-1704 cryostat and ITC-6 temperature controller. Quartz fluorescence cuvettes of path length 1 cm were employed. The absorbance of each solution at the excitation wavelength was below 0.3 to avoid inner filter effect. Second order diffraction effects were obviated by using a cut-off filter to remove the scattered light before it enters the emission monochromator.

Steady state fluorescence anisotropy measurements were made using the Perkin-Elmer LS 50B equipped with polarizing accessory. The instrumental factor '*G*' was determined from the spectra obtained using horizontally polarised excitation.

Excited state lifetime measurements were generally made on the Perkin-Elmer LS 50B (using Phlemming data acquisition written by Dr. A. Beeby, University of Durham) by monitoring the integrated intensity of light (at 618 nm for Eu and 545 nm for Tb complexes) emitted during a fixed gate time, t_g, a delay time, t_d, later. At least 20 different delay times were used, covering two or more lifetimes. The gate time was 0.1 ms, the excitation and emission slits were set to 15 nm bandpass. Where necessary, solutions were degassed by means of three freeze–pump–thaw cycles in a degassing cell fitted with a Young's tap. Lifetimes less than 0.7 ms were measured

using the third harmonic (λ_{ex} 355 nm) of a Q-switched Spectra Physics GCR-150–10 Nd:YAG laser as the excitation source.[11] The phosphorescence decay curves were fitted to a single exponential decay using a curve fitting program (Kaleidagraph software or Excel). An uncertainty of ± 10% was estimated for the values obtained.

Lanthanide luminescence quantum yields were determined relative to similar complexes of known quantum yield. For each of the standards (s) and the unknown (x), five solutions with absorbance between 0.02 and 0.1 were prepared and their absorbance at the excitation wavelength and total integrated emission intensity determined. The slope of the line obtained by plotting the integrated emission against the absorbance for each complex was used to calculate the quantum yield.[11]

Singlet-oxygen quantum yields were measured using the Nd:YAG laser excitation source described above. The phosphorescence from the sample was collected at 90°, passed through an interference filter centred at 1270 nm (Infra Red Engineering Ltd., Essex, UK) and then focussed onto the active area of a liquid nitrogen–cooled germanium photodiode (North Coast EO-817P). The singlet-oxygen emission decay was recorded for the terbium complex and the standard at two different concentrations using five laser energies. Details of the method employed to determine the quantum yields are included in ref. 11.

Circularly polarised luminescence spectra were recorded at the University of Glasgow. Details of the method and equipment used have been reported.[12]

Calf-thymus DNA and poly(dGdC) of the highest available purity were obtained from Sigma and were used as received. HPLC-purifed self-complementary oligonucleotides were purchased from Oswel Ltd. (Southampton, UK) and used as received. For absorbance and luminescence titrations, the nucleic acid solution (typically 1 to 3 mM) was titrated in 5 to 50 μL increments into a fixed concentration of complex (20-50 μM) in a pH 7.4 HEPES buffer containing 10 mM NaCl. Occasionally a minimal volume of methanol was added (< 5% total volume) to aid complex solubilisation.

Difference CD titrations were carried out in a pH 7.4 HEPES buffer containing 10 mM NaCl. When changes in the CD difference spectra of the nucleic acid were monitored, the complex solution (typically 0.1-0.2 mM) was added to the nucleic acid solution (10-20 μM) in 10-20 μL aliquots. The spectrum due to the aqueous buffer was subtracted, followed by subtraction of the complex at the same corrected concentration, allowing for the small dilution effects. When changes in the CD difference spectra of the complexes were recorded, the nucleic acid solution (typically 2-3 mM) was added to the solution of the complex (100 μM) in 10-20 μL aliquots.

5.3. Other Measurements

The longitudinal water proton relaxation rates were measured using a modified Varian VXR instrument tuned to 65.6 MHz (^{1}H), by means of the standard inversion recovery technique. The concentration of the complex was about 0.5 mM in deionized water.[13]

COSY spectra of $[CGCGAATTCGCG]_2$ were acquired on a Varian Unity 500 instrument (11.8 T) employing standard VNMR software. The HOD signal was used as internal reference set at δ 4.75 ppm and was suppressed by a presaturation pulse. An oligonucleotide concentration of 0.8 mM in degassed D_2O (600 μL) was employed and the successive additions of D_2O solutions containing 0.01, 0.02 and 0.05 molar equivalents of Gd complex were carried out such that the total volume added did not exceed 20 μL.

Cyclic voltammetry was performed using an EG&G Versastat II potentiostat operating under the PARC M270 software package. Aqueous solutions of the complexes were used (0.01 M), containing 0.1 M KNO_3 as supporting electrolyte. A glassy carbon working electrode, an Ag/AgCl reference electrode and a Pt counter electrode were employed. The potential was scanned at different scan rates (5-200 mV s^{-1}). All experiments were performed under argon.

References

1 D. Parker, P. K. Senanayake, and J. A. G. Williams, *Journal of the Chemical Society-Perkin Transactions 2*, 1998, 2129.

2 D. Parker, 'Macrocycle Synthesis', Oxford University Press, 1996.

3 J. I. Bruce, R. S. Dickins, L. J. Govenlock, T. Gunnlaugsson, S. Lopinski, M. P. Lowe, D. Parker, R. D. Peacock, J. J. B. Perry, S. Aime, and M. Botta, *Journal of the American Chemical Society*, 2000, **122**, 9674.

4 J. Lewis and T. D. O' Donoghue, *Journal of the Chemical Society-Dalton Transactions*, 1980, 736.

5 A. M. S. Garas and R. S. Vagg, *Journal of Heterocyclic Chemistry*, 2000, **37**, 151.

6 S. Brandes, C. Gros, F. Denat, P. Pullumbi, and R. Guilard, *Bulletin De La Societe Chimique De France*, 1996, **133**, 65.

7 S. Aime, M. Botta, R. S. Dickins, C. L. Maupin, D. Parker, J. P. Riehl, and J. A. G. Williams, *Journal of the Chemical Society-Dalton Transactions*, 1998, 881.

8 C. J. Broan, E. Cole, K. J. Jankowski, D. Parker, K. Pulukkody, B. A. Boyce, N. R. A. Beeley, K. Millar, and A. T. Millican, *Synthesis-Stuttgart*, 1992, 63.

9 H. Gilman and J. Eisch, *Journal of the American Chemical Society*, 1955, **77**, 6379.

10 M. Jastrzebskaglapa and J. Mlochowski, *Roczniki Chemii*, 1976, 987.

11 A. Beeby and A. E. Jones, *Photochemistry and Photobiology*, 2000, **72**, 10.

12 R. S. Dickins, J. A. K. Howard, C. L. Maupin, J. M. Moloney, D. Parker, R. D. Peacock, J. P. Riehl, and G. Siligardi, *New Journal of Chemistry*, 1998, **22**, 891.

13 M. P. Lowe, D. Parker, O. Reany, S. Aime, M. Botta, G. Castellano, E. Gianolio, and R. Pagliarin, *Journal of the American Chemical Society*, 2001, **123**, 7601.

Appendix

^{1}H NMR spectra of ligand **8** and europium complexes **9** and **40**.

8

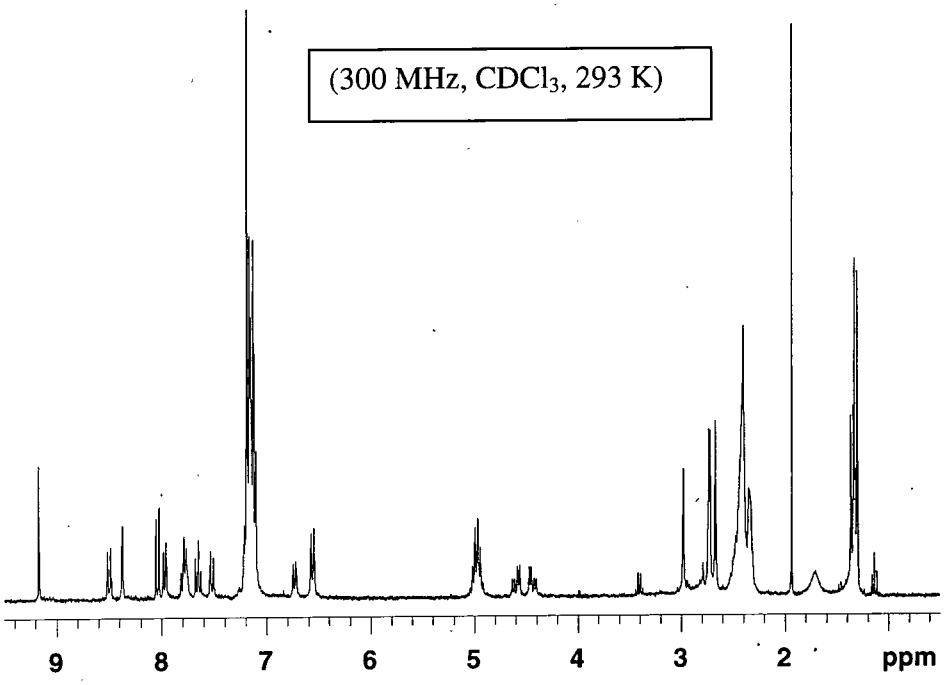

9

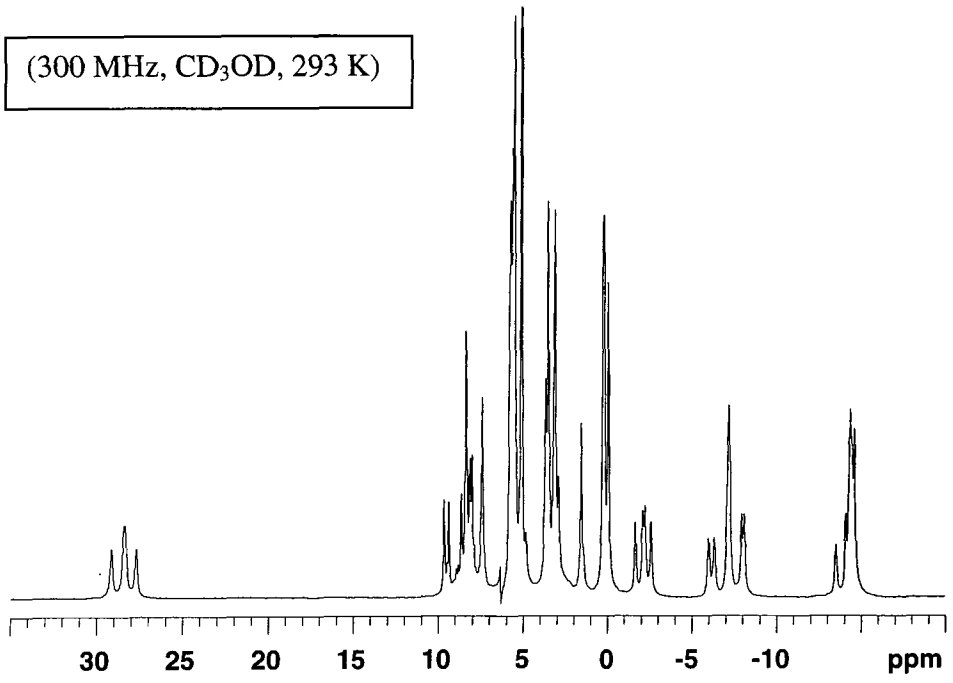
(300 MHz, CD_3OD, 293 K)
30
25
20
15
10
5
0
-5
-10
ppm

40

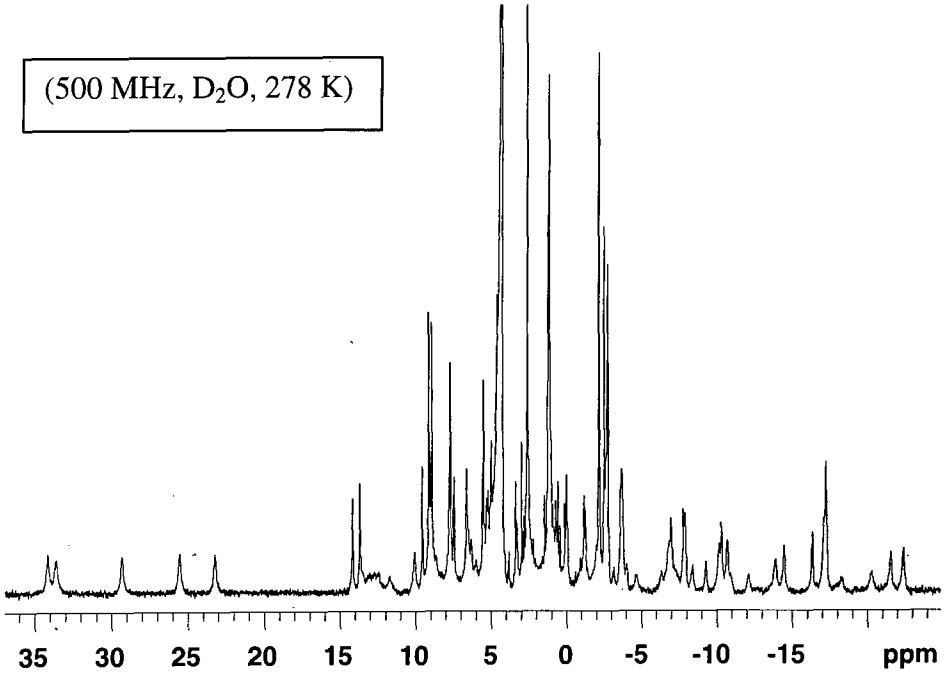
(500 MHz, D_2O, 278 K)
35
30
25
20
15
10
5
0
-5
-10
-15
ppm